Author/s:
Fernando, Hettiya Kandage Dinali Helan

Title:
The AGE/RAGE pathway in NAFLD progression to liver fibrosis: targets for prevention and treatment

Date:
2019

Persistent Link:
https://hdl.handle.net/11343/227044

The AGE/RAGE pathway in NAFLD progression to liver fibrosis: targets for prevention and treatment

ORCID iD: https://orcid.org/0000-0002-2984-6670

Hettiya Kandage Dinali Helan Fernando

B.Sc. (Hons), M.Sc.

Department of Medicine, Austin Health,

The University of Melbourne

Submitted to total fulfilment of the requirements of the degree of

Doctor of Philosophy

March 2019

TABLE OF CONTENTS

ABSTRACT

Non-alcoholic fatty liver disease (NAFLD) is the most prevalent liver disease in Australia and around the world and affects up to 40% of the adult population. It is the leading cause for liver transplantation in the USA and expected to be the leading cause in the next 10 years in Australia. There is no proven medical treatment for NAFLD except for liver transplantation in patients with advanced liver disease. The management involves lifestyle modifications and dietary restrictions, which are difficult to achieve in most patients.

NAFLD can progress to its severe form of non-alcoholic steatohepatitis (NASH) and liver fibrosis which eventually leads to cirrhosis or hepatocellular carcinoma. It has been described that there are several factors which contribute to NAFLD progression such as genetic factors, epigenetic factors, oxidative stress, adipokines and microbiota. These factors constitute the second hit of the so called 'two-hit' hypothesis in which the fatty liver is considered as the first hit.

Advanced glycation end products (AGEs) are formed by the non-enzymatic reaction between reducing sugars and proteins or lipids. These are found in large amounts in the Western diet where high temperatures are applied during food processing. AGEs can also be formed in the body during aging, and the rate of synthesis can be accelerated in conditions such as diabetes due to elevated blood glucose levels. AGEs have been implicated in the progression of many chronic diseases such as diabetic complications. We therefore hypothesized that AGEs are another 'second hit' that drives NAFLD progression to liver fibrosis.

A series of studies in this thesis have been designed to investigate and compare the effects of endogenous AGEs formed in the body and exogenous or dietary AGEs on NAFLD progression to liver fibrosis. The effects of AGEs on NAFLD progression were explored by intraperitoneal administration of AGEs to C57BL/6 mice for 10 weeks following 30

weeks of a high fat (HF) diet. This strategy was used to mimic the effects of endogenously formed AGEs. The effects of intraperitoneal AGEs were compared to those of dietary AGEs by feeding mice with the HF diet for the first 30 weeks, followed by a diet containing high AGEs for the next 10 weeks. The high AGE diet was prepared by baking the HF diet at 160^{o} C for 1 hour. To further evaluate the contribution of endogenous AGEs, HF fed mice were made diabetic by two consecutive daily injections of streptozotocin after 15 weeks of HF diet. RAGE knockout mice were used to evaluate the role of RAGE in AGE-induced effects. We also explored therapeutic strategies targeting the AGE/RAGE pathway in NAFLD progression. Since we found that vinegar marination of HF diet prior to baking reduces AGE content in the diet, in a series of studies we fed diabetic mice with a vinegar marinated baked diet for 40 weeks. Moreover, we used therapeutic drugs that are known to inhibit AGE formation and have been used in phase II clinical trials for other diseases but have not been tested for their therapeutic effects on AGE-induced NAFLD progression. This included the administration of aminoguanidine and pyridoxamine to diabetic or high AGE fed mice via drinking water during the last 10 weeks of the 40-week NAFLD model. In addition, we investigated the effects of alagebrium, an AGE-crosslink breaker, administered by daily gavage injection during the last 10 weeks to mice fed the high AGE diet for 40 weeks. Moreover, an AGE trafficking study was performed by gavaging fluorescent labelled-AGEs to high AGE fed mice treated with alagebrium in the last 2 weeks of a 4-week study.

Dietary AGE content, gene expression of pro-inflammatory and pro-fibrotic cytokines, collagen 1, endotoxin responsive genes and RAGE in the liver and liver injury, oxidative stress and fibrosis were determined. Moreover, to elucidate mechanisms we performed cell culture experiments using two immortalised cell lines, murine Kupffer cells (KUP5 cells) and human hepatic stellate cells (HSCs) (LX2 cells). Gene expression of pro-inflammatory cytokines, ROS generation and HSC activation were determined in cells exposed to AGEs in the presence and absence of RAGE antagonists or alagebrium.

We found that baking the HF diet increased its AGE content by several fold. Whilst the effects of intraperitoneal AGEs on pro-inflammatory and pro-fibrotic cytokine expression and liver fibrosis were not significant, diabetic mice fed the HF diet showed elevated circulating AGE levels which were accompanied by increased liver expression of RAGE, cytokines, endotoxin responsive genes, collagen 1, oxidative stress and liver fibrosis

compared to the HF diet. There was also a positive and strong correlation between circulating AGEs and liver RAGE expression. Similarly, high dietary AGE intake in non-diabetic mice was also associated with an increased expression of the genes measured above, oxidative stress and liver fibrosis compared to HF diet, with diabetic mice fed the high AGE diet showing an additive effect on some parameters such as circulating AGEs, RAGE and oxidative stress. This suggests that increased AGEs formed in diabetes may be responsible for NAFLD progression to liver fibrosis. The concept that AGEs impart their effects by binding to RAGE is supported by the findings that AGE-induced up-regulation of pro-inflammatory cytokines was completely prevented by RAGE blockade in Kupffer cells. Importantly, the finding that liver fibrosis was worse in high AGE fed non-diabetic mice than diabetic mice fed the HF diet suggests that dietary AGEs are more harmful in NAFLD progression to liver fibrosis than endogenous AGEs.

The AGE inhibiting drugs aminoguanidine and pyridoxamine failed to affect NAFLD progression to liver fibrosis in diabetic or high AGE fed mice. In fact, these drugs were apparently enhanced liver fibrosis in HF fed mice, at least under our experimental conditions. On the other hand, we found that dietary intervention with vinegar marination prior to baking the HF diet had a profound inhibitory effect on liver injury, liver expression of RAGE, pro-inflammatory and pro-fibrotic cytokines and HSC activation, leading to a marked improvement in liver fibrosis in diabetic mice fed the marinated high AGE diet compared to diabetic mice fed the high AGE diet without vinegar marination. Pharmacological intervention with the AGE-crosslink breaker alagebrium produced profound inhibitory effects on all of above parameters, leading to a marked improvement in NAFLD progression. The finding that an alagebrium-induced marked reduction in circulating AGEs in high AGE fed mice was supported by AGE-trafficking study which showed that alagebrium apparently promotes AGE clearance. Moreover, cell culture experiments showed that alagebrium directly inhibits AGE-induced pro-inflammatory cytokine secretion and ROS generation by Kupffer cells and thereby reduced the exposure of HSCs to these cytokines and thus, indirectly inhibited HSC activation. Thus, alagebrium in addition to promoting AGE clearance and other than its designated role as an AGE-crosslink breaker, may also have a direct effect on AGE/RAGE signalling.

In summary, the studies in this thesis demonstrate that AGEs could be considered as a second hit that drives NAFLD progression to liver fibrosis. These findings also suggest

that diabetes which is an important source of the circulating pool of AGEs, exacerbates NAFLD progression to liver fibrosis. Moreover, we conclude that dietary AGEs which appear to act directly on liver AGE/RAGE signalling and indirectly via the gut/liver AGE/RAGE axis are more harmful and stronger stimulant than endogenously derived AGEs in driving NAFLD progression. Thus, dietary modifications and changes to food preparation such as vinegar marination provide a feasible strategy to reduce dietary AGE intake and associated liver injury in NAFLD. We also conclude that AGEs directly act on Kupffer cells, leading to indirect activation of HSCs. We also show that alagebrium, a drug considered to be an AGE-crosslink breaker, may also have a direct effect on AGE/RAGE signalling in Kupffer cells. We also provide evidence that alagebrium is a potential therapeutic drug for NAFLD patients that could be trialled in a phase II study since the drug has been trialled in patients with other conditions such as heart failure and diabetic nephropathy.

DECLARATION

This is to certify that

1) this thesis comprises only my original work towards the Doctor of Philosophy except where due acknowledgement has been made in the text to all other material used
2) this thesis is less than 100,000 words in length, exclusive of tables, maps, bibliographies and appendices as approved by the Research Higher Degree Committee.

Dinali Fernando

ACKNOWLEDGEMENTS

I would like to firstly thank my supervisors, Doctor Chandana Herath and Professor Peter Angus, for providing me the opportunity to undertake PhD study in this lab and their guidance and support throughout this process. I am extremely grateful for the constant support and much needed encouragement I received from Dr Chandana Herath. I am extremely grateful for Professor Peter Angus for his endless ideas with clinical acumen.

I would also like to acknowledge Dr Chris Leung, Dr Kai Mak, Dr Indu Rajapaksha and Ms Lakmie Gunarathne for their valuable time and support they gave me throughout this process. I also like to thank Ms Zhiyuan Jia and Ms Ping Huang for their support in lab experiments and my other lab colleagues for their company and friendship.

I am indebted to Professor Josephine Forbes and the lab for their assistance with technical support and Dr Hiroshi Kitani for providing immortalised Kupffer cell line used in this thesis. I also would like to thank Prof Sof Andikopolus and lab, Prof Louise Burrell and lab Dr Peter Wookey and lab for the laboratory facilities provided for this study. A special thank goes to my PhD advisory committee chair person Prof Albert Frauman for his valuable ideas and advices and also for his pleasant company. The staff of department of medicine, Ms Jo Mayall, Ms Susan Hisheh, Ms Minh Nguyen, Ms Gina Barri-Rewell, Meri Kalajdziovski and Mr Joey Santos and the staff of Bioresource facility at Austin Health, Ms Julia Fyfe, Mr Josh Laurima, Ms Eleanor Hunt and other staff for their support, company and friendship shown throughout my study.

I would like to acknowledge the financial assistance I received form Melbourne International Research Scholarship (MIRS) and Melbourne International Fee Remission Scholarship (MIFRS) by The University of Melbourne without which this study would not have been completed. The travel award from Austin Health is also appreciated. Our

research group is also grateful for National Health and Medical Research Council of Australia for their funding support.

Finally, I wish to pay a heartfelt and beloved acknowledgment to my wonderful husband Roshan. Without Roshan's ongoing support, patience, sacrifices and endless moral support and encouragement, I would never have had the strength and determination to complete this work. An utmost and heartfelt thank goes to my parents who spoiled me with unconditional love and would be the happiest people to see me accomplish this achievement. I also wish to pay special thanks to my brother who took the responsibility of me in the absence of my parents and my niece for giving me lovely distractions. A sincere thanks goes to my in-laws and dear friends for their love, moral support and encouragement.

ABSTRACTS AND PUBLICATIONS ARISING FROM THIS THESIS

PAPERS

1. Fernando HKDH, Angus PW, Herath CB. (2019) Development and progression of non-alcoholic fatty liver disease: the role of advanced glycation end products (2019 - Submitted)

2. Fernando HKDH, Rajapaksha DIG, Leung C, Forbes J, Angus PW, Herath CB. (2019) Alagebrium inhibits progression of non-alcoholic fatty liver disease to liver fibrosis via RAGE mediated direct inhibition of Kupffer cells and indirect inhibition of hepatic stellate cell activation in high fat high AGE fed mice (MS in preparation)

3. Fernando HKDH, Leung C, Forbes J, Angus PW, Herath CB. (2019) Advanced glycation end products (AGEs) exacerbate NAFLD progression to liver fibrosis via receptor for AGEs (RAGE) in high fat fed mice (MS in preparation)

4. Fernando HKDH, Leung C, Forbes J, Angus PW, Herath CB. (2019) Dietary advanced glycation end products (AGEs) exacerbates liver fibrosis and are more harmful than diabetes (MS in preparation)

CONFERENCE PROCEEDINGS AND ABSTRACTS

1. Alagebrium ameliorates NAFLD progression in mice fed a high advanced glycation end products diet via direct inhibition of Kupffer cells and indirect inhibition of hepatic stellate cell activation.
   International Liver Congress, April 2019, Vienna, Austria.
   DOI: 10.3252/pso.eu.ILC2019.2019
   (Young Investigator Bursary)

2. Advanced glycation end products (AGEs) exacerbate NAFLD progression to liver fibrosis via receptor for AGEs (RAGE) in high fat fed mice.
   International Liver Congress, April 2019, Vienna, Austria.
   DOI: 10.3252/pso.eu.ILC2019.2019

3. Advanced glycation end products (AGEs) derived from diets have more impact on the progression of fatty liver disease than endogenously derived AGEs.
   Austin Research Festival, October 2018, Melbourne, Australia
   (Winner - AMRF Young Investigator Award)
   (Finalist - AMRF Research Higher Degree Award)
   (Finalist - Austin Life Sciences Award for Science Research)

4. Marinating of food with vinegar offers a simple and effective approach to prevent advanced glycation end products (AGEs)-induced NAFLD progression.
   Austin Research Festival, October 2018, Melbourne, Australia

5. Dietary advanced glycation end products (AGEs) play a major role in exacerbating progression of non-alcoholic fatty liver disease to liver fibrosis in diabetic mice.
   Australian Gastroenterology Week, September 2018, Brisbane, Australia
   (Finalist - Young Investigator Award)

6. Alagebrium inhibits the progression of NAFLD to NASH and liver fibrosis by blocking AGE/RAGE pathway.
   Austin Research Festival, October 2017, Melbourne, Australia

7. Alagebrium inhibits the progression of NAFLD to NASH and liver fibrosis by blocking AGE/RAGE pathway.
   Australian Gastroenterology Week, August 2017, Gold Coast, Australia
   (Finalist - Young Investigator Award)

AWARDS GRANTED FOR THE RESEARCH INCLUDED IN THIS THESIS

1. Young Investigator Bursary: International Liver Congress (EASL) (2019)

2. AMRF Young Investigator Award: Winner. Austin Research Festival (2018)

3. AMRF Research Higher Degree Award: Finalist. Austin Research Festival (2018)

4. Austin Life Sciences Award for Science Research: Finalist. Austin Research Festival (2018)

5. Young Investigator Award: Finalist. Australian Gastroenterology Week (2018)

6. Young Investigator Award: Finalist. Australian Gastroenterology Week (2017)

LIST OF FIGURES

LIST OF TABLES

ABBREVIATIONS

α-SMA	α -smooth muscle actin
AASLD	American association for the study of liver diseases
AGEs	advanced glycation end products
AGE-R1	AGE receptor-1
AGE-R2	AGE receptor-2
AGE-R3	AGE receptor-3
AGE-RSA	AGE modified rat serum albumin
Ala	alagebrium
ALP	alkaline phosphatase
ALT	alanine aminotransferase
ANOVA	analysis of variance
AST	aspartate aminotransferase
ATP	adenosine 5′-triphosphate
BSA	bovine serum albumin
BHT	butylated hydroxytoluene
bw	body weight
cDNA	complementary DNA
CML	N^{ε}1-(carboxymethyl)lysine

CEL	N^{ε}1-(carboxyethyl)lysine
cRAGE	cleaved RAGE
CTGF	connective tissue growth factor
DAB	diaminobenzidine tetrahydrochloride
DCFDA	di chlorofluorescin di acetic acid
DNA	deoxyribonucleic acid
ECM	extracellular matrix
EGF	epidermal growth factor
ELISA	enzyme linked immune sorbent assay
EMT	epithelial-to-mesenchymal transition
ER	endoplasmic reticulum
esRAGE	endogenously secreted RAGE
FBS	fetal bovine serum
FGF	fibroblast growth factor
GC	gas chromatography
GESA	gastroenterological society of Australia
GGT	gamma-glutamyl transpeptidase
GI	Glycaemic index
GWAS	genome-wide association studies
HbA1c	haemoglobin A1c
HCC	hepatocellular carcinoma
HF	high fat
HGF	hepatocyte growth factor

HNE	hydroxy-2-nonenal
HSC	hepatic stellate cells
H&E	Haemotoxylin and Eosin
IL-1β	interleukin-1 β
IL-6	interleukin-6
i.p.	intraperitoneal
IR	insulin resistance
IVIS	*In vivo* imaging system
Kg	kilograms
KO	knockout
LPS	lipopolysaccharides
M	molar
MAP kinases	mitogen-activated protein kinases
mM	millimolar
MMP	matrix metalloproteinase
mg	milligram
mL	millilitre
MCP-1	monocyte chemoattractant protein-1
MG-H1	methylglyoxal derived hydroimidazalone-1
mRNA	messenger RNA
MS	mass spectrometry
NADPH	nicotinamide adenine dinucleotide phosphate-oxidase
NAS	NAFLD activity score

ng	nanograms
nm	nanometre
nM	nanomolar
NAFLD	non-alcoholic fatty liver disease
NASH	non-alcoholic steatohepatitis
NF-kβ	nuclear factor kappaβ
NK	natural killer
PBC	primary biliary cholangitis
PBS	phosphate buffered saline
PCR	polymerase chain reaction
PDGF	platelet-derived growth factor
PFA	paraformaldehyde
PNPLA3	Patatin-like phosholipase domain-containing 3 gene variant I 148M
PPAR-γ	peroxisome proliferator-activated receptor-γ
PSC	primary sclerosing cholangitis
PUFA	polyunsaturated fatty acids
Q-PCR	quantitative real time polymerase chain reaction
RAGE	receptor for advanced glycation end products
RAS	renin-angiotensin system
RCS	reactive carbonyl species
RNA	ribonucleic acid
ROS	reactive oxygen species
RSA	rat serum albumin

SCFA	short chain fatty acids
SEC	sinusoidal endothelial cells
SEM	standard error of the mean
SIBO	small intestinal bacterial over-growth
SNPs	single nucleotide polymorphisms
sRAGE	soluble RAGE
STZ	streptozotocin
TGF	transforming growth factor
TIMPs	tissue inhibitor of metalloproteinases
TLR-4	toll like receptor-4
TNF-α	tumour necrosis factor-α
U	units
VCAM-1	vascular cell adhesion molecule 1
VEGF	vascular endothelial growth factor
VLDL	very low density lipid
WT	wild type
µg	microgram
µl	microlitre
µm	micrometer
µM	micromolar

PREAMBLE

The prevalence of chronic liver diseases is rising worldwide and approximately 1.7 million deaths due to liver disease are reported annually.[1] The aetiology of these diseases is multifactorial and the causative agents vary depending on ethnic groups and geographical area.[2] Among them, non-alcoholic fatty liver disease (NAFLD) is the most common liver disease in Australia as well as in the world. It affects up to 40% of adult Australian population and is a major cause of morbidity and mortality in Australia.[3] The main risk factors for developing NAFLD are central obesity, type 2 diabetes, dyslipidaemia and insulin resistance.[4] Currently, there is no established drug therapy, and treatments are largely based on lifestyle modification which are difficult to achieve in most patients. Therefore, there remains a major need to identify potentially modifiable factors that exacerbate liver injury and NAFLD progression to liver fibrosis and to develop therapies that can prevent or treat fibrosis in this condition.

A two-hit hypothesis has been proposed to explain the establishment and progression of NAFLD.[5] In this hypothesis, the first hit is the accumulation of excess fat in the liver causing fatty liver. There are several factors that have been considered as the second hit that drives NAFLD progression to liver fibrosis. We hypothesized that advanced glycation end products (AGEs) that have been implicated in the progression of many chronic diseases,[6,7] are one factor responsible for NAFLD progression to liver fibrosis. AGEs are formed by the non-enzymatic reaction between reducing sugars and proteins or lipids and are found in large amounts in the Western diet where high temperatures are applied during food processing. AGEs can also be formed in the body during aging, and the rate of synthesis can be accelerated in conditions such as diabetes due to elevated blood glucose levels.[8]

The accumulation of circulating and/or tissue AGEs may result in the activation of pro-inflammatory and pro-fibrotic pathways which lead to changes in extracellular matrix

structure and function. It has been shown that AGEs impart their effects via two pathways; 1) a direct effect independent of receptor binding where crosslinks are formed between AGEs and molecules on the basement membrane, 2) an indirect effect by interaction with their receptors. Most of the harmful effects of AGEs in a wide range of pathological conditions including liver disease have been shown to be mediated via their receptors.[9] To date, at least 8 candidate molecules have been identified which are capable of binding to AGEs. The most characterised receptor among them is known as the receptor for AGEs or RAGE.[10] RAGE is a 35 kDA pattern recognition multiligand receptor and is a member of immunoglobulin super family of cell surface molecules.[10]

The primary approach to manage hepatic fibrosis is concerned with the removal of the causative agent while managing the complications. Fibrosis can eventually result in liver cirrhosis or hepatocellular carcinoma. Liver transplantation is the only curative treatment for end-stage liver disease in patients with cirrhosis. Therefore, it is important to explore strategies that can prevent NAFLD progression to liver fibrosis. Emerging evidence suggests that the AGE-RAGE axis contributes to the progression of many diseases, including cardiovascular disease and diabetic complications.[11-13] Therefore, in this thesis, we investigated the role of the AGE-RAGE axis in the progression of NAFLD to liver fibrosis with special emphasis on the contribution by different sources of AGEs, and dietary and therapeutic interventions.

The central hypothesis of this thesis is that the AGE-RAGE axis plays an important role in NAFLD progression and targeting this axis provides an effective strategy of disease prevention and treatment. The hypothesis was addressed in three main aims.

1) To investigate and compare the effects of dietary versus endogenous AGEs on the progression of NAFLD to NASH and liver fibrosis.
2) To elucidate the role of RAGE in mediating AGE-induced signalling and NAFLD progression using RAGE antagonists and RAGE knockout ($RAGE^{-/-}$) mice.
3) To explore the benefits of dietary modification, and therapeutic role of inhibitors of AGE formation (aminoguanidine and pyridoxamine) and an AGE-crosslink breaker (alagebrium) in NAFLD mice fed a diet high in AGEs.

This thesis is comprised of a brief introduction (preamble), background with literature review (chapter 1), methods and protocols (chapter 2) and experimental chapters

(chapters 3 to 6), followed by chapter 7 with general discussion, conclusions and future directions. Each of the experimental chapters contains a brief introduction, experimental design, study-related specific methods/protocols, results, discussion and a summary.

This thesis commences with chapter 1, which is the literature review, with details of liver anatomy and function and the current understanding of the pathogenesis of NAFLD and liver fibrosis. The structure and formation of AGEs that potentially drive NAFLD progression are also outlined, including RAGE structure and possible interactions of AGE/RAGE. Moreover, current and proposed therapies targeting the AGE/RAGE axis are discussed.

Chapter 2 describes the general experimental methods and protocols used to explore the role of the AGE/RAGE axis in NAFLD and to target this axis to prevent NAFLD progression. In addition, the chapter also discusses statistical methods employed for data analysis.

Chapter 3 is the first experimental chapter which provides the outcome of aim 1 of the thesis. A series of studies presented in this chapter investigated and compared the effects of endogenous (i.e. intraperitoneally administered AGEs) and dietary AGEs on NAFLD progression and demonstrates that dietary AGEs are more harmful than endogenous AGEs.

Chapter 4 describes the effects of diabetes and potentially AGEs formed during hyperglycaemia and compares these with oral AGEs. The latter part of this chapter investigated the role of RAGE in mediating AGE effects, which is related to aim 2 of this thesis. This leads to the next chapters which described the effects of several therapeutic strategies targeting the AGE/RAGE axis in NAFLD.

Chapter 5 addresses aim 3 of this thesis. In this chapter, strategies that can inhibit AGE formation were studied using two approaches. The first was to inhibit endogenous AGE formation using two drugs, aminoguanidine and pyridoxamine. Neither of the two drugs was effective in ameliorating NAFLD progression. The second strategy employed was to inhibit the formation of AGEs in the diet by vinegar marination which showed promising results with improvement of NAFLD progression.

Chapter 6 is the last experimental chapter which described the effects of the AGE-crosslink breaker alagebrium. The studies described in this chapter convincingly showed that alagebrium is an effective drug which ameliorates NAFLD progression. Moreover, they provide evidence that other than its designated mode of action, alagebrium may also have a direct effect on the AGE/RAGE axis in Kupffer cells and indirect effects on hepatic stellate cells.

Chapter 7 contains the general discussion and conclusions where the results from chapters 3, 4, 5 and 6 are discussed. Future directions are also mentioned, to guide future investigations related to the present findings and potential of manipulating the AGE/RAGE axis in formulating future therapies in both diabetic and non-diabetic patients with NAFLD.

CHAPTER 1

Background and aims

1.1 Introduction

The liver is the heaviest and largest internal organ in the human body and is the most important metabolic organ. The wide range of metabolic, secretory and endocrine functions explain its complexity in structure. These functions include synthesis and secretion of bile, excretion of bilirubin, excretion of other toxins and waste products, synthesis of plasma proteins (including clotting factors, albumin and acute phase proteins), gluconeogenesis, and storage of triglycerides, some vitamins and glycogen.

1.1.1 Macroscopic structure of liver

The healthy human liver weighs around 1.5 kg and is located in the upper right quadrant of the abdomen, below the diaphragm, on top of several structures, with imprints showing on the inferior surface. It is divided into eight functionally independent segments; with each segment having its own independent vascular and biliary pedicle and venous drainage (Fig. 1.1). The capsule of the liver, known as Glisson's capsule, is a fibrous connective membrane mainly composed of collagen and elastin fibres. It encompasses the hepatic parenchyma which contributes mechanical support to the liver.[14]

Mouse liver has 4 lobes: the median (or middle), left, right and caudate and all, except the left are further subdivided into 2 or more parts.[15] The large medial lobe is subdivided into left and right portions. The right lateral lobe is divided horizontally into anterior and posterior portions and the caudal lobe subdivided into two leaf shaped dorsal and ventral portions.[16]

Unlike other organs, the liver receives its blood supply from two sources, the hepatic artery and the portal vein. The portal vein supplies the major portion (approximately 75%) of the liver's blood supply. It carries blood from the digestive tract and is therefore rich in compounds which have been absorbed from the gut. After entering the liver, the portal vein divides into increasingly smaller branches, portal venules. The remaining supply (approximately 25%) is from the hepatic artery and it perfuses the liver with highly oxygenated blood. Upon entering the liver, like the portal vein, the hepatic artery divides into increasingly smaller branches, hepatic arterioles. This blood then flows into sinusoids before emptying into hepatic veins, then to the inferior vena cava.[15]

The biliary system in the liver is responsible for the excretion of bile and other products. It begins with small tributaries which fuse together to form increasingly larger branches, hence it is called the biliary tree. These larger branches eventually come together to form two large bile ducts, the left and right hepatic ducts. These two then join to form the common hepatic duct, which is later joined to the cystic duct to form the common bile duct.

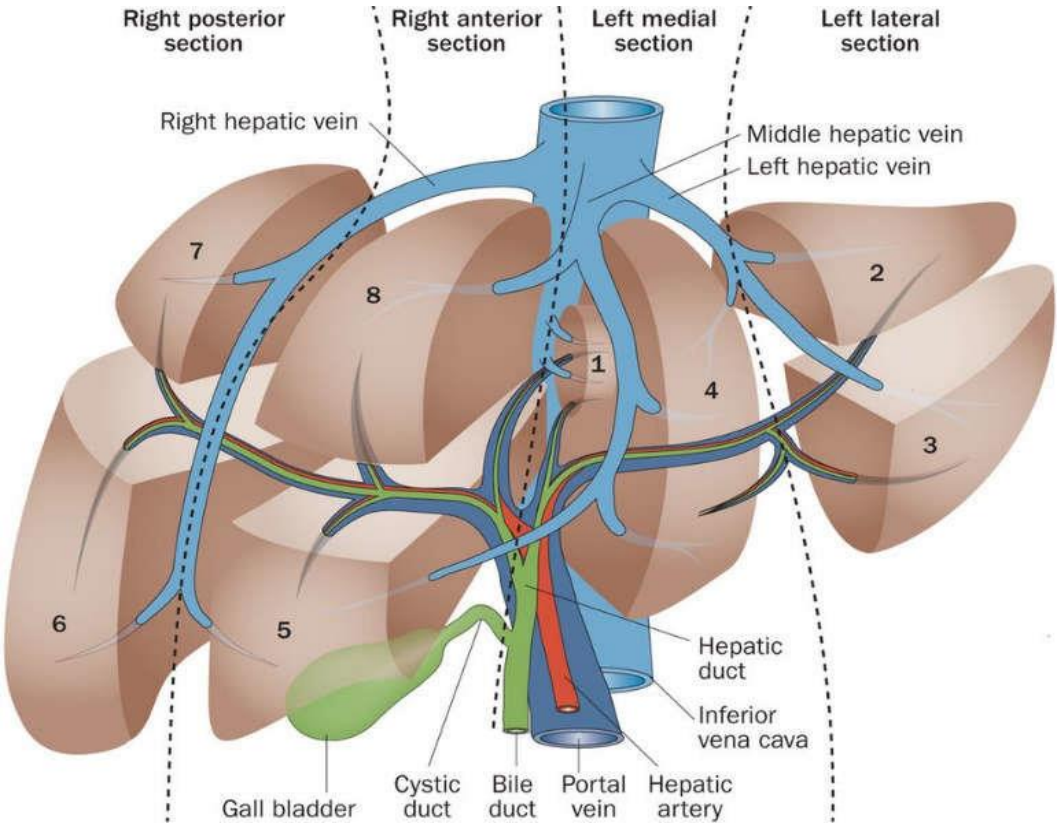

Figure 1.1 Macroscopic anatomy of liver

The liver can be divided into 8 vascular segments, with each subserved with a separate branch of portal vein, hepatic artery and bile duct (Adapted from Ref[17]).

1.1.2 Microanatomy of liver

The classic lobule was defined as the structural and functional unit of the liver for more than a century. It is a hexagonal lobule with portal tracts at the corners of the hexagon and a hepatic vein at the centre. A parallel concept of a lobule based on the portal tract has been described by Mall with a portal tract in the centre and central venules at the periphery and called the portal lobule. In 1954, Rappaport et al. described the liver acinus, defining the functional unit based on the microcirculatory flow within the liver (Fig. 1.2). The concepts of classic lobule, portal lobule, and acinus have never been completely accepted, neither have they been completely discarded. A single concept might not successfully explain all the pathological and physiological processes in the liver, but every concept is useful in explaining some of them.[18]

Both hepatic artery and the portal vein divides into small branches and eventually empty their flow into a system of small vascular channels which is different from capillaries anywhere else in the body. These channels, called 'hepatic sinusoids', are 10-30 μm in diameter. These are lined by endothelial cells with spaces, or fenestrations, between them and are directly contacted on each side by hepatocytes which are arranged in one cell thick plates. The narrow, plasma filled region between hepatocytes and sinusoidal endothelial cells is called the 'space of Disse' through which solutes are exchanged. It contains both extracellular matrix (ECM) and hepatic cells.

A terminal branch of the portal vein, a terminal branch of the hepatic artery and a bile ductule is collectively called a portal triad (or portal tracts) (Fig. 1.2), which is surrounded by a small amount of connective tissue and a layer of hepatocytes. Within the portal tract, there is also a lymphatic channel, but these are difficult to identify on sections as their thin walls are often collapsed.

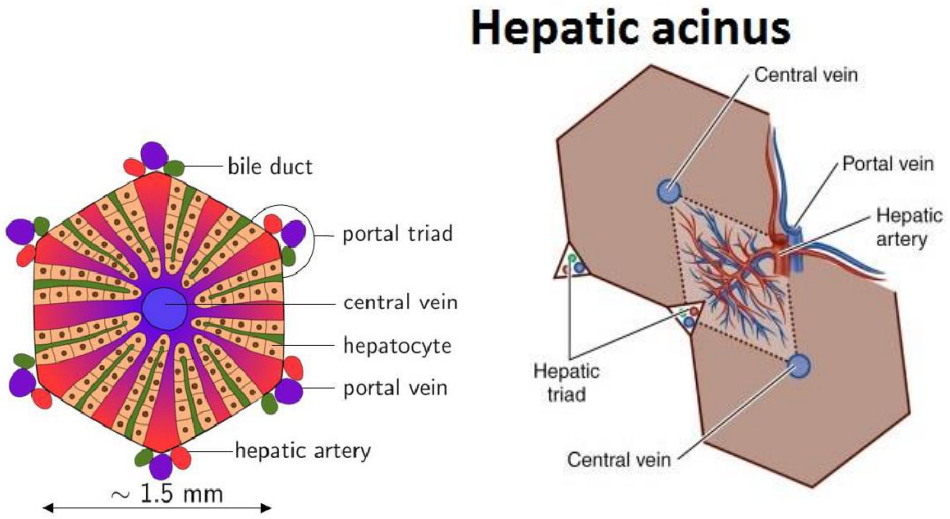

Figure 1.2 Hepatic lobule

Concepts of functional units of the liver. The hepatic lobule is roughly hexagonal in shape with the portal tract located at the angles of the hexagon and a hepatic vein located centrally. Central vein and portal triad belonging to the hepatic acinus are located at each angle of the rhombus (Adapted from Ref[19]).

1.2 Cell types in the liver

The total cell population in the liver can be divided into two; parenchymal cells and non-parenchymal cells.

1.2.1 Parenchymal cells - Hepatocytes

Hepatocytes which are the main functional cells of the liver, constitute of 65% of total liver cell population,[20] and 70-85% of liver volume.[21] They are irregular in shape and variable in dimensions depending on their age, location and the regenerative capacity. The hepatocytes are polarised cells which are joined to one another in anastomosing rows or plates. Each cell has three functional membrane domains; the basolateral domain, canalicular and the lateral domain with each domain having distinct functions.[22] The hepatocytes have abundant rough and smooth endoplasmic reticulum (ER) , reflecting the fact that they execute most of the liver's synthetic, endocrine and metabolic functions.

1.2.2 Sinusoidal endothelial cells (SEC)

Sinusoidal endothelial cells (SECs) constitute the surfaces of the sinusoids, also called endothelium, or endothelial lining. They differ from the endothelial cells present elsewhere in the body, by having open pores or fenestrations within and between them. A group of fenestrate acts as a dynamic filter, which allows free exchange of macromolecules between sinusoidal blood and hepatocytes and protects the hepatocyte from the trauma of passing blood flow. SECs have other important roles, including endocytosis/clearance of endotoxin, bacteria and other compounds, as well as regulation of inflammation and leukocyte recruitment.[23]

1.2.3 Kupffer cells (KC)

Kupffer cells are resident macrophages in the liver and constitute of up to 15% of the cells in the liver.[15] They lie within the walls of liver sinusoids, in between or on top of endothelial cells but are capable of penetrating the endothelial barrier. These cytoplasmic extensions allow direct cell contact with hepatocytes facilitating their signalling function. These cells form a part of the reticuloendothelial system (Fig. 1.3).

Kupffer cells are important in responding to the local changes. The role of Kupffer cells in mediating signalling may have led to alternate roles as damage mediator versus protector.[24] Protective roles include the modulation of immune responses via antigen presentation and suppression of cell activation and proliferation of T-cells, and immune surveillance of the host and regulation of hepatic physiological homeostasis. However, activated KCs can be a damage mediator as they produce many cytokines and release them into the local environment. These cytokines are capable of modulating the metabolism behaviour and integrity of other liver cell types, including hepatocytes which can aggravate liver damage

1.2.4 Hepatic stellate cells (HSC)

Hepatic stellate cells (HSCs) make up 5-8% of cells in the normal liver and are located in the space of Disse.[25] These cells were previously known as lipocytes, Ito cells or perisinusoidal cells. Morphologically, they are characterised by long cytoplasmic

extensions or processes allowing for the cell signalling with a large number of cells, including other HSCs, hepatocytes, endothelial cells and nerve endings.

HSCs are quiescent under normal physiology, with a cytoplasm containing lipid droplets rich in vitamin A playing an important role in vitamin A storage and homeostasis.[26] These cells are not clearly distinguishable in routine histological sections, but can be identified under electron microscope. However, there are other markers for identifying these cells, including cytoskeletal proteins.[27,28] α-smooth muscle actin (α-SMA) is often used as a marker for HSCs which is expressed on activated cells.[29]

There is evidence to suggest that HSCs play an important role in liver development and regeneration through the hepatocyte mitogen, hepatocyte growth factor (HGF). These growth factors provide the necessary signalling to neighbouring cells for cell division and transformation. Another major function is immunoregulation, with HSCs being capable of secreting several chemokines including monocyte chemoattractant protein-1 (MCP-1). They also appear to be involved in the regulation of sinusoidal vascular tone.[30] In response to tissue injury, the HSCs undergo a dramatic phenotypic change and transdifferentiate into myofibroblast-like cells (activated HSCs) that produce ECM.[31]

1.2.5 Cholangiocytes

Cholangiocytes are cuboidal epithelial cells that line the intrahepatic biliary ductules and canals of Hering. They are also referred to as bile duct cells and bile duct epithelial cells**.** The major function of cholangiocytes is to regulate ductal bile secretion.[32] The other functions include absorption and secretion of water, organic anions and cations, lipids and electrolytes and regulate localised immune responses by interacting with immune cells through expression of adhesion molecules and secretion of cytokines.[33] It has been shown that under pathological conditions these cells may be involved in liver fibrosis via epithelial-to-mesenchymal (ETM) transition suggesting that this could be possible mechanism that contributes to chronic cholestatic liver disease.

1.2.6 Hepatic dendritic cells (DC)

Hepatic dendritic cells (DCs) constitute less than 1% of the nonparenchymal cells in the liver and are found in the periportal and pericentral space. DCs are derived from hematopoietic progenitor cells in the bone marrow.[34] Although these are antigen presenting cells, they are poor initiators of immunity in a normal liver, but enhance the immunogenicity upon liver injury such as fibrosis.[35] They can internalise antigen by phagocytosis, receptor mediated endocytosis, or pinocytosis. Like any other DC in other peripheral sites, they are able to efficiently capture, process, and transport antigen to regional lymphoid tissues.[36] In 2009, Connolly et al showed that DCs govern the upregulation of numerous inflammatory mediators by activation of neighbouring cell types and crosstalk with HSCs.[35]

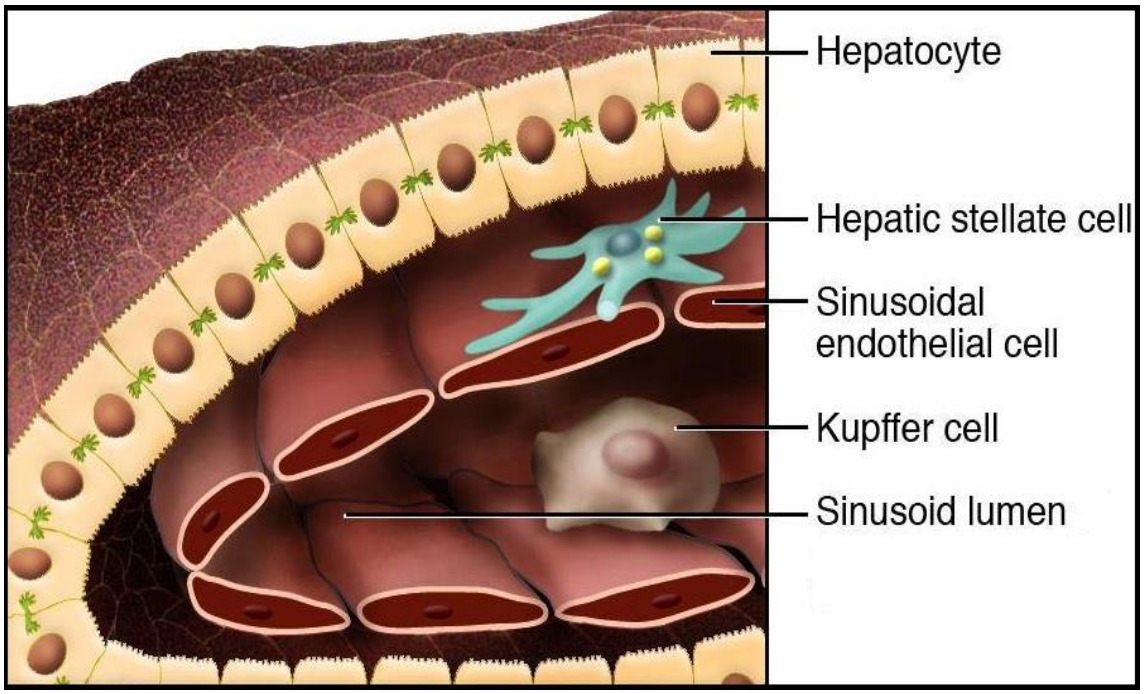

Figure 1.3 Cell types in the liver

Different cell types located differently according to their function in the liver (Adapted from Ref[37] &[38])

1.3 Extra cellular matrix (ECM)

1.3.1 Molecular composition of the ECM

ECM is a 3-dimensional scaffold mainly produced by HSCs which determines the shape of the cell and defines its microenvironment. It's a mesh of proteins and protein components that constitutes less than 3% of relative area[39] and approximately 0.5% of the liver weight.[40] There are 10 types of matrix proteins found in the liver and, the predominant forms of collagen are types I (36%) and type III (36%) in normal liver, 2) structural glycoproteins (fibronectin, laminin, nidogen/entactin, tenascin, osteopontin), 3) proteoglycans (heparin sulphate, etc.) and 4) free glycosaminoglycan hyaluronan.

1.3.2 Function of ECM

The primary function of ECM is to provide a scaffold that maintains the structure of the tissue. However, emerging evidence suggests that in addition to this mechanical support, ECM is now considered as an active component of the liver that can sustain inflammation and fibrosis by its direct signals to cells, i.e. it controls cell phenotype through ECM-cell interactions mediated by receptors and in addition by providing potent signalling fragments. It also serves as a storage site for multiple soluble cytokines and growth factors.[41]

1.3.3 Sources of ECM

Hepatic stellate cells are the major cell type that is responsible for the deposition of ECM in liver, both under normal circumstances and in pathological conditions. Other cell types such as mesenchymal cells and epithelial cells also may play a role in fibrogenesis (Fig. 1.4). There is evidence from studies suggesting that portal mesenchymal cells,[42] bone marrow derived cells[43] and epithelial cells (hepatocytes and cholangiocytes) through the process of ETM transition contribute to the fibrogenesis. The contribution of these different cell populations to fibrogenesis may vary depending on the nature of the underlying liver injury.

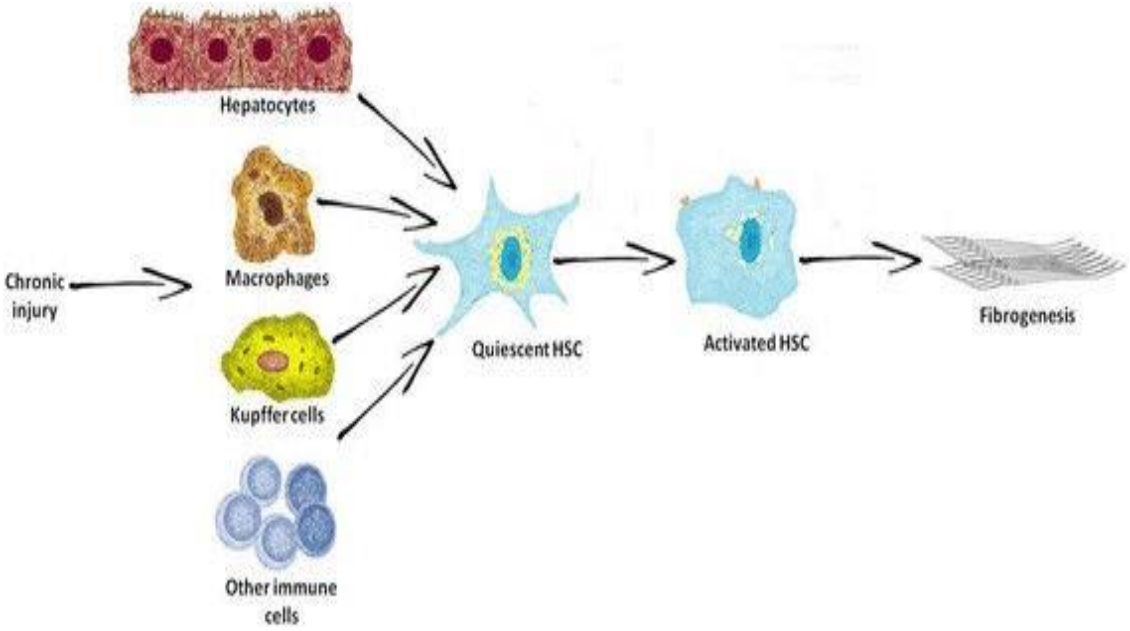

Figure 1.4 Sources of ECM

HSCs are the major cell type contribute to ECM deposition following activation by various other signals (Adapted from Ref[44]).

1.3.4 ECM in liver pathologies

There is constant turnover and remodelling of the ECM with both tissue forming and tissue degradation. A balance between these two processes keeps the quantity and quality of matrix maintained. Fibrosis is a condition with accelerated ECM turnover resulting in increased pathological protein deposition and altered matrix metalloproteinases (MMPs) expression.[45] Activation of HSCs (into myofibroblast like cells) due to tissue injury and inflammation disrupts the normal pattern of ECM leading to deposition of excess ECM. It primarily acts as a wound healing reaction, however, with continuous inflammatory insult excess ECM becomes dominated by fibrillary collagen I and collagen III which generates scar tissue eventually.

1.3.5 Resolution of ECM

Resolution of ECM can be carried out by enzymes, especially, matrix metalloproteinases (MMPs). Different MMPs have specific substrates, and MMP-1 is the main enzyme responsible for degradation of type I collagen, the most abundant form of collagen in hepatic fibrosis. The activity of MMPs is regulated by other enzymes, i.e. MMPs can be activated by factors including membrane-type 1 matrix metalloproteinase (MT1-MMP) or plasmin and inhibited by a family of molecules known as TIMPs (tissue inhibitors of metalloproteinases).[46] Hence, ECM quantity in a system, reflects relative amounts of activated MMPs and their inhibitor TIMPs.

1.4 Chronic liver diseases

There are a large range of chronic liver diseases some of which are discussed below, which can lead to liver fibrosis. Fibrogenesis leads to cirrhosis, a condition which is characterised by the loss of functional parenchymal cells with increased deposition of scar tissue, resulting in distorting of liver structure and the development of parenchymal regenerative nodules. Once cirrhosis is established, it may progress to hepatocellular carcinoma (HCC) and patients with both cirrhosis and HCC have reduced life expectancy and significant morbidity. Therapeutic options for these conditions are limited apart from liver transplant.

1.4.1 Alcoholic liver disease (ALD)

Alcoholic liver disease (ALD) may be the oldest form of liver injury known to us and remains a major cause of liver diseases worldwide. In Australia, 6825 deaths due to ALD were estimated to occur from 1992 to 2001.[47] ALD ranges from simple steatosis to cirrhosis.[48] The risk of developing cirrhosis increases with the ingestion of >60-80 g/day of alcohol for 10 years or longer in men, and >20 g/day in women[49] and mortality is significantly correlated with alcohol consumption.[50] Other factors such as type of alcohol, ethnicity, obesity, iron overload, concomitant infection with viral hepatitis, and genetic factors may affect the severity. The diagnosis of ALD is based on liver biopsy and history of significant alcohol intake. Biochemical tests are less sensitive for the

screening.[51] Long term management of the disease mainly involves abstinence rehabilitation and nutritional therapy.

1.4.2 Viral hepatitis

A collective group of viruses, which can cause liver diseases are called hepatitis viruses. There are six types which can infect humans, Hepatitis A, B, C, D, E and GB viruses.[52] Hepatitis B (HBV) and C (HCV), both transmitted parentally are the most common in Australia, with a prevalence of 1.1% HCV in 2002[53] and 1% HBV in 2012 (Department of Health, Australia). Age (>40-55 years), male sex, HIV co-infection and other liver diseases may accelerate the disease progression[54] and lead to decompensated cirrhosis or hepatocellular carcinoma and death. The initial management includes a complete history and physical examination to assess for signs of cirrhosis, alcohol and metabolic risk factors. Even though multiple highly effective drug treatments have been approved, prevention remains the cornerstone of Australia's response to viral hepatitis.[55]

1.4.3 Hereditary Haemochromatosis (HFE)

The prevalence of HFE was 0.36% in Australia in 1990.[56] This is also known as 'iron storage disease' due to iron overload in parenchymal cells in major organs such as liver, heart and pancreas, due to genetic mutations.[57] There are many complications associated with HFE including hepatomegaly, cirrhosis or hepatocellular carcinoma.[58] Therapeutic management involves venesection mainly, with rarely used erythocytapheresis and iron chelation.[59]

1.4.4 Primary Sclerosing Cholangitis (PSC)

Primary Sclerosing Cholangitis is a rare disease with a low prevalence (4-16/100,000) in adults[60] with estimated 872 cases in 2012, in Australia. A broad range of abnormalities, with narrowing and obstruction of intra- and extra-hepatic bile ducts occur in PSC.[61] Even though the aetiology remains unclear, the genetic background seems to play a significant role in global distribution of the disease.[62] Liver transplantation is the only established

treatment on PSC. Antibiotic and antifibrotic agents have shown beneficial effects in some studies,[63] although the mechanism is unclear.

1.4.5 Primary Biliary Cholangitis (PBC)

The prevalence of PBC was 51 cases per million in 2004 in Australia.[64] It is an autoimmune liver disease characterized by biliary destruction, progressive cholestasis, and potentially liver cirrhosis. Serologically, PBC is characterized by presence of antimitochondrial antibodies, which are present in 90–95 % of patients.
Ursodeoxycholic acid was the only accepted therapy until obeticholic acid received FDA approval recently. However, like PSC, the ultimate treatment for end-stage PBC is liver transplantation.[65]

1.4.6 Non-alcoholic Fatty Liver Disease (NAFLD)

This will be discussed in detail in section 1.6 of this thesis.

1.5 Pathophysiology of liver diseases

1.5.1 Fibrosis

As mentioned above, fibrosis is the excessive accumulation of extracellular matrix proteins including collagens that occurs in most types of chronic liver diseases. It is an essential wound healing response to repeated injury from a wide variety of aetiologies. Regardless of the stimuli, the most advanced stage of fibrosis, cirrhosis is same. In most of diseases, it takes up to 15-20 years for cirrhosis to develop.[37]

1.5.1.1 Histological definition

The degree and the pattern of liver fibrosis is one of the most important diagnostic and prognostic assessments in chronic liver disease. Liver biopsy related histological assessment is recognised as the best standard for the evaluation of fibrosis. It provides

information on fibrosis, inflammation, necrosis and steatosis.[66] There have been several scoring systems introduced by a number of investigators.[67] However, most current studies use well validated Metavir score system, comprised of five progressive stages; F0, normal; F1, portal fibrosis; F2, few fibrotic septae; F3, numerous septae and bridging fibrosis; and F4, cirrhosis (Fig. 1.5A).[68]

Different patterns of the deposition of fibres have been observed depending on the aetiology. For example, in chronic viral hepatitis and chronic cholestatic disorders, the fibrotic tissue is initially located around portal tracts, causing bridging fibrosis. In alcohol-induced liver disease, ECM deposited in the space of Disse, pericentral and perisinusoidal areas, giving a 'chicken-wire' pattern.[69] Biliary fibrosis incorporates the proliferation of bile ductules and periductular myofibroblasts, which leads to the formation of portal-portal fibrotic septa surrounding liver nodules. Conditions that alter venous outflow are the main cause of centrilobular fibrosis, which is characterized by central-central fibrotic septa. In comparison, NASH histology show a great heterogeneity depending on age, but is predominantly centrilobular giving a river-delta pattern.[70]

(A)

Metavir score system	Fibrosis stage
F0	No fibrosis can be detected
F1	Fibrosis exists with expansion of portal zones
F2	Fibrosis exists with expansion of most portal zones, and occasional bridging
F3	Fibrosis exists with expansion of most portal zones, marked bridging, and occasional modules
F4	Presence of cirrhosis

(B)

Appearance	Ishak stage: Categorical description	Ishak stage: Categorical assignment	Fibrosis measurement*
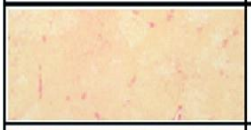	No fibrosis (normal)	0	1.9%
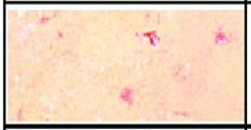	Fibrous expansion of some portal areas ± short fibrous septa	1	3.0%
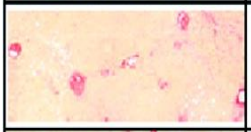	Fibrous expansion of most portal areas ± short fibrous septa	2	3.6%
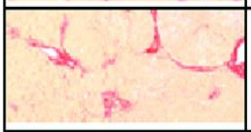	Fibrous expansion of most portal areas with occasional portal to portal (P-P) bridging	3	6.5%
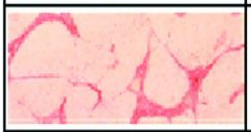	Fibrous expansion of portal areas with marked bridging (portal to portal (P-P) as well as portal to central (P-C))	4	13.7%
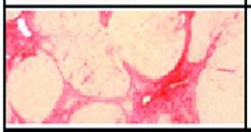	Marked bridging (P-P and/or P-C), with occasional nodules (incomplete cirrhosis)	5	24.3%
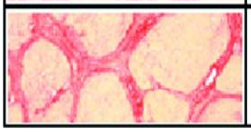	Cirrhosis, probable or definite	6	27.8%

Figure 1.5 Fibrosis score systems

(A) Proportion (%) of area of illustrated section showing sirius red staining for collagen (collagen proportionate area) (Adapted from Ref[67])

(B) Fibrosis stage according to Metavir score system (Adapted from Ref[71])

1.5.1.2 Pathogenesis of fibrosis

Liver parenchymal hepatocytes regenerate and replace necrotic and apoptotic cells after an acute injury with an inflammatory response and a limited ECM deposition. It is a complex, dynamic process in which deposited fibres are removed by fibrolytic enzymes. However, if the injury persists, the dynamic balance is tipped in favour of matrix accumulation, eventually the liver regeneration fails, and hepatocytes are substituted with abundant ECM, including fibrillar collagen. As disease advances, fibrosis progresses

from collagen bands to bridging fibrosis to cirrhosis.[37] Overall, the cirrhotic liver contains approximately six times more ECM overall than normal liver.[72]

Both the quality and quantity of ECM is largely altered during fibrogenesis. In a normal liver, the sub endothelial space of Disse separates hepatocytes from the sinusoidal endothelium and contains a low-density, or 'basement membrane-like matrix'. It contains a defined lattice-like meshwork, mainly composed of collagens IV and VI, and other proteins such as collagen I, hyaluronan, undulin, elastin, and laminin. Its function is to provide cellular support while allowing unimpeded transport of solutes and growth factors.[68] During liver injury, this matrix is disrupted and replaced with fibrillar collagens including collagen I, III and IV. Although all three types of collagens are increased, type I increases most and its ratio to types III and IV therefore increases.[73] Hyaluronan is increased more than eightfold,[74] accompanied by increases in other minor proteins.[75]

These quantitative and qualitative changes in ECM composition alter the matrix microenvironment and create a functional and physical impediment to the bidirectional flow of plasma between sinusoidal lumen and hepatocytes.[39] After injury, ECM not only modulates the activation and proliferation of HSC and angiogenesis, but also provides signals for sinusoidal endothelial cells and hepatocytes. With progressive injury, ECM spurs link the vascular structures, ultimately resulting in the architecturally abnormal nodules that characterise cirrhosis.[76]

1.5.1.3 Role of hepatic stellate cells (HSCs)

There is overwhelming evidence that activated HSCs are the major producers of the fibrotic neomatrix, although other cells and processes can make significant contributions.[77] Activated HSCs produce a wide variety of collagenous and non-collagenous ECM proteins upon wound healing.[76] Activation of HSCs consist of two steps; early events called initiation and followed by perpetuation.[26]

Initiation: Initiation is also called the "pre-inflammatory stage" referring to the early changes in gene expression and phenotypical changes of HSCs, when exposed to the various cytokines and stimuli including the interaction of other cells as well. Death of hepatocytes following an injury releases cellular contents such as DNA and reactive

oxygen species (ROS) which promotes HSC initiation. In addition to injured hepatocytes, hepatic macrophages, endothelial cells, and lymphocytes also drive HSC activation. The dead cells can upregulate the expression of pro-inflammatory factors secreted by Kupffer cells.

Perpetuation: Perpetuation is the next stage of stellate cell activation and, it involves at least seven discrete changes in cell behaviour: proliferation, chemotaxis, fibrogenesis, contractility, matrix degradation, retinoid loss, and white blood cell chemoattractant/cytokine release.[26] Platelet derived growth factor (PDGF),[78] vascular endothelial cell growth factor (VEGF), thrombin and its receptor, epidermal growth factor (EGF), transforming growth factor α (TGF-α), keratinocyte growth factor and fibroblast growth factor (FGF) have been studied in perpetuation.[79] This increase in both the cell numbers and matrix production per cell, results in fibrogenesis.[80] The best-studied component of hepatic scar is collagen type I and the most potent stimulus is transforming growth factor beta1 (TGF-β1). Signals downstream of TGF-β1 include a family of bifunctional molecules known as Smads. Connective tissue growth factor (CTGF/CCN2) is also another potent fibrogenic signal.[81]

Contractility of HSCs may be a major determinant of early and late increases in portal resistance during liver fibrosis. Large number of HSCs impede portal blood flow by constricting individual sinusoids and by contracting the cirrhotic liver. Endothelin-1,nitric oxide[82] and angiotensin II[83] are major counter regulators controlling stellate cell contractility, hence regulators of local microcirculation. As stellate cells activate, the expression of the cytoskeletal protein α-SMA is increased, which confers increased contractile potential.[29] ECM degradation and remodelling is a key event in fibrosis. The matrix remodelling requires matrix-metalloproteinases, and HSCs are the principal source of most of these proteinases. Studies have suggested that stellate cells contain most, if not all, of the molecules necessary to either activate or inhibit metalloproteinases.[84]

Resolution: Despite the earlier belief was that liver fibrosis is irreversible, emerging evidence from biliary obstruction,[85] hepatitis B and C,[86,87] alcoholic liver disease,[88] autoimmune hepatitis[89] and non-alcoholic steatohepatitis (NASH)[90] suggests that even advanced liver fibrosis is potentially reversible. Natural killer (NK) cells can induce

apoptosis of HSCs.[91] In non-recovering liver fibrosis, activated HSCs might persist as a result of a "memory" effect which either promotes HSC activation or protect them from apoptotic stimuli.[76]

1.5.2 Portal hypertension (PHT)

Portal hypertension is the main complication of cirrhosis characterized by hepatic venous pressure gradient (HVPG) of 10 mmHg or greater.[92] It initially results from increased intrahepatic vascular resistance to portal inflow[93] and later, an increase in portal blood flow resulting from splanchnic vasodilatation.[83,94] It can cause the development of ascites and some other syndromes.[95]

1.6 Non-alcoholic fatty liver disease (NAFLD) and its pathogenesis

1.6.1 Introduction

NAFLD is an emerging medical problem worldwide, with a gradually increasing prevalence. It is the most prevalent liver disease in the world (25.24%) and in Australia (<40% of adults over 50 years) (GESA, 2012). NAFLD is defined as either excessive fat accumulation with more than 5% of hepatocytes containing visible intracellular triglycerides or steatosis affecting at least 5% of the liver volume or weight in patients consuming less than 30 g of alcohol per day for men and less than 20 g of alcohol per day for women.[96] The main risk factors for developing NAFLD are central obesity, type 2 diabetes and elements of the metabolic syndrome.[4,97]

1.6.2 Defined by histology

The non-alcoholic form of fatty liver was first reported by Ludwig et al.[98] It is classified into two categories. Simple steatosis, in which only hepatocellular steatosis is observed, which generally follows a benign clinical course. However, there is second and more severe form, non-alcoholic steatohepatitis (NASH), in which both necro inflammatory

reactions and hepatocellular steatosis occur. This can be present in one third of NAFLD cases, and is a progressive disease that can advance to liver cirrhosis and HCC.[99] However, the risk factors for this progression remain unclear.[4]

Histological evaluation and pathological assessment remain the gold standard for diagnosis of NAFLD, despite the limitations of the liver biopsies due to sampling errors and differences in the left and right lobes.[100,101] In 2002, the NASH clinical research network (NASH CRN) designed a NAFLD activity score (NAS) which can be used for the full spectrum of NAFLD in three arms; steatosis (0-3), lobular inflammation (0-3), and ballooning (0-2) (Table 1.1). In the same year, the American Association for the Study of Liver Diseases (AASLD) summarised histopathological abnormalities of NASH. In this report, steatosis, lobular inflammation and hepatocellular ballooning were identified as the necessary components for the diagnosis of NASH. Fibrosis is not necessarily a component for the diagnosis of NASH, although it is usually present. Currently, most pathologists use these criteria, although a complete consensus has not been reached.

Steatosis should be > 5% to be considered as clinically significant NAFLD[102] and is typically macrovascular.[103] Early in the disease course, the steatosis is most prominent in zone 3, but with progression of disease or severity, the steatosis may spread evenly throughout the hepatic acinus or become irregularly distributed.[104]

The hepatocellular injury seen in NASH can range from ballooning, degeneration and apoptosis to less-well characterized reactive changes. A mixture of infiltrating lymphocytes and scattered Kupffer cells are distributed in lobules. Brunt et al concluded that the diagnosis of definite NASH or the absence of NASH does not always correlate with the threshold values of NAS. Moreover, Kleiner et al developed a semi quantitative scoring system and validated using only two stains (haematoxylin & xylene and Masson trichrome stains) and they used “borderline NASH” when the histological patterns are not sufficient to make a diagnosis.[105]

Paediatric NAFLD exhibits different histological features than adult NAFLD and serum diagnosis (alanine aminotransferase) does not reflect the severity of the disease.[106] It can develop to advanced fibrosis without the typical features of NASH.[107] A different diagnostic categorization has been proposed in a paediatric study.[108]

Table 1.1 NAFLD activity score (NAS)

Item	Definition	Score
Steatosis	<5%	0
	5%-33%	1
	>33%-66%	2
	>66%	3
Lobular inflammation	No foci	0
	<2foci per x200 field	1
	2-4 foci per x200 field	2
	>4 foci per x200 field	3
Ballooning	None	0
	Few balloon cells	1
	Many cells	2

1.6. 3 Two hit hypothesis of NAFLD pathogenesis

NAFLD is the hepatic manifestation of metabolic syndrome and the presence and severity are closely related to insulin resistance (IR). However, the relationship between insulin resistance and NAFLD is complex and the pathogenic mechanisms involved in mediating liver damage in this setting are still not fully understood. In 1998, Day and James proposed a mechanism to explain why some NAFLD patients never progress to NASH or more severe forms and they called this model ‘two hit hypotheses. In this model, they described the deposition of fat in the liver or simple steatosis as the first hit, where the development of steatosis into steatohepatitis requires the involvement of other factors. There is a broad range of these factors which can act as the ‘second hit’.[109]

1.6.3.1 Genetic factors

Genetic composition inherited by an individual plays an important role in individual disease onset or the severity. This is supported by clinical studies which have shown familial clustering of NAFLD and the difference of the prevalence of NAFLD in different racial and ethnic groups.[110] Studies have focused on genetic factors such as mutations, especially single nucleotide polymorphisms (SNPs) in both classical and novel contexts such as genome-wide association studies (GWAS).[111] For example, Patatin-like phosholipase domain-containing 3 gene variant I 148M (PNPLA3) has been clearly identified as a major player in NAFLD progression.[112] Recently, transmembrane 6 superfamily member 2 E167K variant has been identified as a relevant contributor in progressive NASH.[113]

PNPLA3 appears to function as an acylglycerol hydrolase and as a lysophosphatidic acid acetyltransferase. It correlates with increased hepatic lipid content and predisposes to steatohepatitis, cirrhosis and HCC.[114] Overexpression of the I 148M variant of PNPLA3 results in a loss of function mutation which promotes hepatic intracellular lipid accumulation by reducing the lipidation of VLDL.[115] Multiple other genetic changes have been identified that correlate with progressive NAFLD. These include possible genes involved with oxidative stress, glucokinase regulatory protein, ectoenzyme nucleotide pyrophosphate phosphodiesterase 1 and insulin receptor substrate-1.[116,117] Furthermore, numerous case-control studies have been performed to elucidate the potential role of candidate genes in the pathogenesis and progression of fatty liver, although findings are sometimes contradictory.[118]

1.6.3.2 Epigenetic factors

Clinical studies investigating epigenetic reprogramming are just beginning to emerge.[119] Although most epigenetic irregularities are transient, some are heritable[120] and epigenetic modifiers are involved in lipid metabolism, ER stress, mitochondrial damage, oxidative stress, and inflammation which can induce NAFLD.[121] The most described epigenetic modifications related to NAFLD are DNA methylation and microRNAs.[122]

DNA methylation: DNA methylation is the addition of a methyl group on cytosine with guanine as the next nucleotide, also known as CpG sites or islands. The effects of DNA methylation have been reported on HSC activation[123], susceptibility to NASH development[124] and severity of NASH.[125,126] Furthermore, HSC activation has been inhibited both *in vitro* and *in vivo* by small molecule epigenetic inhibitors that can alter DNA methylation and histone modifications.[127]

Micro RNA (miRNA): Micro RNAs are small, highly conserved noncoding RNAs of approximately 18–25 nucleotides in length that modulate translation and transcription of target genes. These miRNAs are stable in body fluids and resistance to RNases, therefore, suggested as suitable biomarkers in diagnosis of liver diseases.[128] miR-34a, miR-146b and miR-335 are some miRNAs associated with NAFLD parameters,[129] while miR-122 is the most abundant.[123]

1.6.3.3 Reactive Oxygen Species (ROS) generation and oxidative stress

Impaired fat homeostasis in the liver leads to an overproduction of reactive oxygen species (ROS) via a number of mechanisms involving mitochondria, peroxisomes, cytochrome P-450, reduced nicotinamide adenine dinucleotide phosphate oxidase (NADPH), cyclooxygenase and lipoxygenase[130] which leads to oxidative stress generating free reactive radicals. In addition, fat oxidation in the liver also contributes to oxidative stress and reduction of antioxidants triggers NASH by lipid peroxidation.[131] Oxidative stress may cause damage at a cellular level, such as membrane lipid peroxidation, cell degeneration and necrosis, cell death by apoptotic proinflammatory cytokine expression, HSC activation and fibrogenesis.[132]

It has been shown that increased mitochondrial ROS generation is associated with impaired activity of mitochondrial respiratory chain which is reported to act as a second hit in the development of NAFLD in rodents[133,134] and in human patients.[135] It has also been reported that increased activity of membrane bound NADPH oxidases or NOX are equally important in ROS generation and oxidative stress in the liver.[136] Furthermore, NASH livers are reported to have more than 40% ultrastructural mitochondrial alterations and impaired hepatic adenosine 5′-triphosphate (ATP) synthesis.[137] Moreover, NASH is associated with impaired ATP generation capacity.[138] The decreased electron transport

chain reactions increase TNF-α expression, which then forms a positive loop, leading to a vicious cycle with worsening mitochondrial function.[139] These events enhance the lipid peroxidation in the liver which leads to liver cell injury, consequently to NASH and fibrosis together with increased cytokine secretion.

1.6.3.4 Adipokines

Adipose tissue was thought to be an inert energy storing tissue until leptin was discovered in 1994.[140] It is now recognized as a major and possibly the largest endocrine organ which, synthesizes and releases adipokines. Adipokines play a role in disease development,[141] but the relationship between the adipose communication network and NAFLD is complex.[142] Adiponectin and leptin are the two major adipokines associated with the development of NASH.[143] Adiponectin is a beneficial adipokine, identified in 1995[144] and it improves hepatic and peripheral insulin resistance and has anti-inflammatory and hepato-protective activities.[119] Leptin is suggested to participate in both the first and second hit of NASH development by contributing to the development of insulin resistance and activating HSCs.[145] Resistin,[146] chemerin[147] and visfatin[143] are some other adipokines which play a role in NAFLD.

1.6.3.5 Microbiome

There is emerging evidence suggesting the dysregulation of the microbiota (known as dysbiosis) contributes to the development of NAFLD and the metabolic syndrome.[148] This is endorsed by the fact that 70% of hepatic blood supply is from intestine through the portal vein, and therefore, liver is the first organ to expose to gut derived toxins such as bacteria and bacterial by-products.[149]

SCFA synthesis and energy harvest: Some bacteria use short chain fatty acids (SCFA) as substrates for glucose synthesis (intestinal gluconeogenesis), inducing a signal to the brain that influences food intake and affects satiety, thereby altering the food intake[150] and contributing to NAFLD progression.[151]

Gut permeability, inflammation and immune imbalance: Alterations in intestinal permeability and tight junctions in the gut has been reported in NAFLD patients.[152,153] Leaky gut allows the translocation of lipopolysaccharides (LPS)[154] and bacterial derived products into the liver and systemic circulation.[155,156] These translocated substances act mainly via the toll-like-receptor-4 (TLR-4), a prominent receptor involved in innate immune responses, which triggers a signalling cascade, leading to inflammation, suggesting gut barrier malfunction may act as a promotor of NASH.[157,158]

Choline and methylamine metabolism: Diets deficient in choline, which is an essential phospholipid cell membrane component[159] lead to increased hepatic steatosis and fibrosis.[136] The intestinal microbiota converts dietary choline into toxic methylamine which can induce hepatic inflammation.[160] Also, the intestinal microbiota converts dietary phosphatidylcholine to choline and to hepatotoxic methylamine. Reduced availability of dietary choline inhibits VLDL excretion from the liver, allowing the accumulation of triglycerides causing steatosis. In addition, bacterial biomarkers associated with fatty liver have been identified that respond to choline deficient diet.[161]

Bile acid metabolism: Bile acids have antimicrobial activity[162] and reciprocally, bacteria are capable of modulating bile acid metabolism, thereby changing the composition of the bile acid pool. Bile acid receptor, FXR stimulation not only suppresses nuclear factor κβ (NF-κβ) resulting in decreased hepatic inflammation[163], but also regulates lipogenesis.[164] Moreover, bile acid receptor agonists are currently in clinical trials which have been shown to improve NASH.[165,166]

1.6.3.6 Dietary factors

Diet is an important contributor to the pathogenesis of many diseases. Both the daily energy intake[167] and per capita food consumption has been risen,[168] including significant modifications of diet composition, as well as of frequency and timing of energy and nutrients intake in the last 3 to 4 decades. NAFLD patients tend to have a dietary pattern characterized by a higher consumption of SFAs, cholesterol, and fructose, and lower ingestion of polyunsaturated fatty acids (PUFAs) and antioxidants (vitamin C and E).[169]

Carbohydrates/ Sugars: Carbohydrates, in particular sugars like fructose have been implicated in NAFLD pathogenesis. Even though a healthy diet must provide no more than 5% of total energy intake as simple sugars, currently, 13% of the American population consumes over 25% of their daily energy intake as simple sugar.[170] Results from both animal and clinical studies have confirmed that the sugar added to foods and beverages add considerable excess calories without any beneficial effects and may take place of other nutrients in the diet.[171] Clinical studies with NAFLD patients have shown the consumption of a high carbohydrate diet increases the risk factors for cardiovascular diseases and hepatic inflammation,[172] visceral adiposity and lipids in overweight subjects,[173] circulating insulin, thereby decreased hepatic insulin sensitivity, and elevates inflammation by inducing small intestinal bacterial over-growth (SIBO) and bacterial translocation resulted in concomitant increase in endotoxin levels in the portal vein.[174] This LPS can bind to receptor complexes present on Kupffer cells leading to activation of many harmful signalling pathways.[148]

In addition, genome-wide studies have identified several polymorphisms that contribute to increased liver fat accumulation, with some of these genes relating to dietary carbohydrate and sugar consumption.[175] Although, direct effects of fructose remain to be proven, NAFLD patients are recommended to have simple sugar restrictions in their diet.[176]

Fat/ saturated fatty acids (SFA)/ unsaturated fatty acids (UFA): Increased fat intake and the Western diets have been linked to IR, impaired postprandial lipid metabolism, and the development or progression of NAFLD.[177] Dietary SFA and dietary cholesterol interact synergistically to induce the metabolic and hepatic features of NASH in mice[178] and high-cholesterol diets (1%–2% w/w) have been reported to increase hepatocyte-free cholesterol accumulation in mitochondria and results in glutathione depletion, increased susceptibility to TNF-α and TNF receptor superfamily, member 6-mediated apoptosis, macrophages recruitment, and liver fibrosis.[179] Moreover, SFA enhances transcriptional activity in lipogenic genes, fatty acid synthase, and diacylglycerol acyltransferase and the expression of the unfolded protein response (UPR)-related components and caspase 3 activity, all elicited by ER stress.[180]

However, diets containing 8–10% SFA are likely to be beneficial, whereas extreme reductions in SFA (< 6%) may have deleterious effects on plasma lipid levels.[181] Both monounsaturated and polyunsaturated fatty acids (MUFA & PUFA) on the other hand, are beneficial for the health.[182]

Proteins: There are limited number of studies addressing the association between protein and NAFLD. These studies show beneficial effects in the pathogenesis or progression of NAFLD.[176,183] However, conclusive evidence is lacking to make a definitive statement regarding the effect of dietary protein on NAFLD.[177]

Micronutrients/metals/ antioxidants/ fibres and other food supplements: Deficiency of some nutrients such as choline,[136,184] iron,[185] copper[180] and vitamin D[186] has been shown to induce NAFLD.

1.6.4 Role of liver cell types in NAFLD

1.6.4.1 Kupffer cells

KCs constitute the largest liver tissue specific macrophages, representing 80–90% of all tissue macrophages in the body.[187] [188] They express adhesion molecules and secrete chemokines which can attract and retain non-resident cells such as neutrophils, natural killer T lymphocytes and blood monocyte-derived macrophages. Once KCs recognize an antigen, they engulf, ingest and eliminate solid particles and present antigens to attract cytotoxic and regulatory T cells, thereby contributing to adaptive immunity.[189] Hence, liver damage from KCs may either result from the inability to properly recognize and eliminate danger molecules or from excessive activation of cytotoxic mechanisms and failure to halt inflammation.[190] Emerging evidences confirms the hypothesis that KCs are involved in both initiation and progression of NAFLD.[191] In the early stages of the disease, hepatic macrophages expand rapidly and secrete cytokines and chemokines contributing to a paracrine activation of protective or apoptotic signalling pathways in hepatocytes and the recruitment of other immune cells.[192]

KCs hyper-react to LPS[193] attempting to prevent it spreading to the peripheral circulation. TLR-4[190] and CD-14[194] recognize LPS and signal to adaptor proteins leading to the

activation of NF-κβ and C-Jun N-terminal kinase (JNK).[195] Furthermore, they are involved in free fatty acid activated NF-κβ pathways[196] resulting in oxidative stress and ER stress[197] which triggers the progression of NAFLD dramatically. Rapid release of ROS in response to LPS and other microbial stimuli in KCs occurs through NOX-2 activation.[198] Imbalance in antioxidants and peroxide in KCs eventually drives the activation of fibrogenesis.[199]

KCs initiate insulin resistance (Duarte et al., 2015) by activating insulin receptor substrate 1 (IRS-1) and IRS-2 through the JNK pathway[200] and diminish uncoupling protein-2 (UCP2).[201]

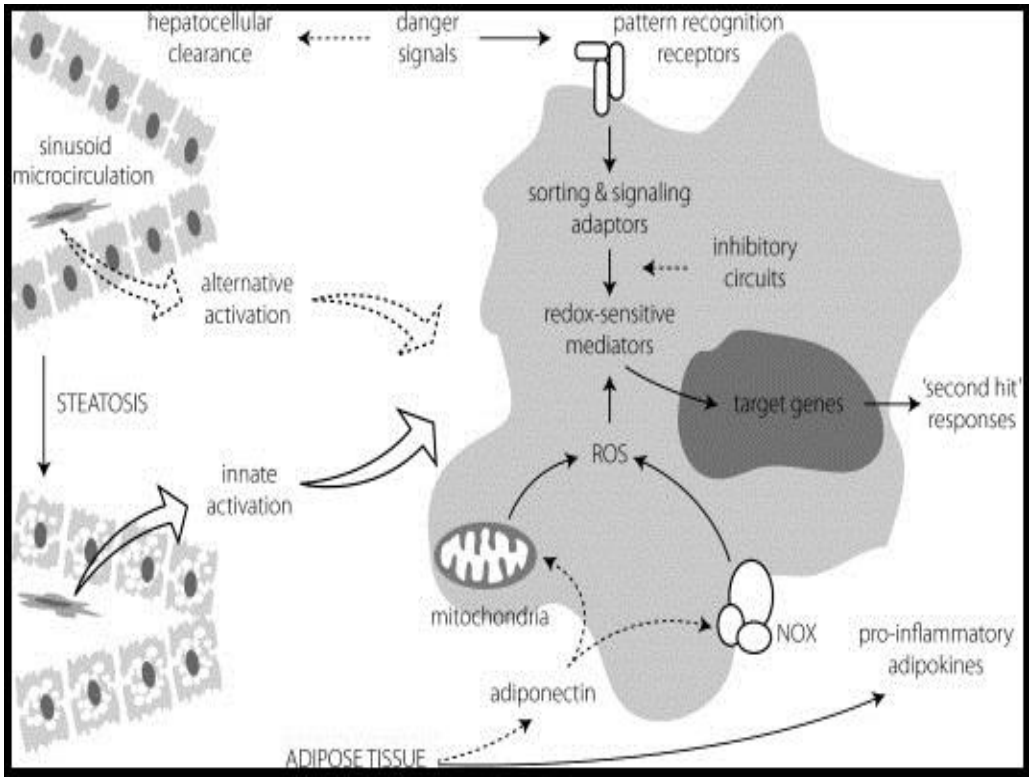

Figure 1.6 Schematic representation of dysfunctional activation of Kupffer cells in NAFLD

Pattern recognition receptors of KCs such as TLR-4 may be increasingly exposed to exogenous and endogenous danger signals (e.g., LPS, excess fatty acids, modified lipoproteins) via the portal circulation. Pattern recognition pathways may intensify due to altered sorting and signalling, impaired inhibitory circuits, or amplification of redox-sensitive signalling loops. Adipokine imbalance may contribute to these events including low adiponectin levels that fail to suppress intracellular ROS generation. Fat-laden

hepatocytes may compromise sinusoid microcirculation leading to entrapment of inflammatory cells. Finally, steatosis may shift away KCs from alternative activation. Solid lines: pro-inflammatory effects, dotted lines: anti-inflammatory mechanisms. Malfunction at one or more steps may promote 'second hit' responses, while cellular targeting of these checkpoints has the potential for identifying novel treatment strategies in NAFLD (Adapted from Ref[190]).

1.6.4.2 Hepatic stellate cells

The role of HSCs is linked primarily to NASH and fibrosis, rather than initial stages of NAFLD and have been discussed in detail in section 1.5.2.3.

1.6.4.3 Hepatocytes

Hepatocytes exert metabolic and detoxifying functions and prompt the acute phase response. The TLR-4 receptor found on the cell surface needed a high dose of LPS to become activated.[202] They also express TLR-2, CD-14 and myeloid differentiation-2 receptors which act in inflammatory conditions. These cells can clear LPS from the systemic circulation, through its uptake and release into the bile.[203] In NAFLD, hepatocytes accumulate a single large vacuole of lipid (mostly triglyceride) that almost fills the entire cell, displacing the nucleus to one side, which is called macrovesicular steatosis, enlargement of these cells then leads to hepatomegaly.[199]

1.6.4.4 Dendritic cells

Dendritic cells are immature and tolerogenic. However, in an environment of chronic inflammation, these cells are transformed to potent inducers of immune responses.[204] The mature proinflammatory DCs facilitate the deposition of monocytes, increase in IL-6 and TNF-α with the activation of HSCs.[34]

1.6.4.5 Sinusoidal endothelial cells

Sinusoidal endothelial cells injury appeared to be necessary for the activation of both KCs and HSCs in NAFLD, which in turn results in the perpetuation of fibrosis.[205] Another study suggested that the changes in SEC phenotype are one of crucial events in human NASH progression.[206] Moreover, endothelial cells subjected to microarray showed different profiles in rats induced NAFLD compared to control rats.[207]

1.6.4.6 Hepatic progenitor cells

Hepatic stem/progenitor cells constitute an adaptive response of the liver to oxidative stress and are activated during NAFLD and involves in ductular reaction correlated with progressive portal fibrosis.[208] Studies in both mice and humans have confirmed that PCs are activated when oxidative stress inhibits the regenerative capacity of more mature hepatocytes of NAFLD, suggesting that PC expansion is a component of the liver's adaptive response to oxidative stress.[209]

1.7 Advanced glycation end products

1.7.1 Introduction

There is accumulating evidence which suggests that in NAFLD, advanced glycation end products (AGEs) play a role as a 'second hit' that triggers progression from steatosis to NASH. Studies published by our laboratory showed that AGEs exacerbate liver injury in rodents with NAFLD by pathways which include ROS generation and lipid peroxidation.[210-212]

AGEs are a chemically heterogeneous and biologically active group of compounds. They are formed as a result of the non-enzymatic reaction between reducing-sugars with proteins, lipids and nucleic acids. This process was named as the 'Maillard reaction' after its first discovery in 1912, by a French biochemist Louis Camille Maillard.[213] Maillard noticed a characteristic yellow colour when proteins are heated in the presence of

reducing sugars. This process can be taken place inside the body (endogenous AGEs) or outside the body, mainly as a result of food processing (exogenous AGEs).

1.7.2 Structure and formation

The structure of AGEs are heterogenous in nature, depending on the reactive groups attending in the reaction. The Maillard reaction begins with nucleophilic addition reaction of the aldehyde group in a reducing sugar with the amino group in a protein to release a water molecule, producing early glycation products (Schiff base). This reaction is reversible, and the product may undergo hydrolysis again or further rearrange into more stable Amadori products. The rate of rearrangement of Schiff bases to Amadori products varies depending on the protein type, but, approximately one sixth of the hydrolysis reaction.[8]

Amadori products may undergo a further series of dehydration and rearrangements, forming advanced glycation end products (AGEs). This may include both oxidative and non-oxidative pathways, both being irreversible; therefore, AGEs are more stable and accumulate with time (Fig. 1.7).

The rate of formation of AGEs depending on various factors. Early glycation rate depends on the concentration of the reactants such as reducing sugars or proteins. It also depends on the life time of the protein; proteins with longer half-life tend to glycate more than a protein with a shorter life-time. The reaction can be catalysed in the presence of some transitional metal ions.[213]

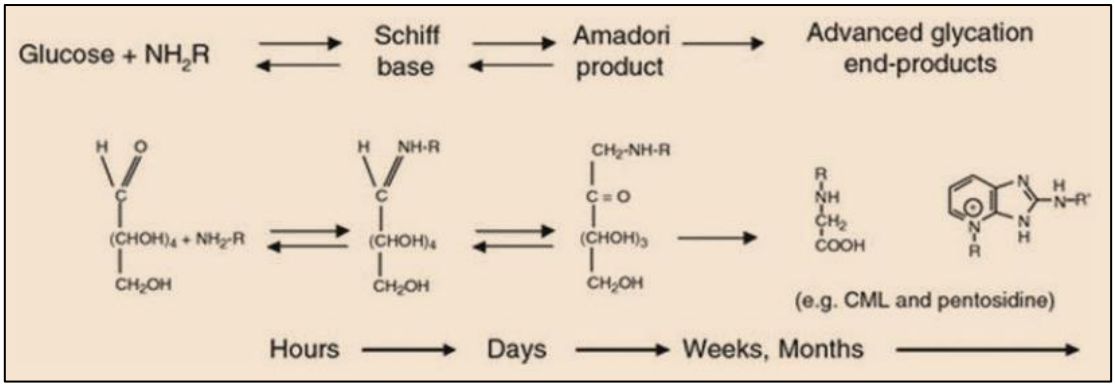

Figure 1.7 Formation of AGEs

Glucose nonenzymatically react with amino acids to form AGEs through a series of intermediates (Adapted from Ref[214]).

1.7.3 Reactive intermediate products

One important by-product of Maillard reaction is reactive carbonyl species (RCS) which are formed in each step of the reaction and are commonly known as α-dicarbonyls or oxoaldehydes.[215] These can be formed by either degradation of glucose or Schiff bases or non-oxidative hydrolysis/ rearrangement of Amadori products. Glyoxal, methylglyoxal, glycolaldehyde and 3-deoxyglucosone are some commonly found oxoaldehydes.[216]

There is a limited work has been done in controlling the generation of RCS in food processing. In 2014, Kokkinidou and Peterson have developed a quantitative method to monitor RSCs. Moreover, they have used some phenolic compounds (off-flavours) to reduce the RSC formation in pasteurised milk.[216] RSC generated during Maillard reaction can react with other available amino acid residues and AGEs in the media.[217] Moreover, the presence of protein- RCS is an excellent marker of oxidative stress.[218]

1.7.4 Endogenous AGEs

AGEs are formed at a low rate in healthy individuals.[219] However, the rate can be accelerated in certain conditions due to the high availability of reactants, especially sugars, for example, in subjects with diabetes[220] and in aging.

Glycaemic index (GI) is the scale that ranks foods according to how much they raise the blood glucose level after consumption[221] which depends on both the quantity and the quality (proportion of simple and complex carbohydrates) of carbohydrates present in food. Consumption of sugar-sweetened food has increased in the last couple of decades and is positively co-related to the metabolic syndrome,[222,223] dyslipidaemia and insulin resistance.[173,224] Food with high GI can result in elevated circulating glucose, acting as a substantial source of endogenous AGEs.[171] Moreover, low GI food lower the AGE levels in both animals and humans.[225-227] However, more work need to be done to confirm the association between the accumulation of AGEs in the body and the intake of high-GI foods.[228]

Diabetes can accelerate AGE formation due to hyperglycaemia. Elevated glucose concentration shifts the equilibrium towards the right facilitating the forward reaction of Schiff's base formation. A variety of diabetic complication such as atherosclerosis,

nephropathy, neuropathy and retinopathy can be exacerbated due to the involvement of AGEs.[213,220,229]

Oxidative stress can accelerate the glycation reaction.[230] It has been demonstrated that the AGEs can be generated by activating the myeloperoxidase pathway in neutrophils.[231] More importantly, the interaction of AGEs with its receptors can generate further oxidative stress forming a positive loop.[232] A study with healthy, non-diabetic twins showed that the correlation for the most common AGE marker, Nε-(carboxymethyl)lysine (CML) levels in serum were much higher in monozygotic compared with di-zygotic twins.[233] This suggests that the formation or accumulation of AGEs is influenced by genetic factors as well.

1.7.5 Exogenous AGEs

Although the formation of AGEs is usually endogenous, it can also be formed in the diet during preparation of food. Despite the bioavailability of orally ingested AGEs is as low as 10%,[234] emerging evidence demonstrates the deleterious effects of AGEs on health,[228] suggesting a significant proportion of dietary AGEs is absorbed by the gut. As mentioned above, the glycation reaction was first observed when reducing sugar was heated in the presence of amino acids demonstrating the heat treatment of food can cause non-enzymatic glycation, forming a characteristic golden-brown colour.

Temperature and time are two key factors that determine the rate and the extent of exogenous AGE formation. Other factors that influence the rate include, type of reactants, pH and the water activity.[235,236] Applying high temperatures, usually above 160^{o} C accelerate glycation whereas food cooked in watery environment (e.g. boiling and steaming) tend to have low levels of AGEs; i.e. the Western diet where dry heat is applied has a large amount of AGEs compared to the Asian diet where slow cooking is involved. The amount of AGEs produced during cooking varies as grilling/barbeque > oven frying > deep frying and broiling > roasting > boiling.[237] Microwaving does not increase AGE content dramatically, as it applies for a short time. Marination of food with vinegar prior processing significantly reduces glycation. Lemon juice has the same effects. Baking with sodium bicarbonate (baking soda) on the other hand, increases the pH of the mixture, enhancing the glycation associated browning.[238] Types of reactants present in the

glycation process also determine the rate. For example, pentose sugars are more reactive than hexoses and monosaccharides are more reactive than disaccharides.[239]

Table 1.2 shows AGE levels present in commonly consumed food. Although in this study AGE levels were measured by ELISA[237] it gives a general idea about the content of AGEs present in commonly consumed food.

Table 1.2 Advanced glycation end products (AGE) content of selected foods prepared by standard cooking methods

Food Item	AGEs (kU/g or /mL of food)
Butter	265
Olive oil	120
Mayonnaise	94
Cheese, American	87
Almonds, roasted	66.5
Chicken breast, fried_15 min	61
Beef, broiled_15 min	60
Chicken breast, broiled_15 min	58
Cheese, Brie	56
Tuna, broiled_10 min	51
Tofu, Broiled	41
Egg, fried	27
Beef, boiled_1 h	22
Egg yolk, boiled	12
Pancake, homemade	10
Tofu, Raw	8
Tuna, roasted_40 min	6
Enfamil (infant formula)	4.86
Bread, whole-wheat centre	0.54
Green Beans	0.18
Apple	0.13
Carrots	0.1
Milk, cow, whole	0.05
Milk, human, whole	0.05
Banana	0.01

(Adapted from Ref[237]).

Smoking is also considered as a source of exogenous AGEs.[213] Upon curing, tobacco products dry in the presence of sugar which can initiate the Maillard reaction. The AGE

species are volatilized during combustion and are inhaled. These glycotoxins (termed by Koschinsky et al in 1997) can then be absorbed through the lungs and conjugate with proteins. Studies have shown higher serum AGE levels in smokers than non-smokers[240] and especially in diabetic smokers, high AGE levels in arteries and ocular lens[241] have been found.

1.7.6 Metabolism of AGEs

The metabolism of AGEs in the body is not fully understood, despite several mechanisms having been proposed in number of organs. It is estimated that the daily average consumption of AGEs in New York city (USA) is 15000kU. Only 10% of this is absorbed through gut and about 30% excrete via urine.[234] The fate of the remaining percentage is unclear.

Studies conducted over the past few decades led to identification of a complex system of specific AGE receptors present in specific organs which are involved in AGE clearance. It is proposed that macrophages expressing AGE receptors can degrade larger AGE molecules into small soluble AGE peptides[242] which are and then cleared by kidneys.[243] Reduction in kidney function can cause accumulation of circulating AGE levels. Liver sinusoidal endothelial cells and Kupffer cells play an important role in clearing AGEs from the system[244] and this was supported by the finding of patients who have impaired hepatic function have higher AGE accumulation than healthy controls.[245]

1.7.7 AGEs in diseases

The accumulation of AGEs inside the body may results in activation of pro-inflammatory and pro-fibrotic pathways which lead to changes in ECM structure and function. This may be mediated through two pathways; 1) interaction with receptors, 2) independent of receptors-via forming crosslinks between molecules in the basement membrane.[246]

AGEs appear to contribute to a wide range of disease states acting through both mechanisms.[247] Most studied has been diabetes (animals/patients), as it can result in accelerated endogenous AGE formation, due to elevated sugar concentration. Increased accumulation of AGEs in serum have been linked to the development of nephropathy,

retinopathy, and coronary artery disease in patients with type 2 diabetes.[248] The formation and accumulation of AGEs have also been implicated in the pathogenesis of a number of seemingly disparate conditions.

The effects of AGEs on biological systems, independent of receptors, are mainly due to the formation of crosslinking during the process of AGE formation. Consequently, structural and functional properties of a protein can be significantly altered.[213] Crosslinks formed between protein backbones makes them less malleable and more resistant to proteolysis and this may lead to entrapment of proteins, lipoproteins and immunoglobulins.[249] A number of clinical studies have shown that this crosslinking can affect tissue structure and function.[250-252] Moreover, it is shown AGE adducts residing in vessel walls can directly inactivate nitric oxide mediated vasodilatation independent of its receptors.[253]

Renal dysfunction and diabetic nephropathy: Numerous studies have demonstrated the role of both dietary and endogenous AGEs in the development of renal diseases. High AGE diets were associated with exacerbated renal dysfunction in mice[254] and development of glomerular sclerosis and albuminuria in rats.[255] In addition to animal studies, there are numerous clinical studies that have demonstrate the engagement of AGEs in the pathogenesis of diabetic nephropathy.[256-260]

Cardiovascular diseases (CVD), atherosclerosis and cardiomyopathy: AGEs also appear to be involved in the development of other microvascular complications of diabetes.[261] Most of these effects appear to act through arterial crosslinks,[250] however it can also be due to receptor dependent pathways[262] or nitric oxide mediated pathways.[246,263] AGE/RAGE pathway plays a pivotal role in the pathophysiology of CVD in patients with chronic kidney disease.[264] Moreover, AGEs are suggested as a good biomarker to evaluate the association between diabetes and atherosclerotic disorders.[265]

Other diseases: Deleterious effects of AGEs have been studied in various other diseases including retinopathy and neuropathy. They also determines the effects of calorie restriction on oxidant stress, age related diseases and life span.[266] AGEs are a key player in skin aging[219] and development of retinopathy in patients with type 1 diabetes,[267] impaired wound healing,[268] development of neuropathy[269] and Alzheimer's disease .[270]

In the amyloid deposits found in patients with haemodialysis-associated amyloidosis, AGE-modified β2-Microglobulin is abundant.[243] They are involved in erectile dysfunction[271] which was managed to reverse with AGE inhibitors,[272,273] early ovarian aging[274] and might contribute to the polycystic ovary syndrome.[275] Additionally, they may contribute to the diabetic GI dysfunction,[276] inflammation[232,239] and oxidative stress.[232,277]

1.7.8 AGEs in liver diseases

Despite many studies carried out to investigate the involvement of AGEs in other diseases, studies investigating the role of AGEs in liver disease commenced recently.[278] Sebekova et al first showed a positive correlation between the CML levels and the severity of liver disease and showed improvement after liver transplantation.[245] This was followed by a few similar studies to investigate the relationship between AGE levels and liver disease which demonstrated similar results.[279,280]

Animal studies from our laboratory showed that AGEs can augment NAFLD and liver fibrosis. In these studies it was shown that the effect of intraperitoneally injected AGEs augmented hepatic fibrosis in a cholestatic model of bile-duct ligated rats.[210] Moreover, dietary AGEs in mice fed a high fat (HF) diet aggravated NAFLD.[212] In both studies, it was suggested that AGEs play a role in steatotic liver acting as a second hit. Similar findings were reported by another study with short-term feeding (4 weeks).[281] Another study, which used oral gavage of mice with different doses of CML for 28 days, corroborated the hypothesis that CML might induce liver injury.[277] Similarly, oral gavage of rats with CML for 12 weeks, significantly increased protein-bound CML in the liver.[282] However, another similar study carried out by the same group showed contrasting results with no significant protein-bound CML in the liver following CML gavage compared to the high-fat fed rats.[283]

It has been shown that liver sinusoidal endothelial cells and sinusoidal resident macrophages Kupffer cells are responsible for 90% of AGE elimination from the liver.[244] Removal of AGEs from by these cells is a slow process which declines with age.[284] Nevertheless, many in-vitro studies investigating possible mechanisms of AGEs effects have focused on HSCs, as these cells play a pivotal role in fibrogenesis.[278] The first

evidence of the involvement of myofibroblastic HSCs in the rat liver was shown by Fehrenbach.[285] HSCs express five different types of AGE receptors: Galectin-3, CD-36, SR-AI, SR-BI and RAGE and four of them were appeared to be up-regulated during HSC activation upon AGE induction.[286] AGEs enhance α-SMA, a marker of HSC activation and the profibrotic cytokine TGF-β1 expression and increase proliferation of HSCs, which is associated with increased ROS generation[287] and autophagy.[288] Increased ROS generation by AGEs activated HSCs suggest a role for AGEs in NAFLD pathophysiology. Moreover, this might also lead to upregulation of several key signalling pathways as shown by the upregulation of Rac1, PKCδ and p47phox.[286]

1.8 Advanced glycation end products receptors

1.8.1 Introduction

Most of the harmful effects of AGE on liver pathology appeared to be mediated via its receptors. To date, there have been at least 8 candidates identified which are capable of binding to AGEs. The most characterised receptor among them is known as the receptor for AGEs or RAGE. Other common receptors are the AGE receptors AGE-R1, AGE-R2, AGE-R3. Some other AGE receptors which have not been studied well include CD-36, as well as newly identified AGE-binding proteins, Nglycans, ezrin, and megalin, macrophage scavenger receptor Type I and II.[289] Some studies suggest that the role of these receptors are more complex and different receptors might interact or influence each other.[290]

AGER-1: AGER-1 (OST-48) is a 48 kDa protein and functions as part of the oligosaccharyltransferase complex.[291] Unlike RAGE, AGER-1 is an AGE-specific receptor that appeared to be a negative regulator of the inflammatory response in mesangial cells.[292]

AGER-2: AGER-2 was initially referred to as 80K-H protein (80 kDa) which is expressed in vascular endothelial cells and kidney cells. It participates in a RAGE recognizing complex[289] in diabetic complications and breast cancers.[293]

AGER-3: AGER-3 (Mac-2 or galectin-3) is a 32 kDa protein shown to play a role in the development of acute inflammation,[294] myofibroblast proliferation and activation,[295] cell migration, adhesion, growth and differentiation.[296] Recently it was shown that in diabetes, AGER-3 (galectin-3) contributes to increased insulin resistance by transactivating insulin receptor.[297]

1.8.3 RAGE

1.8.3.1 Introduction

RAGE is a 35 kDa, multiligand receptor protein encoded by RAGE gene localised to chromosome 6.[290] It has been reported that RAGE is expressed in many cell types, including HSCs and KCs.[298] As RAGE is a pattern recognition receptor, it binds to ligands other than AGEs including amyloid-β peptide, amyloid A and S100/calgranulins.[299]

1.8.3.2 Variants of RAGE

RAGE is composed of three main regions; 1) an extracellular component made up of a single V-type domain and two C type domains which are responsible for the ligand binding, 2) a short transmembrane domain and 3) a relatively long (43 amino acids) cytoplasmic tail which is thought to be crucial for most of the intracellular signalling. The RAGE isoforms can be formed in two different ways, 1) alternative mRNA splicing, and 2) proteolytic cleavage.[300] Alternative mRNA splicing forms endogenous secretory RAGE (esRAGE)[301] while proteolytic cleavage forms cRAGE or simply soluble RAGE (sRAGE) (Fig. 1.8). It has been proposed that these soluble isoforms bind to AGEs prior to binding with membrane-bound RAGE and thereby have a protective role. There is also another functionally inactive isoform due to deletion of V-type domain known as delta RAGE isoform or variant 2.[302]

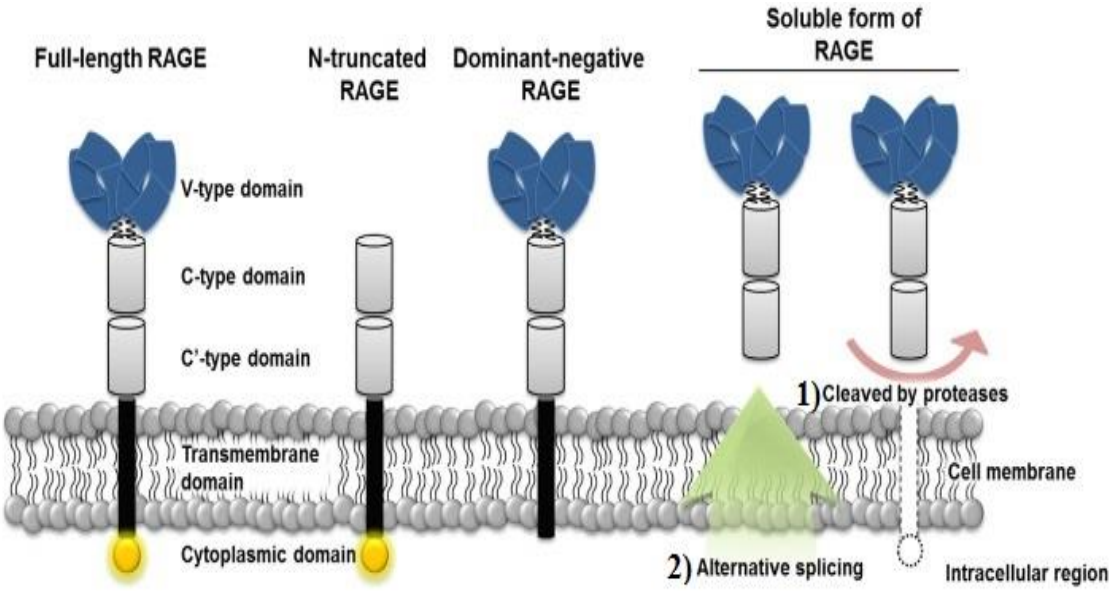

Figure 1.8 Structure and the isoforms of the receptor for advanced glycation end products (RAGE)

RAGE is a multiligand receptor of the immunoglobulin superfamily. The extracellular domain consists of a V domain and two C domains. There is a short transmembrane domain, and a cytosolic tail which confers intracellular signalling. RAGE exists in a soluble form (sRAGE) which lacks the transmembrane and cytosolic domain and can be produced by either 1) alternative mRNA splicing at exon 9 resulting in endogenous secretory RAGE (esRAGE) or 2) proteolytic cleavage of membrane RAGE, which gives rise to cleaved RAGE (cRAGE) (Adapted from Ref[303]).

1.8.3.3 RAGE induced cellular activation

Binding of RAGE to its ligands produces signals from its cytosolic tail which then leads to activation of many signal transduction pathways resulting in altered gene expression in many different cell types. Activation of signalling cascades including ERK 1/2 (p44/p42) MAP kinases,[304] p38 and SAPK/JNK MAP kinases, JAK/STAT pathway[305] and NF-κβ pathway.[306] NF-κβ activates transcription of number of genes under its control[290] such as TGF-β1, CTGF,[307] VEGF,[308] MCP-1,[309] TNF-α and members of the interleukin family.[243,299,310]

The most important consequences of NF-κβ activation is ROS generation and subsequent upregulation of RAGE itself, setting up a positive feedback loop via binding to the promoter region of RAGE gene (Fig. 1.9).[287] A number of *in vitro* studies have shown that blockade of RAGE can improve mitochondrial damage and reduces oxidative stress.[311,312]

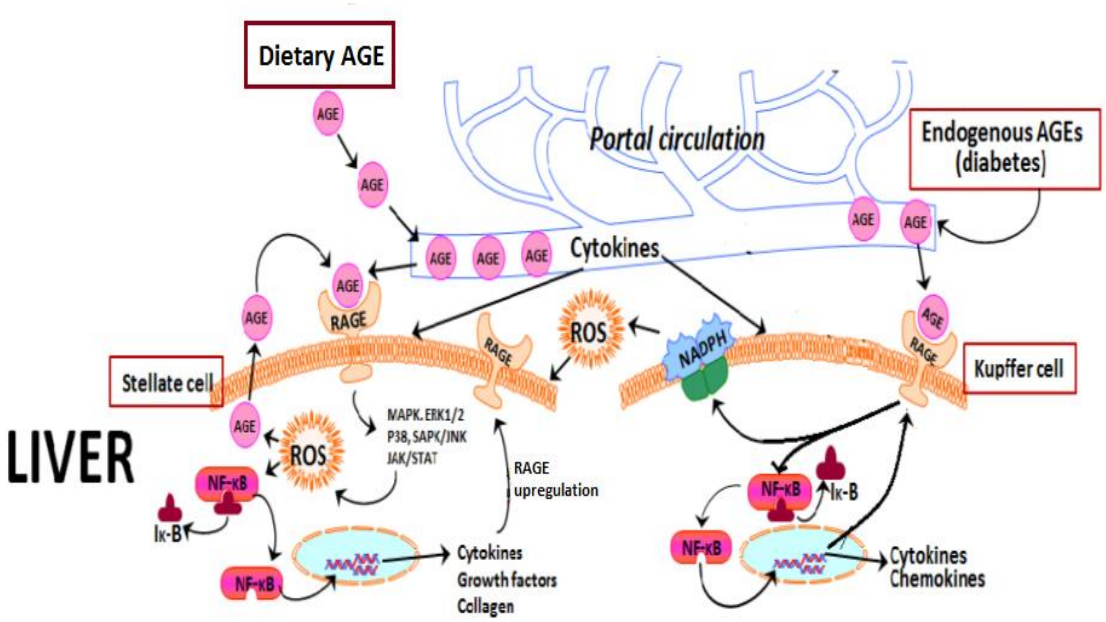

Figure 1.9 A model of RAGE induced cellular activation in liver

Consequences of RAGE activation. Both dietary and endogenous AGEs bind to RAGE expressed by liver cells. RAGE activation causes increased ROS production and gene transcription, including that of RAGE itself, thus inducing a positive feedback loop which forms a vicious cycle.

1.8.3.4 RAGE in diseases

Numerous studies have been carried out to demonstrate the involvement of RAGE in a range of diseases. Most of these involvements appeared to be via its cell signalling upon activation, to influence cell survival, cell proliferation, oxidative stress and inflammatory responses.[313] Deleterious effects of RAGE have been studied in diabetes mellitus, atherosclerosis, neurodegenerative disorders (including Alzheimer's disease), rheumatoid arthritis, chronic renal disease, and inflammatory bowel diseases.[290]

1.9 Therapies targeting AGE/RAGE axis

1.9.1 Introduction

As discussed above, AGEs and RAGE are involved in liver pathology or other diseases or the development of diabetic complications via different mechanisms. It is therefore possible to inhibit the AGE/RAGE axis using several strategies (Fig. 1.10). First, preventive measures can be employed to lower AGE production. Second is to inhibit endogenous AGE formation, and thirdly, break AGEs that have been already formed. Lastly, AGE/RAGE interaction could be disrupted or inhibited.

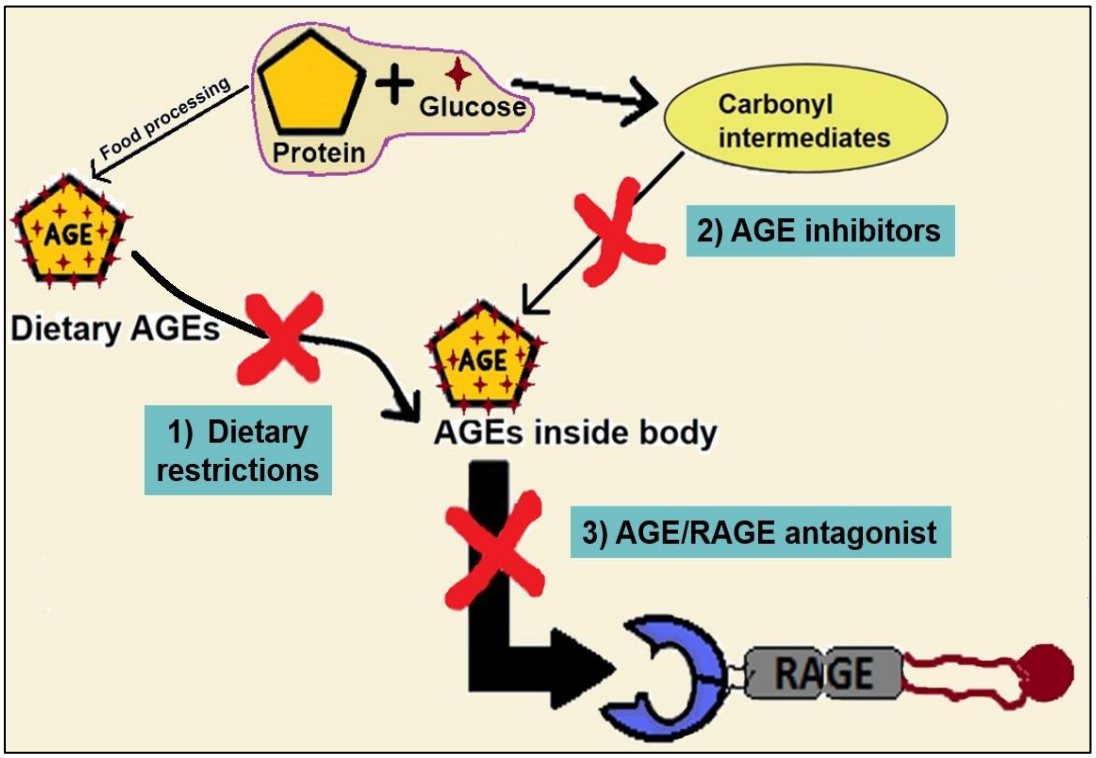

Figure 1.10 Therapies targeting AGE/RAGE axis

In the treatment and prevention of AGEs-induced NAFLD progression, three strategies could be adapted; 1) Lowering dietary AGE and precursors of glycation reaction, 2) Inhibition of endogenous AGE formation and 3) Inhibition of AGE/RAGE interaction.

1.9.2 Dietary restrictions

1.9.2.1 Endogenous AGEs

Hyperglycaemia contributes to AGE formation by providing excess reducing sugar to participate in the Maillard reaction. Therefore, it is logical that a reduction in glucose levels will result in less AGE formation. Glycaemic control reduces AGE accumulation[314] and hypoglycaemic drugs or insulin sensitizers such as metformin and pioglitazone reduce blood glucose levels and AGE formation. In addition, these particular drugs appear to inhibit AGE formation independent of their effects on blood glucose.[315] This appears to be through their ability to trap reactive carbonyl groups.[316]

1.9.2.2 Exogenous AGEs

The food with high fat, sugars and protein contents and those cooked at high temperatures have highest AGE content.[237] High levels of AGEs are found in many commonly consumed foods such as toasted breads, biscuits, potato chips, toasted breakfast cereals and meats that are grilled, fried or roasted. Although intestinal absorption of AGEs is poor, high AGE diets increase circulating AGE levels and levels fall in response to low AGE diets.[220,234] Animal models of diabetes have demonstrated that reducing the intake of dietary AGEs results in prevention of diabetic nephropathy.[254] In humans with diabetes, a low AGE diet for 6 weeks resulted in decreased serum AGE levels and decreased inflammatory markers such as C reactive protein.[229] The lowered AGE content of the food can be achieved by cooking the food for less time and at lower temperatures. Low AGE diets have also been shown to have benefits in non-diabetic animal disease models. For example, in apolipoprotein-E knockout mice, a low AGE diet prevented intimal proliferation after arterial injury.[317]

1.9.3 Inhibition of AGE formation

There have been number of inhibitors of the glycation reaction. Aminoguanidine and pyridoxamine are two of the well-studied inhibitors that prevent the conversion of early glycation end products to AGEs. Even though their mode of action has been proposed

differently in different studies, clinical trial has been successfully completed using these drugs.[318] Thiamine and benfotiamine, lipid soluble derivatives of thiamine have been studied in clinical trials.[319] LR-90 inhibits AGE formation[320] and their interaction with ROS[321] and has anti-inflammatory effects.[322] Metformin is an oral anti-diabetes agent which has been studied in human patients[323] and in-vitro models.[324] OPB-9195 has different modes of anti-AGE actions including anti-oxidant activity,[325] entrapping or reacting with reactive carbonyl compounds.[326,327]

1.9.4 AGE-crosslink breakers

Accumulation of AGEs either from endogenous sources or from the diet can form crosslinks with proteins such as extracellular matrix proteins, connective tissue matrix and basement membrane proteins. The first AGE-crosslink breaker, known as PTB (N-phencylthizolium bromide) showed promising results of decreased AGE accumulation in tissues,[328] but was very unstable.[321] A more stable derivative of PTB, alagebrium or ALT-711 was developed and it has been successfully used in phase 2 clinical trials for diabetic nephropathy and atherosclerosis.[319] However, some of the clinical trials have been terminated due to financial constraints of the drug companies, despite its safety and well tolerability.[329]

1.9.5 Inhibitors of RAGE or AGE/RAGE binding

Many of the harmful effects of AGEs are postulated to be due to the activated cell signalling induced by AGE/RAGE interaction. Studies with RAGE knockout ($RAGE^{-/-}$) animals, not only demonstrated RAGE mediated effects of AGEs, but also, showed the blocking of RAGE or the interaction of AGE/RAGE may be beneficial in attenuating disease progression.

sRAGE: sRAGE acts as a decoy compound by binding to AGEs without inducting cell signalling[330,331] and therefore has protective effects against micro and macrovascular complications in diabetes,[332] neointimal formation,[333] tumour growth and metastasis,[334] colitis,[299] impaired wound healing[335] and associated macrophages function,[336] Alzheimer disease-like conditions,[337] neuronal dysfunction[338] and lung inflammation.[339] Moreover,

studies have also shown that adenoviral over-expression of esRAGE successfully restored the impaired angiogenic response in diabetic mice.[340]

Regulation of angiotensin converting enzyme (ACE):

Forbes et al showed that inhibition of ACE was associated with increased renal expression of sRAGE and decreased renal full-length RAGE protein in rats.[341] Moreover, they showed increased plasma sRAGE levels in type 1 diabetic patients treated with an ACE inhibitor. Thiazolidinediones[342] and statins[343] have shown similar results. In addition, another clinical study performed with rosiglitazone intervention, resulted in significant increases in total sRAGE and esRAGE associated with improved diabetic parameters.[247]

Conclusion:

NAFLD is the most prevalent liver disease in Australia and the world, and effects up to 40% of the adult population. It is the leading cause for liver transplantation in the USA and expected to be the leading cause in the next 10 years in Australia. NAFLD is the hepatic manifestation of the metabolic syndrome. It can progress to NASH and liver fibrosis which eventually leads to cirrhosis or HCC. The first step is the deposition of triglyceride in the liver, especially in obese people. The presence and severity of NAFLD is closely related to the insulin resistance which increases de novo lipogenesis with excess carbohydrate availability. There is no proven medical treatment for NAFLD except for liver transplantation in patients with advanced liver diseases. The management involves lifestyle modifications and dietary restrictions, which can be difficult to achieve in most patients.[344,345] As a result, there remains a major need to identify potentially modifiable factors that exacerbate liver injury and fibrosis in NAFLD and to develop therapies that can prevent or slow liver scarring.

Although the mechanism of NAFLD pathophysiology is complex and not fully understood, a two-hit hypothesis has been proposed. In this model, whilst the deposition of fat in the liver or simple steatosis is the first hit, factors that involved in the progression of steatosis to steatohepatitis is the second hit. For example, triglyceride accumulation is the first hit, and their metabolites result in increased oxidative stress and apoptosis as a second hit. There are many other factors which contribute to progression to NASH which

have been discussed such as genetic factors, epigenetic factors, ROS generation and oxidative stress, adipokines, microbiota and diet.

Diets rich in simple sugars and AGEs have been studied in a range of diseases and AGEs have been proposed as a second hit in the progression of NAFLD to NASH. AGEs are the end product of non-enzymatic glycation reaction between reducing sugars and proteins, lipids or nucleic acids. This reaction takes place in the body under normal physiological conditions, but the rate can be accelerated dramatically in pathological conditions such as diabetes due to the elevated sugar levels. AGEs can be formed in the diet when sugars are exposed to high temperatures and/or longer cooking time with proteins. Cooking methods applying high, dry temperature such as roasting, grilling, barbequing and broiling have been found to elevate dietary AGEs. Hence the Western diets prepared using these cooking methods have higher AGE content compared to Asian diets, where slow cooking with lots of moisture is applied.

AGEs are cleared by the body via binding to its receptors. RAGE is the best characterised of the 8 receptors identified to date. Interaction of AGEs with RAGE has been shown to induce several signalling pathways downstream of NF-κβ, leading to many deleterious effects including increased generation of ROS and RAGE expression itself.

AGE/RAGE has been studied in a vast range of diseases including diabetic nephropathy, retinopathy, cardiovascular diseases and Alzheimer disease. However, there is only a few studies to demonstrate the effects of AGEs on liver diseases, and even those studies which have been carried out are in short term animal models which may not reflect the pathogenesis of human NAFLD. In fact, pathogenesis of NAFLD in diabetes has not been studied. Therefore, in this thesis, I investigated the effects of both endogenous and dietary AGEs on NAFLD in the presence and absence of diabetes using a long-term model that closely mimics the natural progression of the disease in human. Moreover, I have focused on therapeutic agents that have already been used in clinical trials for other diseases but have not been used to investigate their therapeutic effects in liver diseases. The importance of using these drugs is that if these are found to be effective in NAFLD, the findings could be used to justify a clinical trial in the future as these drugs have already been tested for safety in humans.

1.10 Hypotheses of the thesis

1) Dietary AGEs play a prominent role as a second hit in the progression of NAFLD to NASH and liver fibrosis.
2) Effects of AGEs on NAFLD progression are mediated via RAGE.
3) Drugs that lower AGE formation or inhibit AGE/RAGE signalling could be useful in targeting AGE/RAGE axis in NAFLD progression to liver fibrosis.

1.11 Aims of the thesis

1) To investigate and compare the effects of dietary versus endogenous AGEs on the progression of NAFLD to NASH and liver fibrosis.
2) To elucidate the role of RAGE in mediating AGEs-induced signalling and NAFLD progression using RAGE antagonists and RAGE knockout ($RAGE^{-/-}$) mice.
3) To explore the benefits of dietary modification, and therapeutic role of inhibitors of AGE formation (aminoguanidine and pyridoxamine) and an AGE-crosslink breaker (alagebrium) in NAFLD mice fed a diet high in AGEs.

CHAPTER 2

General Methods

2.1 Introduction

In this chapter, the general methods followed through-out the thesis will be described. The first section will be about the animal models and procedures. In the second section, sample collection and analysis methods will be described. The last section describes the cell culture analysis and statistical analysis.

2.2 Animal procedures

2.2.1 Animal housing and welfare

All animal experiments were approved by Austin Health Animal Ethics Committee and conducted in accordance with the National Health and Medical Research Council of Australia Guidelines for Animal Experimentation.

For all animal experiments, 6 weeks old male mice in C57BL/6 background were used. The mice were obtained from two sources; the RAGE knockout ($RAGE^{-/-}$) mice were provided by an in-house breeding colony at bio resource facility at Austin Health, while the wild-type (WT) mice were obtained from Walter and Eliza Hall institute for medical research (WEHI) animal facility, Victoria, Australia. They were housed at the bio resource facility at Austin Health and maintained under a 12-hour light/dark cycle and controlled temperature (21±2° C). Animals had *ad libitum* access to water and different types of diets. Animals were allowed to acclimatise for a week prior to the commencement of any experiment. Mice were caged in groups of 5 in a single cage.

2.2.2 Animal models

There are two types of rodent diets used through-out this thesis. Those are Standard mouse chow and high fat (HF) diet. This is a novel dietary model combining amounts of saturated fat and fructose to mimic unhealthy Western diets. Two percent cholesterol was incorporated as this has been shown to be a critical driver for fibrosis in murine dietary models of NASH.

2.2.2.1 Composition of high fat (HF diet)

Table 2.1 Ingredients in HF diet

Ingredients	
Casein (Acid)	195 g/Kg
Sucrose	211 g/Kg
Fructose	100 g/Kg
Clarified Butter (Ghee)	210 g/Kg
Cellulose	50 g/Kg
Wheat Starch	112 g/Kg
Dextrinised Starch	22 g/Kg
DL Methionine	5.0 g/Kg
Calcium Carbonate	28.5 g/Kg
Sodium Chloride	4.1 g/Kg
AIN93 Trace Minerals	2.3 g/Kg
Potassium Citrate	4.1 g/Kg
Potassium Dihydrogen Phosphate	11.4 g/Kg
Potassium Sulphate	2.7 g/Kg
Choline Chloride (75%)	4.2 g/Kg
AIN93 Vitamins	17 g/Kg
USP Cholesterol	20 g/Kg
Oxicap E2	0.04 g/Kg

Table 2.2 Macro nutrient percentage in HF diet

Calculated Nutritional Parameters	
Protein	19.00%
Total Fat	21.00%
Crude Fibre	4.70%
AD Fibre	4.70%
Digestible Energy	19.4 MJ / Kg
% Total calculated digestible energy from lipids	40.00%
% Total calculated digestible energy from protein	17.00%

Table 2.3 Micronutrients in HF diet

Calculated Amino Acids	
Valine	1.23%
Leucine	1.80%
Isoleucine	0.85%
Threonine	0.80%
Methionine	1.02%
Cystine	0.06%
Lysine	1.50%
Phenylanine	1.00%
Tyrosine	1.00%
Tryptophan	0.30%

Calculated Total Minerals	
Calcium	0.98%
Phosphorous	0.42%
Magnesium	0.15%
Sodium	0.19%
Chloride	0.25%
Potassium	0.64%
Sulphur	0.29%
Iron	120 mg/Kg
Copper	11 mg/Kg
Iodine	0.3 mg/Kg
Manganese	29 mg/Kg
Cobalt	No data
Zinc	72 mg/Kg
Molybdenum	0.3 mg/Kg
Selenium	0.4 mg/Kg
Cadmium	No data
Chromium	1.6 mg/Kg
Fluoride	1.6 mg/Kg
Lithium	0.2 mg/Kg
Boron	1.9 mg/Kg
Nickel	0.8 mg/Kg
Vanadium	0.2 mg/Kg

Calculated Total Vitamins	
Vitamin A (Retinol)	8 330 IU/Kg
Vitamin D (Cholecalciferol)	1 670 IU/Kg
Vitamin E (a Tocopherol acetate)	130 mg/Kg
Vitamin K (Menadione)	2 mg/Kg
Vitamin C (Ascorbic acid)	None added
Vitamin B1 (Thiamine)	10 mg/Kg
Vitamin B2 (Riboflavin)	10 mg/Kg
Niacin (Nicotinic acid)	50 mg/Kg
Vitamin B6 (Pyridoxine)	12 mg/Kg
Pantothenic Acid	27 mg/Kg
Biotin	330 ug/Kg
Folic Acid	3 mg/Kg
Inositol	None added
Vitamin B12 (Cyancobalamin)	170 ug/Kg
Choline	2 400 mg/Kg

Calculated Fatty Acid Composition	
Saturated Fats C12:0 or less	1.80%
Myristic Acid 14:0	2.60%
Palmitic Acid 16:0	7.00%
Stearic Acid 18:0	2.40%
Palmitoleic Acid 16:1	0.40%
Oleic Acid 18:1	5.50%
Gadoleic Acid 20:1	No data
Linoleic Acid 18:2 n6	0.40%
a Linolenic Acid 18:3 n3	0.20%
EPA 20:5 n3	No data
DHA 22:6 n3	No data
Total n3	0.35%
Total n6	0.41%
Cholesterol	0.15%
Total Mono Unsaturated Fats	6.23%
Total Polyunsaturated Fats	0.77%
Total Saturated Fats	13.99%

2.2.2.2 Composition of mouse standard chow

Table 2.4 Ingredients in standard chow

Ingredients	
Casein (Acid)	200 g/Kg
Sucrose	100 g/Kg
Canola Oil	70 g/Kg
Cellulose	50 g/Kg
Wheat Starch	404 g/Kg
Dextrinised Starch	132 g/Kg
DL Methionine	3.0 g/Kg
Calcium Carbonate	13.1 g/Kg
Sodium Chloride	2.6 g/Kg
AIN93 Trace Minerals	1.4 g/Kg
Potassium Citrate	2.5 g/Kg
Potassium Dihydrogen Phosphate	6.9 g/Kg
Potassium Sulphate	1.6 g/Kg
Choline Chloride (75%)	2.5 g/Kg
AIN93 Vitamins	10 g/Kg

Table 2.5 Macro nutrient percentage in standard chow

Calculated Nutritional Parameters	
Protein	19.4%
Total Fat	7.0%
Total Digestible Carbohydrate as defined by FSANZ Standard 1.2.8	56.8%
Crude Fibre	4.7%
AD Fibre	4.7%
Digestible Energy	16.1 MJ / Kg
% Total calculated digestible energy from lipids	16.0%
% Total calculated digestible energy from protein	21.0%
Ash	4.5%

Table 2.6 Micronutrients in standard chow

Calculated Amino Acids	
Valine	1.26%
Leucine	1.80%
Isoleucine	0.87%
Threonine	0.79%
Methionine	0.84%
Cystine	0.05%
Lysine	1.49%
Phenylanine	0.99%
Tyrosine	1.04%
Tryptophan	0.27%
Histidine	0.60%

Calculated Total Minerals	
Calcium	0.47%
Phosphorous	0.35%
Magnesium	0.08%
Sodium	0.15%
Chloride	0.16%
Potassium	0.40%
Sulphur	0.23%
Iron	68 mg/Kg
Copper	7.0 mg/Kg
Iodine	0.2 mg/Kg
Manganese	19 mg/Kg
Cobalt	No data
Zinc	46 mg/Kg
Molybdenum	0.15 mg/Kg
Selenium	0.3 mg/Kg
Cadmium	No data
Chromium	1.0 mg/Kg
Fluoride	1.0 mg/Kg
Lithium	0.1 mg/Kg
Boron	3.3 mg/Kg
Nickel	0.5 mg/Kg
Vanadium	0.1 mg/Kg

Calculated Total Vitamins	
Vitamin A (Retinol)	4 000 IU/Kg
Vitamin D (Cholecalciferol)	1 000 IU/Kg
Vitamin E (a Tocopherol acetate)	78 mg/Kg
Vitamin K (Menadione)	1 mg/Kg
Vitamin C (Ascorbic acid)	None added
Vitamin B1 (Thiamine)	6.1 mg/Kg
Vitamin B2 (Riboflavin)	6.3 mg/Kg
Niacin (Nicotinic acid)	30 mg/Kg
Vitamin B6 (Pryridoxine)	7 mg/Kg
Pantothenic Acid	16.5 mg/Kg
Biotin	200 ug/Kg
Folic Acid	2 mg/Kg
Inositol	None added
Vitamin B12 (Cyancobalamin)	103 ug/Kg
Choline	1 470 mg/Kg

Calculated Fatty Acid Composition	
Myristic Acid 14:0	trace
Palmitic Acid 16:0	0.30%
Stearic Acid 18:0	0.14%
Palmitoleic Acid 16:1	0.02%
Oleic Acid 18:1	3.89%
Gadoleic Acid 20:1	0.07%
Linoleic Acid 18:2 n6	1.51%
a Linolenic Acid 18:3 n3	0.98%
Arachadonic Acid 20:4 n6	No data
EPA 20:5 n3	No data
DHA 22:6 n3	No data
Total n3	0.98%
Total n6	1.51%
Total Mono Unsaturated Fats	3.98%
Total Polyunsaturated Fats	2.50%
Total Saturated Fats	0.50%

2.2.3 RAGE Knockout mice

The RAGE knockout mice used in experiments detailed in chapter 4 were kindly provided by Professor Josephine Forbes at the Mater Institute, University of Queensland.
These mice have a homozygous deletion of RAGE. They appear phenotypically normal with a retained ability to reproduce. $RAGE^{-/-}$ mouse line was generated in mice with a C57BL/6 background using the Cre-Lox system.[346] Briefly, the elements encoding the extracellular domain of RAGE (exons 2–7) were flanked by two loxP sites. Exposure to Cre recombinase resulted in the genomic sequences between the loxP sites being deleted, generating a knockout allele. Mice heterozygous for Cre recombination were bred to homozygosity to generate the $RAGE^{-/-}$ mouse line.

2.2.4 Diabetic model

In order to provide endogenous AGEs, thereby to produce severe liver scaring and fibrosis, some of the mice were induced diabetes after 15 weeks of special diet feeding. Diabetes was induced by destructing ~50% of the pancreatic beta cells using streptozotocin (STZ), (Sigma Aldrich, Australia). STZ was given with a dose of 65 mg/kg of body weight (bw) via intraperitoneal injections in two consecutive days.[347,348] Personal protective equipment including long sleeves lab gowns, face mask, gloves, goggles and covered shoes is a must when handling STZ, as it is being categorized under S4 drugs.

Streptozotocin injection in mice

The baseline blood glucose levels (blood glucose monitoring in mice will be explained in a separate section) were recorded in the previous day of first STZ injection. Since the diabetogenic action of STZ is influenced by the nutritional state, all animals were fasted from solid foods overnight with free access to water before receiving each single bolus injection to attain maximal efficiency in the induction of diabetes.

STZ is delivered as a powder as it decomposes rapidly in solutions. Therefore, it was dissolved in acetic medium just before the injection and kept on ice immediately after dissolving. The maximum stability of STZ can be achieved round pH 4, hence, it was dissolved in a sodium citrate buffer with the pH adjusted to 4.5.

Sodium citrate buffer

- 0.147 g tri sodium citrate (Univar, Australia)
- 50 mL 0.9% sodium chloride (NaCl) (Sigma Aldrich)
- Adjust pH to 4.5
- Store at 4^{o} C

Calculation and preparation of STZ (dose in mice: 65 mg/kg)

- The drug should be dissolved just before the injection. Therefore, only the amount that is required for the number of animals in a single cage (n=5) was dissolved at the time of injection.
- The weight of fasted animals was recorded.
- The weights of animals to be injected with STZ was added up and then, the heaviest weight was added to total and was rounded up to the nearest hundred grams.
- This was the volume (µL) of buffer required.
- STZ dose (65 mg/kg) was multiplied by the volume, which gives the amount of STZ required (mg).
- This amount of STZ was carefully weighed out into a sterile container.
- The required volume of sodium citrate buffer was added to STZ and mixed gently to ensure all STZ is dissolved to produce a light-yellow coloured solution. The drug should be dissolved in a fume hood to prevent any inhalation to the users.
- A separate U-100 fixed needle syringe was used for each animal in the cage. The correct volume (amount in microliter which equals to the body weight of each mouse in grams) of STZ solution was solution was intraperitoneally injected to mice with utmost care.

- The same procedure was carried out the following day.

Post injection monitoring

The animals were closely monitored for any discomfort due to the injection. Diabetic animals with polyuria were housed in larger cages to provide more space. Home cages contained normal bedding and facial tissue to absorb urine and the bedding and tissues were replaced frequently to ensure a warmer and dryer home cage. Diabetic animals have excessive hunger and thirst (together with urination) and hence, cages were provided with ad-libitum water and feed. All the animals were monitored twice daily though out the experimental period with weekly body weight and blood glucose measurements.

Blood glucose measurement

- Five days after the second STZ injection, blood glucose levels were measured to confirm the presence of diabetes in animals.
- Mice were heated under heat lamp for 2-3 minutes.
- Then a single mouse at a time was restrained in mouse restrain device.
- The tail was wiped with 80% ethanol, and the tail vein was pricked using a 26 ½" G needle.
- A drop of blood was collected onto glucometer strip and blood glucose was recorded.
- The tail was wiped with a tissue and made sure no bleeding from the tail before putting back in the cage.
- Diabetes was confirmed if blood glucose level was greater than 15 mmol/L.

2.3 Preparation of advanced glycation end products (AGEs)

2.3.1 For intraperitoneal injection and oral gavage

AGEs conjugated rat serum albumin (AGE-RSA) was prepared using Fraction V Rat Serum Albumin (RSA) (Sigma Aldrich, Australia). First, 40 mg/mL RSA solution was prepared using 0.2 M phosphate buffered saline (PBS) as the solvent. Ideally, it would be better to use mouse serum albumin (MSA) in mice rather than rat serum albumin (RSA). However, commercially available MSA is extremely expensive, and others have used bovine serum albumin (BSA) in rat studies.

10 X Phosphate buffered saline

- 80 g NaCl (Sigma Aldrich)
- 2.0 g KCl (BDH Chemicals, Australia)
- 7.1 g Na_2HPO_4 (BDH Chemicals, Australia)
- 2 g of KH_2PO_4 (BDH Chemicals, Australia)
- Dissolve in 1 L of autoclaved distilled water
- Adjust pH to 7.2
- Dilute as required

To this RSA solution, 90 g/L of D-glucose (Ajax Pharmaceuticals, Australia) was added, giving a final glucose concentration of 0.5 M. The solution was filtered using a 0.22 μm micropore filter into a 50 mL falcon tube in a sterile fume hood. The tubes were then incubated at 37^o C for 6 weeks followed by dialysis against 0.2 M PBS using dialysis flasks (Thermo Fisher Scientific, Australia) at 4^o C for 48 hours, to remove any free glucose. The buffer was changed several times. The solution was then filtered through 0.2 μm micropore filter and pH was adjusted to 7. To ensure the solution was free of endotoxin, it was passed through an endotoxin column. Disposable polypropylene columns (Thermo Fisher Scientific, USA) were prepared prior to use by addition of firstly degassed water, and secondly, degassed gel slurry (Pierce detoxi gel resin, Thermo Fisher Scientific, Australia). The columns were then washed with 5 column volumes of 1% sodium deoxycholate (BDH chemicals, Australia) followed by 10 column volumes of pyrogen free water (Thermo Fisher Scientific, Australia). The samples were then passed through the columns, and samples were collected from the bottom to pyrogen free falcon tubes, aliquoted into 1.5 mL eppendorfs and then stored at -80^o C until further use.

Control RSA (without AGEs) was treated in exactly the same way, without inclusion of D-glucose. All the solutions were detected for endotoxin levels and only the solutions with endotoxin levels <5 U/L were used for the experiments.

2.3.2 Preparation of AGEs in the diet

Dietary AGE content was increased by baking the HF diet at 160^0 C for 1 hour. We have previously shown that baking HF diet at these conditions increases N^{ε}-(1-Carboxymethyl)lysine (CML) by 4 folds.[212] N^{ε}-(1-Carboxyethyl)lysine (CEL) and

methylglyoxal derived hydroimidazalone-1 (MG-H1) content in the diet was assessed by gas chromatography/mass spectrometry (GC/MS). Work from our laboratory showed that this particular temperature and time do not alter the micronutrient composition including the vitamins in the diet.

Dietary AGE content was reduced using vinegar in some of the experiments. In this, 1.5 kg of HF diet was fully submerged in 1 L of vinegar (Coles home-brand, Australia) for 15 minutes and allowed to marinate. Then, the vinegar was strained for another 15 minutes, so that excess vinegar could be removed. After that, it was baked under the same conditions as mentioned above.

2.4 Plasma collection for Biochemistry

Mice were anaesthetised using pentobarbitone (Boehringer Mannheim, Germany) at a dose of 60 mg/kg intraperitoneal injection. Blood was obtained via intracardiac puncture and collected into 1.5 mL eppendorf tubes added 0.02 mL lithium heparin. Blood was centrifuged (6,000 g, 4° C, 10 min; Beckman Optima LE-80K centrifuge, Beckman Coulter, USA) and the separated plasma was stored at -20° C until the time of assay. Plasma alanine amino transferase (ALT), bilirubin, alkaline phosphatase (ALP), aspartate aminotransferase (AST) and gamma-glutamyl transpeptidase (GGT) were measured by Austin pathology, Heidelberg, Australia.

2.5 Liver Collection

Following blood collection, the liver was dissected out and weighed. It was sectioned, a portion from the left lateral lobe was partitioned and collected into RNAse free eppendorf tubes, then immediately snap frozen in liquid nitrogen and stored at -80° C for RNA and protein extraction. The right lobe of the liver was fixed in 4% paraformaldehyde (PFA) (24 g of PFA (Sigma Aldrich, Australia) was dissolved in 600 mL of 1 X PBS and heated below 60^{o} C and pH was adjusted to 7.2) for 24 hours at 4° C, and then transferred to 10% sucrose in 1 X PBS and stored at 4° C until paraffin embedding and histological analysis.

2.6 Quantification of gene expression

2.6.1 Total RNA isolation from the liver

Small sections of liver tissue (that had been snap frozen in liquid nitrogen and stored at -80^{o} C) weighing approximately 50-100 mg were homogenised for 60 seconds in 1 ml of Tri-Reagent (Sigma Aldrich). It was allowed to rest at room temperature for 5 minutes allowing the dissociation of nucleoprotein complexes. Samples were centrifuged at 12,000 g for 15 minutes at 4^{o} C (Beckman Optima LE-80K centrifuge, Beckman Coulter, Fullerton, CA, USA) to remove any cell debris. 0.2 ml of chloroform was added to the supernatant, with 15 seconds of vigorous shaking, followed by incubation at room temperature for 3 minutes. It was again centrifuged using the same conditions, resulting in three distinct phases within the Eppendorf, a lower red phenol-chloroform phase, an interphase, and a colourless upper aqueous phase containing RNA, and this colourless phase was gently pipetted and transferred into a fresh 1.5 mL RNase free eppendorf. To this, 0.5 mL of molecular grade isopropyl alcohol (Sigma Aldrich) was added and allowed to rest at room temperature for 10 minutes. The samples were then centrifuged again at 12,000 g at 4^{o} C for 10 minutes. After this spin, the RNA was visible at the bottom of the eppendorf as a small white pellet. The supernatant was removed and the pellet was washed with 1 ml of 75% molecular grade ethanol (Sigma Aldrich), followed by another centrifugation at 7,500 g for 8 minutes. Then, the pellet was briefly air-dried and re-suspended in 0.05 ml of sterile water treated with 0.1% Diethylpyrocarbonate (DEPC) (Invitrogen, USA). The concentration and quality of RNA was assessed using a Nanodrop (Thermo Fisher Scientific, Australia) at wavelength of optical density (OD) of 260 nm and 280 nm. RNA samples with a ratio from 1.8 to 2.0 indicates a high degree of purity, were stored at -80^{o} C for downstream processing.

2.6.2 rDNase treatment

Following extraction, 2.0 µg of RNA was diluted up to 8 µL with autoclaved milli-Q water. It was treated with 1 µL of DNase buffer and 1 µL of recombinant DNase I (Life technologies, Australia) at 37^{o} C for 25 minutes to remove any contaminating genomic DNA. Then, it was treated with 1.2 µL of DNase inactivation reagent (Life technologies,

Australia) by brief vortexing. Finally, it was centrifuged at 10600 g for 2 minutes prior freezing at -80^{o} C.

2.6.3 cDNA synthesis

Complementary DNA (cDNA) was then synthesized using this DNase treated RNA, which act as the template mRNA for reverse transcriptase reaction. One microgram of mRNA (5 µL of rDNsae treated mRNA prepared in 2.6.2 section) was incubated with 100 ng of random hexamers (Life Technologies) in DEPC treated milli-Q water (total of 10.9 µL) at 70° C for 5 minutes, followed by rapid cooling on ice (at least 1 minute). After cooling it was incubated in room temperature for 5 minutes with a mix containing 2 µL of 0.1 M dithiothreitol (DTT), 2 µL of 10 mM dNTP, 4 µL of 5X RT buffer and 0.1 µL of RNase OUT (Life Technologies). cDNA was synthesized by incubating the samples with 1 µL of Malony murine leukaemia virus reverse transcriptase (M-MLVRT) enzyme (Life Technologies), first at room temperature for 10 minutes, then at 42° C for 50 minutes and finally for 15 minutes at 70° C to stop the reaction. The resulting cDNA was then used for amplification by quantitative real-time PCR (Q-PCR).

2.6.4 Quantitative real-time polymerase chain reaction (q-PCR)

All q-PCR reactions were carried out using multiplexing where both the target and the endogenous reference genes are amplified in a single well of 96 or 384 wells plate. All probes and primers were designed using the software program Primer Express (PE Applied Biosystems, Foster City, CA, USA). The DNA sequences of the probes, forward and reverse primers are shown in Table 2.4.

For each gene of interest, a reaction was set up with a total volume of 25 µL. The reaction contained 50 ng of cDNA (volume of 1 µL), 1.25 µL each of probe (100 nmol/L), forward primer (500 nmol/L) and reverse primer (500 nmol/L), 12.5 µL of Platinum Quantitative PCR SuperMix-UDG with ROX (Invitrogen, Australia), 0.6 µL of 18S VIC pre-developed endogenous control reagent (Applied Biosystems, USA) and 7.2 µL of autoclaved milli-Q water. For 384 gene expression assay, a reaction was set up with a total volume of 5 µL containing 5 ng of cDNA (volume of 1 µL), 0.25 µL of pre-

developed Taqman assay probe and primer mix (Thermo Fisher Scientific), 2.5 μL of Platinum Quantitative PCR SuperMix-UDG with ROX (Invitrogen), 0.2 μL of 18S VIC pre-developed endogenous control reagent (Applied Biosystems) and 1.05 μL of autoclaved milli-Q water.

Samples were amplified on a 7500 Real-Time PCR machine (Applied Biosystems). PCR thermal cycling conditions were as follows: 95° C for 10 minutes, then 45 cycles at 95° C for 15 seconds for denaturing and extension at 60° C for 1 minute. Results were expressed relative to control values, which were arbitrarily assigned a value of 1.

Table 2.7 Sequence of probes and primers for mouse qPCR analysis

Gene	Genebank Accession	Probe/ Primer	Sequence
ColA1	NM_007742	Probe	5'-ATCGACCCTAACCAAG-3'
		Primer-F	5'-GACTGGAAGAGCGGAGAGTACTG-3'
		Primer-R	5'-CCTTGATGGCGTCCAGGTT-3'
TGF-β1	NM_011577	Probe	5'-AAAGCCCTGTATTCCGT-3'
		Primer-F	5'-GCAGTGGCTGAACCAAGGA-3'
		Primer-R	5'-GCAGTGAGCGCTGAATCGA-3'
α-SMA	NM_007392	Probe	5'-TGCCAGATCTTTTCC-3'
		Primer-F	5'-GACGCTGAAGTATCCGATAGAACA-3'
		Primer-R	5'-GGCCACACGAAGCTCGTTAT-3'
CTGF	BC006783	Probe	5'-ACTGCCTGGTCCAGAC -3'
		Primer-F	5'-CTTAGAACAGGCGCTCCACTCT-3'
		Primer-R	5'-ACAGGGTGCACCATCTTTGG-3'
IL-6	NM_031168	Probe	5'-ACAGGGTGCACCATCTTTGG-3'
		Primer-F	5'-ACAGGGTGCACCATCTTTGG-3'
		Primer-R	5'-ACAGGGTGCACCATCTTTGG-3'
MCP-1	NM_011333	Probe	5'-AATGGGTCCAGACATAC-3'
		Primer-F	5'-GTCTGTGCTGACCCCAAGAAG-3'
		Primer-R	5'-TGGTTCCGATCCAGGTTTTTA-3'

RAGE	NM_007425	Probe	5’-CTACCAGATTCCTGGGAAGCCAGAAATTG-3’
		Primer-F	5’-GGGAAGGAGGTCAAGTCCAACTA-3’
		Primer-R	5’-TGAGTTCAGAGGCAGGATCCA-3’
TNF-α	NM_013693	Probe	5’-TCACCCACACCGTCAG-3’
		Primer-F	5’-GGCTGCCCCGACTACGT-3’
		Primer-R	5’-TTTCTCCTGGTATGAGATAGCAAATC-3’
IL-1β	M15131	Probe	5’-CTGAAAGCTCTCCACCTC- 3’
		Primer F	5’-TCGTGCTGTCGGACCCATA- 3’
		Primer R	5’-TTGTTGGTTGATATTCTGTCCATTG- 3’
$p47^{phox}$	NM_010876	Probe	5’-CCCAGCCTTCTGCAGAT-3’
		Primer F	5’-CCGGCTATTTCCCATCCAT-3’
		Primer R	5’-TCGCTGGGCCTGGGTTAT-3’
NOX-1	NM_072203	Probe	5’-CTAGAATAGCTACTGCCCACC-3’
		Primer F	5’-GACCAATGTGGGACAATGAGTTT-3’
		Primer R	5’-CCCCCACCGCAGACTTG-3’
NOX-4	NM_015760	Probe	5’-CATTTTGCTATTTCATCAAA-3’
		Primer F	5’-AAAAATATCACACACTGAATTCGAGACT-3’
		Primer R	5’-TGGGTCCACAGCAGAAAACTC-3’
$gp91^{phox}$	U43384	Probe	5’-CAACTGGACAGGAACCT-3’
		Primer F	5’-AGTGCGTGTTGCTCGACAAG-3’
		Primer R	5’-CCAAGCTACCATCTTATGGAAAGTG-3’

Note: Predeveloped probe/primer kits of TLR-4 and CD-14 were purchased from Thermo Fisher Scientific, Australia.

2.7 Histological techniques

Liver samples that had been collected for histology were mounted in specimen cassettes and then embedded in paraffin blocks by Austin pathology, Heidelberg, Australia. Then the samples were sectioned into 4 μm sections (Leica bio systems, Germany) and then

mounted onto silane coated glass slides (Thermo Fisher Scientific) for use in histological or immunohistochemical techniques.

2.7.1 Picrosirius red staining and morphometric assessment of collagen content

Liver sections (4 μm in size) were deparaffinised twice in xylene (Australia Biostain, Australia), 5 minutes each time. It was dehydrated through descending concentrations of ethanol (100%, 100%, 100%and 95%) for 3 minutes each and washed thoroughly under running tap water for 30 minutes. Next, the sections were stained with 0.1% picrosirius red (Sigma Aldrich) for 2 hours and 30 minutes. Slides were then rinsed thoroughly in running tap water and rapidly dehydrated through graded ethanol (95%, 100%, 100% and 100%), followed by xylene for twice, 5 minutes each time. The slides were then mounted with cover slips using DPX mounting medium (Sigma Aldrich). Total collagen was quantified by analysing liver sections under a standard light microscope (Olympus BX50 Microscope, Japan; magnification x200). Collagen volume fraction was determined by measuring the area of stained tissue (red) within a randomly selected field. A total of 10 fields per section were analysed per animal using computerized image capture (MCID) (Imaging Research, Canada). The mean value was calculated and results were expressed as a percentage of the area positively stained red.

2.7.2 Haematoxylin and Eosin staining

Liver sections were deparaffinised twice in xylene (Australia Biostain), 5 minutes each time, then dehydrated using graded ethanol (100%, 100% and 95%) and washed under running tap water. Slides were immersed in haematoxylin (Merck, Australia) for 8 minutes, and then washed intensively. Then, those were immersed in Scott's blue (AMBER Scientific, Australia) solution for exactly 30 seconds, followed by intensive washing in running tap water for about 45 minutes. Then, it was dipped in 95% ethanol for 10 times, followed by immersion in alcoholic Eosin (Sigma Aldrich) for 10 minutes. The slides were then dehydrated three times using 100% ethanol, 3 minutes each time

followed by twice in xylene, 5 minutes each time. Finally, the slides were mounted with cover slips using DPX mounting medium (Sigma Aldrich).

2.7.3 4-Hydroxy-2-nonenal (4-HNE) immunohistochemistry

Superoxide anion and ROS are key mediators of liver injury and cellular dysfunction associated with the progression of fatty liver disease. 4-HNE is a marker of lipid peroxidation which can result in ROS generation. Immunohistochemistry was performed on 4 μm sections of paraffin embedded mouse liver tissue mounted on silane-coated glass slides. First, specimens were de-waxed in xylene (100% for 5 minutes each) and dehydrated in graded ethanol as described in 2.7.2 and followed by running tap water for 15 minutes. The slides were then washed in dH_2O followed by 3 times with 1 X PBS for 5 minutes each on a rocker at RT. The antigens of the tissues were retrieved by incubating sections in boiling 10 mM trisodium citrate buffer (contained 0.05% Tween 20 adjusted to pH 6) for 2 minutes. The washing step with dH_2O and 1 X PBS was repeated as outlined above. Endogenous peroxidase activity was removed with 3% hydrogen peroxide in PBS at RT for 20 minutes and washed as described above. Non-specific proteins were blocked with 10% normal goat serum (NGS) in PBS for 30 minutes at RT and after the incubation period the excess blocking solution was removed using blotting paper. Then, the primary anti-rabbit 4-HNE antibody (Alpha Diagnostic International, USA) diluted in 1 X PBS (1:100 dilution) in 0.1% NGS was applied and incubated overnight at 4º C in a box locally designed for immunohischemistry. On the following day, sections were rinsed using dH_2O for 5 minutes and PBS with 0.1% Tween 20 for 5 minutes on a rocker at RT. The slides were then incubated with biotinylated secondary goat anti-rabbit antibody (Dako, Agilent Technology, 1:100) in 3% BSA and 3% NGS for 10 minutes at RT. It was rinsed in dH_2O for 5 minutes and PBS with 0.1% Tween 20 for 5 minutes on a rocker at RT. Next, the slides were incubated with avidin-biotin complex (ABC kit) (Dako, Agilent Technology) for 30 minutes at RT and rinsed using dH_2O and PBS as described above. Peroxidase conjugates were subsequently localised using diaminobenzidine tetrahydrochloride chromogen (DAB) (Sigma Aldrich) for 8 minutes. Finally, the slides were counterstained with haematoxylin (Merck) for 8 minutes followed by washing in running tap water for 10 minutes. It was washed in blue Scott tap water (AMBER Scientific) for 15 seconds to clear the background and washed in running tap water for 40

minutes. The relative positive staining in each group was determined by computerised quantification (MCID, Imaging Research) at x200 magnification (10 fields per sample).

2.8 IVIS Imaging and dye preparation

In order to determine how ingested AGEs in the diet traffic through the gastrointestinal tract and body as well as organ exposure to AGEs, a near-infrared tracking approach was used. Tissues have a lower absorption coefficient in the near infrared region and this allows for deeper penetration into mice and a decreased interference from tissue auto-fluorescence.

2.8.1 Preparation of dye conjugated AGEs

1 mg/mL AGE-protein solution was prepared as previously described in section 2.3. It was labelled with IRDye 800CW protein labelling kit-High MW (LI-COR, Lincoln, USA). First, the pH of the protein solution was adjusted to 8.5 using the potassium phosphate buffer provided in the kit. The total volume of labelled AGEs was determined based on the number of mice in the study, and the volume of dye needed was calculated according to the molecular weight of the protein (i.e. dye volume needed for 1 mL of 65 kDA protein is 17.9 µL (1:1 = dye: protein), thereby the total number of dye vials needed was calculated). The protein and the dye were warmed to room temperature without exposing the dye to light (carried out in a dark room) and 1 vial of dye was dissolved in 25 µL of ultrapure water provided in the kit and vortexed until the dye is completely dissolved. The appropriate volume was added to protein vials and mixed thoroughly by inversion and incubated at room temperature for 2 hours.

2.8.2 Separation of conjugate from unreacted free dye

To avoid false signals due to free dye moieties, the conjugate was purified from its free dye moieties using Zebra spin desalting column kits (Pierse Biotechnology, USA) which remove more than 95% free dye from the sample.

First the bottom caps of the columns were loosened and placed in 15 mL collection tubes and centrifuged at 1000g for 2 minutes to remove storage solution. Columns were washed with 2.5 mL of 1 X PBS and centrifuged as given above for 3 times. Then, the caps were removed, and the columns were placed in new sterile collection tubes and the sample was added (approximately 1 mL) and centrifuged in the same conditions. The conjugate free from unreacted dye was collected in the collection tube and the resin was discarded.

2.9 Cell culture experiments

As described in the background, Kupffer cells are the major cell type involved in NAFLD progression and stellate cells are the major cell type responsible for ECM secretion. In addition to that, these two are the major cell types in the liver that present RAGE receptor. Therefore, *in vitro* experiments using immortalised cell lines of these two cell types were carried out to explore mechanistic insight. Immortalised Mouse Kupffer cells (KUP5) were developed using C57BL/6 background mice by Dr Hiroshi Kitani, Japan and kindly provided to us.[349] Immortalised Human hepatic stellate cells (LX2) have been extensively characterised and used in literature and provided to us by Associate professor William Sievert and Jorge Tchongue from the Monash Medical Centre, Clayton, Victoria.

2.9.1 Maintaining and growing cells

Both cell types were grown and maintained routinely as monolayer cultures in DMEM high glucose (4.5 g/L L-Glucose) media (Thermo Fisher Scientific) supplemented with 10% fetal bovine serum (FBS) (Sigma Aldrich) with 5% CO_2 at 37^o C. In addition to that, for Kupffer cells 10 µg/mL bovine insulin (Sigma Aldrich) and 250 µM monothioglycerol (Sigma Aldrich) were added as supplements. For LX2 cells 1% penicillin and streptomycin (Thermo Fisher Scientific) was added.
Cells were passaged once they reached approximately 80% confluency.

KUP5 cells: First the cells were washed twice with 1 X HBSS (Thermo Fisher Scientific) and then, 0.5 mL to 2 mL of 10 X trypsin (Invitrogen) was added depending on the size of the flask. The flask was incubated at 37^o C for 2-3 minutes and tapped to detach the cells from the plastic surface.

LX2 cells: First, the cells were washed twice with 1 X PBS (Thermo Fisher Scientific) and then, 0.5 mL to 2 mL 1 X trypsin (Invitrogen) was added depending the size of the flask. The flask was tapped to detach the cells from the plastic surface and if necessary, it was incubated at 37^{o} C for 1 minute to facilitate cell detachment.

Once the cells were detached, they were collected to a falcon tube by adding media into the flask. Cell suspension was centrifuged, and the pellet was resuspended in fresh media. The cells were used for experiments or passaged depending on the number of cells required for the experiments. The media was refreshed as required and subsequent passages were performed every 2-3 days for KUP5 cells and 5-7 days for LX2 cells.

2.9.2 Counting the cells

Cells were counted manually using a microscope and a haemocytometer (Weber Scientific International). 10 µL of cell supernatant was mixed thoroughly with equal volume of trypan blue and carefully filled into the haemocytometer. The cells were counted using 4 sets of 16 squares of the haemocytometer (Fig. 2.1) and average cell count was considered for the calculation of total number of cells in the cell suspension. Trypan blue stains the dead cells with blue colour, therefore, blue stained cells were not counted.

$$\text{Number of cells/mL of cell suspension} = N \times \text{dilution factor} \times 10^4$$

Where, N = average cell count obtained from 4 sets of 16 squares

Dilution factor in trypan blue is 2.

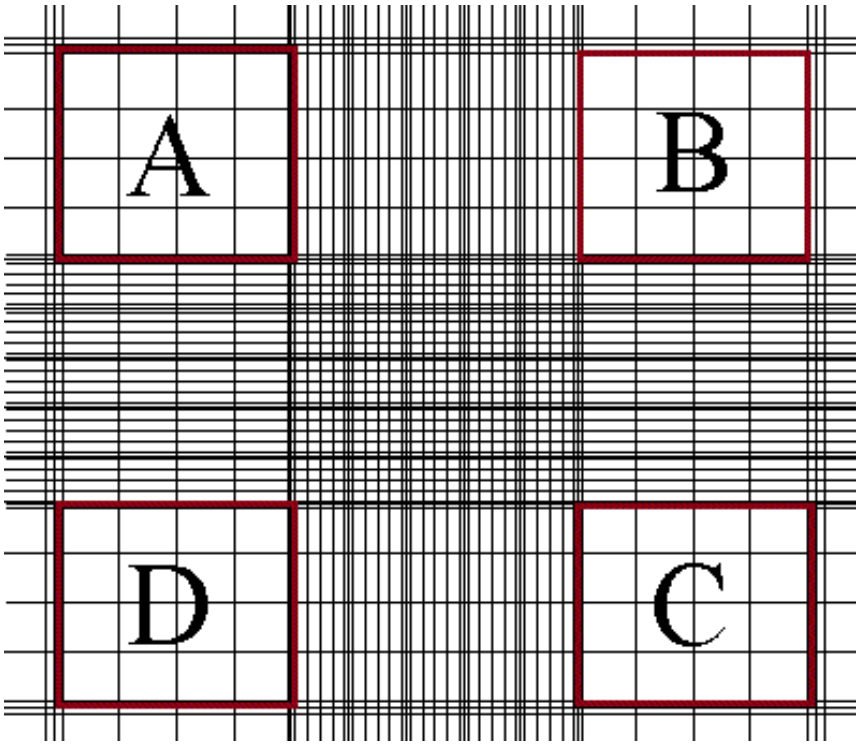

Figure 2.1 Haemocytometer gridlines

Cells in 16 squares of each A, B, C and D (outlined in brown colour) sets were counted and average was calculated for the determination of number of cells present in the cell supernatant.

2.9.3 Cell harvest

At the end of each experiment, cells were harvested for analysis of supernatant components, protein and RNA. Firstly, the supernatant from each well was aspirated (with care taken not to aspirate any cells adherent to the base of the well) into sterile 1.5 mL eppendorfs and immediately frozen at -80^{o} C. Prior to analysis, the samples were centrifuged at 10,000 g for 15 minutes at 4^{o} C to remove debris.

Once the supernatant was removed, cells were collected for q-PCR using Tri-reagent (Sigma Aldrich). Firstly, the wells were washed twice with 1 mL ice-cold 1 X PBS (LX2) or HBSS (KUP5). Then, 0.5 ml Tri-reagent was added to each well, followed by multiple aspirations to mix thoroughly and break up any adherent cells. The Tri-reagent/cell mix

from each well was then collected into 1.5 mL eppendorf tubes and immediately frozen at -80^{o} C until the time of RNA extraction as outlined in section 2.6.

2.11 Statistical Analysis

Results are expressed as mean $\pm$ standard error of means (SEM) unless otherwise stated. Data were analysed by one-way or repeated measures analysis of variance (ANOVA) with Tukey's post-hoc and Student's two tailed, unpaired t-test where appropriate. A p value of less than 0.05 was considered statistically significant. Statistical analyses were performed using GraphPad Prism 7 software (GraphPad Software, CA, USA).

CHAPTER 3

The effect of endogenous and exogenous advanced glycation end products (AGEs) on non-alcoholic fatty liver disease

3.1 Introduction

Advanced glycation end products are formed via a series of reversible and irreversible reactions as outlined in section 1.7.2. The rate of each reaction varies on the substrate availability.[213] Hence, the rate of endogenous formation of AGEs is accelerated in diabetic conditions due to both elevated sugar level and increased oxidative stress.[247]

We have previously shown in our laboratory that AGEs did not induce liver injury, oxidative stress or fibrosis in normal liver, i.e. coexisting liver injury is required to induce hepatic injury by AGEs. Therefore, all the animals used for the experiments in this thesis were fed on a high fat (HF, 21% of fat) diet to induce fatty liver or non-alcoholic fatty liver disease (NAFLD). This diet, as discussed in general methods, has comparable fat and fructose percentage to unhealthy Western diet, but a relatively higher percentage of cholesterol to induce mild fibrosis.[350] Moreover, as discussed in chapter 1, the deleterious effects of AGEs are induced via activation of the receptor for AGEs (RAGE), resulting in the release of cytokines and growth factors and producing oxidative stress. We have recently shown that deleting RAGE gene protects the liver from fibrosis in animals fed on the HF diet with a high AGE content induced by baking.[212]

AGEs plays a role in the pathogenesis of many diabetic complications[213] and it has been suggested that high AGE levels in diabetic subjects may directly contribute to liver disease. However, it is not possible to determine the quantity of AGEs which are produced in the circulation in diabetic subjects or diabetic animals. Therefore, this chapter aimed

to investigate the effect of exogenously administered AGEs to mimic the effect of endogenous AGEs on NAFLD progression. Mice fed the HF diet were intraperitoneally (i.p.) injected with *in vitro* prepared AGEs daily, thus modelling endogenous AGEs formed as a result of diabetes. The objective of this experiment was therefore, to determine the effect of endogenous AGEs on NAFLD progression and compare these effects to the effect of dietary AGEs. Although this may not represent a full spectrum of changes that take place in diabetic subjects or animals, the objective of the study was to examine the effect due to AGEs alone.

3.2 Materials and Methods

3.2.1 Experimental design

Six to eight weeks old male C57BL/6 mice were randomized into 6 groups as follows.

1)Standard chow

2)High fat (HF) diet

3)HF + (HF Baked/ HF+B) diet

4)HF+ AGE (20 mg/kg/day)

5)HF + AGE (40 mg/kg/day)

6)HF + AGE (60 mg/kg/day)

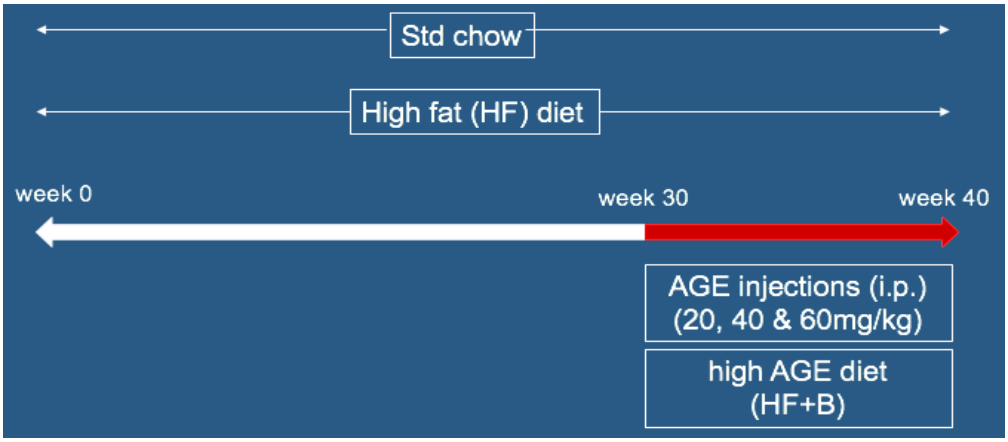

A group of mice was fed on standard chow for 40 weeks (control group). Another 4 groups of mice were fed on the HF diet for 40 weeks. *In vitro* prepared AGEs (see section 3.2.2) were intraperitoneally (i.p.) injected daily in varying doses for 10 weeks

commenced at 30 weeks of the HF diet. Similar to this, a group of mice was fed the HF diet for the first 30 weeks, followed by baked-HF diet (HF+B) to increase dietary AGE content during the remaining 10 weeks for comparison between endogenous AGEs (i.p. injected AGEs for 10 weeks) vs dietary AGEs.

3.2.2 Preparation of AGEs for i.p. injection

AGEs for i.p. injections were prepared as outlined in section 2.3.1. In brief, 40 mg/mL RSA (Sigma Aldrich, Australia) solution was prepared using 0.2 M phosphate buffered saline (PBS) as the solvent. To this RSA solution, 90 g/L of D-glucose (Ajax Pharmaceuticals, Australia) was added, giving a final glucose concentration of 0.5 M. This mixture was incubated at 37^{o} C for 6 weeks followed by dialysis against 0.2 M PBS using dialysis flasks (Thermo Fisher Scientific, Australia) at 4^{o} C for 48 hours, to remove any free glucose. The pH was adjusted to 7. The control was treated the same way without adding glucose. At the end CML levels were measured by ELISA (Jomar Life Research, Australia)

3.2.3 Preparation of AGEs in the diet

Dietary AGE content was increased by baking at 160^{0} C for 1 hour. CML, CEL and MG-H1 content in the diet was assessed by gas chromatography/mass spectrometry (GC/MS).

3.2.4 Tissue harvesting and storage

The animals were sacrificed at 40 weeks using pentobarbitone (120 mg/kg bw) as described in chapter 2. Blood and livers were collected from the mice as described in chapter 2.

3.2.5 Biochemical assessment of liver function

Liver function testing was carried out in plasma that had been stored at -20^{o} C, using Beckman Coulter LX20 autoanalyzer (Beckman Coulter) at Austin Pathology, Austin Health.

3.2.6 Liver gene expression

Total RNA was extracted from snap-frozen liver samples stored at -80^{o} C as described in chapter 2.6. cDNA was synthesized from this RNA and qPCR reactions were carried out using multiplexing to assess the expression of RAGE, LPS-binding receptors, pro-inflammatory and pro-fibrotic genes. The details of dual fluorescent-labelled oligonucleotide probes and primers are given in Table 2.4 in chapter 2.

3.2.7 Histological assessment of liver injury and fibrosis

Haematoxylin and Eosin (H&E) staining

Haematoxylin and Eosin (H&E) staining was performed in 4 µm liver sections as described in chapter 2.7.2.

Picrosirius red staining

Picrosirius red staining was performed in 4 µm liver sections as described in chapter 2.7.1. Briefly, total collagen was quantified by analysing liver sections under a standard light microscope (Olympus BX50 Microscope, Japan; magnification x200). Collagen volume fraction was determined by measuring the area of stained tissue (red) within a randomly selected field. A total of 10 fields per section were analysed per animal using computerized image capture (MCID) (Imaging Research, Canada). The mean value was calculated per section/animal before analysis, and results were expressed as a percentage of the area positively stained red.

3.2.8 Cell culture Experiments

Immortalised murine Kupffer cells (KUP5) were kindly provided us to by Dr Hiroshi Kitani (REKEN cell bank, JAPAN).[349] These cells were seeded for 24 hours and exposed to three different doses of AGEs, 25 μg/mL, 50 μg/mL, 100 μg/mL for 3 hr, 6 hr, 12 hr, 24 hr, 48 hr and 72 hr. At the end of the experiment 0.5 mL of tri-reagent (Sigma Aldrich) was applied to cells to harvest total RNA for gene expression analysis as outlined in chapter 2. Lipopolysaccharide (LPS) was used at three different doses, 1 ng/mL, 5 ng/mL and 10 ng/mL as the positive control.

Since using this protocol, we could not observe any changes in gene expression and there was a possible cell death on 24-hour seeding, the cells were seeded for 6 and 12 hours and exposed to 200 μg/mL of AGEs for 6 and 12 hours. Gene expression of RAGE and pro-inflammatory cytokines was analysed.

Immortalised human hepatic stellate cells (HSCs/LX2) were exposed to 200 μg/mL of AGEs for 6 hr, 12 hr, 24 hr, 48 hr and 72 hours and gene expression of RAGE and α-SMA was determined. LX2 cells were also exposed to conditioned medium collected from KUP5 cells treated with AGEs for 6 hours and harvested for gene analysis. LX2 cells activated by TGF-β1 at 10 ng/mL was used as the positive control.

3.2.9 Statistical analysis

Results are expressed as mean ± SEM and analysed by one-way analysis of variance (ANOVA) and Tukey's comparison test or calculated by Student's two-tailed unpaired t test where appropriate using Prism 7 software (GraphPad Software, San Diego, United States). $p < 0.05$ was considered significant.

3.3 Results

3.3.1 AGE content in the baked diet and injectable AGEs

Baking at 160^{o} C for 1 hour dramatically increased 3 common AGE types, CML, CEL and MG-H1 (Fig. 3.1A) as measured by GC/MS. CML concentration in injectable AGEs was significantly ($p<0.01$) higher compared to that in the control RSA (Fig. 3.1B) as measured by CML ELISA. Note: no statistical analysis was performed as food samples were pooled across before GC/MS analysis.

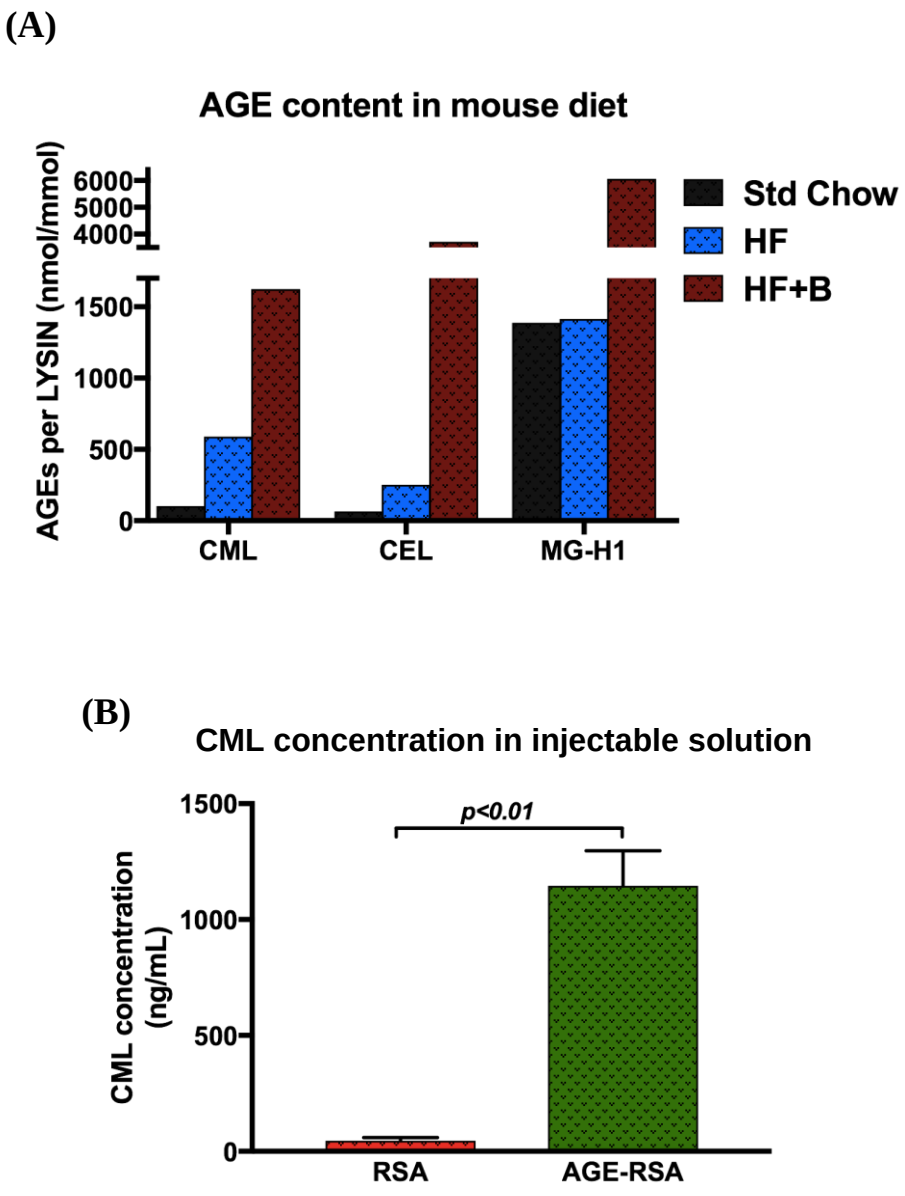

Figure 3.1 AGE content in the diet and injectable AGEs

Standard chow contains the least amount of all three AGE types. High fat (HF) diet has higher CML and CEL levels compared to standard chow, however MG-H1 content is similar in the two diets. In contrast to this, all three AGE types in the baked diet were dramatically increased compared to HF diet (A). CML concentration in AGE-RSA solution was significantly ($p<0.01$) higher compared to RSA solution (B). Each bar in (B) represents the mean ± SEM profile of 2 samples per group as calculated by Student's two-tailed unpaired t test. CML: N^{ε}-(Carboxymethyl)lysine, CEL: N^{ε}-(Carboxyethyl)lysine, MG-H1: methylglyoxal-derived hydroimidazolone 1, HF: high fat, B: baking, RSA: rat serum albumin.

3.3.2 Effect of high fat and AGEs on weight gain and liver

Feeding high fat for 40 weeks caused a massive increase in body weight and epidydimal fat mass compared to the mice fed on the standard chow for 40 weeks. Intraperitoneal injections of AGEs or feeding diet high in AGEs did not affect food or water intake (data not shown) or body weight gaining (Table 3.1). Non-fasting blood glucose concentration was similar (8.2 ± 2.10 mmol/L) between HF and AGE administered mice suggesting that these mice do not develop insulin resistance.

Table 3.1 Body, liver and epididymal fat weight and physical appearance of mice and macroscopic appearance of livers at 40 weeks of the experiment

Animal group	Body weight (g)	Liver weight (g)	Epididymal fat weight (g)
Standard chow	39.0 ± 1.5 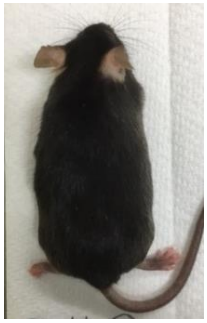	1.4 ± 0.0 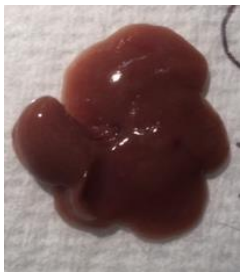	0.75 ± 0.1

HF	44.1 ± 1.8 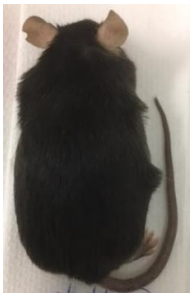	3.2 ± 0.2 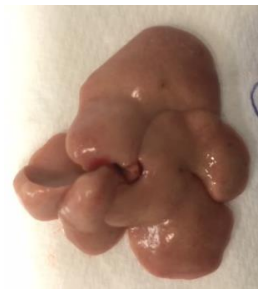	Not measured
HF + AGE (20 mg/kg bw)	45.9 ± 1.2 	3.3 ± 0.2 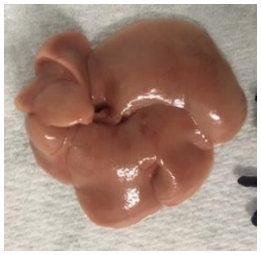	1.59 ± 0.1
HF + AGE (40 mg/kg bw)	46.8 ± 1.3 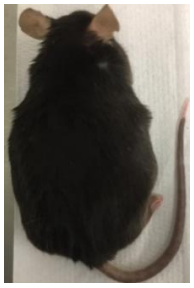	3.1 ± 0.0 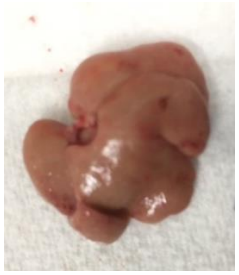	1.43 ± 0.2
HF + AGE (60 mg/kg bw)	43.8 ± 1.3 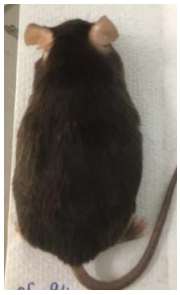	3.0 ± 0.0 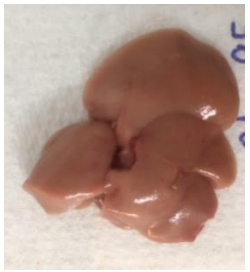	1.34 ± 0.1
HF + (HF+B)	46.4 ± 1.7 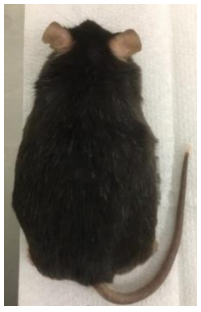	3.3 ± 0.2 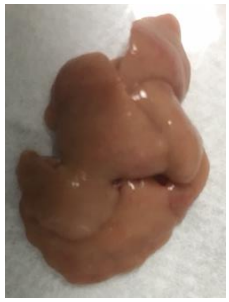	1.36 ± 0.1

3.3.3 Effect of high dietary AGEs on liver injury

Liver injury determined by liver function test showed standard chow fed mice had alanine aminotransferase (ALT) (Fig. 3.2A) and alkaline phosphatase (ALP) (Fig. 3.2B) in the normal range. However, mice fed the HF diet showed significantly ($p<0.05$) elevated ALT and ALP levels compared to standard chow fed mice. In the Figure, because the effect of three doses of AGEs on LFT's represented by green colour-bars was not different, they are indicated within brackets for clarity. Plasma ALT (Fig. 3.2A), but not ALP (Fig. 3.2B), levels were significantly ($p<0.05$) elevated in AGE injected mice compared to HF group. Importantly, mice fed the diet containing high AGEs (HF+B) in the last 10 weeks showed highest levels of ALT and ALP levels in plasma compared to HF group. Moreover, the enzyme levels were significantly ($p<0.05$) more elevated in the AGE (HF+B) fed mice than AGE injected mice. There were no significant differences in plasma AST, bilirubin and GGT levels between groups (data not shown).

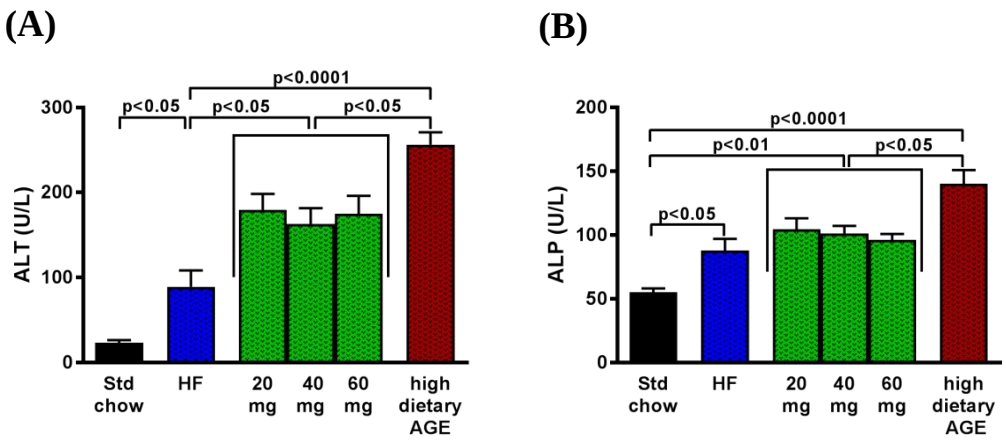

Figure 3.2 Plasma concentration of ALT and ALP in mice

Forty weeks of high fat feeding significantly ($p<0.05$) increased ALT (A) and ALP (B) enzyme concentration in plasma compared to those fed a standard chow diet. ALT levels were further increased ($p <0.05$) by i.p. injections (three doses are indicated within brackets for clarity) of AGEs compared to HF fed mice (A). In contrast, ALP concentration was not elevated by AGE injections compared to HF fed mice (B). However, the highest concentration of both ALT and ALP was found in the plasma of mice fed the high AGE (HF+B) diet for the last 10 weeks of the experiment with ALT showing a significance ($p<0.05$) compared to the IP treated group. Each bar represents the mean ± SEM profile of 10 mice per treatment group as calculated by one-way

ANOVA with Tukey's comparison test. Std chow: standard chow, HF: high fat diet, 20-60 mg AGEs: different AGE doses injected into HF fed mice, ALP: alkaline phosphatase, ALT: alanine aminotransferase.

3.3.4 Effects of AGEs on RAGE and LPS binding receptors

Whilst AGE injections did not increase RAGE, CD-14 and TLR-4 expression compared to the HF diet, mice fed the diet containing high AGEs showed the highest levels of the expression of these genes (Fig. 3.3). Whilst HF failed to up-regulate the expression of RAGE compared to std chow fed mice, it was significantly ($p<0.05$) up-regulated by i.p. AGEs compared to std chow fed mice, however, was not different from HF fed mice. Similar to ALT and ALP levels, RAGE expression was highest in HF+B fed mice which was significantly ($p<0.05$) more elevated than AGE injected mice (Fig. 3.3A).

Endotoxin responsive gene CD-14 was significantly ($p<0.01$) upregulated by HF feeding (Fig. 3.3B). However, endotoxin responsive gene TLR-4 was not significantly increased by HF diet compared standard chow fed mice. Although both i.p. and dietary AGEs increased RAGE, CD-14 and TLR-4 expression compared to standard chow fed mice, only TLR-4 showed a significantly ($p<0.0001$) elevated level compared to HF group (Fig. 3.3C).

(A)

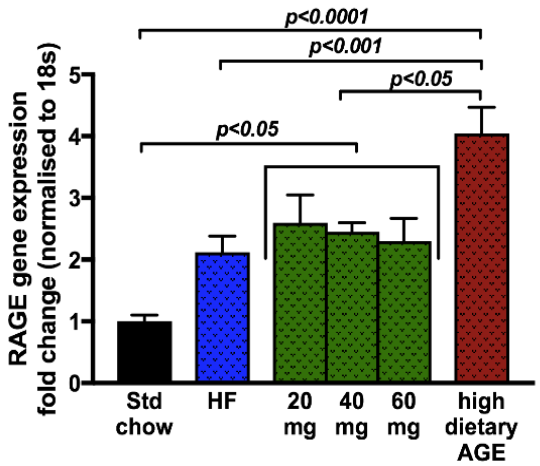

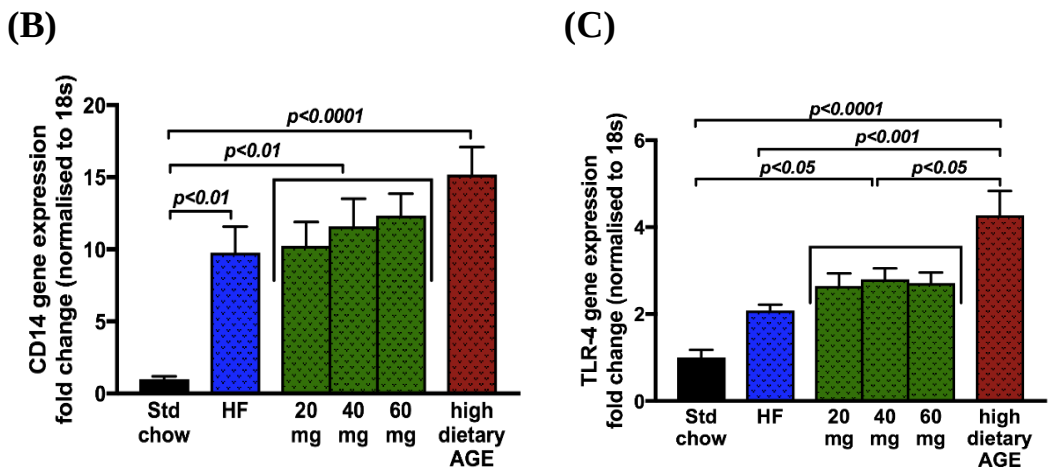

Figure 3.3 Liver gene expression of RAGE and LPS binding receptors

High fat feeding failed to increase RAGE (A) and TLR-4 (C), however, significantly increased endotoxin responsive gene CD-14 expression (B) compared to standard chow fed mice. Although AGE injections showed a significant increase in all three genes compared to standard chow fed mice, they were not significantly different from those of HF fed mice (three doses are indicated within brackets for clarity). However, dietary AGEs caused the highest expression of these genes with RAGE and TLR-4 being significantly ($p<0.05$) higher in dietary AGE group than standard chow and HF fed groups. The data have been normalised to endogenous control gene, 18S and std chow control group was given an arbitrary value of 1. Each bar represents the mean ± SEM profile of 10 mice per treatment group as calculated by one-way ANOVA with Tukey's comparison test. Std chow: standard chow, HF: high fat, 20-60 mg AGEs: different AGE doses injected into HF fed mice.

3.3.5 Effects of AGEs on pro-inflammatory cytokines and histology

Pro-inflammatory genes TNF-α (Fig. 3.4A) and MCP-1 (Fig. 3.4B) were significantly ($p<0.05$) increased by HF diet. Importantly, the expression of these genes was further elevated ($p<0.05$) by high dietary AGEs but not by i.p. AGEs compared to HF group (Fig. 3.4A, B). Evaluation of steatosis and inflammation using H&E staining showed normal histology at 40 weeks in standard chow fed animals (Fig. 3.4C). Compared to this, HF fed mice showed dramatic changes in histology with small (arrows) and large (arrow heads) fat vesicle formation representing steatosis. Hepatocyte ballooning was observed;

however, no inflammatory cell infiltration could be identified in HF diet fed mice livers (Fig. 3.4D). Liver histology showed some inflammatory cell infiltration (area marked by red line) and hepatocyte degeneration (area marked by green line) in AGE injected mice (data not quantified). However, despite the dose difference, there was no difference in histological changes in the liver between different doses of AGE injection (Fig. 3.4E-G). Most importantly, as reflected by elevated liver enzyme and gene expression profiles, there was an apparent and greater inflammatory cell infiltration in high AGE fed mice (HF+B) in the last 10 weeks (data not quantified) (Fig. 3.4H), suggesting these mice had worse liver injury compared to other groups.

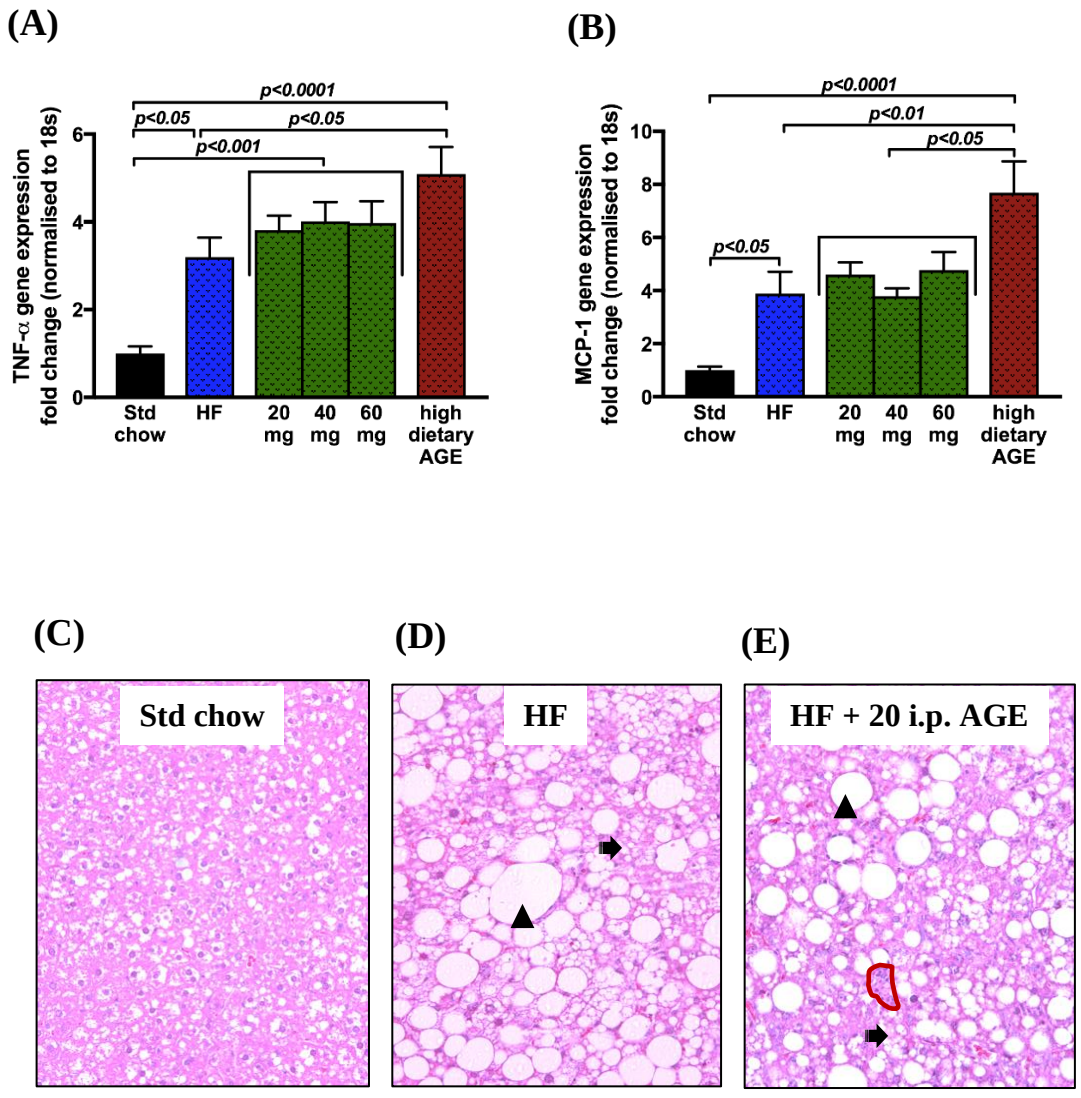

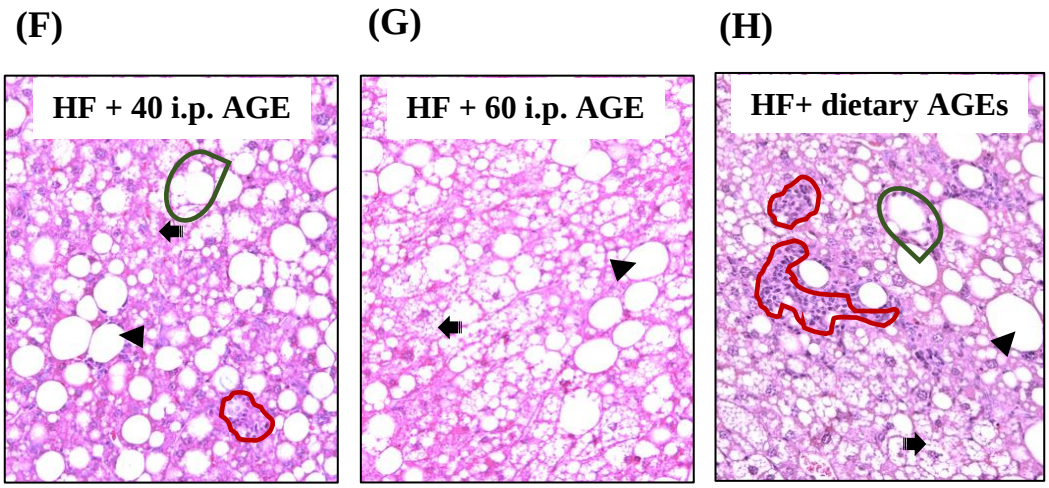

Figure 3.4 Liver gene expression of pro-inflammatory genes and H&E stained histological assessment of liver

High fat feeding significantly increased pro-inflammatory gene expression of TNF-α (A) and MCP-1 (B). Intraperitoneal injections of AGEs did not cause further increase (three doses are indicated within brackets for clarity). However, dietary AGEs showed the highest gene expression of TNF-α (A) and MCP-1 (B). The data have been normalised to endogenous control gene, 18S and std chow control group was given an arbitrary value of 1. Each bar represents the mean ± SEM profile of 10 mice per treatment group as calculated by one-way ANOVA with Tukey's comparison test. Inflammation determined by H&E staining did not show any change or inflammatory cell infiltration in standard chow fed mice (C). Forty weeks of HF feeding caused fat vesicle formation (steatosis) as well as hepatocyte ballooning but did not cause inflammatory cell infiltration (D). Ten weeks of AGE injections (E-G) showed all above changes including hepatocyte degeneration as well as small patches of inflammatory cell infiltration (data not quantified). However, there was an apparent and greater inflammatory cell infiltration in high AGE fed mice (HF+B) (data not quantified) (H). Arrows: small fat vesicles, arrow heads: large fat vesicles, area marked by red line: inflammatory cell infiltration, area marked by green line: hepatocyte degeneration. Magnification x200. Std chow: standard chow, HF: high fat diet, 20-60 mg AGEs: different AGE doses injected into HF fed mice.

3.3.6 Effects of AGEs on pro-fibrotic cytokines and HSC activation

Gene expression of HSC activation marker α-SMA was significantly ($p<0.05$) increased by AGE injection but not by HF feeding compared to standard chow fed mice (Fig. 3.5A), suggesting AGEs activate HSCs. However, mice fed the high dietary AGEs (HF+B) showed the highest α-SMA gene expression which was significantly ($p<0.05$) higher than that in the AGE injected mice. Activated HSCs secrete large amount of pro-fibrotic cytokines such as TGF-β1 and extracellular matrix proteins such as collagen. Although HF feeding significantly ($p<0.05$) increased the expression of TGF-β1 and collagen 1 genes compared to standard chow fed mice, i.p. AGEs did not further increase their expression (Fig. 3.5B, C). Importantly, similar to the expression of pro-inflammatory genes (see Fig. 3.4) and α-SMA, high AGE fed mice showed significant ($p<0.05$) increases in the expression of TGF-β1 and collagen 1 compared to HF group and AGE injected groups (Fig. 3.5B, C).

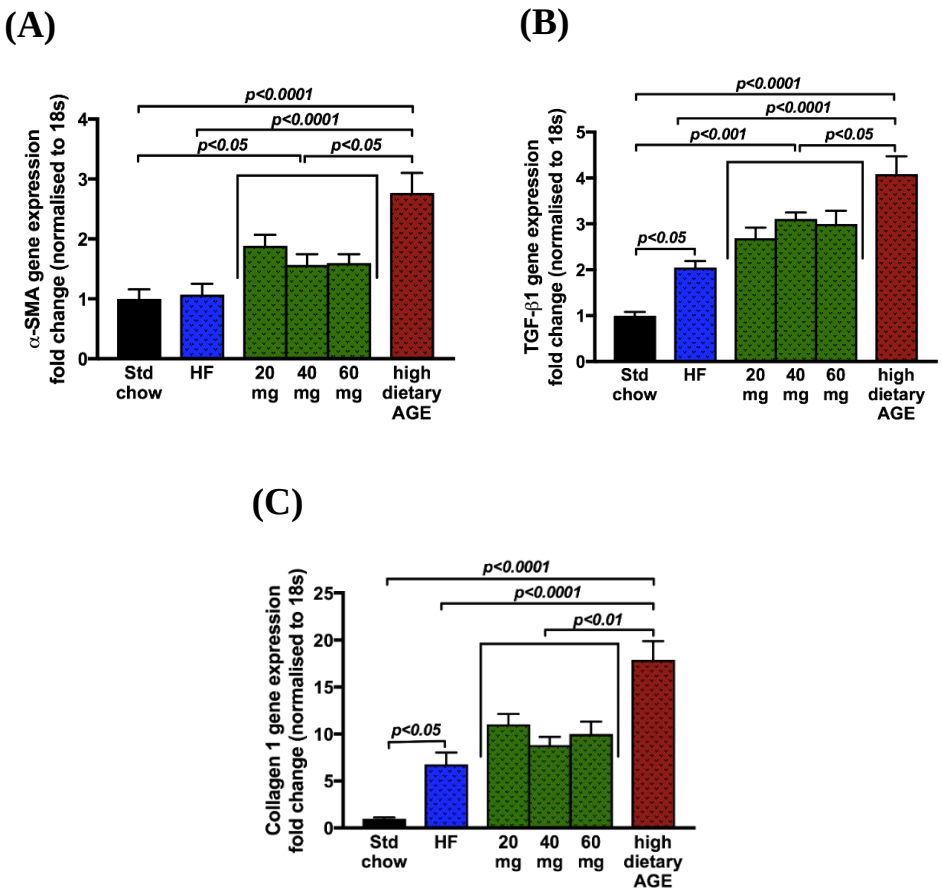

Figure 3.5 Gene expression of HSC activation marker and pro-fibrotic and fibrotic genes

Hepatic stellate cell activation marker α-SMA was not upregulated in HF fed mice compared to std chow fed mice. Although both i.p. and dietary AGEs significantly ($p<0.05$) increased its expression compared to std chow fed mice, AGE injections did not up-regulate α-SMA expression compared to HF fed mice (A). Both TGF-β1 (B) and collagen 1 (C) were significantly ($p<0.05$) increased in HF fed mice compared to std chow fed mice and did not further increase in AGE injected mice (three doses are indicated within brackets for clarity) compared to HF fed mice. Importantly, high dietary AGE fed mice showed the highest expression of α-SMA, TGF-β1 and collagen 1 which was significantly ($p<0.05$) higher than all other groups. The data have been normalised to endogenous control gene, 18S and std chow control group was given an arbitrary value of 1. Each bar represents the mean ± SEM profile of 10 mice per treatment group as calculated by one-way ANOVA with Tukey's comparison test. Std chow: standard chow, HF: high fat diet, 20-60 mg AGEs: different AGE doses injected into HF fed mice.

3.3.7 Effects of AGEs on liver fibrosis

Collagens are a major ECM protein in the fibrotic liver. Standard chow fed mice did not show any collagen deposition as reflected by no positive staining of picrosirius red staining of liver sections (Fig. 3.6A). Moreover, as discussed in the previous section, standard chow fed mice did not show fat vesicles. Livers of HF fed mice showed red fibres and enlarged hepatocytes to some extent (Fig. 3.6B). However, mouse livers after AGE injections showed a greater extent of fibrosis with river-delta pattern, but similar to HF fed mice and between different i.p. AGE doses (Fig. 3.6C-E). Importantly, as reflected by gene expression and liver enzyme profiles, mice fed the high AGE diet (HF+B) for the last 10 weeks of the experiment showed the highest positive staining (Fig. 3.6F) with significant ($p<0.05$) increase of fibrosis compared to AGE injected mice (Fig. 3.6G).

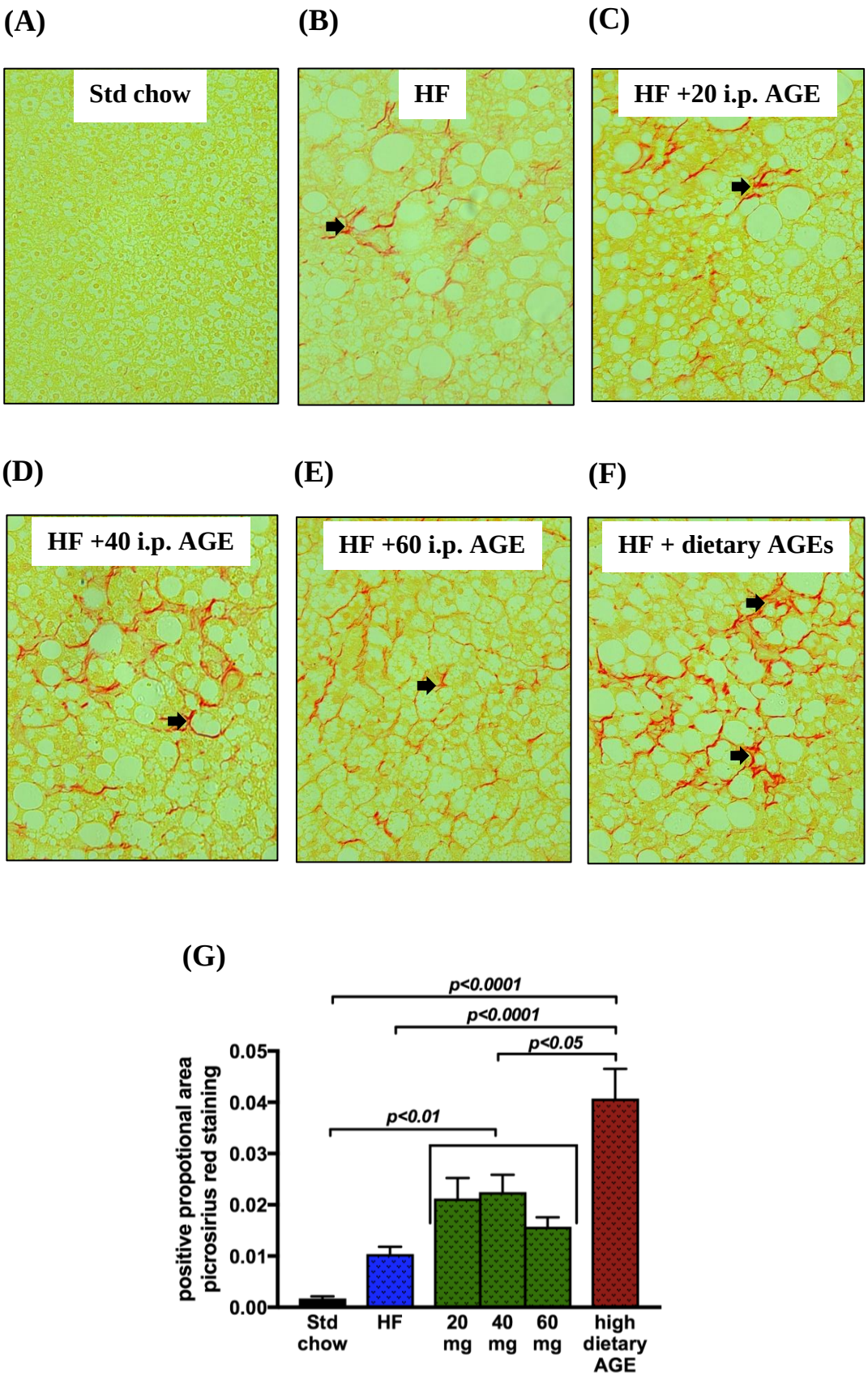

Figure 3.6 Quantification and comparison of liver fibrosis between endogenous and dietary AGE fed mice using picrosirius red staining

Standard chow fed mice (A) did not show any sign of fat accumulation or fibrosis while HF (B) feeding caused mild fibrosis but this was not significant compared to std chow fed mice (G). All three doses of i.p. injections of AGEs (C-E) increased fibrosis, which was significantly ($p<0.01$) higher than that of std chow fed mice. However, high dietary AGE (F) feeding showed the highest positive staining with a significant ($p<0.05$) increase compared to AGE injected mice (G). Each bar represents the mean ± SEM profile of 10 mice per treatment group as calculated by one-way ANOVA with Tukey's comparison test. Arrows: pericellular fibrosis. Magnification x200. Std chow: standard chow, HF: high fat, 20-60 mg AGEs: different AGE doses injected into HF fed mice.

3.3.8 Effects of AGEs on RAGE and pro-inflammatory gene expression by Kupffer cells (KUP5)

We conducted a time course study with different doses of AGEs and LPS (a positive control), to investigate appropriate incubation time for RAGE, TNF-α and IL-1β gene expression induction. KUP5 cells grown for 24 hours and treated with AGEs for 6, 12, 24, 48 or 72 hours did not show RAGE, IL-1β (data not shown) or TNF-α up-regulation at any time point in response to AGEs (Fig. 3.7). However, LPS at 5 and 10 ng/mL doses increased TNF-α and IL-1β gene expression compared to untreated cells (UT) within the first 12 hours (Fig. 3.7A and B show TNF-α as an example); however, their expression was diminished beyond 12 hours, likely due to dying KUP5 cells. Moreover, LPS did not up-regulate RAGE gene expression at any time point (data not shown).

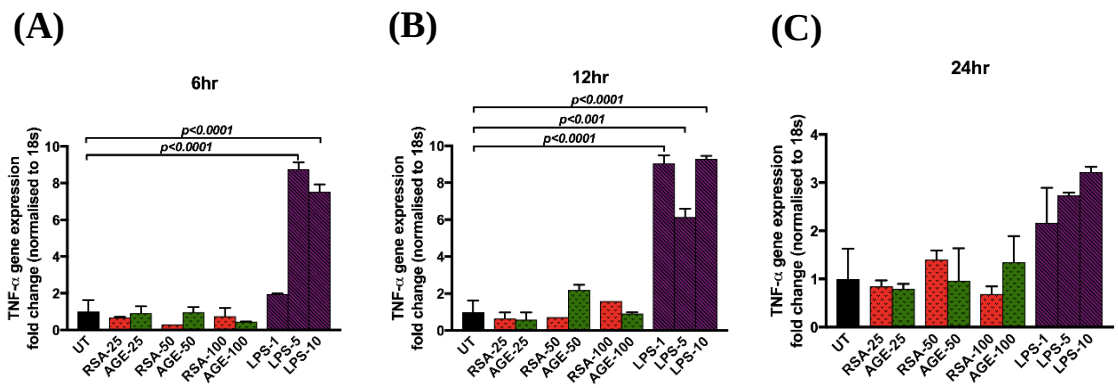

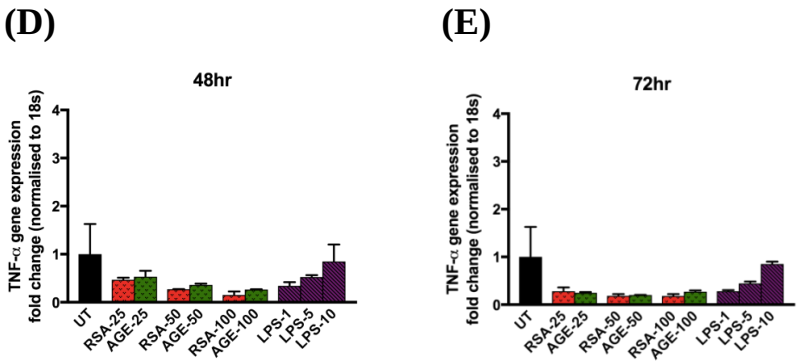

Figure 3.7 Time course study to investigate gene expression of TNF-α by KUP5 cells exposed to AGEs and LPS at varying doses over different time points

Gene expression of TNF-α did not up-regulate by AGEs at any treated doses whereas LPS showed an increased expression up to 12 hours (A, B). The data have been normalized to endogenous control gene, 18S and UT control was given an arbitrary value of 1. Each bar represents the mean ± SEM profile from 1-3 independent experiments as calculated by one-way ANOVA with Tukey's comparison test. UT: untreated cells, RSA: rat serum albumin, LPS: lipopolysaccharide.

Since KUP5 cells did not respond to AGEs at any dose or at any time point, we then evaluated the effect of AGEs on RAGE and TNF-α gene expression by changing cell growing time and treatment duration. First, we reduced the growing time of the cells to 12 hours and treated cells with AGEs for 6 and 12 hours at 50 µg/mL and 200 µg/mL doses. In this experiment we found that the positive control LPS (5 ng/mL) treatment increased TNF-α gene expression at both time points (data not shown). However, AGEs still failed to induce the gene expression of RAGE or TNF-α (data not shown). We then employed 6 hour growing time and treatment with AGEs at two different doses; 50 µg/mL and 200 µg/mL for 6 and 12 hours.

We found that KUP5 cells, grown for 6 hours and exposed to AGEs for 6 hours, showed a significant ($p<0.01$) increase in RAGE expression (Fig. 3.8) at 200 µg/mL dose. However, treatment with AGEs at 50 µg/mL did not up-regulate RAGE gene expression. Therefore, we selected 6 hours growing time, 6 hours treatment time with 200 µg/mL dose of AGEs for further experiments.

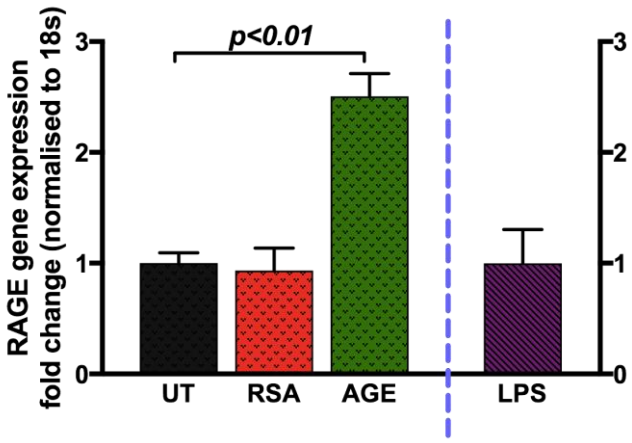

Figure 3.8 Gene expression of RAGE by KUP5 cells exposed to AGEs for 6 hours

Gene expression of RAGE was significantly ($p<0.01$) increased after exposing KUP5 cells to AGEs at 200 μg/mL dose for 6 hours compared to untreated or RSA treated cells. Positive control LPS indicated at right Y axis did not affect RAGE gene expression. The data have been normalized to endogenous control gene, 18S and UT control was given an arbitrary value of 1. Each bar represents the mean ± SEM profile from 3 independent experiments as calculated by one-way ANOVA with Tukey's comparison test. UT: untreated cells, RSA: rat serum albumin, LPS: lipopolysaccharide.

Similar to up-regulated RAGE expression, gene expression of pro-inflammatory cytokines also increased in KUP5 cells exposed to AGEs for 6 hours. Thus, the expression of TNF-α (Fig. 3.9A), MCP-1 (Fig. 3.9B), IL-1β (Fig. 3.9C) and IL-6 (Fig. 3.9D) genes was significantly ($p<0.05$) increased in response to AGE treatment compared to UT or RSA treated cells. Moreover, there was a massive up-regulation of cytokine expression by KUP5 cells in response to the positive control LPS and is plotted on the right Y axis (Fig. 3.9 A-D).

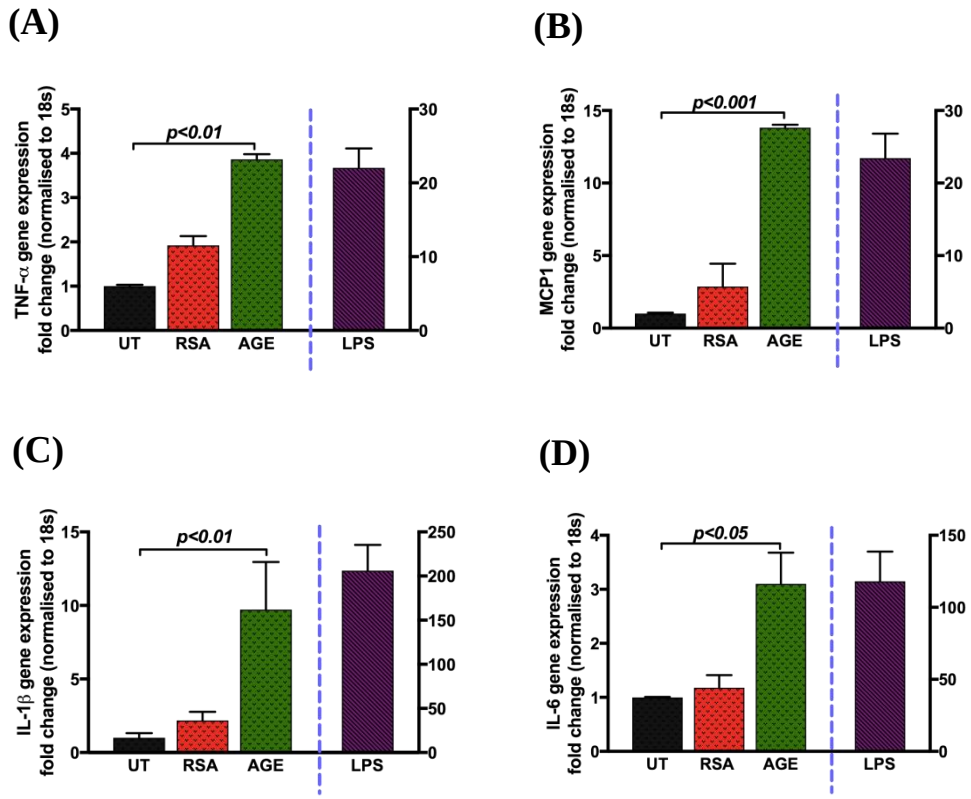

Figure 3.9 Gene expression of pro-inflammatory cytokines by KUP5 cells exposed to AGEs for 6 hours

Pro-inflammatory gene expression (A-D) were significantly ($p<0.05$) increased after exposing KUP5 cells to AGEs at 200 μg/mL dose for 6 hours compared to untreated or RSA treated cells. Positive control LPS induced gene expression is indicated on the right Y axis in a different scale as cytokine expression in response to LPS was dramatically increased. The data have been normalized to endogenous control gene, 18S and UT control was given an arbitrary value of 1. Each bar represents the mean ± SEM profile from 3 independent experiments as calculated by one-way ANOVA with Tukey's comparison test. UT: untreated cells, RSA: rat serum albumin, LPS: lipopolysaccharide.

3.3.9 Effects of AGEs on ROS generation by Kupffer cells (KUP5)

Reactive oxygen species (ROS) generated by NADPH oxidase or NOX activity function as key secondary messengers in numerous downstream signalling pathways in liver inflammation and fibrosis. We therefore assessed gene expression of the regulatory subunit $p47^{phox}$ which translocates to the cell membrane for enzyme activity, thus acting

as a rate limiting subunit, and membrane-bound catalytic subunit gp91^{phox}/NOX-2 and vascular isoforms paralogs to NOX-2, NOX-1 and NOX-4.[351] Both NOX-2 and NOX-4, as well as regulatory subunit p47^{phox} were significantly ($p<0.05$) upregulated in KUP5 cells treated with AGEs (Fig. 3.10A- C), however, the expression of NOX-1 was not affected (Fig. 3.10D).

We then investigated real-time ROS generation by Kupffer cells exposed to AGEs for 150 minutes and found ROS generation was increased in the first 10 minutes and then decreased with time (Fig. 3.10E). Importantly, we found that AGE exposure significantly ($p<0.05$) increased ROS generation in KUP5 cells compared to untreated or RSA treated cells and the level attained with AGEs was almost similar to ROS production in response to LPS (Fig. 3.10F).

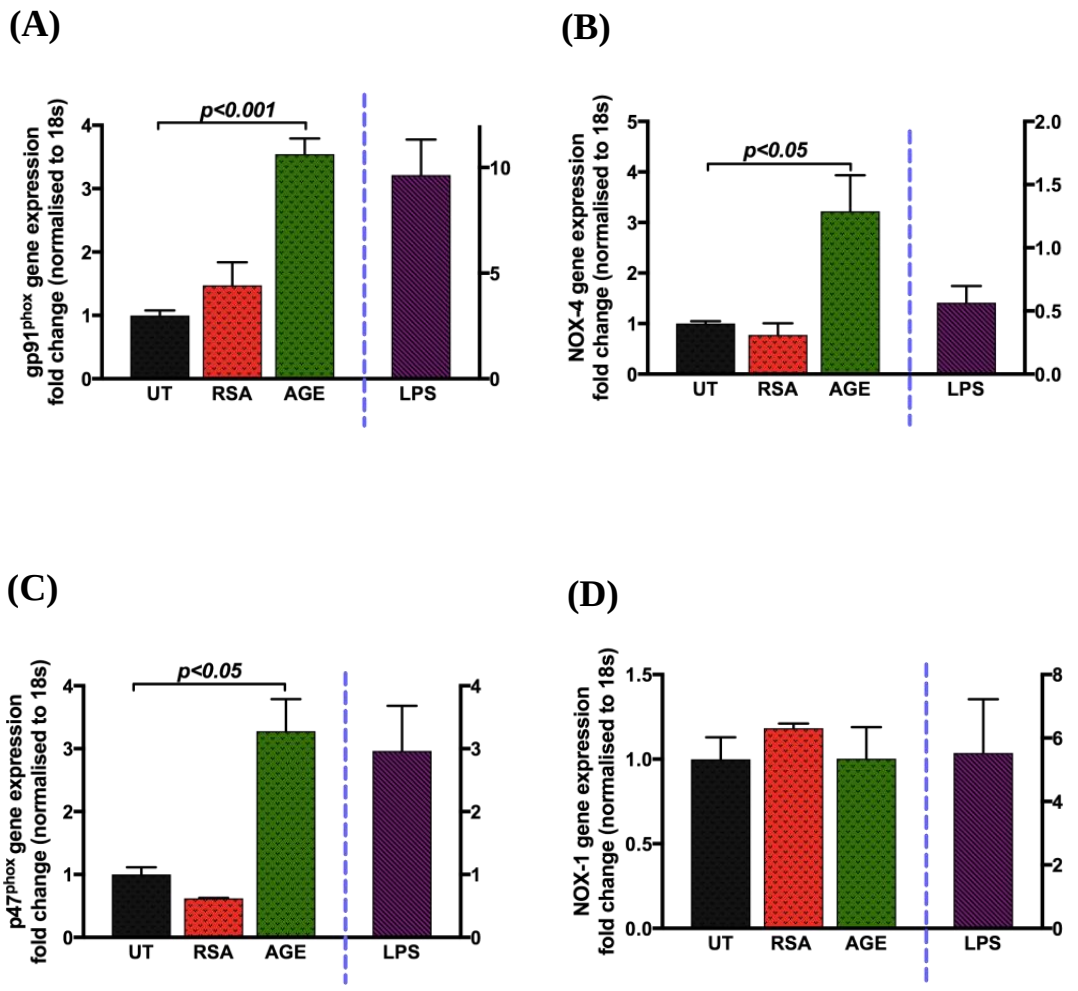

(E)

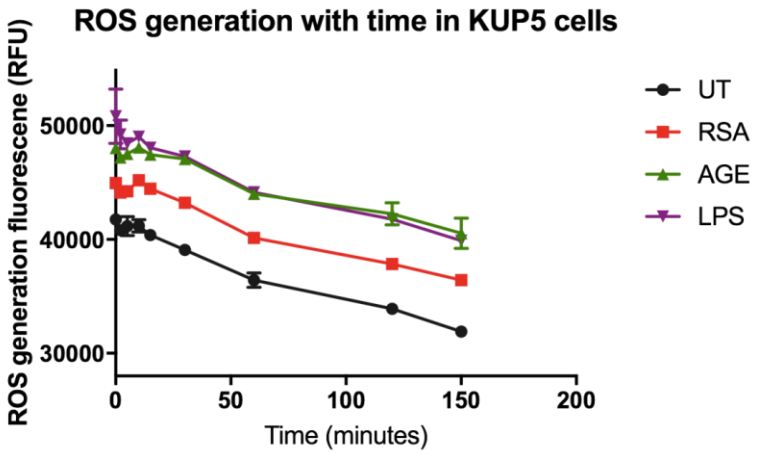

(F)

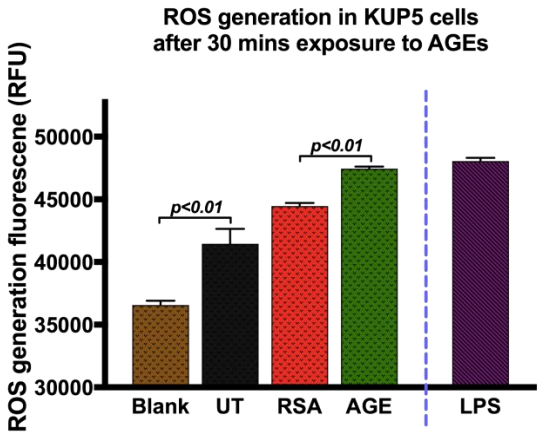

Figure 3.10 Gene expression of NOX enzyme subunits and real time ROS generation by KUP5 cells in the presence of AGEs

AGEs significantly ($p<0.05$) increased gene expression of subunits of $gp91^{phox}$/ NOX-2 (A) NOX-4 (B) and $p47^{phox}$(C) whilst it did not affect NOX-1 expression (D). The positive control LPS, however, increased the expression of $gp91^{phox}$ and NOX-1. Real time ROS generation measured using a 2,7-DCFDA showed the highest ROS generation by both AGEs and LPS in 10 minutes and then it gradually decreased over time (E). ROS generation analysed at 30 minutes showed that AGEs generated significantly ($p<0.01$) higher ROS compared to those generated by untreated cells or cells treated with RSA (F). Gene expression data (A-D) have been normalized to endogenous control gene, 18S and UT control was given an arbitrary value of 1. Each bar represents the mean $\pm$ SEM profile

from 3 independent experiments as calculated by one-way ANOVA with Tukey's comparison test. UT: untreated, RSA: rat serum albumin, LPS: lipopolysaccharide.

3.3.10 Effects of AGEs on HSCs (LX2)

Since LX2 cells are myofibroblastic cells that secrete ECM, we investigated the effect of AGE exposure on these cells. The time-course experiment with a potent activator of HSCs, TGF-β1, showed that this pro-fibrotic cytokine activates α-SMA gene expression by LX2 cells after 6 hours of incubation (Fig. 3.11B). In contrast, AGEs did not activate LX2 cells at any time point (Fig. 3.11A-D).

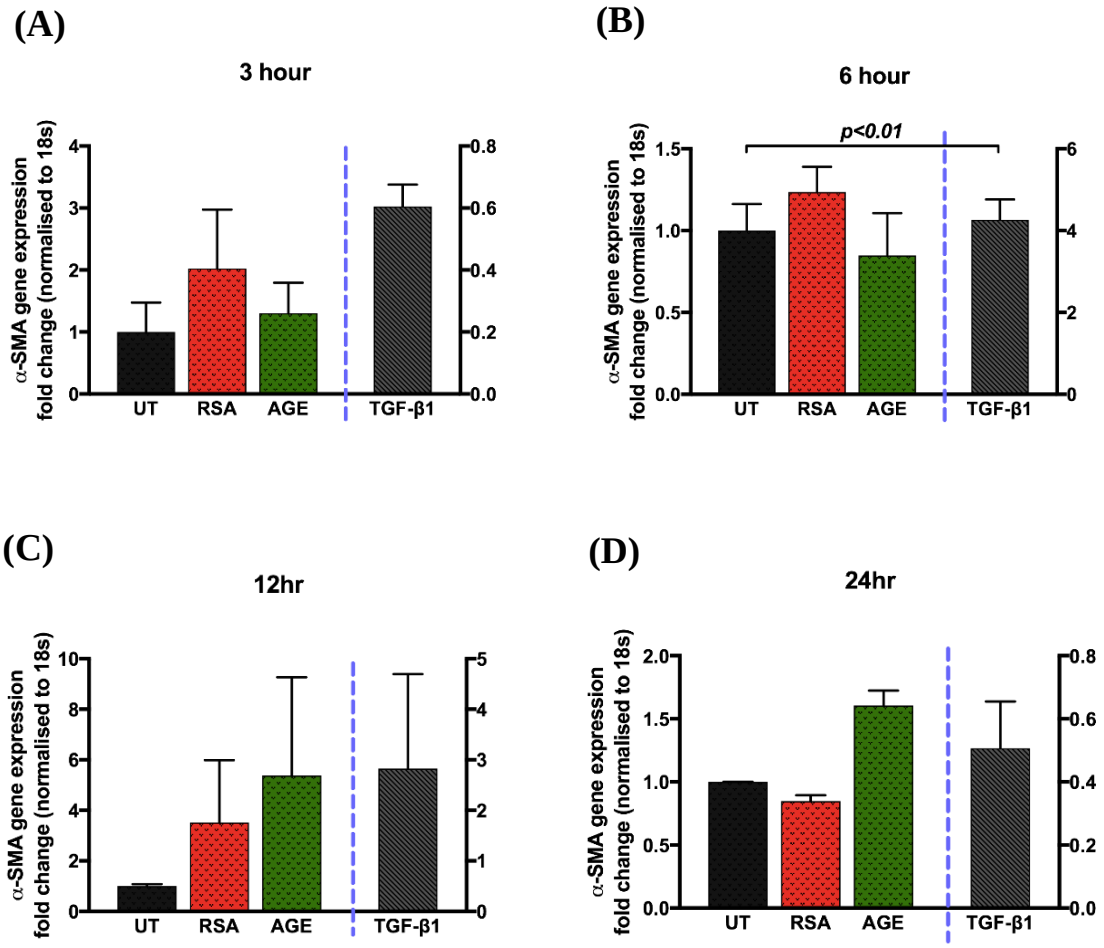

Figure 3.11 Gene expression of HSC marker gene α-SMA by LX2 cells exposed to AGEs at different time points

Hepatic stellate cell activation marker, α-SMA gene expression was not up-regulated by AGEs, or the positive control and also a potent pro-fibrotic cytokine TGF-β1 after treating the cells for 3 hours (A), 12 hours (C) or 24 hours (D). However, cells treated for 6 hours with TGF-β1 showed significantly ($p<0.01$) increased α-SMA gene expression as shown on the right Y axis in a different scale (B). The data have been normalized to endogenous control gene, 18S and UT control was given an arbitrary value of 1. Each bar represents the mean ± SEM profile from 3 independent experiments as calculated by one-way ANOVA with Tukey's comparison test. UT: untreated cells, RSA: rat serum albumin, TGF-β1: transforming growth factor-β1.

Since we failed to detect increased expression of α-SMA in cells treated with AGEs, we decided to treat LX2 cells with the conditioned medium from KUP cells which had been treated with AGEs. In marked contrast, we found that there was an increased expression of α-SMA by LX2 cells when these cells were treated with the conditioned media collected from AGE-treated KUP5 cells (Fig. 3.12), suggesting that products secreted by KUP5 cells, possibly the cytokines, activated LX2 cells.

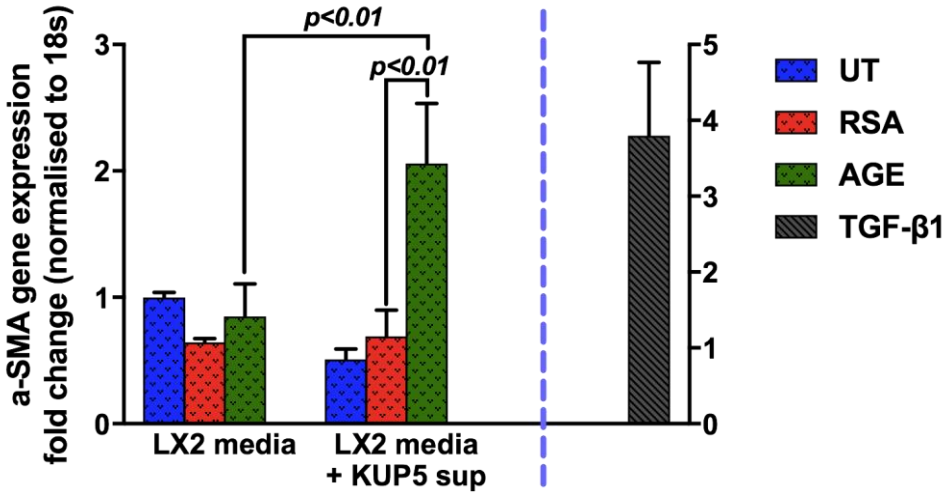

Figure 3.12 Gene expression of α-SMA by LX2 cells exposed to AGEs and conditioned media collected from AGE-treated KUP5 cells.

Hepatic stellate cell activation marker, α-SMA gene expression was not upregulated by AGE treatments. However, cells treated for 6 hours with the conditioned media collected from AGE-treated KUP5 cells showed a significantly ($p<0.01$) increased α-SMA gene

expression compared to AGE treated LX2 cells in the absence of conditioned media as well as conditioned media collected from UT or RSA treated KUP5 cells. Positive control TGF-β1 induced gene expression is shown on right Y axis in a different scale. The data have been normalized to endogenous control gene, 18S and UT control was given an arbitrary value of 1. Each bar represents the mean ± SEM profile from 3 independent experiments as calculated by one-way ANOVA with Tukey's comparison test. UT: untreated cells, RSA: rat serum albumin, TGF-β1: transforming growth factor-β1.

3.4 Discussion

This study was carried out to investigate and compare the effects of endogenous and dietary AGEs on NAFLD progression to NASH and liver fibrosis in mice and to explore mechanistic insights. Our group has previously shown that feeding AGEs for 33 weeks in fatty liver mice induces fibrosis,[212] and injecting AGEs to bile duct ligated rats with liver injury augmented liver fibrosis.[210] However, this is the first study to document the effects of AGEs in a 40 weeks HF model and to explore the effects of endogenous versus dietary AGEs. After 40 weeks, liver enzyme levels were elevated in HF fed mice compared to standard chow fed mice, suggesting that this diet causes liver injury in mice. This is in keeping with our published work which reported an elevated ALT levels in 33 weeks model of HF feeding.[212] One of the key findings of this study was that mice fed the high AGE diet had greater liver fibrosis compared to AGE injected mice. In keeping with this, administration of oral AGEs increased the expression of RAGE, liver inflammatory cell infiltration and pro-inflammatory cytokine expression compared to those of HF fed or AGE injected mice.

Increased expression of RAGE and pro-inflammatory cytokines in the liver of mice fed the high AGE diet, along with our previous findings,[212] are likely to be a major driving force for HSC activation, as reflected by increased α-SMA gene expression. Activated HSCs led to an increased secretion of pro-fibrotic cytokine TGF-β1 in high AGE fed mice, which is a key stimulus for ECM deposition since TGF-β1 is a critical regulator of liver fibrosis.[352] Gene expression of collagen 1, a major component of ECM, also showed a similar pattern to TGF-β1. In contrast, even though i.p. AGEs elevated plasma ALT levels compared to HF fed mice, they did not affect gene expression of RAGE, pro-

inflammatory or pro-fibrotic cytokines. In keeping with these findings, i.p. AGEs failed to cause a significant exacerbation in liver fibrosis compared to HF fed mice as assessed by picrosirius red staining, whilst mice fed the high AGE diet showed a dramatic increase in fibrosis which was much higher than those of AGE injected mice. This suggest that dietary AGEs play a more harmful role in liver inflammation and fibrosis.

A few factors may have affected this difference between oral AGEs and i.p. AGEs. An obvious factor is a difference of the doses between oral and i.p. AGEs. However, we prepared i.p. AGEs according to the oral AGE intake of a mouse within a day, so that the i.p. dose of 40 mg/kg/day is roughly equal to the AGE content received from the diet. Since this dose of i.p. AGEs or the higher dose did not affect liver fibrosis, the dose factor can be eliminated. However, it has been suggested that in addition to quantity of AGEs, the rate of AGE accumulation is also related to the severity of the diseases.[8] In this study, the rate of AGE accumulation was very different in mice fed the high AGE diet as AGEs are added to the system throughout the day whereas i.p. AGEs were added once. Dietary AGEs which are bound to proteins are usually digested by proteases in the gut, releasing modified (glycated) lysine or arginine which are then absorbed into the circulation. This might be a reason for the differential effects we saw between oral and i.p. AGEs.

Most AGEs that have been parenterally administered are cleared by Kupffer cells and hepatic sinusoidal endothelial cells.[353] However, this elimination may be different if intestinal permeability is elevated with oral AGEs.[354] Therefore, in this experiment the elimination of i.p. AGEs may be more efficient than dietary AGEs. In high AGE fed mice this may lead to accumulation of AGEs in hepatic cells for a prolonged period of time before they are eliminated from the body.

It is important to mention that dietary AGEs likely play a prominent role in NAFLD progression to liver fibrosis because AGEs not only have direct effects on liver cells, including the Kupffer cells, but may also affect the integrity of the gut and probably the microbiota.[148] Disrupted intestinal permeability allows LPS derived from microbiota to translocate to portal blood stream which then stimulate the LPS binding receptors present on the membrane of hepatic cells, in particular, the Kupffer cells.[212] In support of this, LPS binding receptors CD-14 and TLR-4 were significantly upregulated in mice fed the high AGE diet but not in mice intraperitoneally administered AGEs, suggesting that the livers of high AGE fed mice may have been exposed to LPS. In this experiment, mice

administered with AGEs via the i.p. route did not or barely showed elevated expression of LPS responsive receptors, suggesting that the livers of these mice are unlikely to have been exposed to LPS. It is therefore possible that in addition to direct effects on the liver, oral AGEs may also have a plethora of effects in the gut and perhaps on the integrity of the microbiota whilst i.p. AGEs are unlikely to cause similar pathological changes in the gut as this route bypasses gut absorption.

In vitro experiments carried out using immortalized Kupffer cell line, KUP5 cells, showed significant increases in gene expression of pro-inflammatory genes such as TNF-α, MCP-1 and interleukins when exposed to high AGEs compared to untreated or vehicle treated cells. These findings agree with published work which showed the interaction of AGEs with its receptors promotes the transcription of genes that control inflammation.[355,356] One of the most important consequences of RAGE activation by binding to AGEs is the generation of ROS which in turn affect the rate of formation of AGEs in the body.[357] In keeping with published work by others and our laboratory using primary Kupffer cells[212] as well as HSCs,[286] in the present studies we showed that AGEs generate large amounts of ROS in cultured Kupffer cells. ROS generation was a rapid response to AGEs or LPS but gradually reduced with time. The NOX enzyme consists of membrane-bound catalytic subunits, and cytosolic regulatory subunits that need to be translocated into the membrane for enzyme assembly and activity. The NOX enzyme plays an important role in the defence mechanism and is abundantly expressed in macrophages such as the Kupffer cells, the liver resident macrophages as well as in other liver cell types.[37,351] The findings show gene expression of membrane-bound catalytic subunits of NOX-2 and NOX-4 as well as the cytosolic regulatory subunit $p47^{phox}$ of NOX enzyme was increased in response to AGEs treatment compared to untreated or vehicle treated cells. In line with this, positive control LPS caused upregulation of membrane-bound NOX-2 and cytosolic regulatory subunit $p47^{phox}$. However, the expression of NOX-1 subunit, which was increased in response to LPS, was not affected by AGEs, suggesting a differential regulation of NOX subunit expression and ROS generation. Nevertheless, we show that AGEs are a potent stimulant of ROS generation and oxidative stress, forming a vicious cycle of RAGE upregulation, which could be a key mechanism that propagates liver inflammation and NAFLD progression to liver fibrosis.

Despite the effects of AGEs in stimulating pro-inflammatory gene expression and ROS generation by Kupffer cells, they failed to directly activate myfibroblastic HSCs. This contrasted with published work by other investigators, who reported that AGEs increased the activation of HSCs.[287,358] However, in these studies they used different types of immortalised and primary HSCs and this may have led to the differences between the current study and those published previously. Another possible reason may be that the cells in these published works were pre-activated by cell culture medium and/or culture on plastic plates and this may have caused the cells to become responsive to exogenous AGEs. In marked contrast, in the present study, the HSCs which did not directly respond to exogenous AGEs, were activated by the addition of conditioned media collected from AGEs-treated KUP5 cells as reflected by increased expression of α-SMA. This phenomenon fits nicely with the hypothesis that Kupffer cells, which highly express RAGE and are the first line of defence in the liver, react with AGEs, causing widespread inflammatory milieu and oxidative stress.[359] This in turn activates myofibroblastic HSCs which then begin to secrete pro-fibrotic cytokines such as TGF-β1 (see Figure 3.12), a potent cytokine that activates and perpetuates activated HCS phenotype causing uninterrupted liver fibrosis. We could not see this effect in AGE injected mice, perhaps because the injected dose was not able to induce Kupffer cells without an additional stimulation for example by cytokines and LPS derived from a leaky gut.

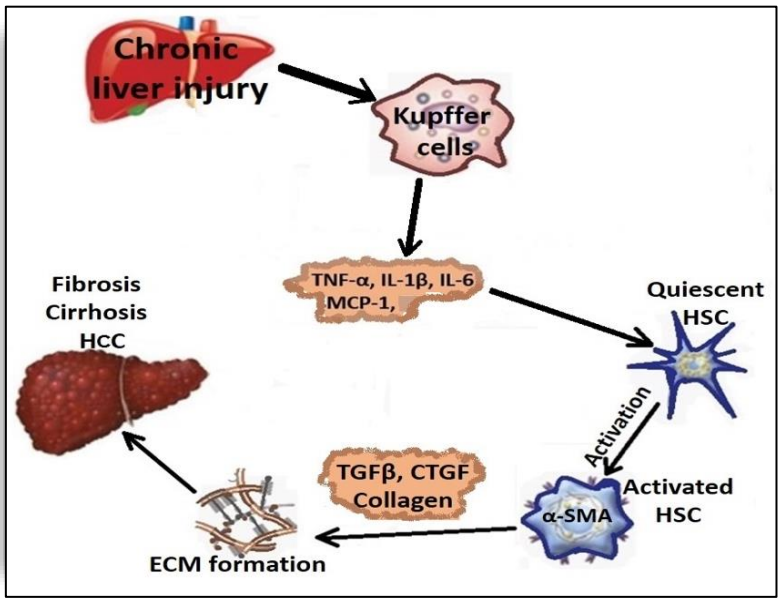

Figure 3.13 Proposed mechanism by which AGE-induced Kupffer cells activate HSCs

In conclusion, dietary AGEs play a critical role in the progression of NAFLD to liver fibrosis. The major cell type which is responsible for AGE elimination is liver resident macrophages known as Kupffer cells and therefore, these cells appear to act as the first line of defence against AGEs. However, by binding to its cell surface receptor RAGE, AGEs cause the activation of Kupffer cells, leading to the generation of ROS and oxidative stress which in turn leads to the secretion of large amounts of pro-inflammatory cytokines. This in turn activates HSCs, which respond with a continuous deposition of ECM, causing NAFLD progression to liver fibrosis.

Dietary AGEs contribute to NAFLD progression whilst i.p. AGEs have minimal effects on plasma ALT levels. However, it appears that dietary AGEs have more powerful effects in this process because unlike endogenously derived AGEs, AGEs derived from diet may also have detrimental effects on gut homeostasis and integrity of the microbiota, causing leaky gut and thus, exposing the liver to gut derived toxins in addition to direct AGE effects on the liver. Therefore, consumption of dietary AGEs may have more harmful effects on NAFLD progression to liver fibrosis than endogenously derived AGEs.

CHAPTER 4

Effects of advanced glycation end products (AGEs) on diabetic fatty liver in a mouse model of non-alcoholic fatty liver disease

4.1 Introduction

It was shown in chapter 3 that AGEs augment the progression of non-alcoholic fatty liver disease (NAFLD) to liver fibrosis where dietary AGEs having more remarkable effects than endogenous AGEs administered by means of intraperitoneal (i.p.) injections. In that study, both dietary and intraperitoneal AGEs were given to high fat (HF) fed mice from week 30 to week 40 for comparison and the doses of i.p. AGEs administered were in a range that was comparable to AGEs concentrations found in diabetic patients. However, unhealthy dietary habits are usually commenced at an early stage of life. Therefore, a series of experiments described in this chapter was designed on the basis of the results obtained in chapter 3 to address the next relevant question i.e. the effect of high dietary AGEs ingested throughout life. Therefore, in this study, mice were fed the diet containing high AGEs throughout the 40 weeks of the experimental period.

Intraperitoneal injections of AGEs that were given to HF fed mice in chapter 3 were to mimic the endogenous AGEs that could be derived as a result of hyperglycaemia in diabetic subjects. AGEs are formed at a lower rate in healthy individuals, and the rate is accelerated in diabetic conditions due to elevated level of sugar.[360] There are numerous studies that have used diabetic models to study the effects of AGEs in a range of diseases including renal deseases,[361,362] cardiovascular diseases[363] and neurodegenerative diseases.[364] Most NAFLD patients have diabetes and this makes their condition worse.[365]

However, the dietary interventions for diabetic patients have focused mainly on reducing sugar consumption and balanced diets and paid less attention on reducing the consumption of AGEs.[366,367] Furthermore, there are very limited studies that investigated the effects of a high AGE diet which would be expected to exacerbate disease progression in diabetes. For these reasons, it was important to study the effects of AGEs on diabetic fatty liver, and therefore, one of the objectives of this study was to study the effects of AGEs on diabetic fatty liver and compare the outcome with those of diabetes alone.

Most of the harmful effects of AGEs are mediated via their receptors. The receptor for AGEs (RAGE) is the best characterized receptor among many AGE receptors described in chapter 1.[368] RAGE is expressed on a number of cell types in the liver including Kupffer cells and hepatic stellate cells (HSCs),[369] but usually at low levels under physiological conditions. However, RAGE expression is increased when its ligands accumulate or when its regulatory transcription factors are activated. Interaction of AGEs with RAGE appears to induce several signalling pathways in vast range of diseases including diabetic nephropathy, retinopathy, cardiovascular diseases, Alzheimer and other neurodegenerative disease and other inflammatory diseases,[7,370-372] RAGE has been shown to play a role in liver disease,[373] including a role in liver-transplanted patients[374] and it inhibits regeneration after massive liver injuries.[375] In fibrogenesis, there have been a number of studies demonstrating the importance of RAGE in the pathogenesis of extracellular matrix (ECM) expansion in a variety of tissues, including the kidney, peritoneal membrane and heart.[376] In addition, animal studies have shown that blockade of RAGE protects against acute liver injury[377] as well as long term NAFLD associated fibrosis.[212] Therefore, the second objective of this study was to investigate whether RAGE contributes to AGE-induced NAFLD progression and whether these AGE effects could be ameliorated by blocking RAGE at the cellular level.

4.2 Materials and Methods

4.2.1 Experimental design

Six to eight weeks old male C57BL/6 mice were randomized into 2 groups and fed on either high fat (HF) diet or HF+B (HF baked=high AGE diet) diet for 40 weeks. One group of mice from each diet was made diabetic at 15 weeks of the diet using streptozotocin (STZ) as outlined in chapter 2.

1) HF (high fat fed non-diabetic mice)

2) HF+D (high fat fed diabetic mice)

3) HF+B (high fat baked/high AGE diet fed non-diabetic mice)

4) HF+B+D (high AGE fed diabetic mice)

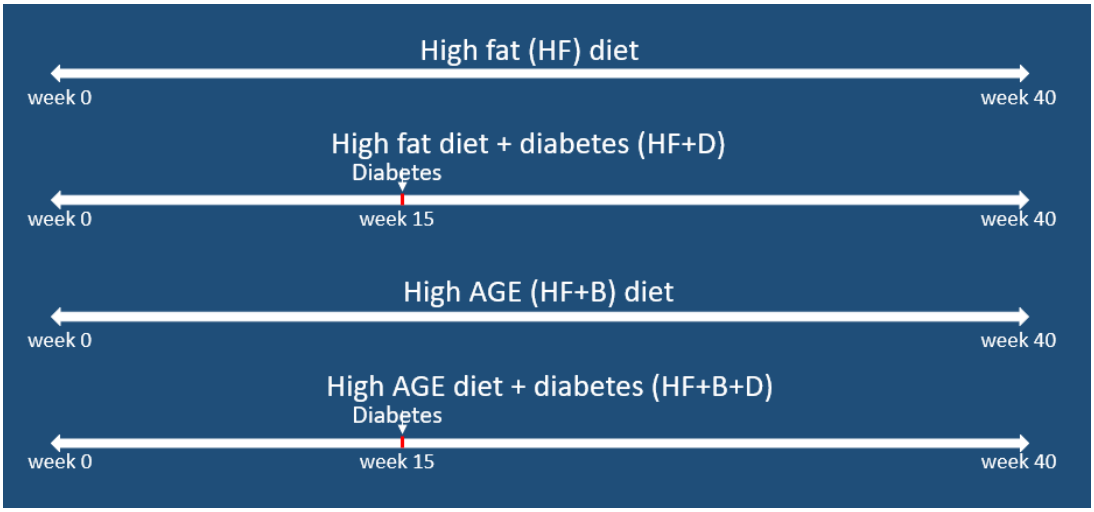

Additionally, to study the role of RAGE, RAGE knockout ($RAGE^{-/-}$) mice were used. These mice were used with kind permission of Prof Angelika Bierhaus, University of Heidelberg, Germany and bred in the BRF at Austin Health. Only male mice were allocated for the study and they were maintained in similar conditions as wild type (WT) mice. Since we have previously studied $RAGE^{-/-}$ mice in a short-term NAFLD model in

the absence of diabetes,[212] in this study, two groups (n=10per group) of RAGE$^{-/-}$ mice were fed on either the HF or HF+B diet for 40 weeks and made diabetic similar to control WT mice.

1) HF WT
2) HF+D WT
3) HF+D RAGE$^{-/-}$
4) HF+B+D WT
5) HF+B+D RAGE$^{-/-}$

4.2.2 Induction of diabetes

As in published studies,[348] diabetes was induced using STZ (Sigma Aldrich) by destroying some population of pancreatic β cells as described in detail in section 2.2.4 of chapter 2. Briefly, blood glucose in mice was measured at 15 weeks after diet. Then, they were fasted overnight, and body weights were measured. STZ was injected according to individual body weight as per the calculation given in chapter 2. This procedure was repeated the following day and measurement of blood glucose was commenced after 5 days and repeated every two weeks to confirm diabetes.

4.2.3 Preparation of AGEs in the diet

Dietary AGE content was increased by baking at 160^{0} C for 1 hour. CML N$^{\varepsilon}$(1-carboxymethyl)-L-lysin, CEL N$^{\varepsilon}$(1-carboxyethyl)-L-lysin and MG-H1 (methylglyoxal-derived hydroimidazolone 1) content in the diet was assessed by gas chromatography/mass spectrometry (GC/MS).

4.2.4 Tissue harvesting and storage

The animals were sacrificed at 40 weeks using pentobarbitone (120 mg/kg bw) as described in chapter 2. Blood and livers were collected from the anesthetized mice as described in chapter 2.

4.2.5 Biochemical assessment of liver function

Liver function test was carried out in plasma that had been stored at -20^{o} C, using Beckman Coulter LX20 autoanalyzer (Beckman Coulter) at Austin Pathology, Austin Health.

4.2.6 Plasma CML concentration measurement

Plasma CML concentration was measured using Cirulex anti-CML mouse antibody ELISA kit (MBL international) following manufacturer's protocol. Briefly, samples were diluted with dilution buffer provided and added to both anti-CML-BSA and BSA coated microplates and incubated at room temperature (RT) for 60 minutes. The plates were washed and incubated with HRP conjugated antibody for 60 minutes at RT, followed by incubation with substrate reagent for 15 minutes at RT. Then, stop solution was added and the absorption was measured immediately at 450/540 nm wavelengths. The difference between absorption reading of CML-BSA coated microplate and BSA coated microplate was calculated to determine CML concentration using a standard curve.

4.2.7 Liver gene expression

Total RNA was extracted from snap-frozen liver samples stored at -80^{o} C as described in chapter 2.6. cDNA was synthesized from this RNA and qPCR reactions were carried out using multiplexing to assess the expression of RAGE, lipopolysaccharide (LPS) binding receptors, pro-inflammatory and pro-fibrotic genes. The details of dual fluorescent-labelled oligonucleotide probes and primers are given in Table 2.4 in chapter 2.

4.2.8 Histological assessment of liver injury and fibrosis

Haemotoxylin and Eosin (H&E) staining

Haemotoxylin and Eosin staining was performed on 4 µm liver sections as described in section 2.7.2 in chapter 2.

Picrosirius red staining

Picrosirius red staining was performed on 4 µm liver sections as described in section 2.7.1 in chapter 2. Briefly, total collagen was quantified by analysing liver sections under a standard light microscope (Olympus BX50 Microscope, Japan; magnification x200). Collagen volume fraction was determined by measuring the area of stained tissue (red) within a randomly selected field. A total of 10 fields per section were analysed per section using computerized image capture (MCID) (Imaging Research, Canada). The mean value was calculated per animal and treated as one observation for statistical analysis, and results are expressed as a proportional positively stained (red) area.

4.2.9 4-hydroxynonenal (4-HNE) immunohistochemistry for lipid peroxidation

Marker of lipid peroxidation, 4-HNE was assessed using 4 µm sections of mouse liver tissues as described in section 2.7.3.4. Primary antibody of 4-HNE (Alpha Diagnostic International) was applied in 1:100 dilutions for overnight and secondary antibody (Dako, Agilent technology) was used in 1:100 dilution. The positive staining in each section was determined using MCID (Imaging Research, Canada) software at x200 magnification. A total of 10 fields per section were analysed per animal. The mean value was calculated per animal and treated as one observation for statistical analysis. The results are expressed as a proportional positively stained (brown) area.

4.2.10 Cell culture experiments

Immortalized murine Kupffer cell line (KUP5 cells)[349] that has been used for experiments described in chapter 3 was used in this study. Since these cells exposed to 200 µg/mL of AGEs induced RAGE and pro-inflammatory cytokine expression (chapter 3), in the present studies, the cells were treated with two RAGE antagonists; RAGE antagonist peptide (RAP) (Sigma Aldrich) and FPS-ZMI (Sigma Aldrich) at the same time when AGEs were added. After 6 hours of treatment, the cells were tested for gene expression to investigate if blockade of RAGE could inhibit or reduce AGE-induced gene expression of the cytokines.

4.2.11 Statistical analysis

Results are expressed as mean ± standard error of means (SEM) unless otherwise stated. Data were analysed by one-way or repeated measures analysis of variance (ANOVA) with Tukey's post-hoc. A p value of less than 0.05 was considered statistically significant. Statistical analyses were performed using GraphPad Prism 7 software (GraphPad Software, CA, USA).

4.3 Results

4.3.1 AGE content in the baked diet and injectable AGEs

Baking at 160° C for 1 hour increased three common AGE types, CML, CEL and MG-H1 more than 100%, as measured by GC/MS (Fig. 4.1). Note: no statistical analysis was performed as food samples were pooled across before GC/MS analysis.

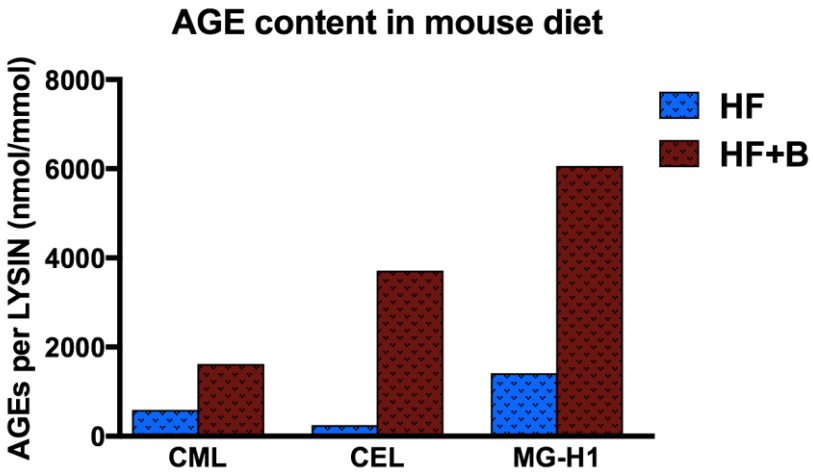

Figure 4.1 AGE content in mouse diets
All three AGE types in the diet were increased with baking. The fold change in CEL and MG-H1 were much dramatic compared to the increase of CML level. CML: N^{ε}-(carboxymethyl)Lysine, CEL: N^{ε}-(Carboxyethyl)Lysine, MG-H1: methylglyoxal-derived hydroimidazolone 1, HF-high fat, B-baking.

4.3.2 Effects of AGEs on physical parameters, liver macroscopic appearance and biochemistry

The initial body weight of the mice in all groups were similar and increased in a similar pattern up to 15 weeks irrespective of the AGE content in the diet. However, after the induction of diabetes at 15 weeks, the STZ injected mice started to lose weight due to diabetes. The weight loss in these mice was a dramatic drop in the first 3-4 weeks after induction of diabetes and gradually slowed down, and about 10 weeks after diabetes induction, it reached a plateau (Fig. 4.2). Blood glucose levels were similar between two diabetic groups (HF+D and HF+B+D). Similar to body weight pattern, liver weight also was higher in non-diabetic mice compared to diabetic mice, with no difference between HF or HF+B groups (Table 4.1).

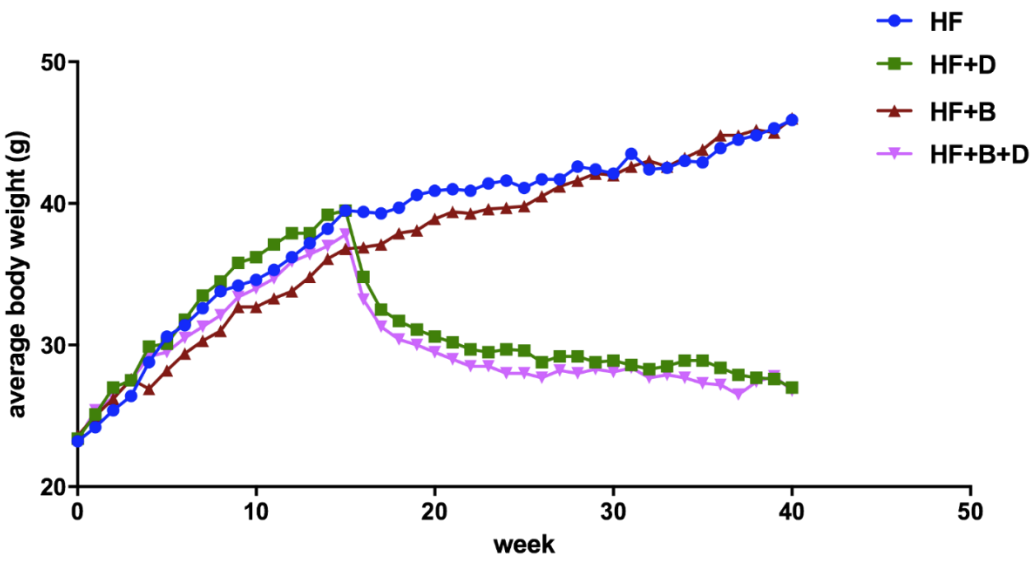

Figure 4.2 Body weight with time in mice fed different diets in the presence and absence of diabetes

Non-diabetic mice fed on both HF and HF+B gradually increased body weight and tend to continue until the end of the experiment, whereas diabetic mice gained body weight until they were rendered diabetic and then they lost body weight dramatically in the first few weeks but reached a level at which it was maintained till the end of the experiment. Each point represents the mean profile of 10-15 mice per treatment group. HF-high fat, D-diabetes, B-baking.

Table 4.1 Body weight and liver weigh of mice fed with different diets in the presence and absence of diabetes

Mice group	Body weight(g)	Liver weight(g)	Epidydimal fat mass (g)	Blood glucose (mmol/L)
HF	45.9 ± 1.3	3.18 ± 0.3	Not measured	9.9 ± 0.8
HF+D	27.0 ± 0.9	3.04 ± 0.2	Not measured	>33.3
HF+B	46.0 ± 1.3	3.50 ± 0.3	1.2 ± 0.1	10.1 ± 1.0
HF+B+D	26.8 ± 1.1	4.10 ± 0.2	0.1	>33.3

Liver injury determined by liver function tests showed that diabetes alone did not increase alanine aminotransferase (ALT) (Fig. 4.3A) and alkaline phosphatase (ALP) (Fig. 4.3B) compared to HF fed mice. In fact, ALT showed a decreased trend in HF+D mice. In contrast, both high AGE fed groups of mice (HF+B and HF+B+D) increased both ALT and ALP concentration in plasma which was significantly ($p<0.05$) higher compared to both HF and HF+D groups of mice, corroborating the findings in chapter 3. Whilst there was no difference in plasma ALT levels between two high AGE fed groups, plasma ALP levels were much higher in diabetic mice fed on the high AGE diet, suggesting an additive effect of diabetes on ALP levels in mice fed the high AGE diet.

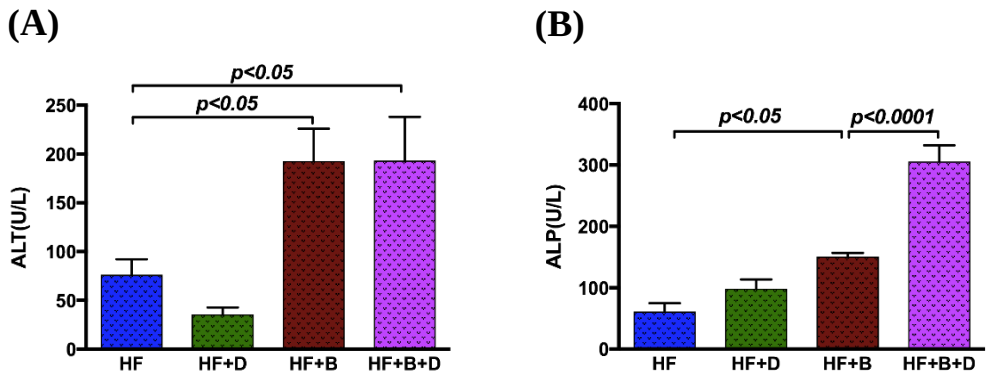

Figure 4.3 Plasma concentration of ALT and ALP in mice

Diabetes alone did not increase plasma concentration of liver enzymes. However, 40 weeks of high AGE feeding significantly increased ALT (A) and ALP (B) enzyme concentration in plasma compared to HF fed mice. ALP (B) levels were further increased by diabetes in mice fed the high AGE diet. Each bar represents the mean +/- SEM profile of 10-15 mice per treatment group as calculated by one-way ANOVA with Tukey's comparison test. HF-high fat, D-diabetes, B-baking.

4.3.3 Tissue CML accumulation and RAGE up-regulation

We also measured the plasma CML concentration in mice and found HF fed mice had the lowest CML concentration. Both diabetes and high AGE consumption increased circulating CML level in plasma which was reflected by significant ($p<0.01$) increase of CML in plasma of HF+D and HF+B mice (Fig. 4.4A). Moreover, diabetic mice receiving dietary AGEs (HF+B+D) showed the highest CML concentration as expected (Fig. 4.4A). We showed in chapter 3 that i.p. AGE administration could up-regulate RAGE gene expression. In this experiment, in keeping with CML concentration, gene expression of RAGE was up-regulated in both endogenous AGE group (HF+D) and high dietary AGE groups (HF+B and HF+B+D), suggesting that the liver has exposed to high AGE levels. Interestingly, diabetic mice fed the high AGE diet (HF+B+D) showed the highest expression of RAGE, suggesting that the livers of these mice were continuously exposed to AGEs coming from both dietary and endogenous sources (Fig. 4.4B). Moreover, we found that there was a strong positive correlation of plasma AGE/CML levels and liver RAGE expression (Fig. 4.4C).

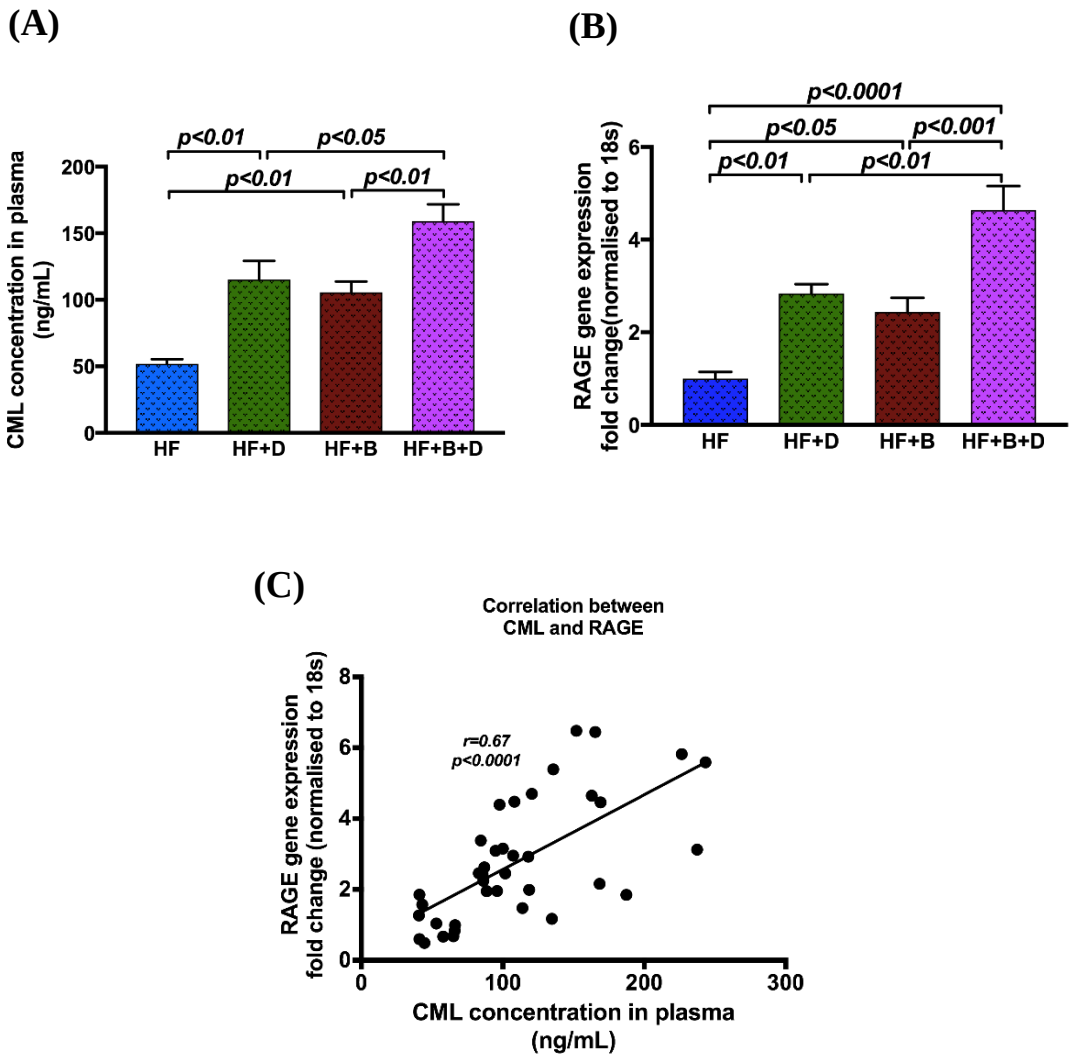

Figure 4.4 Liver gene expression of RAGE and plasma CML concentration

Both diabetes and high dietary AGEs significantly increased plasma CML concentration compared to HF fed mice (A). HF+B+D mice showed the highest CML concentration, suggesting the exposure of livers to AGEs derived from both endogenously as well as via the diet. Expression of RAGE showed a similar pattern to plasma CML levels (B). Plasma CML levels were positively and significantly correlated with liver RAGE expression (C), suggesting that circulating AGEs, produced in the circulation of diabetic animals as well as derived from high AGE diet, stimulate liver RAGE expression. The data have been normalized to endogenous control gene, 18S and HF control group was given an arbitrary value of 1. Each bar represents the mean +/- SEM profile of 10-15 mice per treatment group as calculated by one-way ANOVA with Tukey's comparison test. HF: high fat, D: diabetes, B: baking.

4.3.4 Effects of AGEs on LPS binding receptors

In keeping with plasma CML levels and RAGE expression, the LPS binding cell surface molecule of CD-14 was significantly ($p<0.05$) up-regulated in high dietary AGE groups compared to the HF fed animals (Fig. 4.5A). The LPS binding receptor TLR-4 was increased in both diabetes and high dietary AGE groups, with no difference between HF+B and HF+B+D groups of mice (Fig. 4.5B). However, although not different from HF+D and HF+B groups, CD-14 showed the highest expression in HF+B+D mice, probably suggesting that the livers of mice exposed to the highest amount of CML have the highest CD-14 expression, suggesting that CML contributes to the leaky gut which in turn increase the bacterial translocation to circulation, which in turn increased liver exposure to LPS.

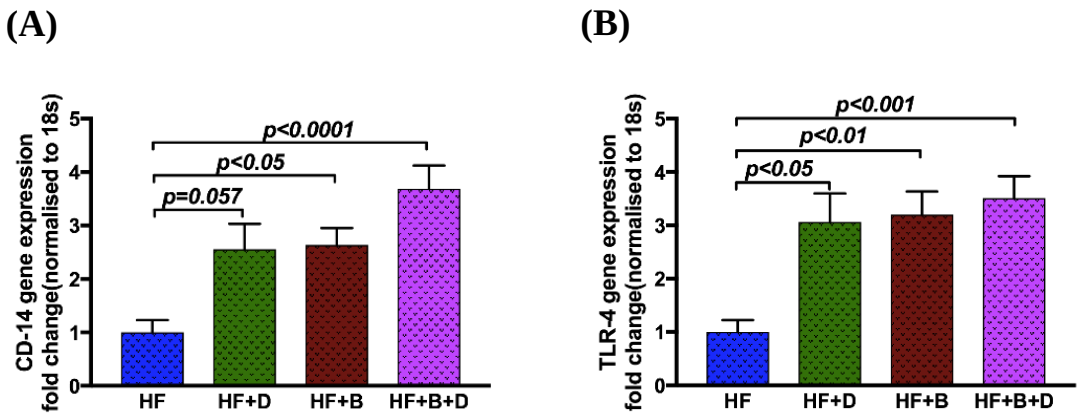

Figure 4.5 Liver gene expression of LPS binding receptors

Whilst only high AGE feeding significantly ($p<0.05$) increased gene expression of cell surface LPS binding receptor CD-14 (A) compared to HF fed mice, LPS binding receptor of TLR-4 (B) was significantly increased in mice exposed to both types of AGEs (HF+D, HF+B). However, high dietary AGEs + diabetes showed the highest expression of both genes. The data have been normalized to endogenous control gene, 18S and HF control group was given an arbitrary value of 1. Each bar represents the mean +/- SEM profile of 10-15 mice per treatment group as calculated by one-way ANOVA with Tukey's comparison test. HF: high fat, D: diabetes, B: baking.

4.3.5 Effects of AGEs on pro-inflammatory cytokine expression and inflammatory cell infiltration

All four inflammatory genes, TNF-α ($p<0.0001$), MCP-1($p<0.05$), IL-6 ($p<0.05$) and IL-1β were significantly ($p<0.0001$) increased by both diabetes and dietary AGEs compared to HF feeding alone (Fig. 4.6). However, there were no significant differences among different groups of AGE exposure i.e. diabetes versus dietary AGEs. Moreover, the livers of mice exposed to both endogenous and dietary AGEs did not show any additive effect on cytokine expression.

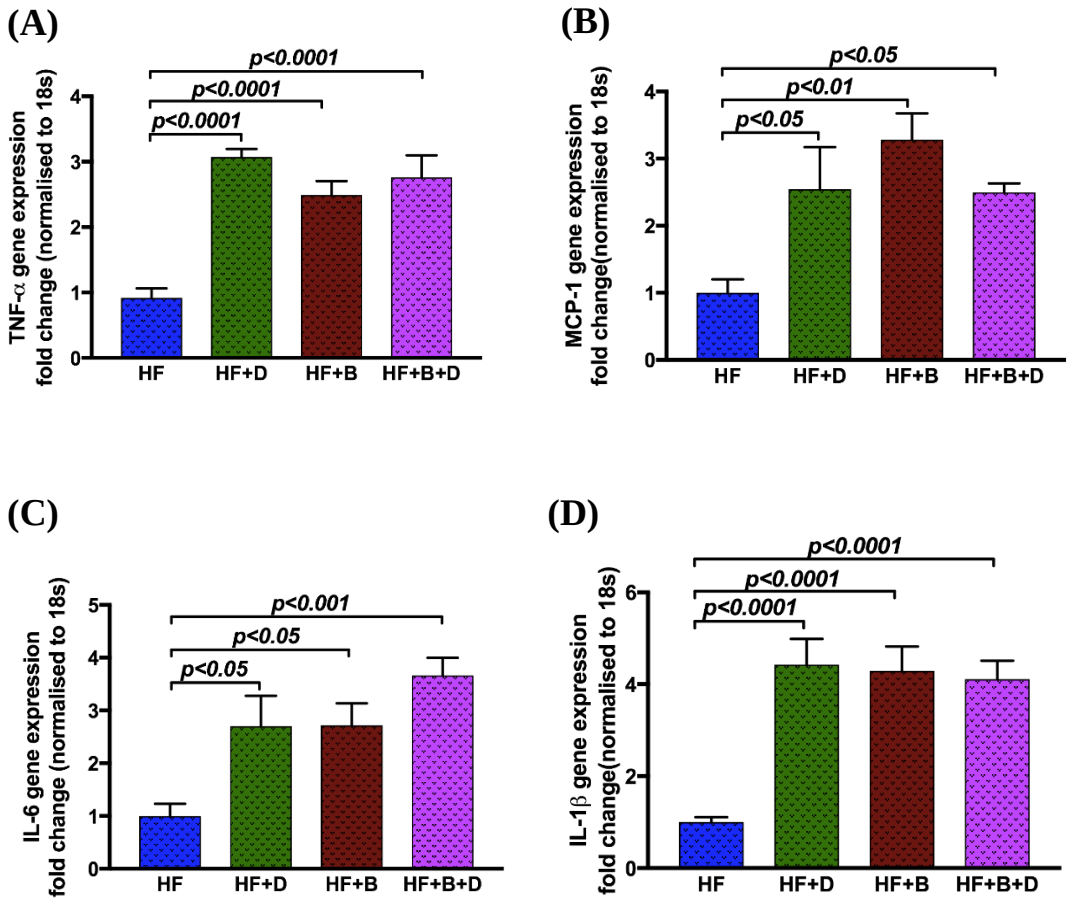

Figure 4.6 Liver gene expression of pro-inflammatory cytokines

Diabetes and dietary AGEs significantly increased pro-inflammatory cytokine expression compared to HF fed mice. However, there was no difference between diabetes and dietary AGEs on cytokine expression. The data have been normalized to endogenous control gene, 18S and HF diet control group was given an arbitrary value of 1. Each bar represents the mean +/- SEM profile of 10-15 mice per treatment group as calculated by one-way ANOVA with Tukey's comparison test. HF: high fat, D: diabetes, B: baking.

Evaluation of steatosis and inflammation using H&E staining showed 40 weeks of HF feeding caused dramatic changes in histology with numerous micro (arrows) and macro-fat vesicle formation (arrow heads), representing steatosis (Fig. 4.7A). There was also noticeable of hepatocyte ballooning; however, no inflammatory cell infiltration could be identified in HF diet fed mice livers. There was however hepatocyte degeneration in HF fed mice livers (area marked by green colour). In keeping with inflammatory cytokine gene expression profiles (see Figure 4.6), liver histology showed inflammatory cell infiltration (area marked by red colour) in both diabetic (Fig. 4.7B) and high dietary AGE fed mice (Fig. 4.7C) with micro- and macro-vesicular steatosis similar to HF fed mice livers. However, although not quantified, there was apparent increase in inflammatory cell infiltration in mice fed the high AGE diet in the presence or absence of diabetes (Fig. 4.7C, D) compared to diabetic mice fed the HF diet (Fig. 4.7B).

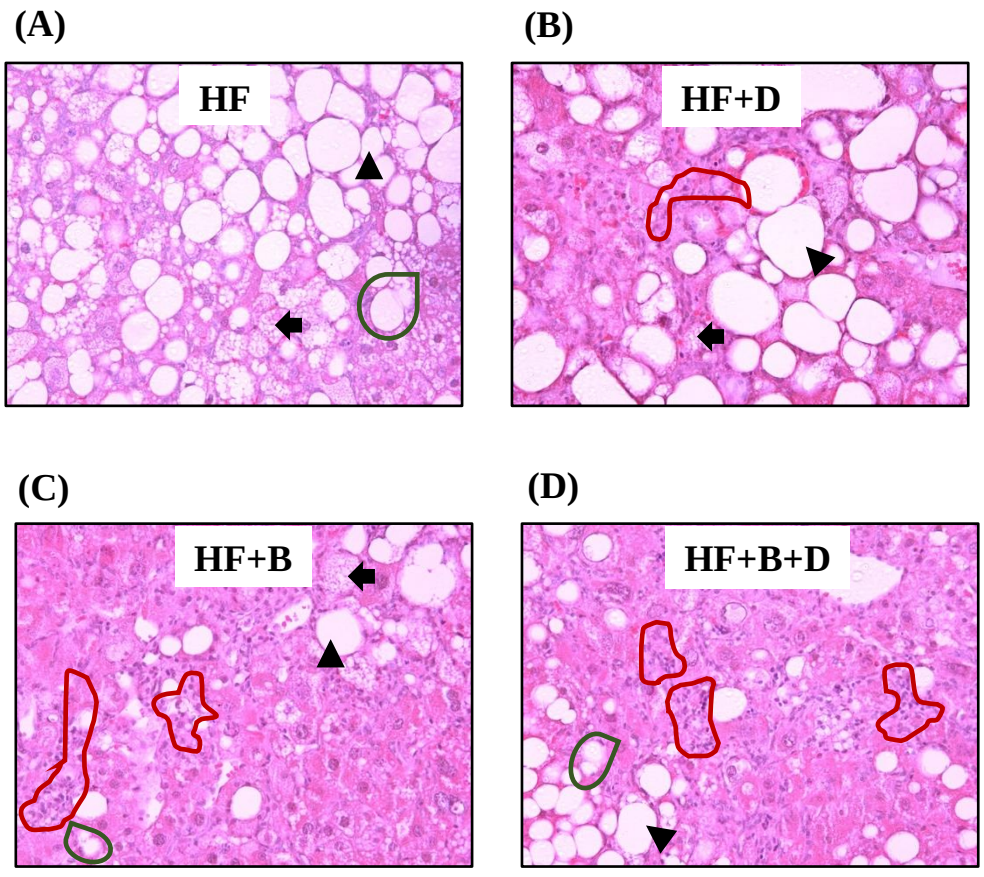

Figure 4.7 H&E stained histological assessment of liver

Inflammation determined by H&E staining showed 40 weeks of high fat feeding caused micro- and macro-fat vesicle formation (steatosis) as well as hepatocyte ballooning, but no inflammatory cell infiltration (A). Administration of AGEs by means of both diabetes and diet (B to D) showed all of above hepatocyte changes including hepatocyte degeneration as well as inflammatory cell infiltration with the highest inflammatory cell infiltration noticed in mice fed the high AGE diet. Arrows: micro-vesicular steatosis, arrow heads: macro-vesicular steatosis, area under red margins: inflammatory cell infiltration, green drops: hepatocyte degeneration. Magnification x200. HF: high fat, D: diabetes, B: baking.

4.3.6 Effects of AGEs on HSC activation and pro-fibrotic cytokine expression

As discussed in the previous chapter, activated Kupffer cells can secrete many pro-inflammatory cytokines, which trigger HSC activation. Activation of HSCs can be monitored by measuring α-SMA gene expression. We found significantly ($p<0.05$) up-regulated α-SMA expression in all three high AGE groups (Fig. 4.8A) compared to HF fed mice and there was no difference between the three high AGE groups. Activated HSCs in turn produced large amounts of pro-fibrotic cytokines. TGF-β1 was significantly ($p<0.0001$) increased in all three high AGE groups of mice (Fig. 4.8B), whereas CTGF, another potent pro-fibrotic cytokine, was significantly ($p<0.05$) increased in the two diabetic groups compared to HF fed mice (Fig. 4.8C). Increased cytokine release is known to activate HSCs which in turn lead to secretion of excess amount of ECM proteins, including collagens. Thus, in comparison with to HF fed mice, all three high AGE groups showed a significantly ($p<0.05$) increased expression of collagen 1, a major component of ECM (Fig. 4.8D). The livers of HF+B+D mice, which were potentially exposed to high AGEs derived from endogenous production as well as from the diet, showed the highest expression of collagen 1, although it did not reach statistical significance.

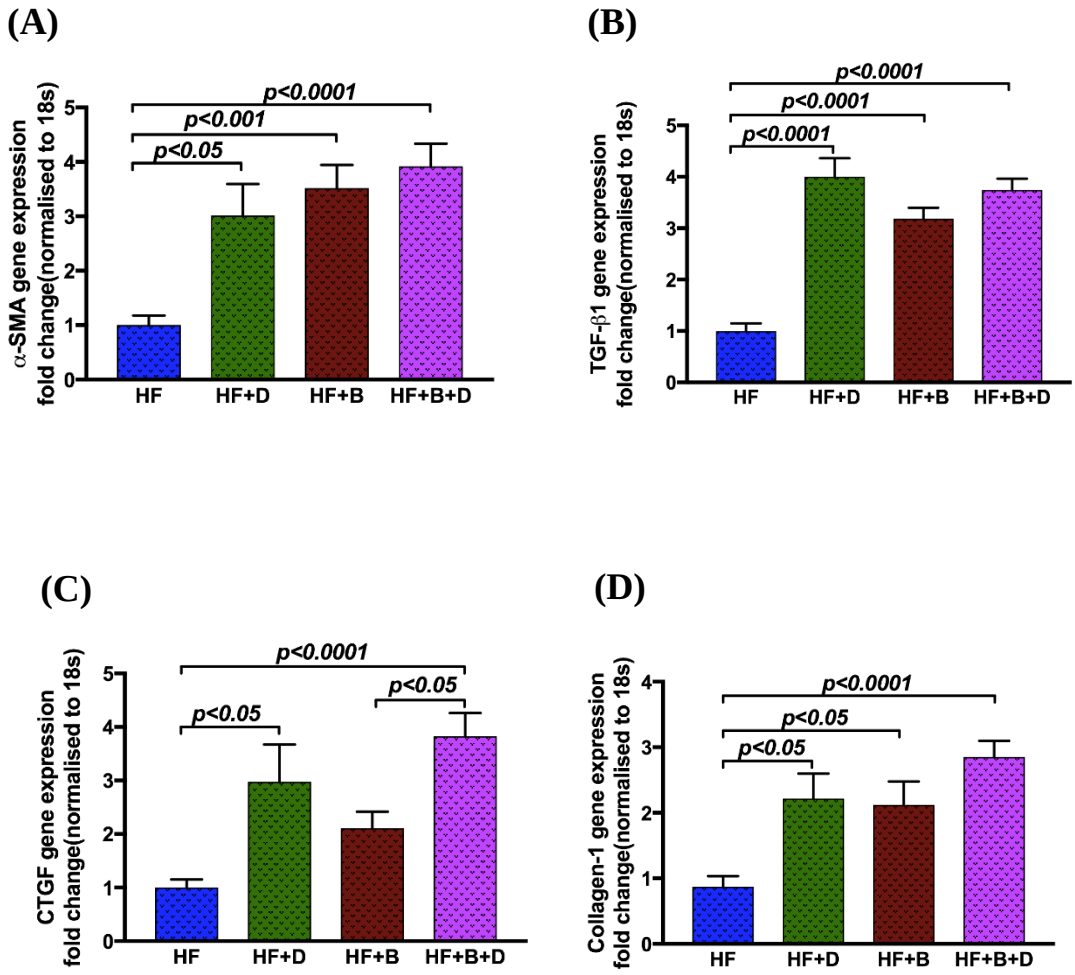

Figure 4.8 Gene expression of HSC activation marker and pro-fibrotic and fibrotic markers secreted by HSCs

HSC activation marker α-SMA was significantly up-regulated in all three groups, compared to HF fed control mice (A). Both TGF-β1 (B) and collagen 1 (D) showed a similar pattern with significant increase compared to HF fed mice. However, CTGF (C) was significantly ($p<0.05$) increased only by diabetes. The data have been normalized to endogenous control gene, 18S and HF fed control group was given an arbitrary value of 1. Each bar represents the mean +/- SEM profile of 10-15 mice per treatment group as calculated by one-way ANOVA with Tukey's comparison test. HF: high fat, D: diabetes, B: baking.

4.3.7 Effects of AGEs on liver fibrosis

Collagen 1 is a major ECM protein in fibrogenesis. High fat feeding for a long period (40 weeks) caused mild fibrosis. Histologically, this is reflected by picrosirius red stained collagens in liver sections with the typical 'river delta' appearance of lobules which is similar to features of human NASH (Fig. 4.9A). Moreover, as discussed in the previous section with H&E staining, these mice showed enlarged hepatocytes. Importantly, collagen deposition was exacerbated in HF+D mice implying that endogenous AGEs play a role in exacerbating liver fibrosis (Fig. 4.9 B). Animals fed the high dietary AGEs (Fig. 4.9C, D) showed even worse fibrosis which was significantly ($p<0.05$) higher than that of HF+D group of mice, suggesting dietary AGEs cause severe liver fibrosis compared to endogenously derived AGEs i.e. diabetes. This confirms the findings reported in chapter 3 that dietary AGEs have more deleterious effects in NAFLD than endogenous AGEs. Although HF+B+D mice showed the highest level of fibrosis which was significantly ($p<0.01$) higher than HF+D mice, there was no significant difference between two high AGE groups (Fig. 4.9E). This suggests that diabetes may not cause an additive effect on liver fibrosis in diabetic mice fed the high dietary AGEs. This may also suggest that high dietary AGE-associated liver fibrosis has attained the maximum induction of fibrosis.

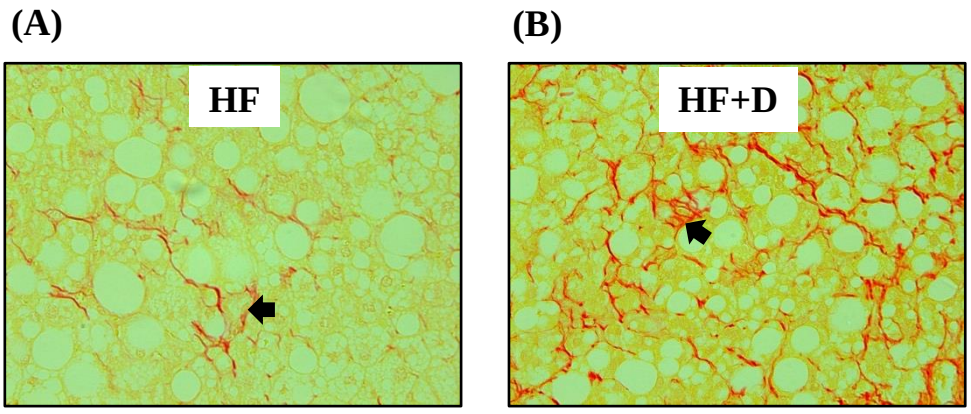

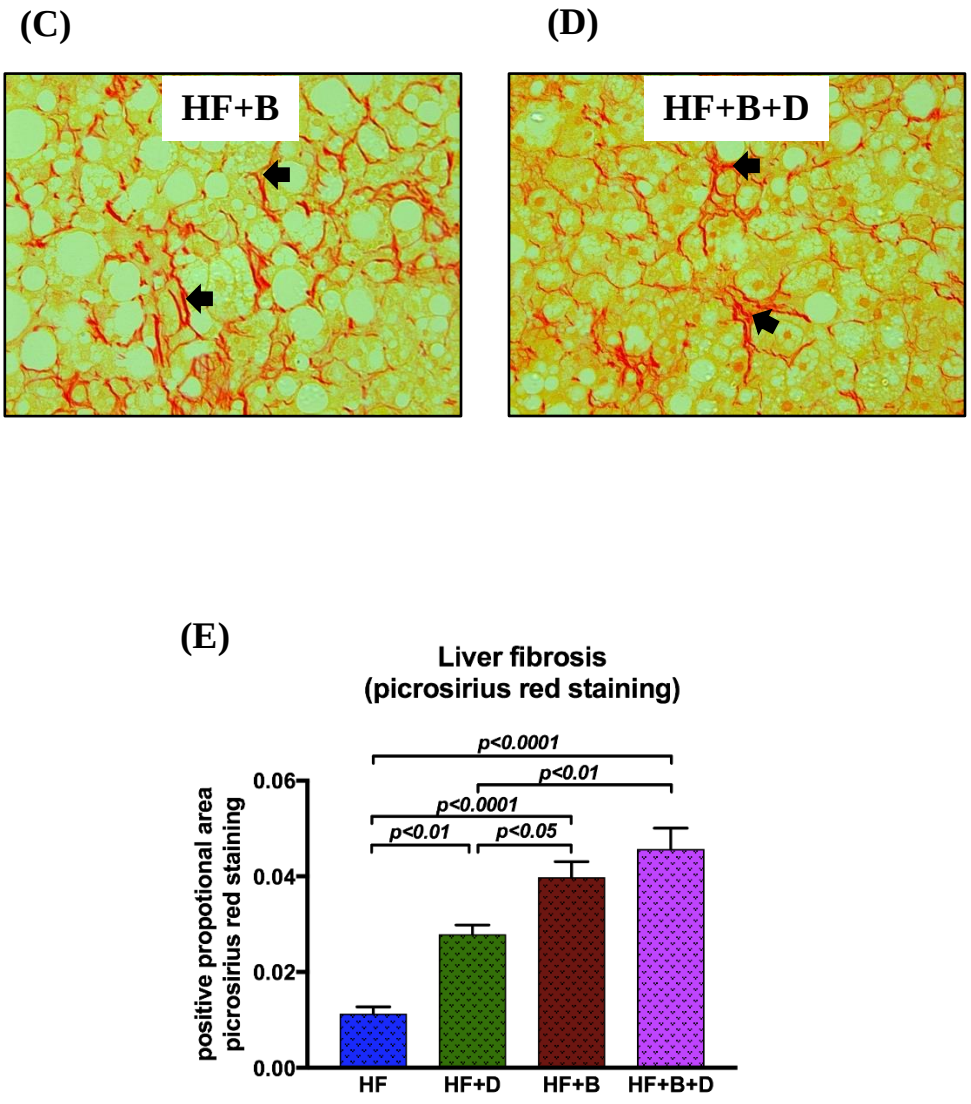

Figure 4.9 Quantification and comparison of liver fibrosis between diabetic and dietary AGE fed mice using picrosirius red staining

Forty weeks of high fat feeding caused mild fibrosis (A). Both diabetes and high dietary AGEs significantly (B, C) increased liver fibrosis. However, diabetic mice fed the high dietary AGEs (D) showed the highest positive staining, although it was not significantly different from HF+B mice (E). Each bar represents the mean ± SEM profile of 10-15 mice per treatment group as calculated by one-way ANOVA with Tukey's comparison test. Arrows: pericellular fibrosis. Magnification x200. HF: high fat, D: diabetes, B: baking.

4.3.8 Effects of AGEs on lipid peroxidation in the liver

4-Hydroxy-2-nonenal (HNE) is an end product of lipid peroxidation and it's adducts can be easily detected in the liver. Quantification of HNE protein adducts in the liver is considered a good marker of lipid peroxidation and thus, oxidative stress.[378] Assessment of oxidative stress was performed through immunohistochemical detection of 4-HNE adducts in liver sections. Forty weeks of high fat feeding caused mild accumulation of 4-HNE adducts, as indicated by small amount of positive staining (brown colour) in liver sections (Fig. 4.10A). Both high dietary AGEs and diabetes significantly ($p<0.001$) increased lipid peroxidation in the liver as reflected by high amounts of 4-HNE adducts compared to HF fed mice (Fig. 4.10B, C). However, in contrast to liver fibrosis, lipid peroxidation appeared higher in the HF+D mice compared to HF+B group of mice but it was not significantly different (Fig. 4.10E). In keeping with fibrosis quantification, the livers of HF+B+D mice (Fig. 4.10D, E) showed the highest positive staining which was significantly ($p<0.001$) higher than those of diabetic (Fig. 4.10B, E) and dietary AGE fed (Fig. 4.10C, E) mice.

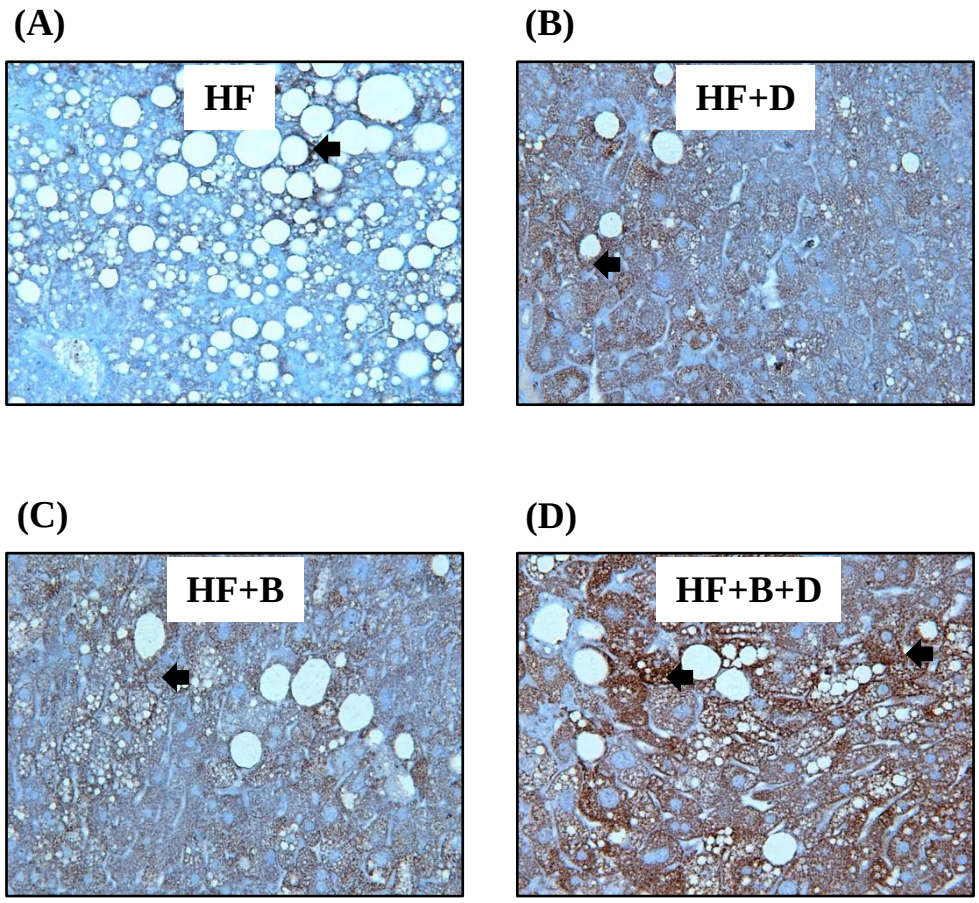

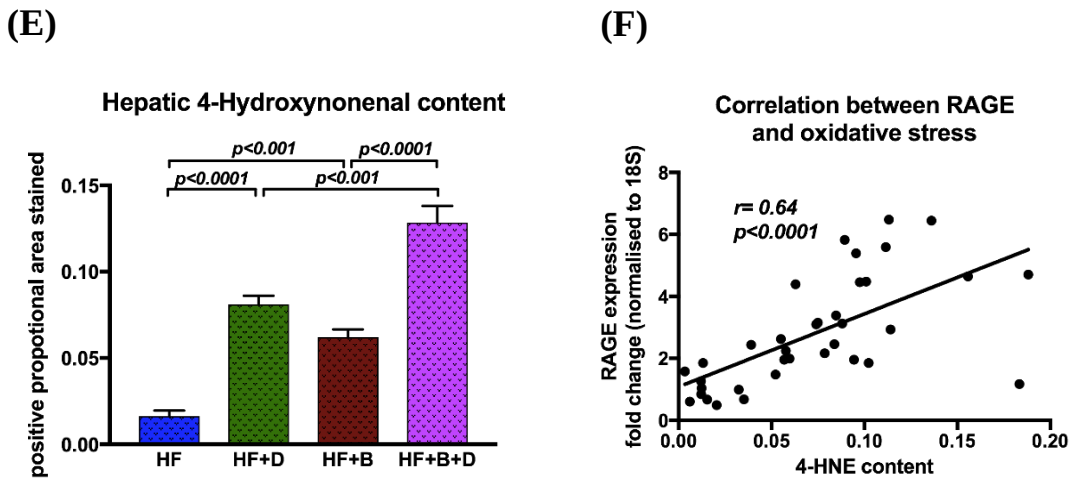

Figure 4.10 Quantification and comparison of lipid peroxidation in the liver between diabetic and dietary AGE fed mice using 4-HNE immuno staining

Forty weeks of high fat feeding caused mild lipid peroxidation (A). Both diabetes and high AGE diet further increased lipid peroxidation in liver tissues, which was reflected by significant increases in positive staining of liver sections compared to HF fed mice (B, C). However, diabetic mice fed the high dietary AGEs (D) showed the highest positive staining which was significantly higher than those of other high AGE groups (E). Hepatic 4-HNE content was positively and significantly correlated with liver RAGE expression (F), suggesting that the activation of RAGE initiates downstream signalling that generates ROS and oxidative stress. Each bar represents the mean ± SEM profile of 10-15 mice per treatment group as calculated by one-way ANOVA with Tukey's comparison test. Arrows: 4-HNE adducts. Magnification x200. HF: high fat, D: diabetes, B: baking.

4.3.9 Effects of RAGE on body weight and blood glucose concentration

At the beginning of the experiment the average body weight of both WT and RAGE$^{-/-}$ groups were similar (~24 g). However, despite similar food and water intake, RAGE$^{-/-}$ mice gained weight faster than WT mice. The average body weight of RAGE$^{-/-}$ mice at the time of STZ injection (to induce diabetes) was over 40 g, whereas the body weight of WT type was below 40 g. Following STZ injection, both WT and RAGE$^{-/-}$ mice started to lose body weight. Whilst WT mice continued to lose body weight towards the end of the 40 weeks experimental period with an average end-weight of approximately 27 g at the culling point, RAGE$^{-/-}$ mice started to gain weight within 3-5 weeks of diabetes

induction (Fig. 4.11A). Although RAGE$^{-/-}$ did not gain weight in the same rate as before prior to induction of diabetes, they had an average body weight of approximately 37 g at the culling point (Fig. 4.11A). The physical appearance of mice is shown in Figure 4.11B, C.

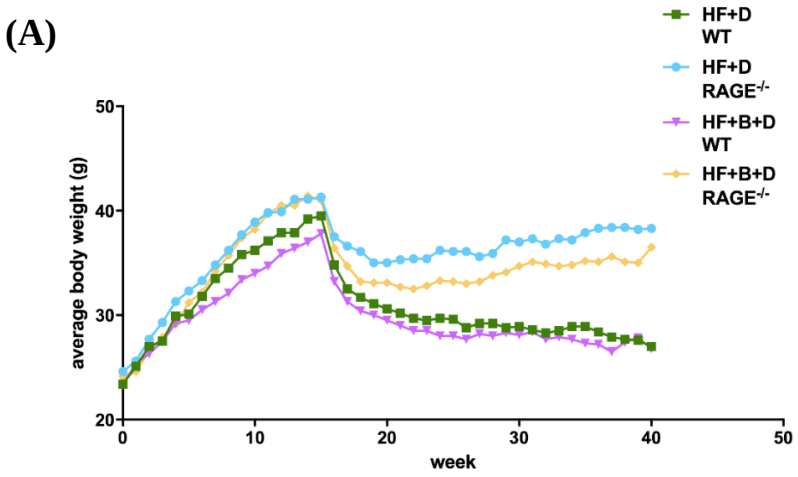

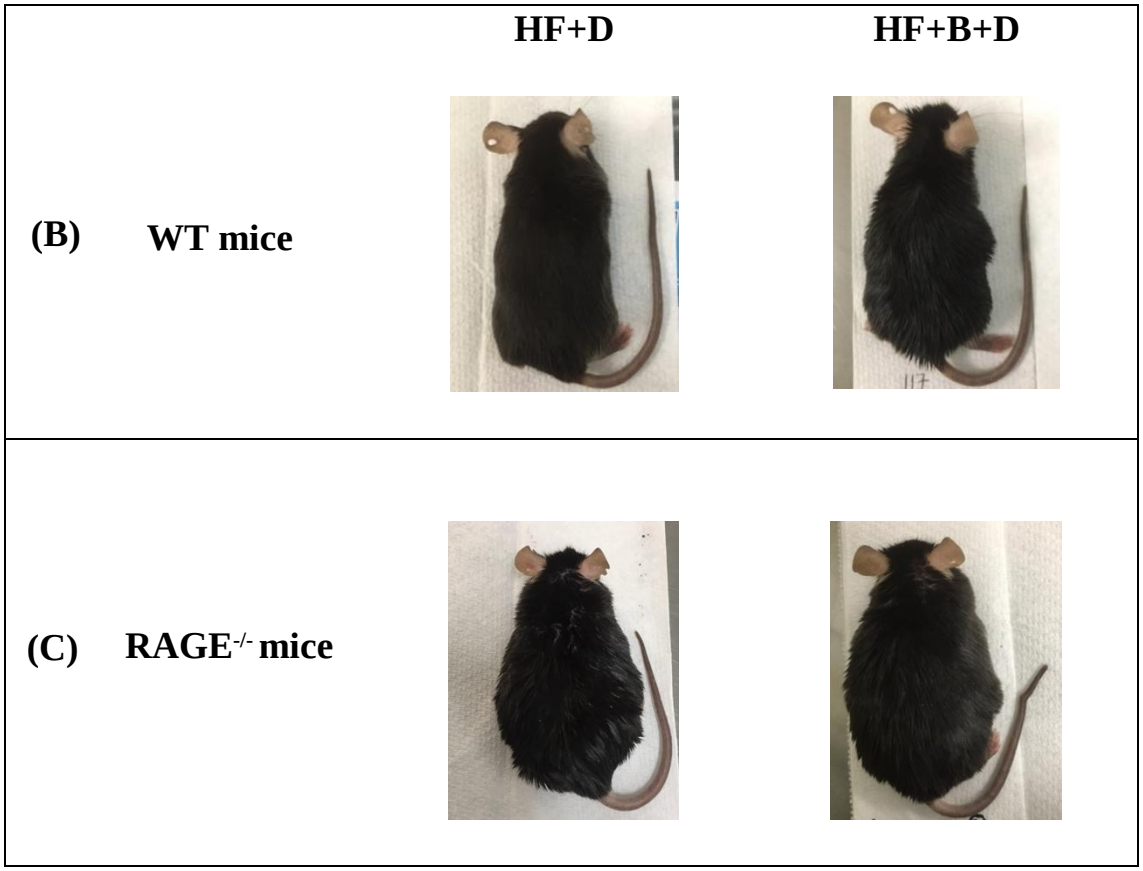

Figure 4.11 Body weight and physical appearance comparison between WT and RAGE$^{-/-}$ mice

Both WT and RAGE$^{-/-}$ mice started gaining body weight at the beginning of the experiment; however, RAGE$^{-/-}$ mice gained weight at a faster rate. Both WT and RAGE$^{-/-}$ lost weight after induction of diabetes at week 15 and WT mice continued to lose weight until 40 weeks. Interestingly, RAGE$^{-/-}$ mice started to gain weight 3-5 weeks post-induction of diabetes (A). WT mice showed a lean body appearance (B) whereas RAGE$^{-/-}$ mice showed fatty appearance (C). Each point represents the mean profile of 10-15 mice per treatment group. HF: high fat, D: diabetes, B: baking, WT: wild type.

As described in methods section (chapter 2), diabetes was induced by two daily injections of STZ on two consecutive days. The basal blood glucose level before the injection was similar between WT and RAGE$^{-/-}$ mice (~10 mmol/L). After 5 days of the second STZ injection, blood glucose levels were increased to about 12-17 mmol/L in both WT and RAGE$^{-/-}$ mice. However, from second week onwards post-STZ injection, WT mice continued to increase blood glucose reaching the highest reading (33.3 mmol/L) of glucometer reading (Fig. 4.12). In marked contrast, instead of continous increases of blood glucose levels, diabetic RAGE$^{-/-}$ mice showed blood glucose levels around 17 mmol/L which was increased to around 25 mmol/L when they were fed the high AGE diet (Fig. 4.12).

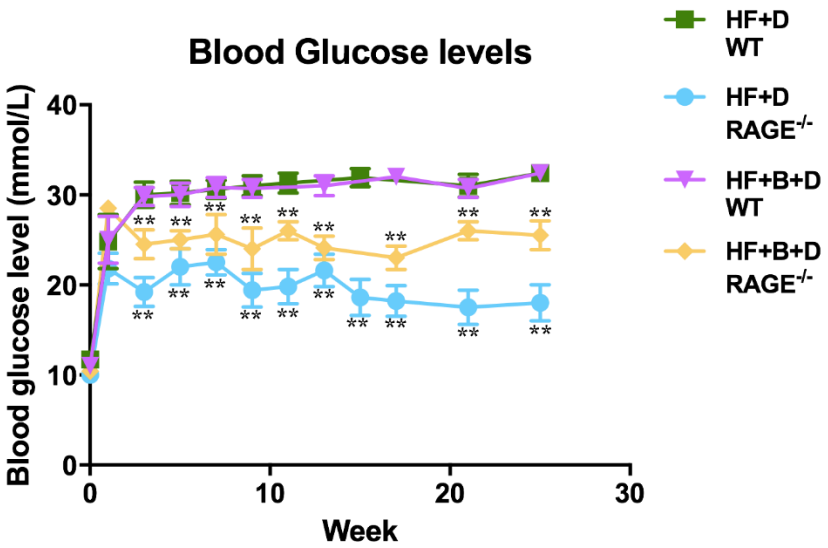

Figure 4.12 Blood glucose levels in WT and RAGE$^{-/-}$ mice
Both WT and RAGE$^{-/-}$ mice showed increased blood glucose during the first week after diabetes induction. Whilst blood glucose level in RAGE$^{-/-}$ mice were maintained around

17 mmol/L (diabetic + high fat fed) and 25 mmol/L (diabetic + high AGE fed), WT mice continued to increase blood glucose until 40 weeks, but 33.3 mmol/L is the highest reading that could be recorded by the glucometer. Each point represents the mean ± SEM profile of 10-15 mice per treatment group calculated by repeated measures ANOVA with Tukey's comparison test. Significance is donated by stars for clarity (**p<0.01). HF: high fat, D: diabetes, B: baking, WT: wild type.

4.3.10 Effects of RAGE on AGE-induced endotoxin responsive genes in the liver

As previously described by our laboratory[212] consumption of diets high in AGEs makes the gut leaky which exposes the liver to microbiota-derived endotoxins (LPS). This can be determined by the up-regulated expression of LPS binding receptors on the surface of liver cells. RAGE$^{-/-}$ diabetic mice fed the high AGE diet showed a significantly (p<0.0001) lower liver CD-14 expression compared to the WT group (Fig. 4.13A). Similarly, we found that TLR-4 expression was also significantly (p<0.01) lower in RAGE$^{-/-}$ diabetic mice with or without high AGE diet compared to their WT controls (Fig. 4.13B), suggesting that the absence of RAGE protects the liver from exposure to high LPS resulting from a leaky gut.

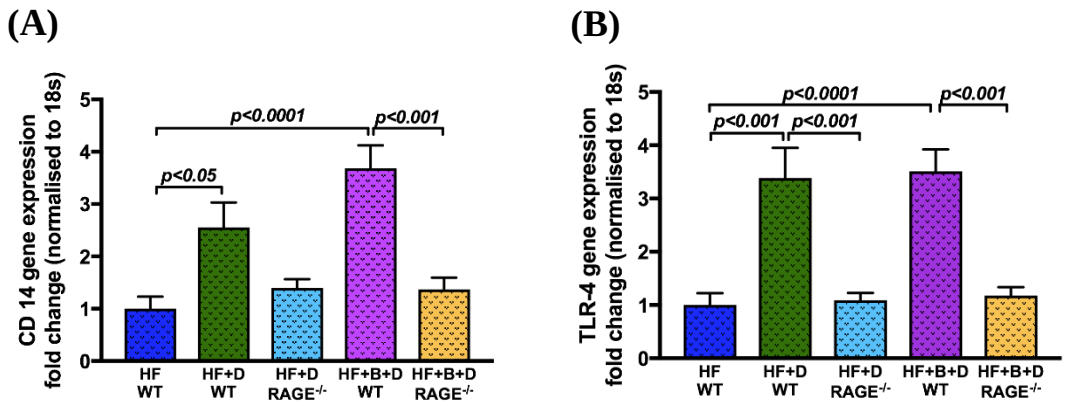

Figure 4.13 Endotoxin responsive liver gene expression in WT and RAGE$^{-/-}$ mice
Gene expression of CD-14 and TLR-4 was significantly lower in RAGE$^{-/-}$ diabetic mice fed the HF or HF baked (high AGEs) diets (A, B). The data have been normalized to

endogenous control gene, 18S and HF fed non-diabetic control group was given an arbitrary value of 1. Each bar represents the mean +/- SEM profile of 10-15 mice per treatment group as calculated by one-way ANOVA with Tukey's comparison test. HF: high fat, D: diabetes, B: baking, WT: wild type.

4.3.11 Effects of RAGE on AGE-induced pro-fibrotic gene expression in the liver

Secretion of pro-inflammatory and pro-fibrotic cytokines is an essential response in wound healing. TGF-β1 is a well-known potent pro-fibrotic cytokine implicated in liver fibrosis. Deletion of RAGE completely abrogated TGF-β1 gene expression in diabetic mice and in diabetic mice fed the high AGE diet compared to respective WT controls, suggesting that RAGE deletion protects mice from TGF-β1 activation (Fig. 4.14A). The expression of α-SMA, the HSC activation marker gene, was however not significantly affected by RAGE deletion (Fig. 4.14B). On the other hand, collagen 1, a major fibrotic gene, did not show a significant reduction in diabetic RAGE$^{-/-}$ mice compared to diabetic WT mice fed the HF diet (Fig. 4.14C). In contrast, RAGE deletion significantly ($p<0.05$) prevented the up-regulation of collagen 1 in diabetic mice fed the high AGEs (Fig. 4.14C).

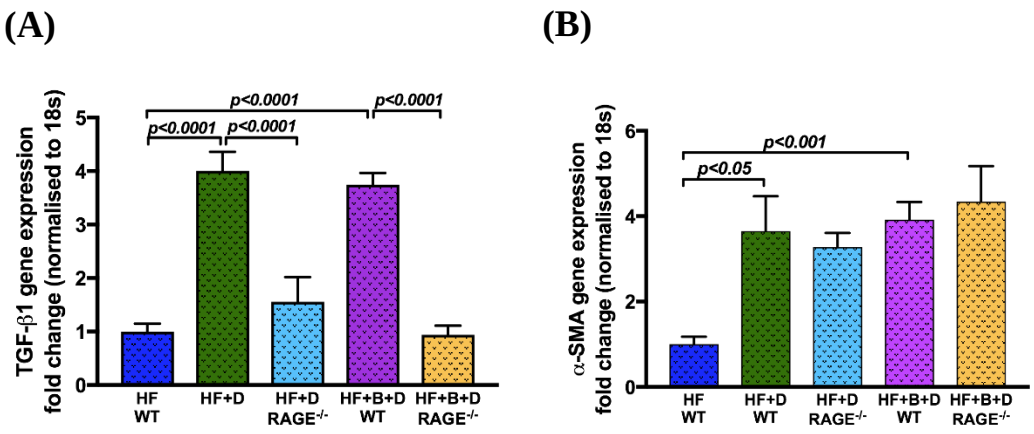

(C)

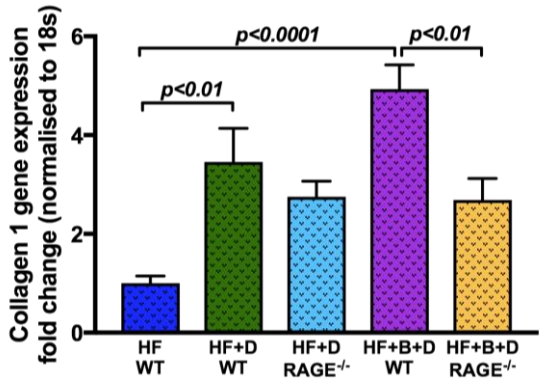

Figure 4.14 Gene expression of the markers of pro-fibrotic, HSC activation and fibrosis in WT and RAGE$^{-/-}$ mice

TGF-β1 gene expression was significantly ($p<0.0001$) down-regulated in both RAGE$^{-/-}$ groups (A). However, α-SMA only showed a small but non-significant reduction in diabetic RAGE$^{-/-}$ mice compared to WT diabetic mice (B). Collagen 1, on the other hand, was significantly ($p<0.05$) reduced in RAGE$^{-/-}$ mice fed the high AGE diet (C). The data have been normalized to endogenous control gene, 18S and HF fed control group was given an arbitrary value of 1. Each bar represents the mean ± SEM profile of 10-15 mice per treatment group as calculated by one-way ANOVA with Tukey's comparison test. HF: high fat, D: diabetes, B: baking, WT: wild type.

4.3.12 Effects of RAGE on mediating AGE-induced liver injury and liver fibrosis

Liver injury is reflected by plasma liver enzyme profiles. Although plasma AST levels in RAGE$^{-/-}$ mice did not show any change compared to WT controls fed the HF diet, RAGE$^{-/-}$ diabetic mice fed the high AGE diet (HF+B+D) showed a significant ($p<0.05$) reduction in plasma AST levels compared to WT control (Fig. 4.15A). In keeping with plasma AST levels, liver fibrosis which was increased in diabetic WT mice fed the high AGE diet was significantly ($p<0.0001$) reduced by RAGE deletion (B, E, F). However, RAGE$^{-/-}$ diabetic mice fed the HF diet showed a non-significant reduction in fibrosis compared to HF fed diabetic WT mice (Fig. 4.15B), although histological assessment showed an apparent reduction in fibrosis in these HF fed RAGE$^{-/-}$ mice compared to WT mice (Fig 4.15C, D).

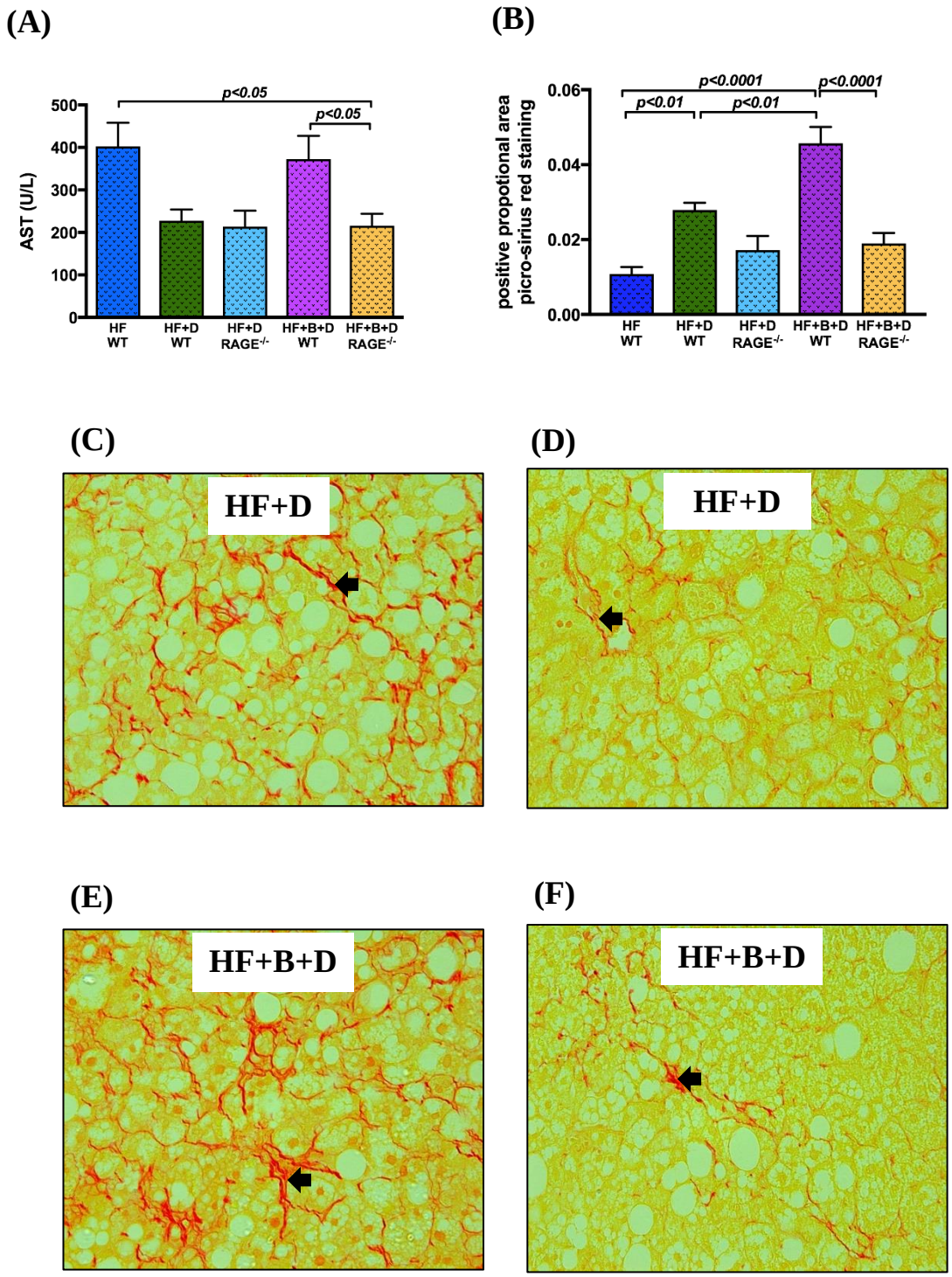

Figure 4.15 Comparison of liver injury and liver fibrosis between WT and RAGE$^{-/-}$ mice

Plasma AST levels were not significantly reduced in RAGE$^{-/-}$ diabetic mice fed on HF diet, however, it was significantly ($p<0.05$) reduced in RAGE$^{-/-}$ diabetic mice fed the high AGE diet (HF+B+D) compared to their relevant WT controls (A). Liver fibrosis showed a similar pattern to this (B). Moreover, picrosirius red staining showed an obvious

reduction in fibrosis in RAGE deleted mice (C-F). Each bar represents the mean ± SEM profile of 10-15 mice per treatment group as calculated by one-way ANOVA with Tukey's comparison test. Arrows: pericellular fibrosis. Magnification x200. HF: high fat, D: diabetes, B: baking, WT: wild type.

4.3.13 Effects of RAGE on AGE-induced pro-inflammatory gene expression in Kupffer cells – mechanistic studies

We have shown that deletion of RAGE in mice could be protective against AGE-induced liver injury and fibrosis. Moreover, we have shown in chapter 3 that Kupffer cells treated with AGEs at 200 μg/mL for 6 hours induced gene expression of a number of pro-inflammatory cytokines including TNF-α, MCP-1 and IL-1β (see Figure 3.9B-D). Pro-inflammatory cytokine release by Kupffer cells is an essential process in wound healing. In this experiment, we found that Kupffer cells treated with specific RAGE antagonist RAP[379] and FPS-ZM1[380] completely abrogated ($p<0.0001$) AGE-induced pro-inflammatory cytokine expression, restoring their expression to those of untreated or RSA treated cells (Fig. 4.16). This corroborated the *in vivo* findings suggesting that RAGE is essential to mediate AGE-induced signalling in liver injury and liver fibrosis.

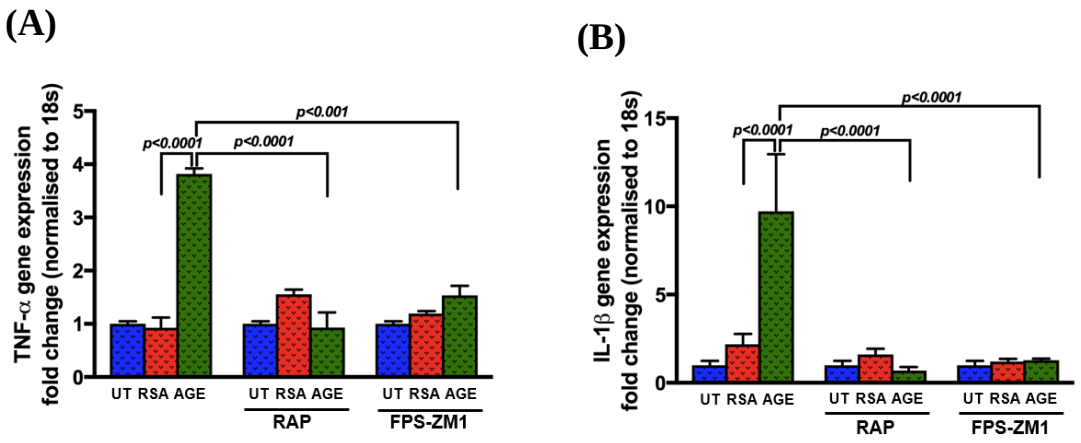

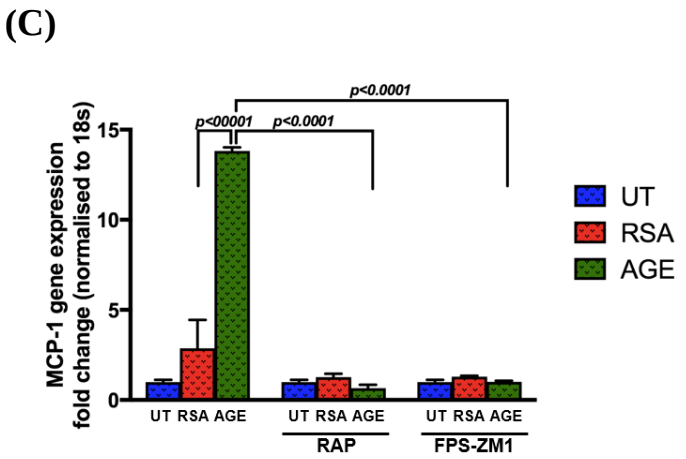

Figure 4.16 Gene expression of pro-inflammatory cytokines by Kupffer cells and the role of RAGE

The expression of all three pro-inflammatory genes, TNF-α (A), MCP-1 (B) and IL-1β (C) were significantly ($p<0.0001$) increased in the presence of AGEs compared to untreated or control RSA treated cells. In the presence of both RAGE antagonists, RAP and FPS-ZM1, AGE-induced gene expression was completely abrogated ($p<0.0001$). The data have been normalized to endogenous control gene, 18S and UT group was given an arbitrary value of 1. Each bar represents the mean ± SEM profile 3 independent experiments per treatment group as calculated by one-way ANOVA with Tukey's comparison test. UT: untreated, RSA: rat serum albumin, RAP: RAGE antagonist peptide.

4.4 Discussion

The experiments described in this chapter provide further evidence showing that AGEs play an important role by contributing to the progression of NAFLD to liver fibrosis. The current findings are consistent with our previous studies which showed both dietary or intraperitoneally administered AGEs exacerbate liver injury and fibrosis.[210,211] However, our previous studies were conducted for only 33 weeks and did not evaluate the contribution of diabetic status to NAFLD progression to liver fibrosis. Therefore, the present study was designed to evaluate whether oral AGEs contribute to NAFLD progression in diabetic NAFLD and whether RAGE plays a role in the disease

progression. Moreover, we also sought to determine whether AGE/RAGE axis acts as a 'second hit' in progressing NAFLD to liver fibrosis in animals fed a diet containing high AGEs for 40 weeks. Whilst the current findings agree with those described in chapter 3, we found that a direct contribution of diabetes is not greater in perpetuating NAFLD progression to liver fibrosis when compared with those produced by diets high in AGEs. Thus, i.p. administration of AGEs to mimic the role of endogenously produced AGEs described in chapter 3 caused a relatively mild effects on pro-inflammatory and profibrotic cytokine expression and NAFLD progression compared to those produced by high dietary AGEs. Thus, whilst the present findings in a diabetic model are important as many fatty liver patients have diabetes, the findings in high dietary AGEs fed animals suggest that dietary intake of AGEs have a profound effect on NAFLD progression to liver fibrosis, at least equivalent to the effect of diabetes. Moreover, RAGE deletion improves blood glucose and prevents weight loss in diabetic animals. This was associated with less expression of endotoxin responsive genes and less TGF-β1 expression and possibly by preventing the exposure of liver to gut-derived endotoxins.

In this experiment we found the highest plasma concentration of CML in diabetic mice fed the high AGE diet, indicating that these mice received AGEs from two sources, i.e. hyperglycaemic condition and high AGE diet. This in turn may have contributed to NAFLD progression to liver fibrosis as supported by findings that oxidative stress was greatest in this group. In chapter 3, we showed that AGEs induced Kupffer cell activation and oxidative stress. Oxidative stress and the accumulation of superoxide anions in tissues is a key mediator of hepatocyte ballooning, cellular dysfunction and fibrosis in NAFLD.[381] 4-Hydroxynonenal (4-HNE) adducts, an end product of peroxidation of membrane N-6-polyunsaturated fatty acids, is a particularly good marker of lipid oxidation during liver injury and is related to the intensity of necroinflammation.[382] Thus, in the present studies, the assessment of oxidative stress in the liver was performed by measuring 4-HNE adducts which reflect the degree of oxidative stress during disease progression. Although HF feeding over 40 weeks tended to increase liver 4-HNE adducts, corroborating the findings described in chapter 3, high dietary AGEs markedly increased HNE content, suggesting that dietary intake of high AGEs causes oxidative stress, a likely pathway of so called 'second-hit' that drives NAFLD progression to liver fibrosis. However, despite oxidative stress being greater, most pro-inflammatory and pro-fibrotic cytokines as well as inflammatory cell infiltration and fibrosis were not significantly

higher in the diabetic high AGE group than high AGE group alone. On the other hand, despite the expression of RAGE and other cytokines and oxidative stress being similar between diabetic and high AGE fed animals, liver fibrosis was higher in high AGE fed animals than HF fed diabetic animals. These findings point to a possibility that factors other than oxidative stress alone were also involved in disease progression.

Supporting a role for AGE/RAGE axis in liver oxidative stress, there was a strong positive correlation between plasma AGEs and liver RAGE expression. Moreover, there was a significant positive correlation between oxidative stress as measured by hepatic 4-HNE content and liver RAGE expression. This would be in keeping with the suggestion that in the liver, AGEs activate RAGE with subsequent increases in oxidative stress,[383] which in turn increases AGE formation and contributes to a vicious cycle of AGE formation, generation of oxidative stress and further RAGE activation as depicted in Figure 4.16. We show further evidence that diets high in AGEs have a remarkable effect on NAFLD progression to liver fibrosis, likely associated with detrimental effects of AGE/RAGE axis in the gut/microbiota as increased expression of endotoxin responsive genes in the liver of high AGEs fed mice was completely prevented by RAGE deletion. This is in keeping with previous reports,[354] that dietary AGEs may contribute to leaky gut and dysbiosis which in turn increases the translocation of bacteria and bacterial products.

As outlined in chapter 1, AGEs have been shown to exert their effects through several receptors, the best studied of which is RAGE. Similar to published reports[212] and the findings presented in chapter 3, we showed above that high exposure to AGEs induced RAGE expression in mice. Activation of RAGE stimulates multiple signal transduction pathways, including the uncoupling of inhibitor factor from NF-κβ, leading to activation of this redox sensitive transcription factor.[384] Upon translocating into the nucleus, activated NF-κ β binds to NF-κ β binding site in the promoter region of the RAGE gene and thereby up-regulates the expression of RAGE itself. This sets up a positive feedback loop and ensures maintenance of RAGE signalling and ROS generation, as mentioned above.[385] In chapter 3 we showed that RAGE expression in healthy livers was minimal and was not affected significantly in a non-diabetic model of fatty liver disease. In this study, similar to that of high AGE fed animals, increased RAGE expression in diabetic animals and the positive correlation of RAGE expression with circulating AGEs/CML, probably reflects that diabetes may contribute to circulating pool of AGEs which causes

RAGE up-regulation.

On the other hand, in the absence of RAGE, the loss of body weight in diabetic mice was markedly reduced despite similar food intake to those of diabetic wildtype animals, suggesting that $RAGE^{-/-}$ were in fact less diabetic as reflected by improved blood glucose levels. This suggested that RAGE may also have a role in blood glucose homeostasis and body weight regulation.[386] Although we have not explored the relationship between RAGE and insulin secretion, markedly reduced plasma glucose levels in RAGE deleted diabetic mice compared to wild type diabetic mice suggest that the absence of RAGE may favour either insulin release with subsequent reduction in plasma glucose levels or improve insulin sensitivity in peripheral tissues in diabetes.[387] This raises an important point that RAGE is possibly involved in many pathogenic pathways. Indeed, RAGE deletion, especially when exposed to high dietary AGEs, improves liver injury, pro-inflammatory and pro-fibrotic cytokine secretion, gut homeostasis and NAFLD progression to liver fibrosis. Further supporting the role of RAGE in pro-inflammatory events mediated by liver resident macrophages, Kupffer cells, we showed that RAGE blockade completely abrogated the expression of potent pro-inflammatory cytokines by immortalized Kupffer cell line, KUP5 cells.[349] Furthermore, previous experiments in our laboratory have shown that AGE trafficking across the gut wall is markedly reduced in RAGE deleted mice (unpublished data). Thus, these findings suggest that although RAGE deleted diabetic mice developed fibrosis to some extent in response to the high fat diet they are protected from the additional harmful effects of high dietary AGEs. This protective effect in RAGE deleted mice could reflect less susceptibility of NAFLD to AGE-induced injury due to a lack of a gut/liver RAGE axis and hepatic AGE/RAGE signalling.

In addition to AGEs, diabetes may play a vital role in the progression of NAFLD via several critical pathways, including insulin resistance, and hyperglycaemia-induced oxidative stress, resulting in inflammatory responses.[388] However, as liver plays a key role in regulating glucose metabolism, it forms a complex bi-directional relationship linking liver disease and diabetes.[389]

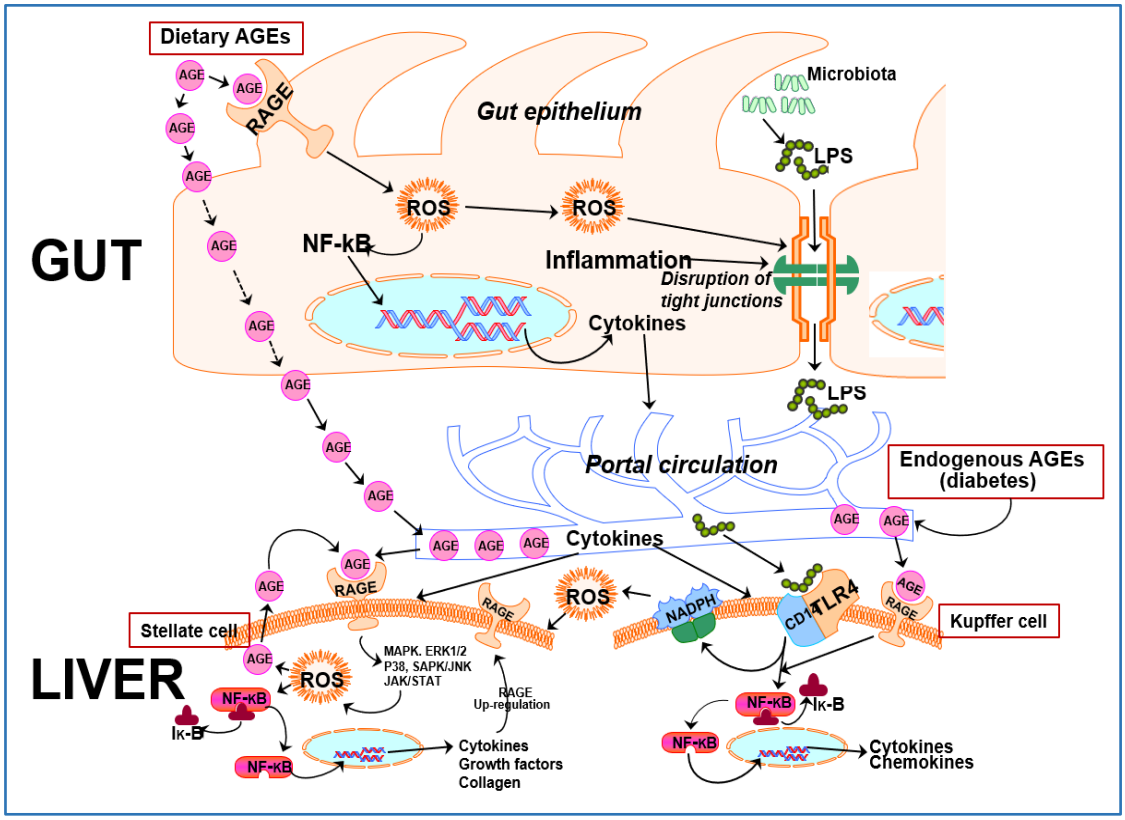

Figure 4.17 RAGE-induced cell signalling in the gut and liver

AGEs bind to RAGE present on the surface of both the gut and liver cells, resulting in ROS generation and oxidative stress which in turn leads to the activation of proinflammatory and pro-fibrotic pathways.

In these experiments, wild type and RAGE$^{-/-}$ mice were not littermates and may add some limitation to the results. Nevertheless, the housing conditions including temperature and lighting were identical for both wild type and knockouts, and more importantly, *in vitro* experiments confirmed the involvement of RAGE in AGEs-induced cell signalling. It is therefore likely that there is minimal or no effect due to this difference on the final outcome.

In summary, the current findings provide further evidence in support of the idea that AGEs contribute to the progression of NAFLD to liver fibrosis. In addition, they drive further oxidative stress and disease progression in diabetes associated NAFLD. It should however be mentioned that based on published studies, AGEs formed endogenously in diabetes may contribute to NAFLD progression, although there could be some other factors that may also be responsible for the observed effects on NAFLD progression in

diabetes. In addition, although high dietary AGEs increased plasma AGEs/CML levels similar to those in diabetic animals fed the high fat diet, dietary AGEs appear to cause more harmful effects than endogenously derived AGEs/CML due to diabetes because there is a possible disruption to gut homeostasis and microbiota integrity due to high dietary AGEs causing dysbiosis. However, this phenomenon of AGEs effect on the gut/microbiota needs to be confirmed by further investigations. Nevertheless, this suggests that dietary modifications may be effective in the control of NAFLD progression to liver fibrosis. Moreover, regardless of the source, the deleterious effects of AGEs are mediated via its receptor RAGE. Therefore, RAGE blockers or antagonists may be effective pharmacotherapies for AGE-induced NAFLD progression to liver fibrosis.

CHAPTER 5

The effects of inhibiting endogenous and exogenous AGE formation on NAFLD progression to liver fibrosis

5.1 Introduction

There have been several mechanisms proposed to suppress the impact of advanced glycation end products (AGEs) on disease progression. Inhibiting the formation of endogenous AGEs by trapping dycarbonyl compounds, intermediate products of Maillard reaction, was a promising pharmacological tool, which was first introduced by Brownlee[390] with the identification of aminoguanidine. Since then, many investigators have studied the effects of aminoguanidine, as well as attempted to discover more compounds that have the ability to trap dycarbonyl compounds.

Aminoguanidine has been widely studied for its AGE inhibiting effects with majority of studies being conducted in diabetic complications. The drug has been shown to be effective in ameliorating diabetic nephropathy,[391-395] cardiovascular diseases,[396-398] reverses functional hyperaemia in diabetic retinopathy[399] and mitigate the effect of AGEs on retinopathy,[400,401] ameliorates skin tissue microenvironment,[402] restores mast cell number[403] and erectile dysfunction,[404,405] and partially prevents a reduction of pyruvate kinase activity in the liver.[406]

With the identification of aminoguanidine, investigators attempted to search for other similar compounds. Pyridoxamine is one of three naturally occurring forms of vitamin B6, and is a critical transient intermediate of transamination reactions by vitamin B6-

dependent enzymes.[407] It was originally described as a post-Amadori inhibitor, but later it was discovered be an inhibitor of the formation of advanced lipoxidation end-products (ALEs) during lipid peroxidation reactions.[408] It has been used in numerous pre-clinical models of diabetic complications. Pyridoxamine has been shown to be effective in diabetic nephropathy, the disease which has been mostly studied with this drug.[408-413] It has also been shown that pyridoxamine ameliorates diabetic cardiovascular disease and retinopathy,[414,415] insulin resistance,[416] glomerular and mesangial cell estrogen receptor α expression in aged female mice,[417] cardiovascular complication and rheumatoid artherites.[257,418-420]

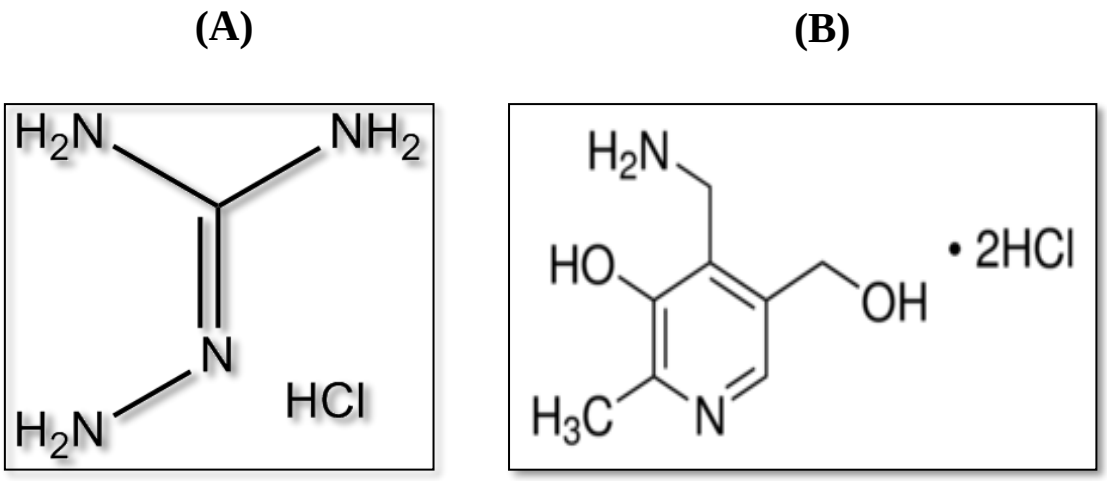

Figure 5.1 Chemical structure of aminoguanidine hydrochloride (A) and pyridoxamine dihydrochloride (B)

However, there are a limited number of studies carried out to investigate the efficacy of aminoguanidine in liver disease and there are no studies that investigated the effects of pyridoxamine in liver disease. One study suggested that a dose of 1 g/L of aminoguanidine is not toxic to liver.[421] However, there are studies providing controversial and conflicting conclusions of the effect of these drugs on the liver.[422] On the other hand, there are no studies that have been carried out in pre-clinical models of non-alcoholic fatty liver disease (NAFLD). Therefore, one of the objectives of this chapter was to investigate the effects of endogenous AGE inhibitors, aminoguanidine and pyridoxamine, in ameliorating AGE-induced progression of NAFLD to liver fibrosis.

It is well documented that the Mediterranean diet has many health benefits compared to the Western diet. Accumulating evidence suggests that the Mediterranean diet could be protective against a range of diseases including atherosclerosis, cancer, diabetes, pulmonary diseases, cognition diseases, obesity and metabolic syndrome.[423,424] The Mediterranean diet is mainly a plant based diet where fruits, vegetables and nuts are consumed frequently[425] and it has been documented that most beneficial effects appear to be mediated via anti-inflammatory and anti-oxidant potential of this diet.[426] The Mediterranean diet has been trialled in NAFLD in Australia and it was found that even modified traditional Mediterranean diet is still beneficial to these patients.[427]

In addition to fresh plant produce used in the Mediterranean diet, it has been shown that food preparation largely involves vinegar-marination prior to processing.[212] We have been shown that the use of vinegar (acetic acids) reduces the formation of AGEs in high fat baked diet and mice fed this vinegar marinated-baked diet for 33 weeks showed improved liver fibrosis compared to high fat baked diet without vinegar marination.[212] Therefore, the second objective of this chapter was to study the effects of vinegar marination on exogenous AGE formation and the effects of vinegar marinated-baked diet on NAFLD progression to liver fibrosis in a long term (40 weeks) diabetic mice.

5.2 Methods

5.2.1 Experimental design

Endogenous AGE inhibitors (aminoguanidine and pyridoxamine):

A group of C57BL/6 mice were fed the high fat (HF) diet for 40 weeks. Another group of mice was fed the HF diet for 40 weeks with diabetes induced at 15 weeks commencing the diet, using 2 consecutive injections of (65 mg/kg body weight) of STZ (Sigma Aldrich, Australia). A third group was fed the baked-HF (HF+B) diet (to increase the AGE amount, as described in chapter 2) for 40 weeks. These 3 groups were used as the control groups for the interventional groups who received aminoguanidine and pyridoxamine.

To investigate the therapeutic effects of aminoguanidine and pyridoxamine, the interventional groups were treated the same way and also commenced the interventions at week 30 and continued for the remaining 10 weeks of the experiment. Both aminoguanidine (1 g/L) and pyridoxamine (2 g/L) were given in drinking water. In diabetic animals, the concentration was halved (i.e. aminoguanidine- 0.5 g/L and pyridoxamine- 1 g/L) as the water intake of diabetic mice was two times higher than that of non-diabetic mice. The nine groups of mice are summarised below.

no treatment	aminoguanidine	pyridoxamine
1) HF	4) HF+ aminoguanidine	7) HF+ pyridoxamine
2) HF+D	5) HF+D+ aminoguanidine	8) HF+D+ pyridoxamine
3) HF+B	6) HF+B+ aminoguanidine	9) HF+B+ pyridoxamine

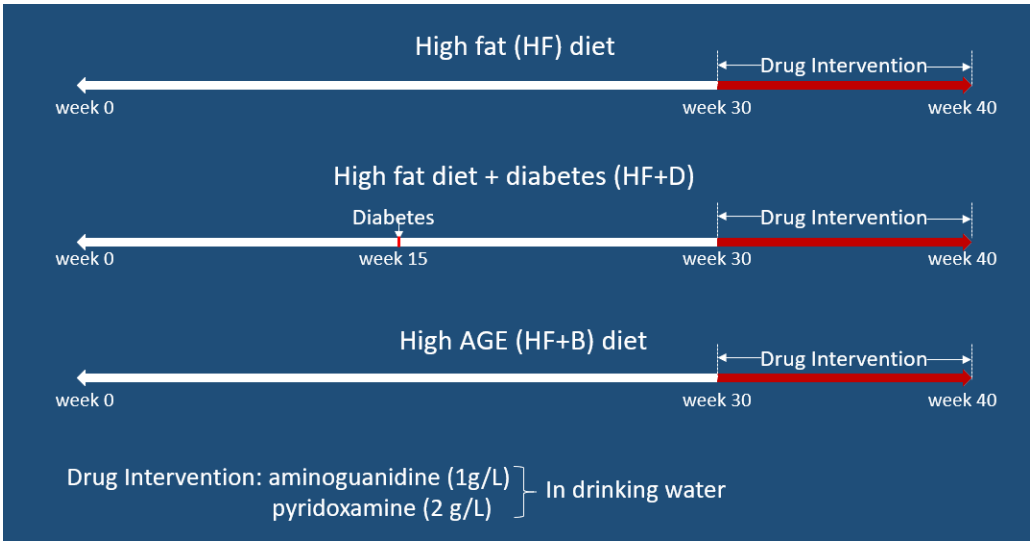

Exogenous AGE inhibitors (vinegar marination):

Three groups of mice were used to investigate the effects of vinegar marination prior to baking the diet as this is expected to reduce the formation of AGEs in the diet. First group was fed on HF diet and used as the control group. Second group of mice were fed the high AGE diet for 40 weeks with induction of diabetes at week 15 of the diet (HF+B+D). A third group of mice were fed the vinegar marinated high AGE diet for 40 weeks with

induction of diabetes at week 15 of the diet (HF+VB+D). The three groups of mice are summarised below.

1) HF
2) HF+B+D
3) HF+VB+D

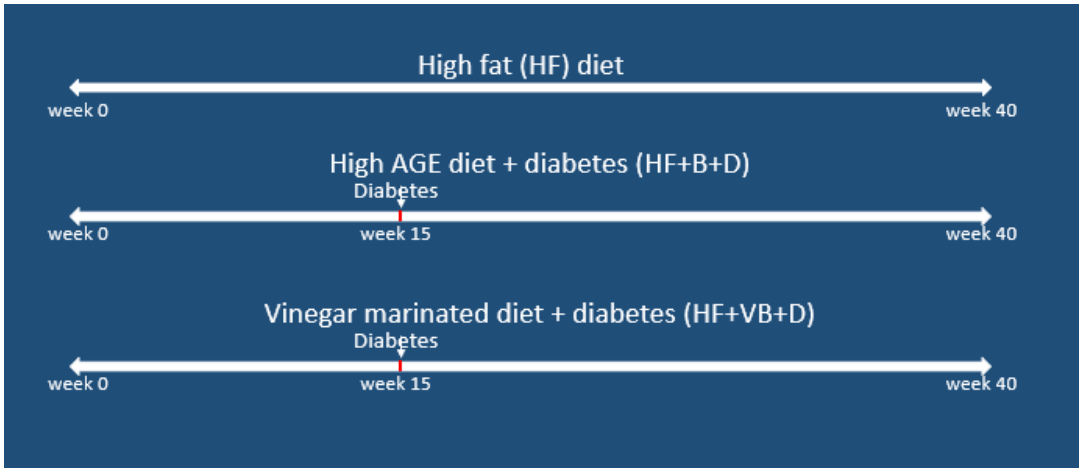

5.2.2 Marination of diet to reduce AGE formation during baking

High fat diet was submerged (150 g/100 mL) in vinegar (Coles home brand) for 15 minutes and the excess vinegar was allowed to drain for another 15 minutes. Then, the diet was baked at 160^{o} C for 1 hour.

5.2.3 Tissue harvesting and storage

The animals were sacrificed at 40 weeks using pentobarbitone (120 mg/kg bw) and blood and livers were collected as described in chapter 2.

5.2.4 Biochemical assessment of plasma

Plasma was separated form whole blood as outlined in chapter 2 and liver function test was carried out at Austin pathology, Heidelberg, Australia.

5.2.5 Liver gene expression

Total RNA was extracted from snap-frozen liver samples stored at -80^{o} C as described in section 2.6. cDNA was synthesized from RNA and qPCR reactions were carried out using multiplexing to assess gene expression of pro-inflammatory cytokine mainly secreted by Kupffer cells such as TNF-α, hepatic stellate cell activation marker, α-SMA and fibrosis marker collagen 1. The oligonucleotide primer and probe sequences of these genes are given in Table 2.4 of chapter 2.

5.2.6 Picrosirius red staining

Picrosirius red staining was performed in 4 µm liver sections as described in section 2.7.1. Briefly, total collagen was quantified by analysing liver sections under a standard light microscope (Olympus BX50 Microscope, Japan; magnification x200). Collagen volume fraction was determined by measuring the area of stained tissue (red) within a randomly selected field. An average of the total 10 fields per section was used as one observation during the analysis of positively stained proportional area using MCID (Imaging Research, Canada).

5.2.7 Statistical analysis

Results are expressed as mean ± SEM and analysed by one-way analysis of variance (ANOVA) using Prism 7 software (GraphPad Software, San Diego, United States). $p < 0.05$ was considered significant.

5.3 Results

5.3.1 Endogenous AGE inhibitors (aminoguanidine and pyridoxamine)

5.3.1.1 Body weight and Liver weight

Body weight and liver weights were not significantly different among the non-diabetic groups. Diabetic mice gained weight in a similar pattern as non-diabetic mouse until they

were made diabetic at 15 weeks of diet. However, after induction of diabetes, they started losing weight. Drug treatments with aminoguanidine or pyridoxamine did not affect the body weight (Table 5.1).

Table 5.1 Body weight and liver weights of animals fed on different diets and treated with different drugs

Parameter	Mouse model	Control	aminoguanidine	pyridoxamine
Body weight (g)	HF	44.1 ± 0.9 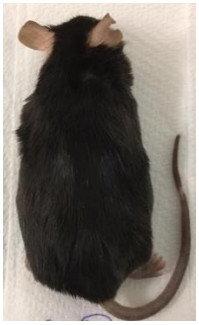	50.2 ± 0.9 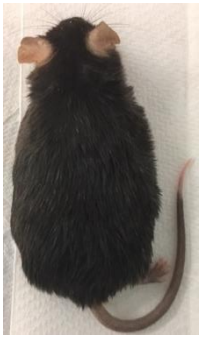	47.5 ± 1.1 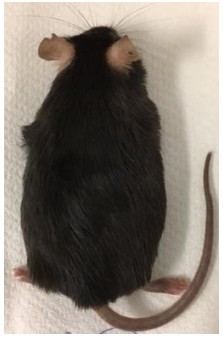
	HF + D	27.8 ±0.8 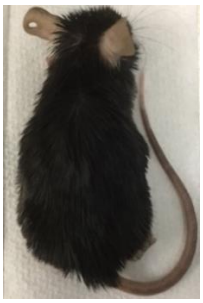	35.4 ± 0.7 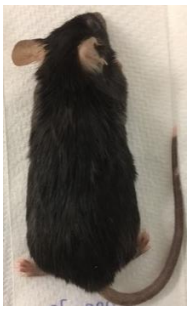	35.7 ± 1.4 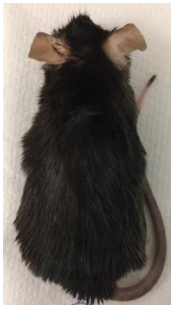
	HF + B	43.0 ± 1.5 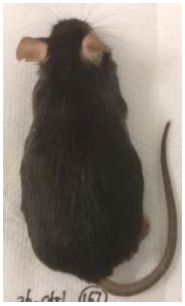	49.1 ± 1.0 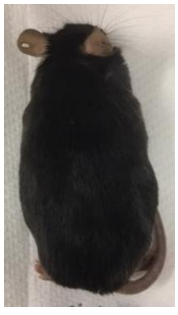	44.9 ± 0.8 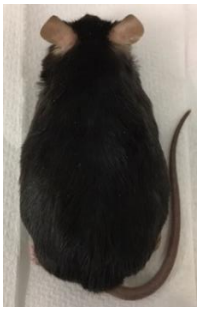

Liver weight (g)	HF	3.2 ± 0.2 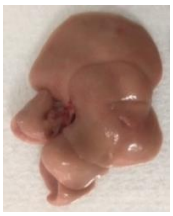	4.8 ± 0.2 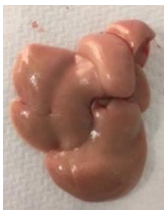	4.6 ± 0.1 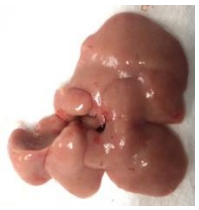
	HF + D	3.0 ± 0.2 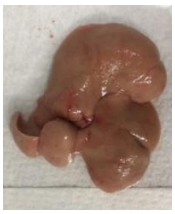	3.3 ± 0.2 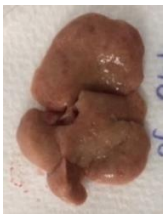	3.2 ± 0.2 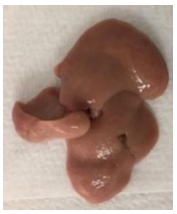
	HF + B	3.5 ± 0.3 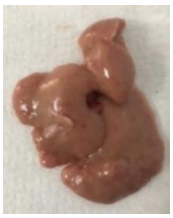	5.1 ± 0.3 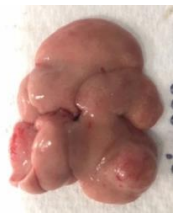	4.4 ± 0.2 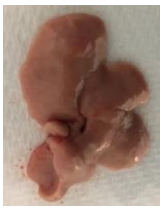
Liver body weight ratio (%)	HF	7.3	9.6	9.7
	HF + D	10.8	9.3	9.0
	HF + B	8.2	10.3	9.8

5.3.1.2 Effects of aminoguanidine and pyridoxamine on AGE-induced gene expression of pro-inflammatory cytokines, hepatic stellate cell activation and collagen 1

Gene expression of pro-inflammatory cytokine TNF-α showed no difference in aminoguanidine treated HF fed mice compared to untreated mice; however, it was significantly ($p<0.001$) increased by pyridoxamine in HF fed mice compared to HF fed untreated mice (Fig. 5.2A). On the other hand, in diabetic HF fed mice, aminoguanidine caused a significant ($p<0.05$) down-regulation of the cytokine expression compared to

untreated diabetic mice. Although TNF-α gene expression was reduced by pyridoxamine in this group it did not reach significance. Moreover, TNF-α gene expression was not affected by both drugs in high AGE diet fed mice (Fig. 5.2A).

Similar to TNF-α gene expression, α-SMA expression was significantly ($p<0.0001$) up-regulated by pyridoxamine in HF fed mice compared to untreated mice. However, there was no change by both drugs in diabetic or high AGE fed mice (Fig. 5.2B).

Similar to TNF-α and α-SMA expression, collagen 1 gene expression was significantly ($p<0.001$) up-regulated by pyridoxamine compared to untreated HF diet fed mice. There was no change in collagen 1 expression by both drugs in diabetic mice. However, both drugs significantly ($p<0.05$) increased collagen 1 expression in mice fed the high AGE diet (Fig. 5.2C).

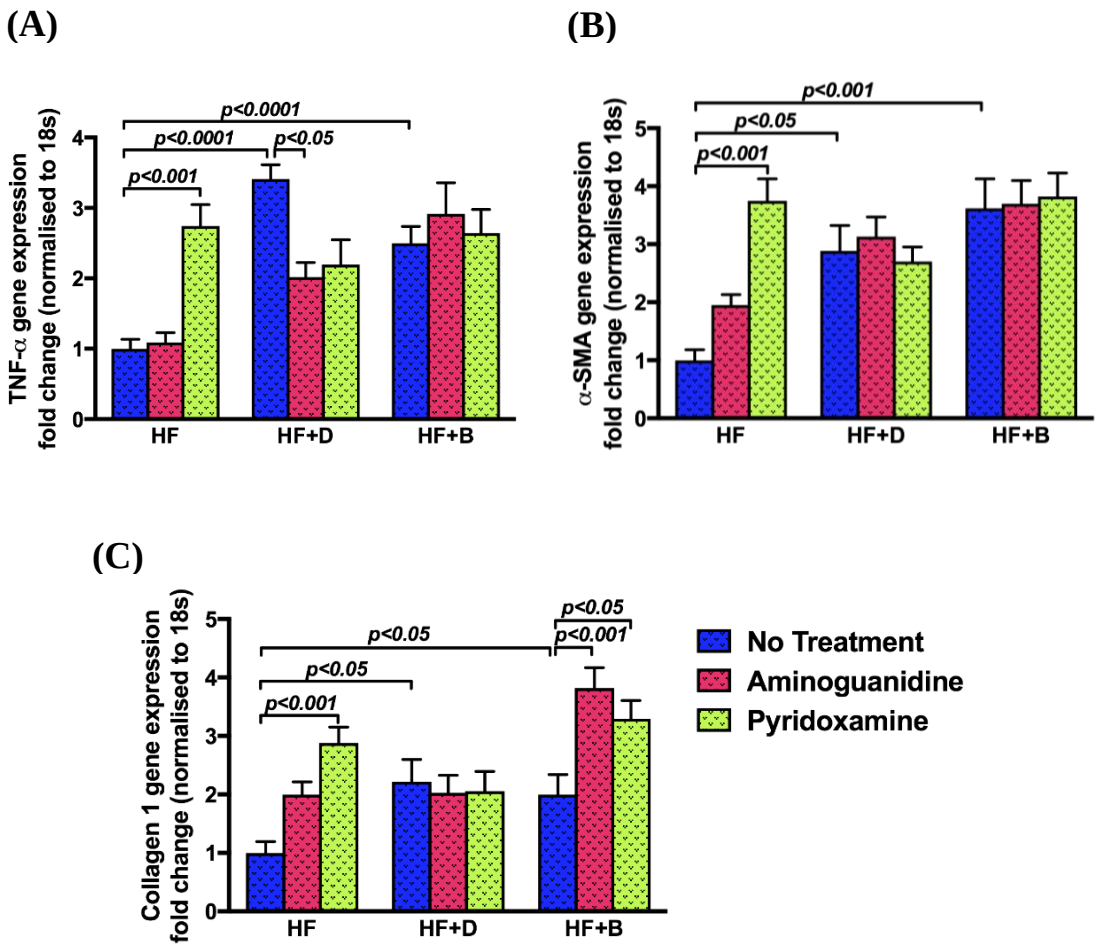

Figure 5.2 Liver gene expression of TNF-α, α-SMA and collagen 1

Pyridoxamine significantly increased the expression of TNF-α in HF fed mice whereas aminoguanidine significantly down-regulated the expression of the cytokine in diabetic mice fed the HF diet (A). The effect of pyridoxamine on α-SMA gene expression showed a similar pattern where its expression in HF fed mice was up-regulated by pyridoxamine while both drugs did not affect α-SMA expression in diabetic or high dietary AGEs fed mice (B). Similarly, pyridoxamine significantly increased collagen 1 expression in HF fed mice. Both drugs did not have any effect on collagen 1 gene expression in diabetic mice; however, they both increased collagen 1 expression in mice fed the high AGE diet (C). Each bar represents mean ± SEM profile from 10-15 mice per treatment group as calculated by one-way ANOVA with Tukey's comparison test. HF: high fat, D: diabetes, B: baking.

5.3.1.3 Effects of aminoguanidine and pyridoxamine on liver fibrosis

Confirming the findings of chapter 4 studies, mice fed the HF diet in the presence of diabetes or high AGE diet showed increased liver fibrosis compared to non-diabetic HF fed mice (Fig. 5.3A, B). In line with pro-inflammatory and pro-fibrotic cytokine expression data, liver fibrosis was augmented by both aminoguanidine and pyridoxamine treatments in HF fed mice compared to the untreated group (Fig 5.3B). Both drugs did not affect liver fibrosis in diabetic mice fed the HF diet or in mice fed the high AGE diet (Fig 5.3A).

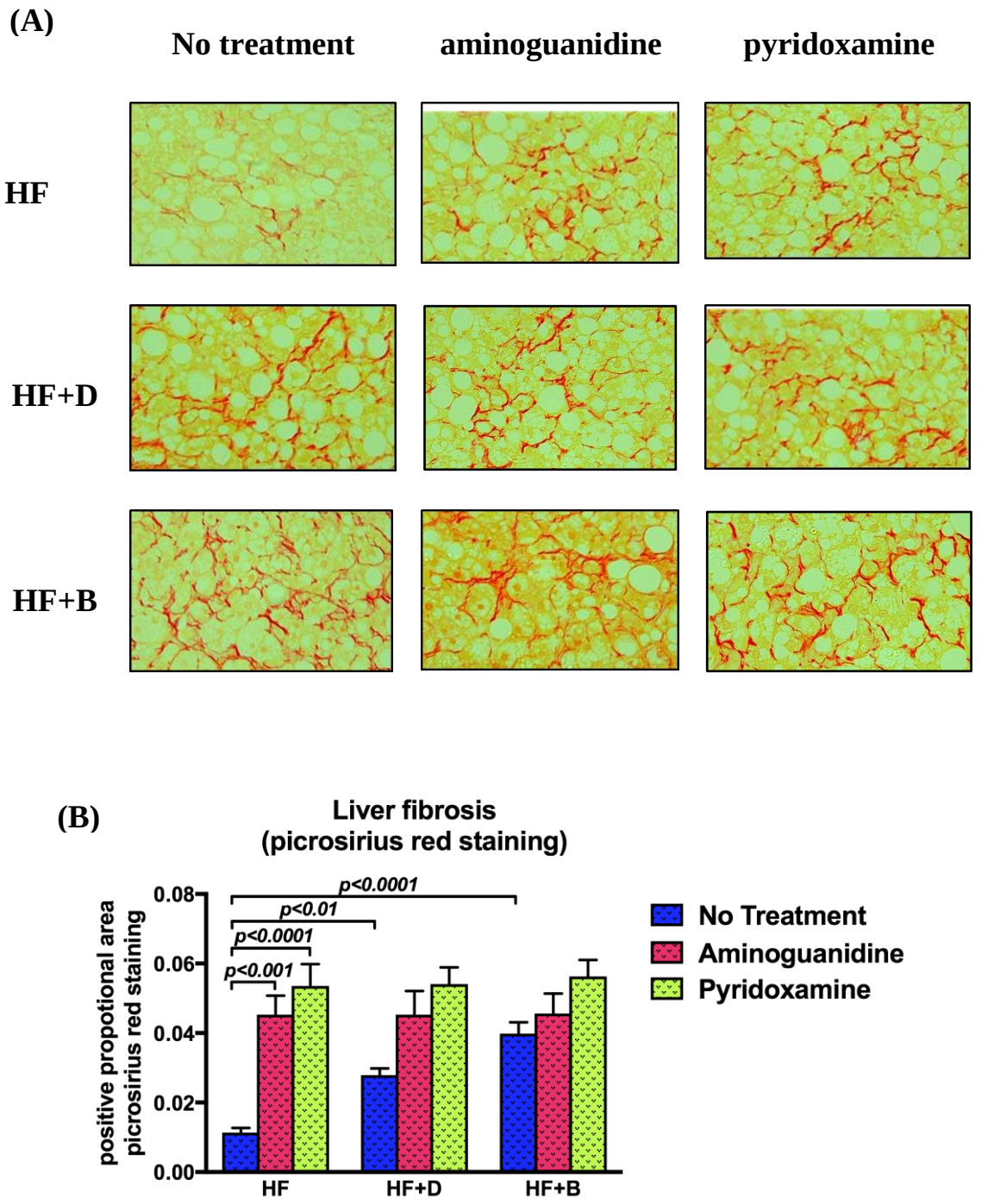

Figure 5.3 Liver fibrosis determined by picrosirius red staining. A) Liver histology panels, B) fibrosis quantification by MCID.

Both Diabetes (HF+D) and high dietary AGEs (HF+B) worsen liver fibrosis compared to HF fed mice (A: top panels). Both aminoguanidine and pyridoxamine significantly increased liver fibrosis in mice fed the HF diet as measured by proportional positively red stained area (B) compared to HF fed untreated control mice. Both aminoguanidine and pyridoxamine had no effect on liver fibrosis in diabetic mice fed the HF diet (HF+D) or in mice fed the high dietary AGEs (HF+B). Each bar represents mean ± SEM profile

from 10-15 mice per treatment group as calculated by one-way ANOVA with Tukey's comparison test. Images are liver histology panels of picrosirius red stained sections with or without drug treatments. Magnification x200. HF: high fat, D: diabetes, B: baking.

5.3.2 Exogenous AGE inhibitors (vinegar marination)

5.3.2.1 Effects of vinegar marination on AGE formation in the diet

It was shown in chapters 3 and 4 that baking the HF diet at 160^{o} C for 1 hour dramatically increased AGEs formation as measured by GC/MS. On the other hand, marinating the HF diet with vinegar for 15 minutes prior to baking reduced the AGE content in the diet (Fig. 5.4). Although the reduction in CML content was small, CEL content in vinegar-baked HF diet was reduced by 50% whereas MG-H1 content was reduced by 20%. Note: no statistical analysis was performed as food samples were pooled across before GC/MS analysis.

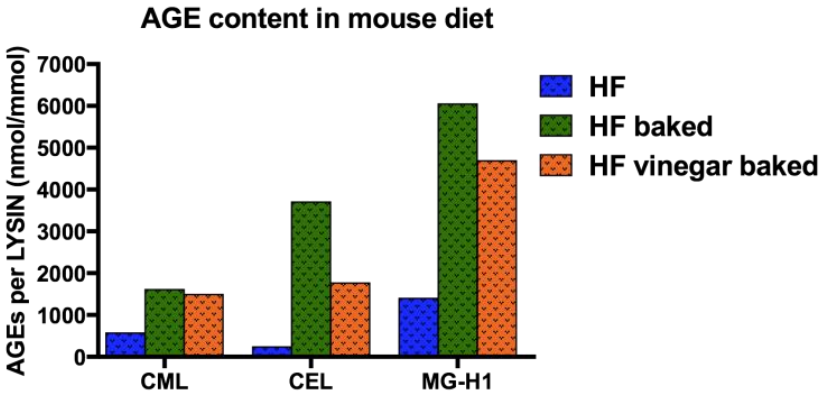

Figure 5.4 AGE content in the diet

All three AGE types in the diet were increased with baking at 160^{o} C for 1 hour. The fold change in CEL and MG-H1 were much dramatic compared to CML increase. However, vinegar marination of HF diet prior to baking reduced different AGE types with CEL and MG-H1 showing a major reduction. CML: N$^{\varepsilon}$-(carboxymethyl)lysine, CEL: N$^{\varepsilon}$-(Carboxyethyl)lysine, MG-H1: methylglyoxal-derived hydroimidazolone 1, HF: high fat.

5.3.2.2 Effects of vinegar marination on AGE-induced liver injury

The findings show that high AGE diet (HF+B+D) significantly increased ($p<0.05$) alanine aminotransferase (ALT) and alkaline phosphatase (ALP) in diabetic mice compared to HF fed mice (Fig. 5.5). We found that reduced AGE formation in HF baked diet by vinegar marination (HF+VB+D) completely inhibited ($p<0.05$) plasma ALT levels compared to high AGE fed mice (Fig. 5.5A). Plasma ALP level which was significantly ($p<0.0001$) increased by high AGE diet, was significantly ($p<0.01$) reduced by vinegar marination prior to baking compared to high AGE fed mice (Fig. 5.5B).

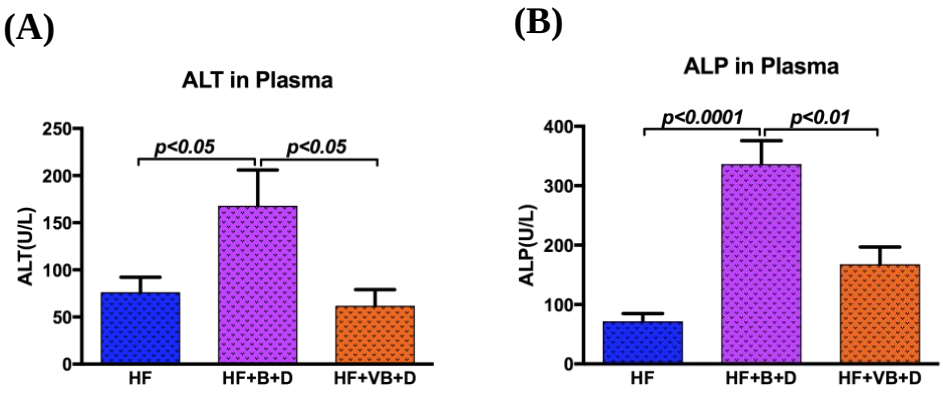

Figure 5.5 Liver function test in mice fed on different diets
Baking (HF+B+D), which increases dietary AGE content, significantly increased plasma ALT ($p<0.05$) (A) and ALP ($p<0.0001$) (B) levels in diabetic mice. On the other hand, feeding mice with vinegar marinated diet prior to baking (HF+VB+D) which reduces AGE formation in the diet, led to a significantly reduced liver injury as indicated by a reduction in both ALT (A) ($p<0.05$) and ALP (B) ($p<0.01$). Each bar represents mean $\pm$ SEM profile from 10-15 mice per treatment group as calculated by one-way ANOVA with Tukey's comparison test. HF: high fat, B: baking, D: diabetes, VB: marination with vinegar prior baking, ALT: alanine aminotransferase, ALP: alkaline phosphatase.

5.3.2.3 Effects of vinegar marination on AGE-induced RAGE and LPS binding receptor gene expression

As described in chapters 3 and 4, high dietary AGEs significantly ($p<0.0001$) increased the expression of a range of genes mainly secreted by Kupffer cells, namely RAGE (Fig. 5.6A), LPS responsive genes CD-14 (Fig. 5.6B) and TLR-4 (Fig. 5.6C). However, we

found that marinating the HF diet prior to baking markedly ($p<0.0001$) reduced liver expression of these genes compared to mice fed the high dietary AGEs (Fig. 5.6). Most importantly, the expression levels of these genes in the liver were returned to the levels of HF fed mice.

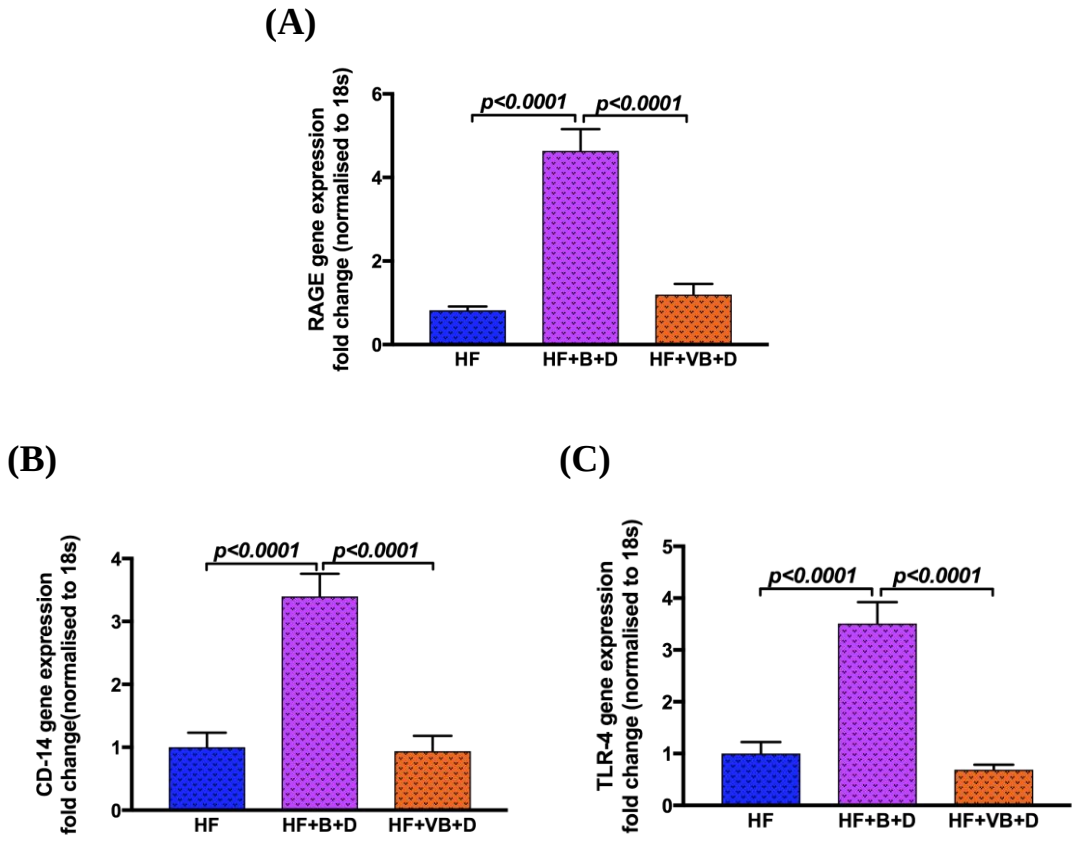

Figure 5.6 Gene expression of RAGE and LPS binding receptors in the liver
High dietary AGEs significantly increased the expression of AGE receptor RAGE, and LPS responsive genes, CD-14 and TLR-4. However, marinating the high fat diet with vinegar prior to baking significantly ($p<0.0001$) reduced the expression of RAGE (A), LPS binding receptors CD-14 (B) and TLR-4 (C). The data have been normalized to endogenous control gene, 18S and HF fed control group was given an arbitrary value of 1. Each bar represents mean $\pm$ SEM profile from 10-15 mice per treatment group as calculated by one-way ANOVA with Tukey's comparison test. HF: high fat, B: baking, D: diabetes, VB: marination with vinegar prior baking.

5.3.2.4 Effects of vinegar marination on AGE-induced pro-inflammatory cytokines in the liver

Consistent with the findings presented in previous chapters, high dietary AGEs caused significant ($p<0.01$) increases of pro-inflammatory cytokine expression compared to HF fed mice. However, We now demonstrate that marinating the HF diet prior to baking markedly reduced liver expression of MCP-1 ($p<0.01$) (Fig. 5.7A), IL-6 ($p<0.01$), (Fig. 5.7B), TNF-α ($p<0.05$) (Fig. 5.7C) and IL-1β ($p<0.05$) (Fig. 5.7D), compared to mice fed the high dietary AGEs. Most importantly, the expression levels of these genes, especially MCP-1, IL-6, and TNF-α in the liver, were returned to the levels of HF fed mice by vinegar marination.

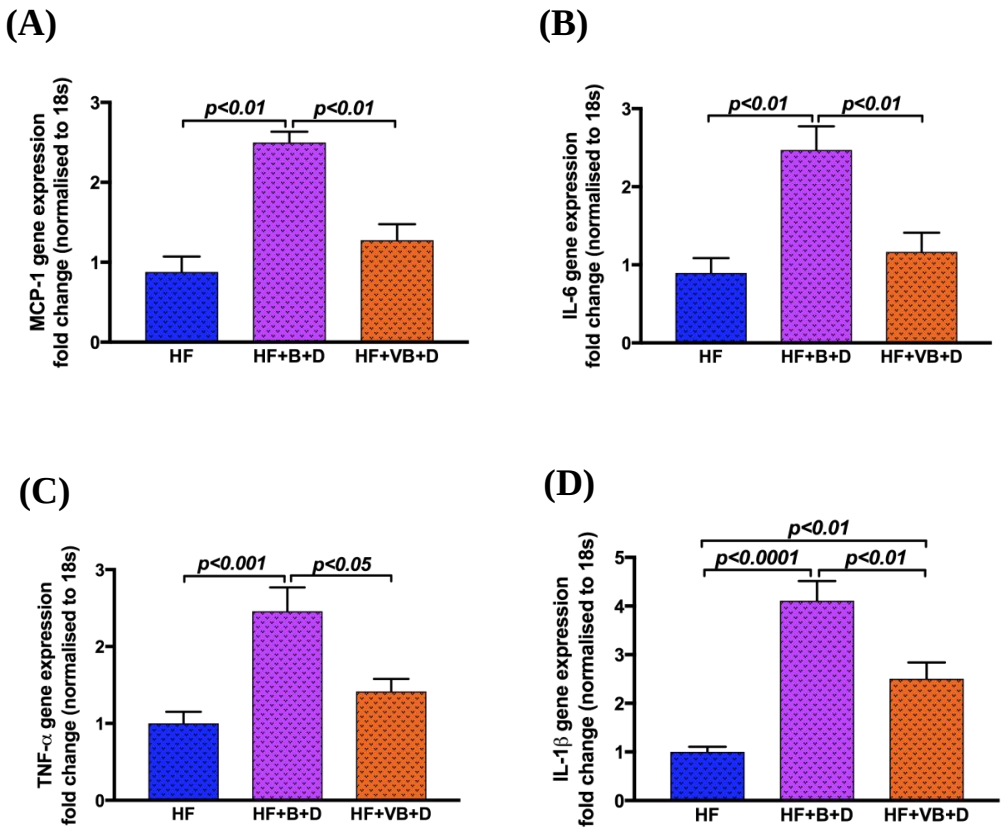

Figure 5.7 Gene expression of pro-inflammatory cytokines in the liver
Feeding mice with vinegar marinated HF diet prior to baking (VB) significantly reduced the expression of (A) TNF-α, (B) MCP-1, (C) IL-1β and (D) IL-6 compared to high AGE fed mice. The data have been normalized to endogenous control gene, 18S and HF fed control group was given an arbitrary value of 1. Each bar represents mean ± SEM profile from 10-15 mice per treatment group as calculated by one-way ANOVA with Tukey's

comparison test. HF: high fat, B: baking, D: diabetes, VB: marination with vinegar prior baking.

In Haemotoxylin and Eosin stained liver sections it clearly showed micro (arrow) and macro (arrowhead) fat vesicle formation in mice fed the HF diet for 40 weeks (Fig 5.8A). In comparison with this, high AGE diet also caused an increased inflammatory cell infiltration (Fig 5.8B). Interestingly, liver histology of mice fed the vinegar baked diet showed a similar pattern to that of HF fed mice with no sign of inflammatory cell infiltration (Fig. 5.8C).

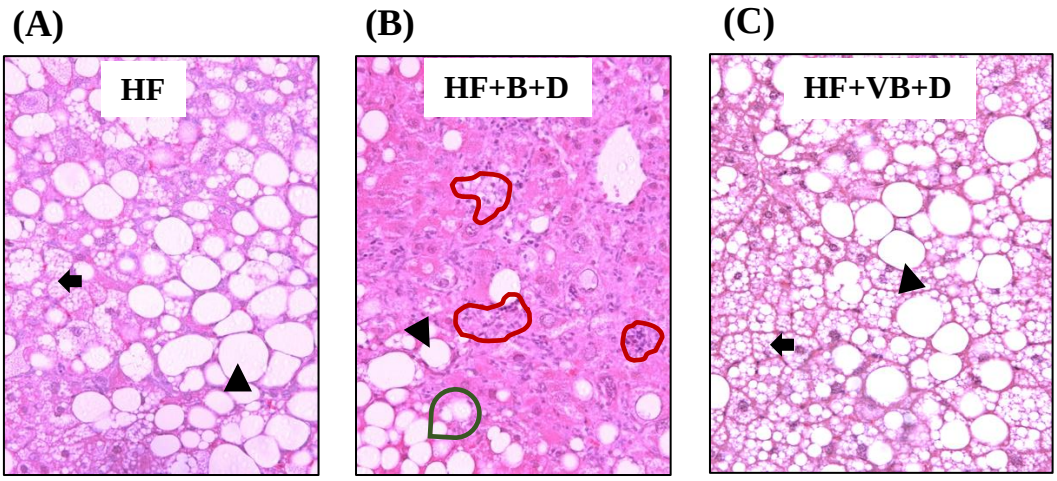

Figure 5.8 Steatosis and inflammatory cell infiltration in the liver of mice fed on different diets

The liver sections from mice fed the HF diet and stained with H&E showed micro (arrow) and macro (arrowhead) vesicular fat vacuoles (A). High AGE diet on the other hand caused an inflammatory cell infiltration in addition to the changes seen in HF fed mice (B). Importantly, vinegar marinated diet showed a similar histological appearance of liver to those of HF mice with no sign of inflammatory cell infiltration (C). Arrow: micro fat vesicles, Arrowhead: macro fat vesicle, area marked by red line: inflammatory cell infiltration, green line: hepatocyte degeneration. Magnification x200. HF: high fat, B: baking, D: diabetes, VB: marination with vinegar prior baking.

5.3.2.5 Effects of vinegar marination on HSC activation and pro-fibrotic gene expression

We then investigated the expression of HSC activation marker gene α-SMA, pro-fibrotic cytokines TGF-β1 and CTGF and fibrotic marker gene collagen 1. Consistent with the findings presented in previous chapters, high dietary AGEs caused HSC activation as reflected by a significant ($p<0.01$) increase of α-SMA (Fig. 5.9A). Moreover, high dietary AGEs caused significant increases in pro-fibrotic cytokines TGF-β1 (Fig. 5.9B) and CTGF (Fig. 5.9C), and fibrotic marker collagen 1 expression (Fig. 5.9D) compared to HF fed mice. However, we now demonstrate that marinating the HF diet prior to baking markedly reduced liver expression of α-SMA ($p<0.01$) (Fig. 5.9A), TGF-β1 ($p<0.0001$), (Fig. 5.9B), CTGF ($p<0.001$) (Fig. 5.9C) and collagen 1 ($p<0.0001$) (Fig. 5.9D), compared to mice fed the high dietary AGEs. Most importantly, by vinegar marination returned the expression levels of these genes to similar or even less than the levels of HF fed mice.

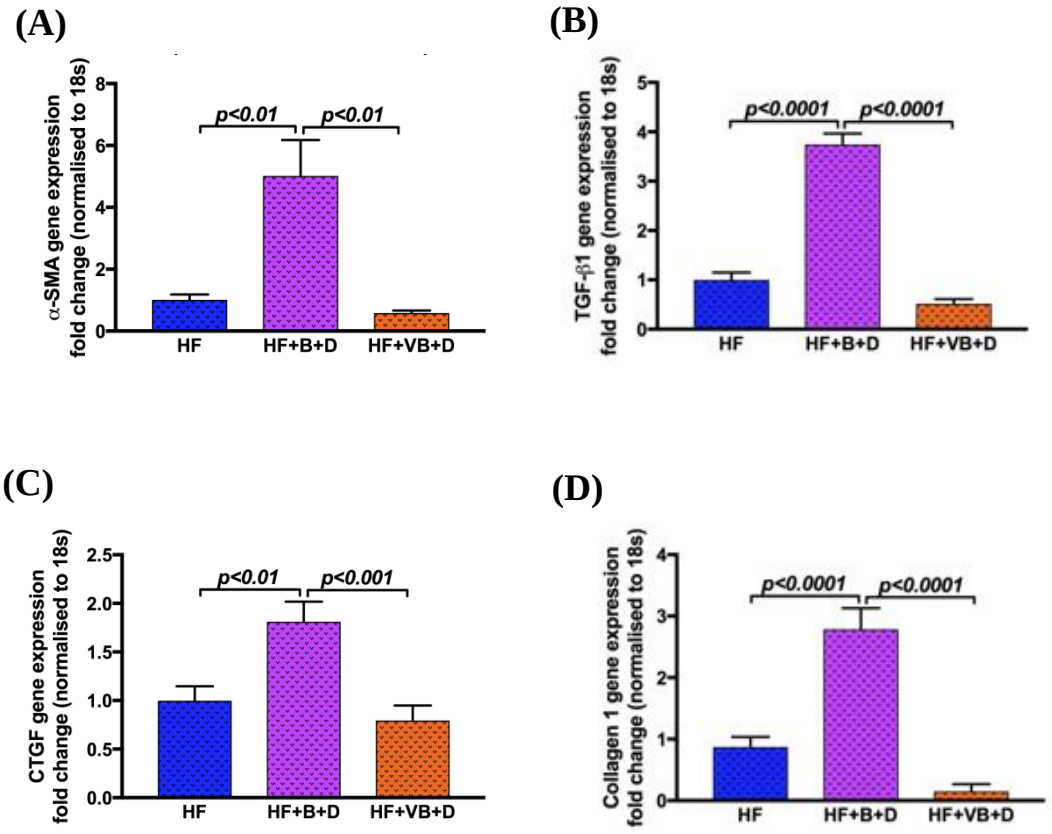

Figure 5.9 Gene expression of HSC activation marker, pro-fibrotic cytokines and fibrosis marker

High dietary AGEs (HF+B+D) significantly increased the expression of α-SMA (A), TGF-β1 (B), CTGF (C) and collagen 1 (D) compared to HF fed mice. However, marinating the high fat diet with vinegar prior to baking reduced the activation of collagen secreting HSCs as reflected by significant reduction in α-SMA expression (A) and thereby reduced the expression of pro-fibrotic cytokines TGF-β1 (B) and CTGF (C), leading to a significant reduction in a major extracellular matrix gene collagen 1 (D). The data have been normalized to endogenous control gene, 18S and HF fed control group was given an arbitrary value of 1. Each bar in represents mean ± SEM profile from 10-15 mice per treatment group as calculated by one-way ANOVA with Tukey's comparison test. HF: high fat, B: baking, D: diabetes, VB: marination with vinegar prior baking.

5.3.2.6 Effects of vinegar marination on AGE-induced liver fibrosis

As presented in pervious chapters, liver fibrosis as assessed by picrosirius red stained liver sections showed that mice fed the HF diet for 40 weeks had mild fibrosis (Fig. 5.10A, D). In keeping with pro-inflammatory and pro-fibrotic cytokine gene expression, mice fed the high AGE diet (HF+B+D) for 40 weeks showed massive increases in liver fibrosis compared to HF fed mice (Fig. 5.10B, D). Interestingly, mice fed the HF diet marinated with vinegar prior to baking showed a markedly reduced liver fibrosis compared to high AGE fed mice (Fig. 5.10C, D). Quantification of these data clearly showed that feeding mice on the vinegar marinated diet reduced the fibrosis level to that of HF fed mice (Fig. 5.10D).

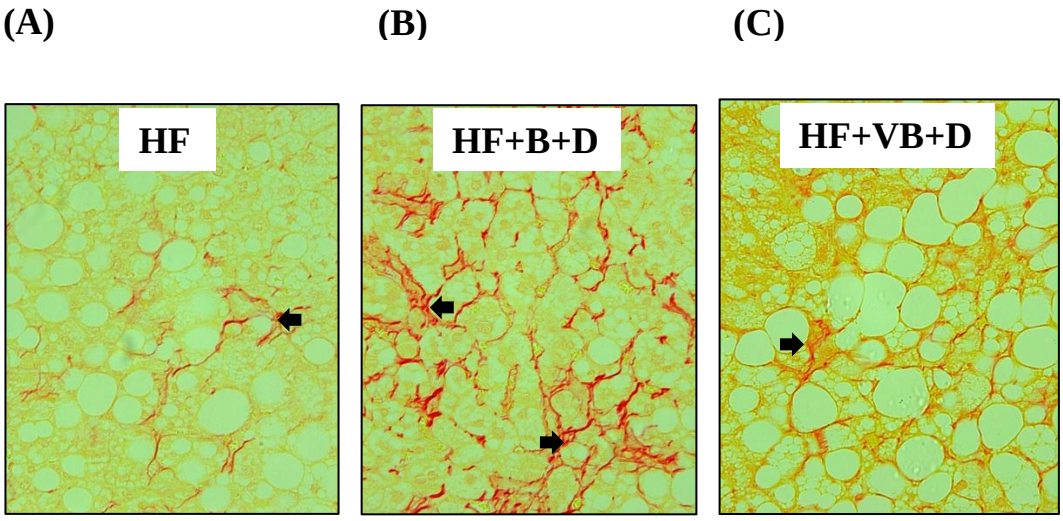

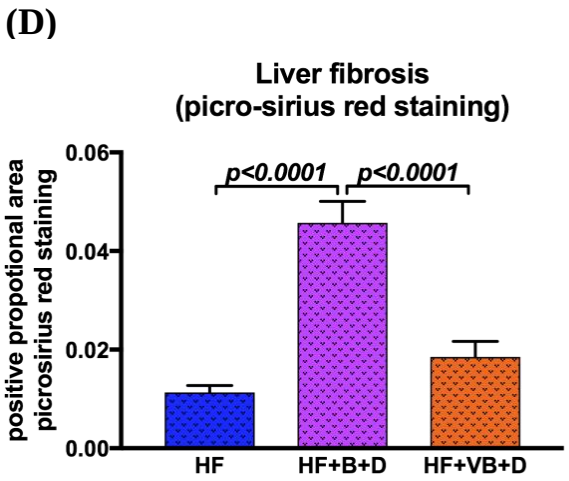

Figure 5.10 Quantification of collagen content in liver sections stained with picrosirius red in mice fed on different diets

Liver collagen deposition was significantly ($p<0.0001$) increased in high AGE diet fed diabetic mice (HF+B+D) after 40 weeks compared to HF fed mice (B). Marinating the HF diet with vinegar prior to baking markedly reduced ($p<0.0001$) liver fibrosis (C, D). Each bar represents mean ± SEM profile from 10-15 mice per treatment group as calculated by one-way ANOVA with Tukey's comparison test. Images are liver histology sections stained with picrosirius red staining. Arrows: pericellular fibrosis. Magnification x200. HF: high fat, B: baking, D: diabetes, VB: marination with vinegar prior baking.

5.4 Discussion

In chapters 3 and 4, we showed that primarily dietary AGEs and endogenously AGEs which possibly formed during diabetes, contribute to NAFLD progression to liver fibrosis. This indicated that pharmacological or non-pharmacological interventions to reduce the formation AGEs would be expected to provide therapeutic strategies to arrest or reduce AGEs-induced NAFLD progression, especially in diabetes. In this chapter, we therefore investigated several strategies to inhibit or reduce AGE formation. Whilst this constituted an endogenous approach, we also attempted to use dietary modification of food as an exogenous approach. As illustrated by Figure 5.11, indeed dietary restriction of AGE formation by vinegar marination, a common food preparation method in the Mediterranean diet, improved NAFLD progression to liver fibrosis. We found that diet

prepared using this method has low AGE content. Interestingly, in mice fed this diet, there were a plethora of beneficial effects which included reduced liver injury, reduced expression of RAGE, endotoxin responsive genes, pro-inflammatory cytokine expression, HSC activation which were associated with a marked reduction in pro-fibrotic and fibrotic genes, leading to a profound reduction in liver fibrosis. In marked contrast, drugs that were used to inhibit AGE formation in diabetic animals failed to affect NAFLD progression to liver fibrosis, although aminoguanidine showed improvement in the expression of TNF-α. On the other hand, we noticed that both drugs, which are known to inhibit or reduce endogenous AGE formation in diabetes[428] but not known to affect AGE/RAGE signalling, also showed some deleterious effects, including worsening of fibrosis in HF fed mice. More carbonyl reactive traps are likely to be toxic because of their reaction with depletion of vitamin B6.[429] This may explain the deleterious effects of these drugs in HF fed mice as the presence of carbonyl intermediates in these mice are low.

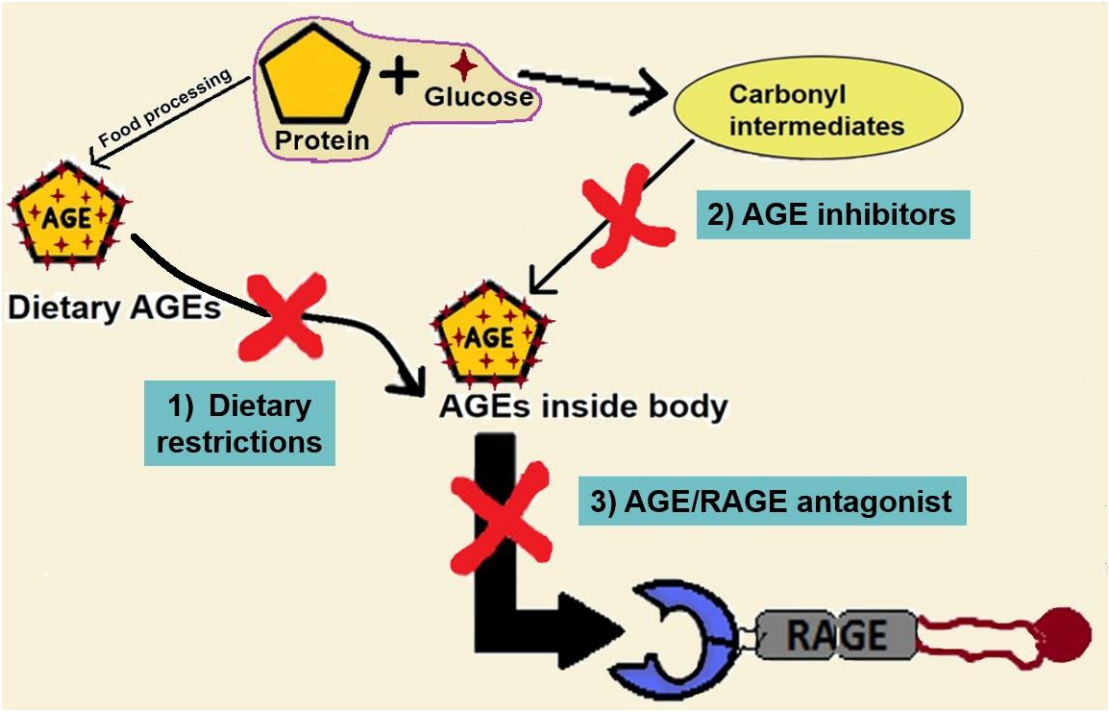

Figure 5.11 Approaches to Inhibit AGE/RAGE axis to prevent NAFLD progression to liver fibrosis

Both aminoguanidine and pyridoxamine have been widely used in pre-clinical studies to improve disease status by reducing AGE formation.[428,430] Moreover, these drugs which are classified as AGE inhibitors, have also been used in Phase I-III clinical trials, mostly in diabetic complications.[319] In addition, these drugs do not alter body weight as shown in the present and previous studies.[431]

In chronic liver disease, fibrosis is driven by pro-inflammatory cytokines primarily secreted by Kupffer cells such as TNF-α[432] which is critically involved in the pathogenesis of liver disease. Although pyridoxamine has been shown to reduce TNF-α expression in adipose tissue,[433] the current study showed an opposite trend in that pyridoxamine in fact increased TNF-α expression in the liver of mice fed a HF diet. In agreement with its positive effect in adipose tissue, pyridoxamine has also been shown to reduce TNF-α gene expression in rats with experimental diabetic nephropathy.[411] This finding was somewhat similar to those in the current study where there was a trend in reducing TNF-α gene expression in diabetic mice. On the other hand, aminoguanidine, the first AGE inhibitor identified to effectively prevent the formation of AGEs *in vitro*,[319] did not change TNF-α expression in high fat fed mice; however, it markedly reduced its expression in diabetic mice fed the same diet, suggesting that like pyridoxamine, aminoguanidine likely inhibits endogenous AGE formation in diabetes. We also found that neither aminoguanidine nor pyridoxamine affected TNF-α gene expression in high dietary AGE fed mice. This is expected as there is no strong evidence to suggest that these drugs are effective in blocking the interactions between AGEs derived from diet and tissue RAGE.

Activation of HSC takes place in two stages as mentioned in section 1.7 of chapter 1. The first step essentially is the initiation which is the pro-inflammatory stage which is followed by perpetuation of inflammation. In the present study, the expression of the HSC activation marker α-SMA, followed a similar pattern as the expression of TNF-α in diabetic mice treated with aminoguanidine. Similar to TNF-α, both drugs did not have any effect on disease progression in high dietary AGE fed mice. On the other hand, collagen 1 expression, which has been shown to be reduced in the adipose tissue by HF diet in mice treated with pyridoxamine,[433] was in fact increased by both drugs in HF fed mice. Nevertheless, the increased collagen 1 expression by both drugs in HF and high AGE fed mice, which is generally expected to increase liver fibrosis, was associated with

increased fibrosis in HF fed mice but not in the high AGE fed mice. This is possibly due to the fact that has also been shown in chapters 3 and 4, diabetes and high dietary AGEs caused an increased liver fibrosis, so that fibrosis promoting effect of the drugs was not visible. Thus, the findings of this study do not support published studies which have been reported both aminoguanidine and pyridoxamine inhibit AGE formation and improves disease in other conditions.[434-437] On the other hand, however there is one study that reported no beneficial effects of aminoguanidine on liver.[438] It should also be noted that some clinical trials reported that aminoguanidine causes pancreatic and renal-neoplastic tumors.[439] It was further noticed that in ACTION 1 clinical trial, the drug has caused the elevation of liver enzyme levels and development of autoantibodies.[440] Moreover, ACTION 2 trials were terminated due to unfavourable risk to benefit ratio.[441] Similar to aminoguanidine, eight weeks of pyridoxamine treatment failed to produce positive results in haemodialysis patients.[442] Thus, the clinical utility of these drugs may be limited.

The most promising outcome from studies described in this chapter comes from dietary intervention. We demonstrate that inhibiting AGE formation in the diet produced promising results in terms of reducing liver fibrosis. It has been shown that food processed in the presence of weak organic acids such as lime juice (citric acid) and vinegar (acetic acid) contained low AGEs compared to foods that have been processed using the same cooking method but without acids,[443] while effects of vinegar on other nutrients have not been reported. The formation of AGEs involves a series of reactions, which includes a reversible first reaction as depicted in Figure 1.7 in chapter 1. Reversible reactions are in an equilibrium, where any disruption to the system results in favouring the opposite reaction. In the presence of an acidic medium, there is an excessive amount of H^+ ions which prevent the dissociation of H^+ ions from amino acids or lipid which is necessary to initiate the reaction with reducing sugar. This results in lower amount of Schiff bases (product of the first reaction between sugar and proteins or lipids) in the medium. The second step of formation of Amadori products influenced by these low amounts of Schiff bases by favouring the backward reaction resulting in low amounts of Amadori products which lead to the production of less AGEs.[444]

Confirming our findings presented in chapters 3 and 4, in this study high dietary AGEs caused an increased expression of two major LPS binding receptors, CD-14 and TLR-4, in the liver. Although we did not measure circulating LPS levels in the present study,

unpublished data from our laboratory show that mice fed a HF diet increased LPS entering the systemic circulation via portal blood, likely due to high fat-induced dysbiosis and leaky gut.[445] Most importantly, vinegar marination prior to baking the HF diet markedly down-regulated both CD-14 and TLR-4 expression in the liver, likely due to a reduced exposure of the liver to LPS, resulting from a reduced AGE levels in the diet (see Figure 5.4). This also supports a marked reduction in liver RAGE expression in mice fed the vinegar marinated diet, likely due to reduced levels of AGEs reaching the liver or less LPS entering the portal circulation or both.

Support for beneficial effects of vinegar marination on gut microbiota comes from a study which highlighted that the Mediterranean diet is associated with beneficial microbiome profiles compared to subjects consumed the Western diets in an adult population.[446] Moreover, it has also been shown that adherence to the Mediterranean diet for three months lowered the prevalence of NAFLD in a human population.[447] Another study showed that the Mediterranean diet not only improved insulin sensitivity, but also reduced the severity of hepatic steatosis in 12 non-diabetic subjects after consuming the diet for 6 weeks.[448] This was further supported by a trial, which included 259 obese patients with type-2 diabetes who were allocated to consume three different diets including a modified Mediterranean diet for 12 months.[449]

The study reported that plasma ALT levels were reduced in those patients who consumed the Mediterranean diet after 6 and 12 months.[449] This was supported by another study which showed that subjects with metabolic syndrome adhered to the Mediterranean dietary pattern had a moderate association of aminotransferases with the prevalence of metabolic syndrome.[450] The present study showed that mice fed the vinegar marinated diet had a markedly reduced ALP and ALT levels compared to those fed the baked diet without marination. Thus, the finding that vinegar marination of diet resulted in the improvement of a number of end points including NAFLD progression to fibrosis could be explained by the diet containing low AGE content compared to the baked diet without vinegar marination.

In summary, aminoguanidine and pyridoxamine were associated with detrimental effects on liver fibrosis in HF fed animals and had minimal effects in diabetic or high AGE fed animals. It is not known whether drug doses employed in the present study reached toxic levels under our experimental conditions which counteracted any positive effects due to

inhibition of AGE formation. On the other hand, our second approach that was employed to reduce AGE formation in the diet by dietary modification using vinegar marination resulted in profound reduction in the expression of RAGE, pro-inflammatory and pro-fibrotic cytokines and LPS responsive genes in the liver, leading to a remarkable improvement in NAFLD progression to liver fibrosis. This highlights the fact that a simple dietary modification of food with vinegar marination may provide an unprecedented benefit for patients with diabetes associated NAFLD.

CHAPTER 6

Effects of an AGE-crosslink breaker alagebrium on AGE-induced NAFLD progression to liver fibrosis

6.1 Introduction

We have shown in chapter 3 and 4 that exposure of fatty livers to advanced glycation end products (AGEs) exacerbates the progression of non-alcoholic fatty liver disease (NAFLD) to fibrosis. We have used two sources of AGE exposure; exposure of fatty liver to endogenously produced AGEs by means of intraperitoneal injections (chapter 3) or due to the presence of diabetes (chapter 4 and 5), and exposure of fatty liver to exogenously produced AGEs i.e. dietary AGEs (chapters 3, 4 and 5). We then demonstrated that AGEs derived from the diet were more harmful and strong stimuli to induce a plethora of effects that resulted in the progression of NAFLD to liver fibrosis than endogenously derived AGEs. We then investigated whether pharmacological blockade of AGE formation *in vivo* using known AGE inhibitors and non-pharmacological blockade of AGE formation *in vitro* using dietary modification (chapter 5). These studies conclusively showed that vinegar marination of the high AGE diet, but not pharmacological inhibitors was able to improve NAFLD progression to liver fibrosis. Since the drugs used in chapter 5 are not expected to block AGE/RAGE signalling, in this chapter, we employed a known AGE-crosslink breaker, alagebrium (Ala), which might also block AGE/RAGE signalling, and investigated the effects of this drug on NAFLD progression to liver fibrosis in mice fed the high fat or high AGE diet.

Alagebrium (Ala) was first named as ALT-711 or 4,5-dimethyl-3-(2-oxo-2-phenylethyl)thiazolium chloride as it contains a thiazolium structure (Fig. 6.1). Although it was developed as an AGE-crosslink breaker by the company Alteon Inc. (later known as Synvista therapeutics), the exact mechanism of action of Ala remains controversial. The crosslink breaking activity was supported by the observation that low molecular weight proteins were aggregated when human diabetic lens containing high molecular weight AGE compounds were incubated with Ala.[451] In contrast, other studies performed by incubating rat tail and tendon skin with Ala did not result in the breaking of pre-formed AGE-crosslinks.[452] Although the mechanism by which Ala works is unclear, pre-clinical studies showed the drug is effective in reducing renal dysfunction and cardiovascular diseases.[319]

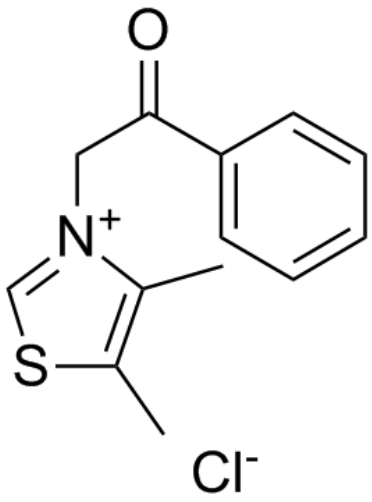

Figure 6.1 Chemical structure of alagebrium

Ala has been extensively used in a number of clinical trials, sponsored by Synvista Therapeutics from 2002 to 2010 such as DIAMOND (NCT00043836), SAPPHIRE (NCT00045981), SILVER (NCT00045994), SPECTRA (NCT00089713), BREAK-DHF-I (NCT00662116) and BENEFICIAL (NCT00516646).[428] Most of the trials has been focused on cardiovascular diseases and has shown improved ventricular function, arterial stiffness and improved atherosclerosis. Despite not all data having been published as some clinical trials were terminated due to financial issues of the company,[430] published data showed that Ala has been well tolerated by subjects.[319]

In addition to use of Ala in pre-clinical and clinical trials related to cardiovascular impairments,[453-459] Ala has also been shown to be effective in diabetic nephropathy[460] central nervous system complications,[364] diabetic retinopathy[461] and erectile dysfunction.[273,462] Although, Ala improved arterial compliance in a clinical trial, it also modestly increased serum triglyceride level,[463] prompting Synvista Therapeutics to conduct a safety and efficacy study of Ala. A subsequent phase I clinical trial, which was conducted with a higher dose of Ala to evaluate the effects of Ala on serum levels of triglycerides and total cholesterol, reported no detrimental effects of Ala on liver function. However, other than these safety trials, there are no studies carried out to investigate the beneficial effects of Ala on liver disease. Therefore, the objective of the current study was to investigate the effects of Ala on NAFLD progression. Moreover, to provide mechanistic insights at the cellular level, cell culture experiments using immortalized Kupffer cell line KUP5 cells and immortalized hepatic stellate cells LX2 cells were also performed.

6.2 Materials and Methods

6.2.1 Experimental design

AGE trafficking studies with Alagebrium (4 weeks)

To study the effects of Ala on AGE trafficking, 6 to 8-weeks-old male C57BL/6 mice were randomized into 5 groups (n=10 per group) and fed on either standard chow, HF diet or HF+B (high AGE) diet for four weeks. Two groups of mice i.e. one from each fed the high fat (HF) diet or the high AGE diet (HF+B), were gavaged with Ala daily at a dose of 10 mg/kg bw in the last two weeks. At the end of the experiment, animals were fasted for 12 hours and the fasted animals received 0.5 mL of fluorescently-labelled AGEs by oral gavage. Then, they were sacrificed after 20 minutes of oral gavage (To determine the time point at which the best AGE trafficking occurs, a time course experiment was carried out by sacrificing a mouse at each time point of 10, 20, 30, 60 and 120 minutes after AGE gavage and 20 minutes was selected as the optimal time). Urine, blood, whole body, liver, kidney and whole intestine were subject to IVIS detection of fluorescent emission using the living image software. The five groups of mice used in this experiment are as follows:

1) Std chow (Standard chow fed mice)

2) HF (high fat fed mice)

3) HF + Ala (high fat fed mice treated with Ala for last 2 weeks)

4) HF + B (high AGE fed mice)

5) HF + B + Ala (high AGE fed mice treated with Ala for last 2 weeks)

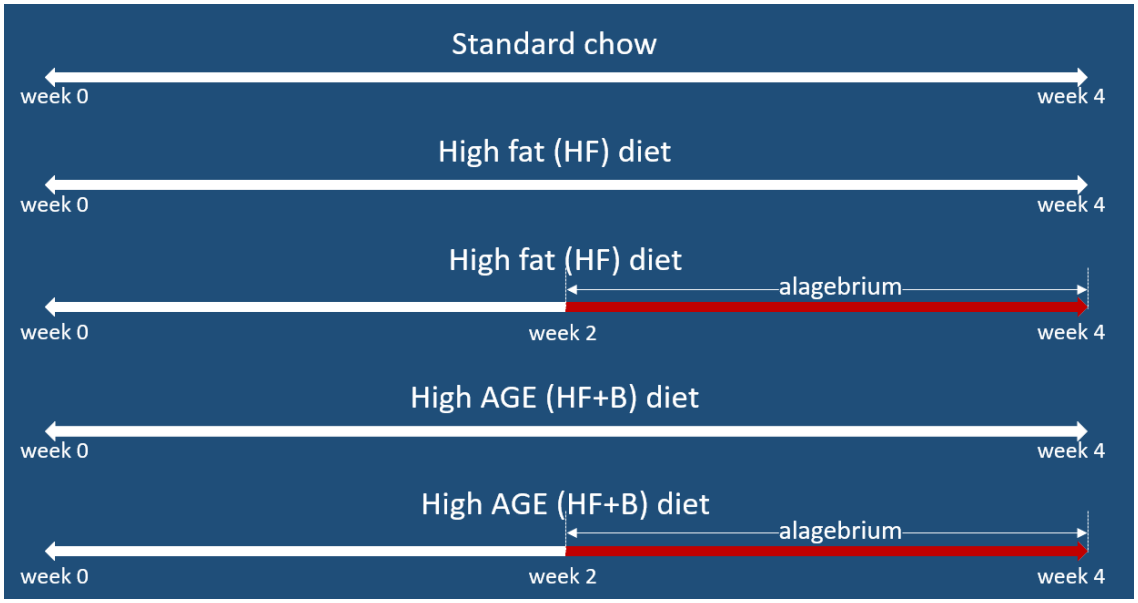

Effect of Alagebrium on AGE-induced NAFLD progression (40 weeks)

To study the effects of Ala on AGE-induced NAFLD progression to liver fibrosis, 40 weeks of HF dietary mouse model was used. Mice were randomized into 3 groups (n=10-15 per group) and fed on the HF or HF+B for 40 weeks. In keeping with the treatment schedule described in chapter 5, Ala was administered to one group of mice in the last 10 weeks (from week 30 to 40) by daily oral gavage at a dose of 10 mg/kg bw. At the end of the experiments, blood and liver tissues were harvested for analysis as mentioned in chapter 2. The three groups of mice used in this experiment are as follows:

1) HF (high fat fed mice)

2) HF + B (high AGE fed mice)

3) HF + B + Ala (high AGE fed mice treated with Ala for last 10 weeks)

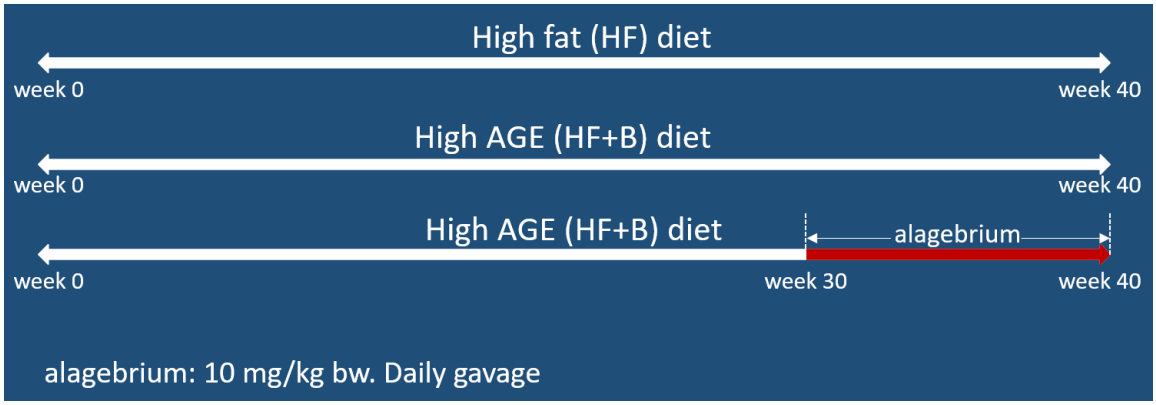

6.2.2 Preparation of AGEs for AGE trafficking and cell culture experiments

Solutions of AGEs for i.p. injections were prepared as outlined in section 2.3.1 of chapter 2. In brief, 40 mg/mL RSA (Sigma Aldrich, Australia) solution was prepared using 0.2 M phosphate buffered saline (PBS) as the solvent. To this RSA solution, 90 g/L of D-glucose (Ajax Pharmaceuticals, Australia) was added, giving a final glucose concentration of 0.5 M. This mixture was incubated at 37^{o} C for 6 weeks followed by dialysis against 0.2 M PBS using dialysis flasks (Thermo Fisher Scientific, Australia) at 4^{o} C for 48 hours, to remove any free glucose. The pH was adjusted to 7. The control was treated the same way without adding glucose. At the end, CML levels were measured by ELISA (Jomar Life Research, Australia).

To prepare fluorescently-labelled AGEs, LI-COR IR dye conjugation (Lincoln, USA) was used as described in section 2.8.2 of chapter 2. In brief, the pH of the AGE solution was adjusted to 8.5 using potassium phosphate buffer. Next, 1 vial of dye was dissolved in 25 µL of ultrapure water. Then, appropriate volume of the dye and AGEs were mixed thoroughly and incubated at room temperature for 2 hours. Finally, the free dye from the conjugate was removed using Zebra spin desalting columns (Pierse Biotechnology, USA).

6.2.3 Preparation of AGEs in the diet

Dietary AGE content was increased by baking the HF diet at 160^0 C for 1 hour. CML, CEL and MG-H1 content in the diet was assessed using GC/MS.

6.2.4 Tissue harvesting and storage

The animals were sacrificed at 40 weeks using pentobarbitone (120 mg/kg bw) as described in chapter 2. Blood and livers were collected as described in chapter 2.

6.2.5 Biochemical assessment of liver function

Liver function test was carried out in plasma that had been stored at -20^o C, using Beckman Coulter LX20 autoanalyzer (Beckman Coulter) at Austin Pathology, Austin Health.

6.2.6 Liver gene expression

Total RNA was extracted from snap-frozen liver samples stored at -80^o C as described in section 2.6 of chapter 2. Synthesis of cDNA from RNA and qPCR reactions were carried out using multiplexing to assess the expression of RAGE, LPS-binding receptors, pro-inflammatory and pro-fibrotic genes. The details of dual fluorescent-labelled oligonucleotide probes and primers are given in Table 2.4 in chapter 2.

6.2.7 Histological assessment of liver injury and fibrosis

Haematoxylin and Eosin (H&E) staining

Liver sections of 4 µm was used to perform H&E staining as described in section 2.7.2 of chapter 2. The type of NAFLD was categorised according to the steatosis and parenchymal degenerative changes in the liver as described previously.[464]

Picrosirius red staining

Picrosirius red staining was performed in 4 μm liver sections as described in section 2.7.1 of chapter 2. Briefly, total collagen was quantified by analysing liver sections under a standard light microscope (Olympus BX50 Microscope, Japan; magnification x200). Collagen volume fraction was determined by measuring the area of stained tissue (red) within a randomly selected field. An average of 10 fields per section was derived for each animal using computerized image capture (MCID) (Imaging Research, Canada) and used in the analysis. Results are expressed as a proportional area positively stained red.

6.2.8 4-hydroxynonenal (4-HNE) immunohistochemistry for lipid peroxidation

The marker of lipid peroxidation, 4-HNE was assessed using 4 μm sections of mouse liver tissues as described in section 2.7.3.4 of chapter 2. Primary antibody to 4-HNE (Alpha Diagnostic International) was applied in 1:100 dilution for overnight and secondary antibody (Dako, Agilent technology) was used in 1:100 dilution. The positive staining in each section was determined using MCID (Imaging Research, Canada) software at x200 magnification. An average of 10 fields per section was derived for each animal using MCID (Imaging Research) for use in the analysis. The results are expressed as a proportional area positively stained brown.

6.2.9 Cell culture Experiments

Kupffer cells (KUP5)[349] were treated with 200 μg/mL AGEs for 6 hours. To investigate the prophylactic effects of Ala, the drug was added to the medium in 1 μM and 100 μM doses at the time of AGEs treatment and incubation continued for 6 hours. To investigate the therapeutic effects, cells were incubated with AGES for 5 hours and then Ala was added to the cells in the same two doses and incubated for 1 hour. Cells were harvested for gene expression of RAGE and pro-inflammatory cytokine analysis. However, we have also measured the expression of RAGE and pro-inflammatory cytokines 5 hours after incubation with AGEs to show that gene expressions were increased when Ala was added to the cells (therapeutic approach).

Immortalised human HSCs (LX2) were exposed to 200 μg/mL of AGEs as well as to the conditioned media collected from KUP5 cells treated with AGEs for 6 hours or both AGEs and Ala as mentioned above under therapeutic approach. Cells were harvested for gene expression analysis of RAGE and α-SMA. Gene expression induced by TGF-β1 at 10 ng/mL was used as the positive control.

6.2.10 Statistical analysis

Results are expressed as mean ± SEM and analysed by one-way analysis of variance (ANOVA) with Tukey's post-hoc test using Prism 7 software (GraphPad Software, San Diego, United States). $p < 0.05$ was considered significant.

6.3 Results

6.3.1 Effects of alagebrium on AGE clearance from the liver

The time course study performed from 10 minutes to 2 hours following labelled-AGE administration showed that at any time point, the fluorescence was emitted only from liver and kidney (Fig. 6.2A), and the gut (discussed below). The highest emission of florescence by livers could be seen 20 minutes after the administration of labelled-AGEs (Fig. 6.2B). After 30 minutes of labelled-AGE administration, an emission could be seen near the rectal area of mice, suggesting that AGEs have been passed through the gut within 30 minutes. After this time point, radiant intensity of kidneys was brighter than the intensity of livers. Although we measured the emission of stool, we could not detect a measurable amount of radiant from stool, suggesting a large proportion of AGEs has been absorbed through the gut. In addition, there was a weak signal emanated from a urine sample although this was not detected in the blood sample. Overall, based on the time course study, 20 minutes after administration of labelled-AGEs was selected as the best time point to detect fluorescence in different treatment groups.

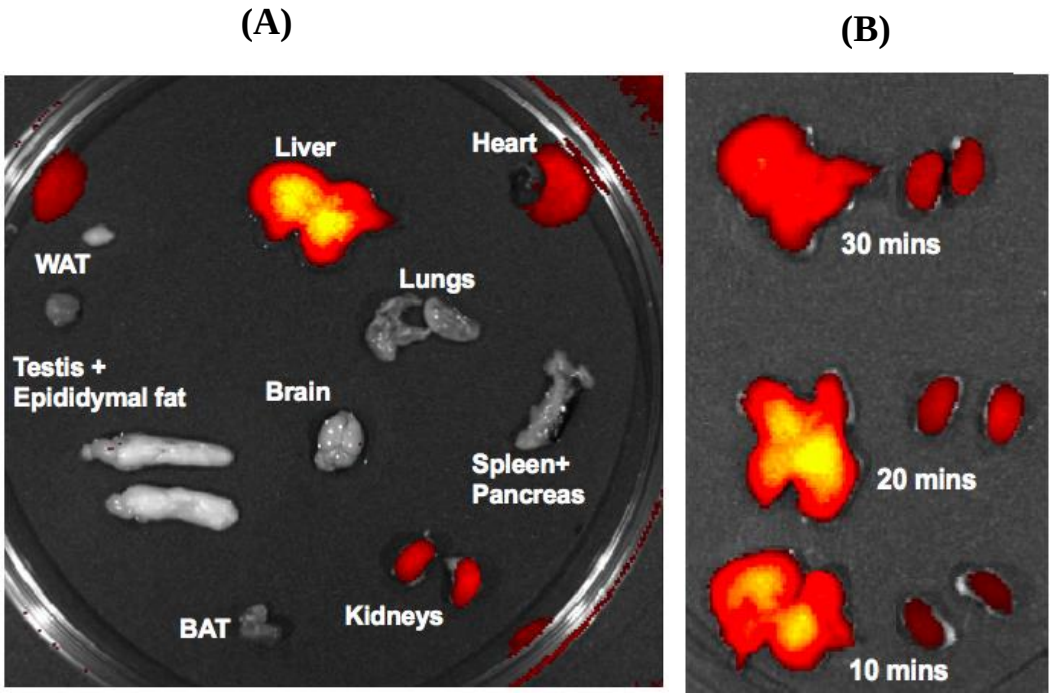

Figure 6.2 Fluorescence intensity of organs after 20 minutes of labelled AGE administration

Liver and the kidneys were the only organs that showed fluorescence following the administration of labelled AGEs as measured by IVIS scanner (A). The livers emitted the brightest fluorescence after 20 minutes of labelled-AGE administration (B).

Mice fed the standard chow showed the maximum clearance of labelled-AGEs from the liver, represented by the highest fluorescence emission in the liver as well as bright fluorescence in the kidneys (Fig. 6.3A). This was significantly ($p<0.01$) reduced by both HF and high AGE (HF+B) diets (Fig. 6.3B). In marked contrast, Ala treatment in high AGE fed mice restored AGE clearance by the liver as indicated by significantly higher florescence in the liver and kidneys than those fed the HF, HF+ Ala or HF+B (Fig. 6.3B, C). However, Ala treatment in HF fed mice failed to improve AGE clearance from the liver (Fig. 6.3B, C), suggesting that Ala appears to work only when liver exposed to high AGEs. We also measured the florescence in blood and urine and found no florescence was emitted by blood with weak signal detected in urine. We also detected fluorescence emission by the gut, showing bright intensity in jejunum area in mice fed the standard chow or high AGE fed (HF+B) mice receiving Ala treatment whilst other groups of mice

showed dull fluorescence. After 20 minutes AGEs have not been reached to latter part of the small intestine such as the ileum or large intestine (Fig. 6.3C).

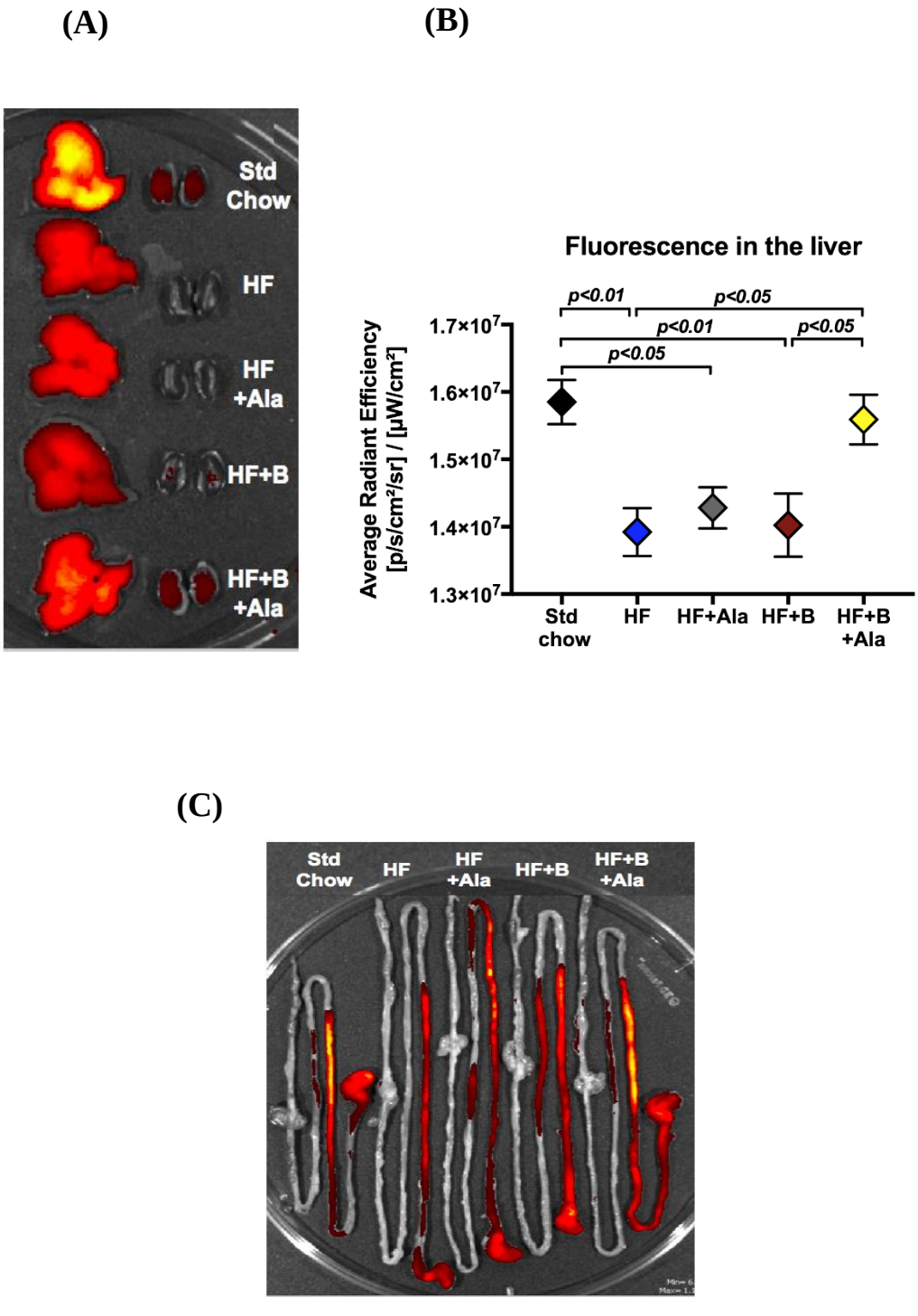

Figure 6.3 Alagebrium normalized the clearance of AGEs from the liver

The livers of the mice fed the standard chow diet showed the highest fluorescence radiant which was significantly reduced by HF or HF+B feeding (A, B). The fluorescence was

significantly increased in HF+B fed mice treated with Ala (A, B). Kidneys showed a similar pattern to that of liver (A, B). Whilst there was no detectable difference of radiant emission between groups in the gut, bright intensity was seen in the jejunum area in mice fed the standard chow and HF+B+ Ala (C). Each point represents the mean ± SEM profile of 10 mice per treatment group as calculated by one-way ANOVA with Tukey's comparison test. Std chow: standard chow, HF: high fat, B: baking, Ala: alagebrium.

6.3.2 Effects of alagebrium on liver function tests and liver injury

In 40 weeks model, physical appearance (not shown), body weight (45.9 ± 2.0 g), liver weight (3.4 ± 0.4 g), food intake (~6 g/day) and water intake (~5 mL) was similar in all 3 experimental groups of mice. However, liver function test determined in plasma was improved in Ala treated mice. Both alanine aminotransferase (ALT) (Fig. 6.4A) and alkaline phosphatase (ALP) (Fig. 6.4B) were significantly ($p<0.01$) elevated due to high AGE diet compared to HF fed mice. Interestingly, mice fed on high AGE diet and treated with Ala significantly ($p<0.01$) reduced these liver enzyme levels compared to high AGE fed mice (Fig. 6.4A, B). However, aspartate aminotransferase (AST) levels, which was not significantly increased in high AGE fed mice, were significantly ($p<0.01$) reduced by Ala treatment (Fig. 6.4C). Plasma bilirubin (<3 µmol/L) did not show any difference between the groups (data not shown).

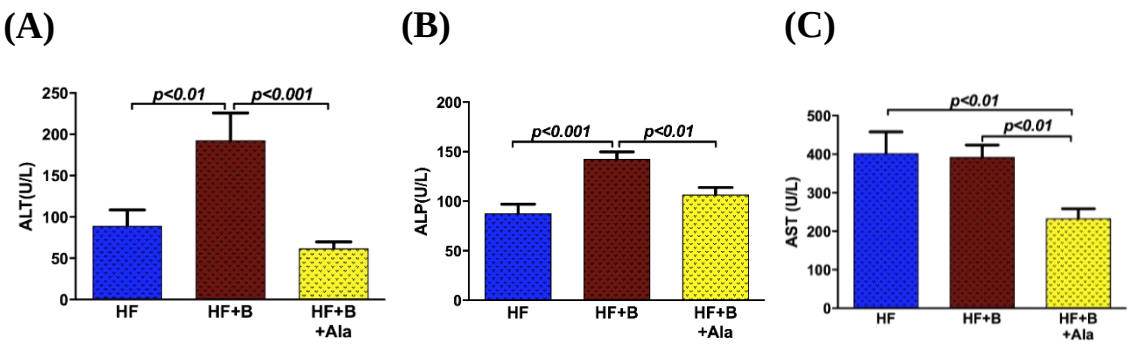

Figure 6.4 Alagebrium significantly reduced liver enzymes elevated due to high AGE diet

The liver enzymes ALT (A) and ALP (B) were significantly elevated in mice fed the high AGE diet compared to HF mice. However, the increased enzyme levels were normalized by Ala treatment. The enzyme AST was not elevated by high dietary AGEs; however, Ala treatment significantly reduced its level in high AGE fed mice compared to both HF

and HF+B fed mice. Each point represents the mean ± SEM profile of 10-15 mice per treatment group as calculated by one-way ANOVA with Tukey's comparison test. HF: high fat diet, B: baking, Ala: alagebrium.

6.3.3 Effects of alagebrium on plasma CML levels and liver RAGE expression

Circulating CML concentration which represents circulating AGEs was significantly ($p<0.0001$) higher in the high AGE fed mice compared to HF fed mice (Fig. 6.5A). However, Ala treatment significantly ($p<0.0001$) reduced plasma CML level compared to high AGE fed mice (Fig. 6.5A). This supports the finding that Ala may improve AGEs uptake by the liver for processing and secretion into the systemic circulation for excretion via the kidneys. In keeping with increased circulating levels of CML/AGEs, liver RAGE expression was significantly ($p<0.0001$) up-regulated by high dietary AGEs compared to HF fed mice. Most importantly, Ala treatment markedly ($p<0.0001$) reduced it to the levels seen in HF fed mice (Fig. 6.5B). Thus, circulating CML levels were strongly and positively ($p<0.001$, $r=0.62$) correlated with liver RAGE expression (Fig. 6.5B).

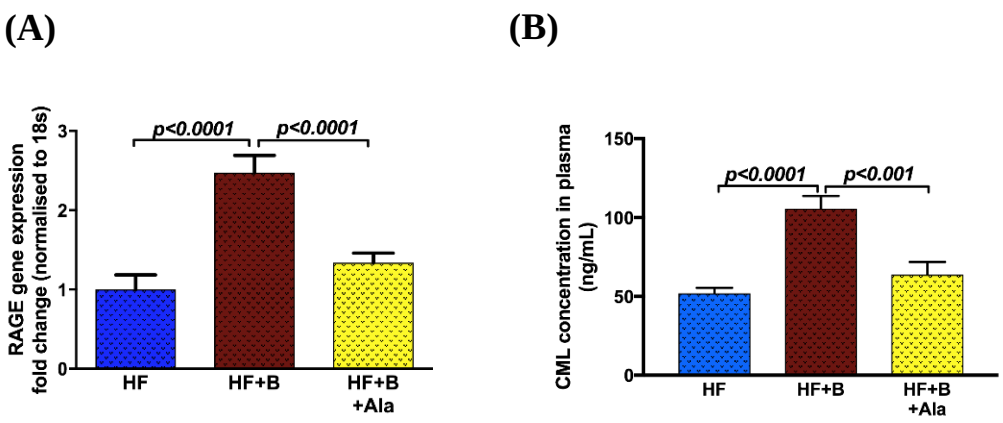

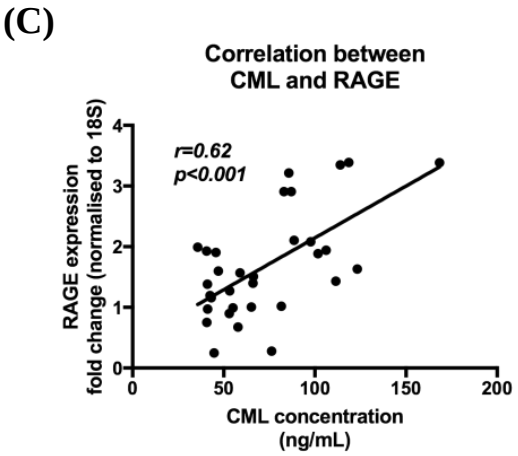

Figure 6.5 Alagebrium significantly reduced plasma CML concentrations and liver RAGE expression

Plasma CML concentration was significantly increased by high AGE (HF+B) diet compared to high fat (HF) diet. However, CML levels were restored to those of HF fed mice by Ala treatment (A). Interestingly, RAGE gene expression followed the same pattern as plasma CML concentration which showed Ala treatment markedly down-regulated RAGE expression (B). Plasma CML levels showed a positive and significant correlation to liver RAGE gene expression. The data have been normalized to endogenous control gene, 18S and HF fed control group was given an arbitrary value of 1. Each point represents the mean ± SEM profile of 10-15 mice per treatment group as calculated by one-way ANOVA with Tukey's comparison test. HF: high fat diet, B: baking, Ala: alagebrium.

6.3.4 Effects of alagebrium on the expression of liver LPS binding receptor genes

It was shown in both chapter 3 and 4 that LPS binding receptors CD-14 and TLR-4 were significantly increased by high dietary AGEs. In keeping with those findings, in the present experiments, we found that hig dietary AGEs significantly ($p<0.0001$) increased liver expression of CD-14 (Fig. 6.6A) and TLR-4 compared to high fat fed mice (Fig. 6.6B). However, the mice fed the high dietary AGEs and also treated with Ala for the last 10 weeks of study showed a significant ($p<0.01$) down-regulation of the expression of LPS binding receptors, CD-14 (Fig. 6.6A) and TLR-4 (Fig. 6.6B).

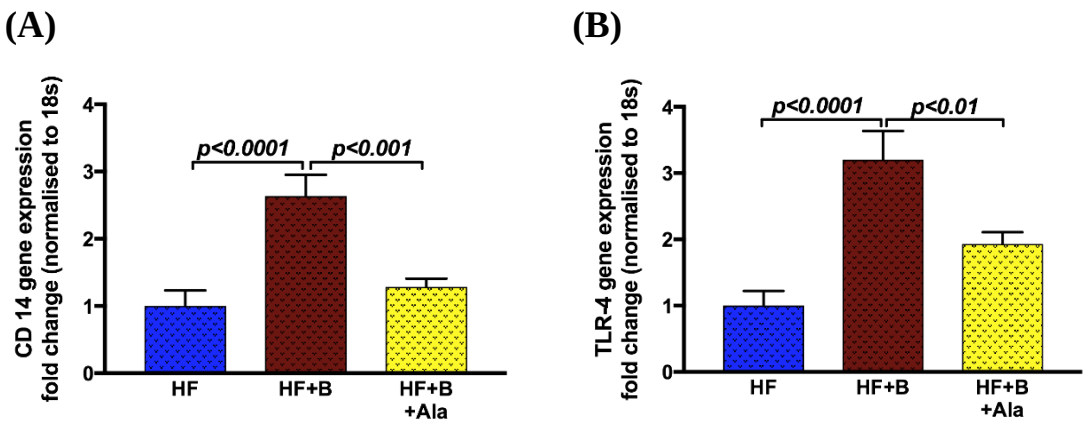

Figure 6.6 Alagebrium significantly reduced the gene expression of LPS binding receptors in the liver

The LPS binding receptors CD-14 (A) and TLR-4 (B) were significantly ($p<0.0001$) increasded by high dietary AGEs (HF+B) compared to high fat (HF) feeding. However, CD-14 (A) and TLR-4 expression was significantly ($p<0.01$) reduced by Ala treatment. The data have been normalized to endogenous control gene, 18S and HF fed control group was given an arbitrary value of 1. Each point represents the mean ± SEM profile of 10-15 mice per treatment group as calculated by one-way ANOVA with Tukey's comparison test. HF: high fat diet, B: baking, Ala: alagebrium.

6.3.5 Effects of alagebrium on the expression of pro-inflammatory cytokines

As shown in chapter 3 and 4, the present study also showed that high dietary AGEs caused significant ($p<0.01$) increases in pro-inflammatory cytokine gene expression in the liver. However, the interventional group fed the high dietary AGEs and treated with Ala showed a marked ($p<0.01$) reduction in hepatic TNF-α (Fig. 6.7A), MCP-1 (Fig. 6.7B) and IL-6 (Fig. 6.7C), suggesting that alagebrium protects the liver from inflammation induced by AGEs. Although we did not quantify NAFLD activity score (NAS score) or inflammation, there was an apparent reduction in inflammatory cell infitration in the liver of Ala treated mice compared to high AGE fed mice (Fig. 6.7E, F).

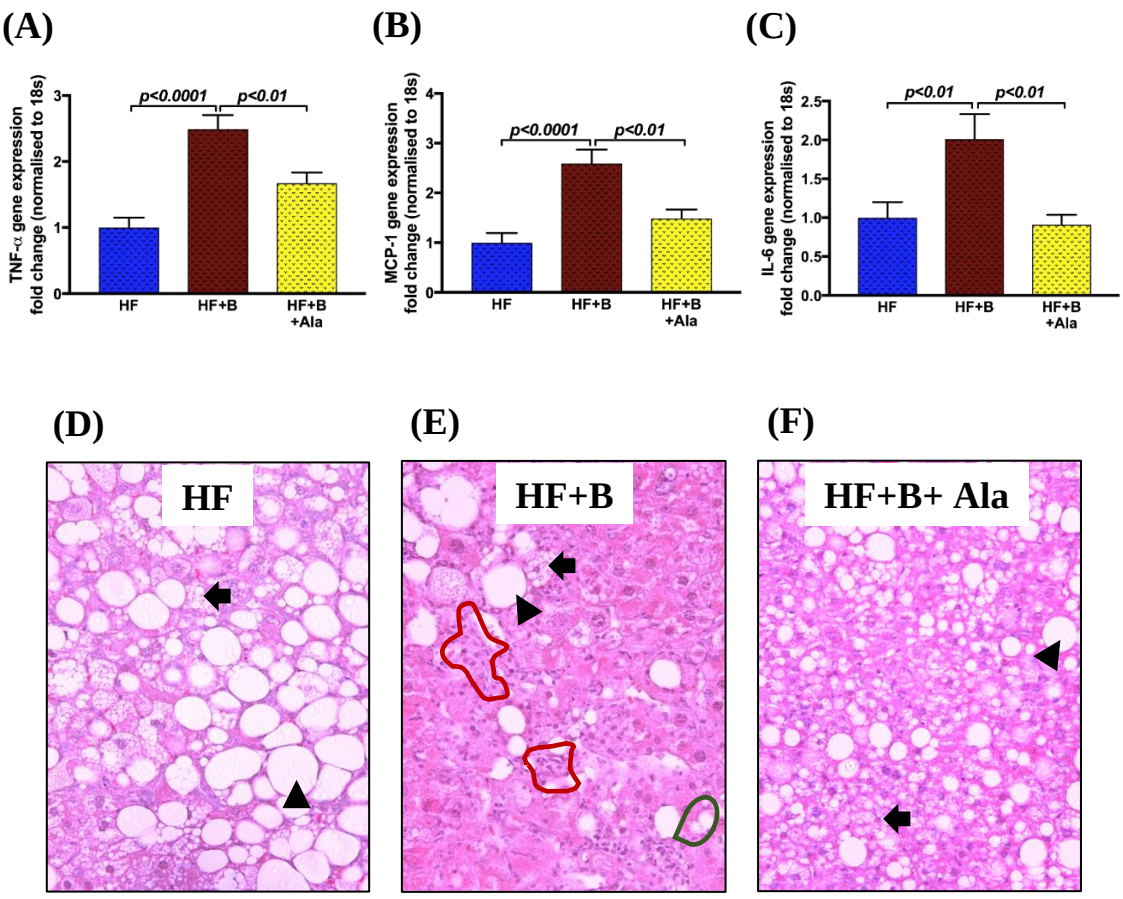

Figure 6.7 Alagebrium significantly reduced liver inflammation

Gene expression of pro-inflammatory cytokines TNF-α (A), MCP-1 (B) and IL-6 (C) was significantly ($p<0.0001$) increased by high dietary AGEs (HF+B) in the liver compared to high fat (HF) fed mice. However, in animals fed the high AGE diet and Ala treatment, there was a significant reduction in the expression of these cytokines. Ingestion of high dietary AGEs was associated with hepatocyte degeneration (marked by green line and inflammatory cell infiltration (marked by red line) (E). Importantly, Ala treatment prevented inflammatory cell infiltration (F) and thus, the livers were histologically similar to HF fed mice (D). However, quantification of cell infiltration was not performed. The data have been normalized to endogenous control gene, 18S and HF fed control group was given an arbitrary value of 1. Each point represents the mean ± SEM profile of 10-15 mice per treatment group as calculated by one-way ANOVA with Tukey's comparison test. Arrows: micro-vesicular steatosis, arrow heads: macro-vesicular steatosis, area under red margins: inflammatory cell infiltration. Magnification x200. HF: high fat diet, B: baking, Ala: alagebrium.

6.3.6 Effects of alagebrium on hepatic stellate cell activation and thereby reduced pro-fibrotic cytokine release and extracellular matrix deposition

It is well known that secretion of pro-inflammatory cytokines by activated Kupffer cells in turn leads to activation of HSCs. High dietary AGEs caused HSC activation, as reflected by increased ($p<0.01$) gene expression of α-SMA, the activated HSC marker, compared to high fat fed mice (Fig. 6.8A), Ala treatment significantly ($p<0.05$) down-regulated high dietary AGE-induced α-SMA expression similar to its effect on pro-inflammatory cytokines secreted by Kupffer cells, suggesting that the cytokines secreted by Kupffer cells likely activate HSCs (see also Figure 3.13 in chapter 3). On the other hand, activated HSCs expressed high levels ($p<0.0001$) of pro-fibrotic cytokine TGF-β1 in mice fed the high AGE diet. However, in keeping with α-SMA expression, Ala treatment significantly ($p<0.0001$) reduced TGF-β1 expression in mice fed the high AGE diet (Fig. 6.8B). Consequently, high dietary AGEs by activating pro-fibrotic TGF-β1 caused an increased ($p<0.001$) expression of a major fibrotic and ECM gene collagen 1 (Fig. 6.8C). However, Ala treatment completely prevented ($p<0.001$) the up-regulation of collagen 1 expression (Fig. 6.8C).

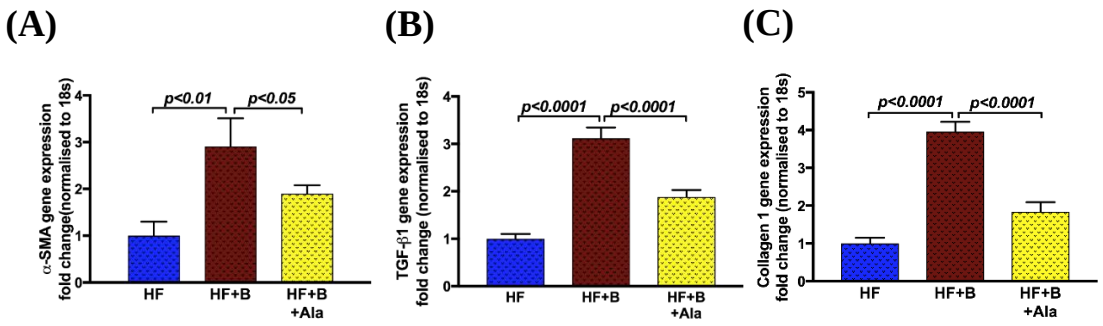

Figure 6.8 Alagebrium significantly reduced gene expression of HSC activation marker and pro-fibrotic and fibrotic markers in the liver

Activation of HSCs by high dietary AGEs is reflected by significant increase in α-SMA expression (A). However, Ala teatment abrogated HSC activation as reflected by significant reduction in α-SMA expression (A). Upon activation, increased expression of pro-fibrotic cytokine TGF-β1 by HSCs in mice fed the high dietary AGEs was significantly inhibited by Ala treatment (B). As a result, increased gene expression of a major ECM protein collagen 1 in the liver of high dietary AGEs fed mice was completely

prevented by Ala treatment (C). The data have been normalized to endogenous control gene, 18S and HF fed control group was given an arbitrary value of 1. Each point represents the mean ± SEM profile of 10-15 mice per treatment group as calculated by one-way ANOVA with Tukey's comparison test. HF: high fat diet, B: baking, Ala: alagebrium.

6.3.7 Effects of alagebrium on NAFLD progression to liver fibrosis

In keeping with increased gene expression of pro-fibrotic cytokines and fibrotic collagen 1, high dietary AGEs caused an increased liver fibrosis (Fig. 6.9A) compared to high fat fed mice (Fig. 6.9B), as shown by increased positive staining of liver sections from high AGE fed mice (Fig. 6.9B). Most importantly, Ala treatment dramatically reduced positive staining of collagens compared to high AGE fed mice (Fig. 6.9C). Quantification of these liver sections showed that a significantly ($p<0.0001$) increased liver fibrosis in high AGEs fed mice was completely prevented by Ala treatment compared to high AGE fed mice without treatment (Fig. 6.9D).

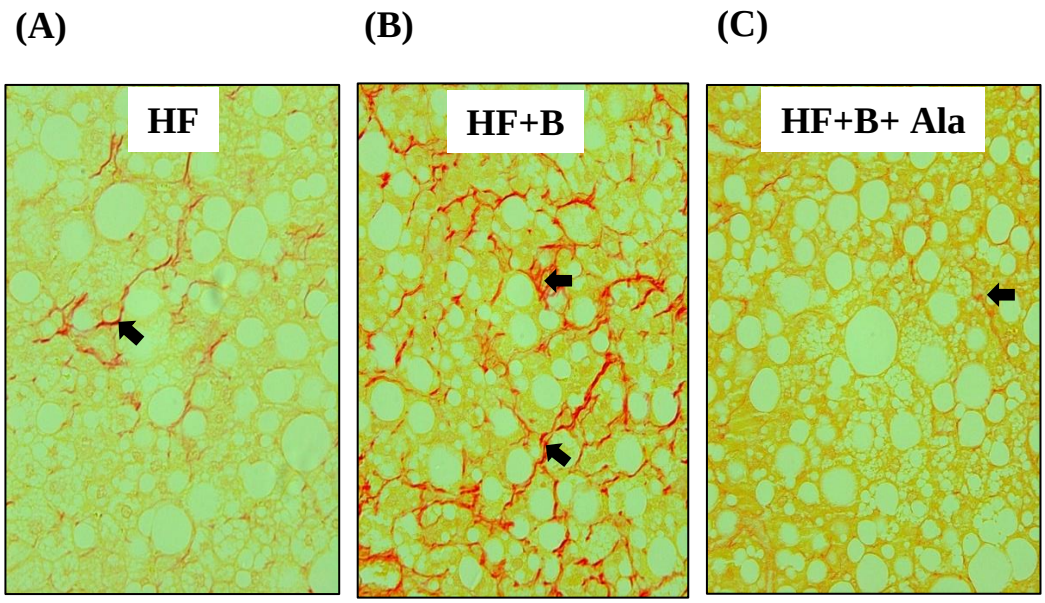

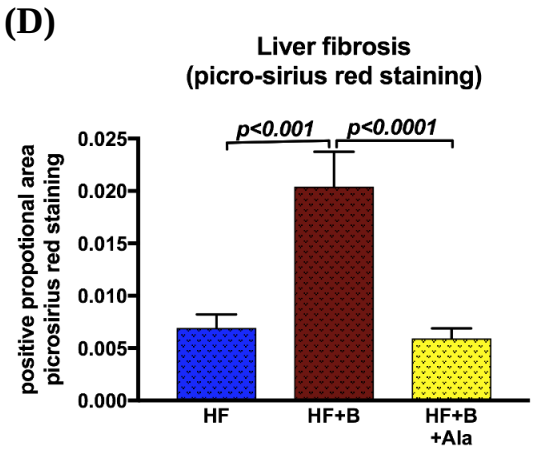

Figure 6.9 Alagebrium significantly reduced liver fibrosis in mice fed the high dietary AGEs

Picrosirius red staining of liver sections from 40 weeks of HF feeding showed mild fibrosis (A). On the other hand, high dietary AGEs (HF+B) significantly increased liver fibrosis compared to HF fed mice (B). However, high AGE fed mice treated with Ala showed a profound reduction in liver fibrosis (C). Quantification of positively stained picrosirius red stained in liver section showed that increased fibrosis caused by high AGE diet was completely prevented by Ala treatment (D). Each bar represents the mean ± SEM profile of 10-15 mice per treatment group as calculated by one-way ANOVA with Tukey's comparison test. Arrows: pericellular fibrosis. Magnification x200. HF: high fat diet, B: baking, Ala: alagebrium.

6.3.8 Effects of alagebrium on lipid peroxidation in the liver of high AGE fed mice

Forty weeks of high fat feeding caused some oxidative stress as reflected by small brown patches (arrow) of positively stained 4-hydroxynonenal (4-HNE) adducts performed on liver sections (Fig. 6.10A). It was shown in chapters 3 and 4 that exposure to high AGEs dramatically increased ROS generation by Kupffer cells and oxidative stress in the liver. In keeping with those findings, in the present study, 4-HNE staining showed wide spread brown patches, reflecting increased lipid peroxidation/oxidative stress in mice fed the high AGE diet (Fig. 6.10B). Interestingly, Ala treatment showed a profound reduction in positively staining 4-HNE adducts compared to high AGE fed mice without Ala

treatment, resulting in a similar histological appearance to that of high fat fed mice (Fig. 6.10C). Quantification of these liver sections showed that high AGE-induced significant ($p<0.0001$) increases in lipid peroxidation adducts were completely abrogated by Ala treatment compared to high AGE fed mice without treatment (Fig. 6.10D).

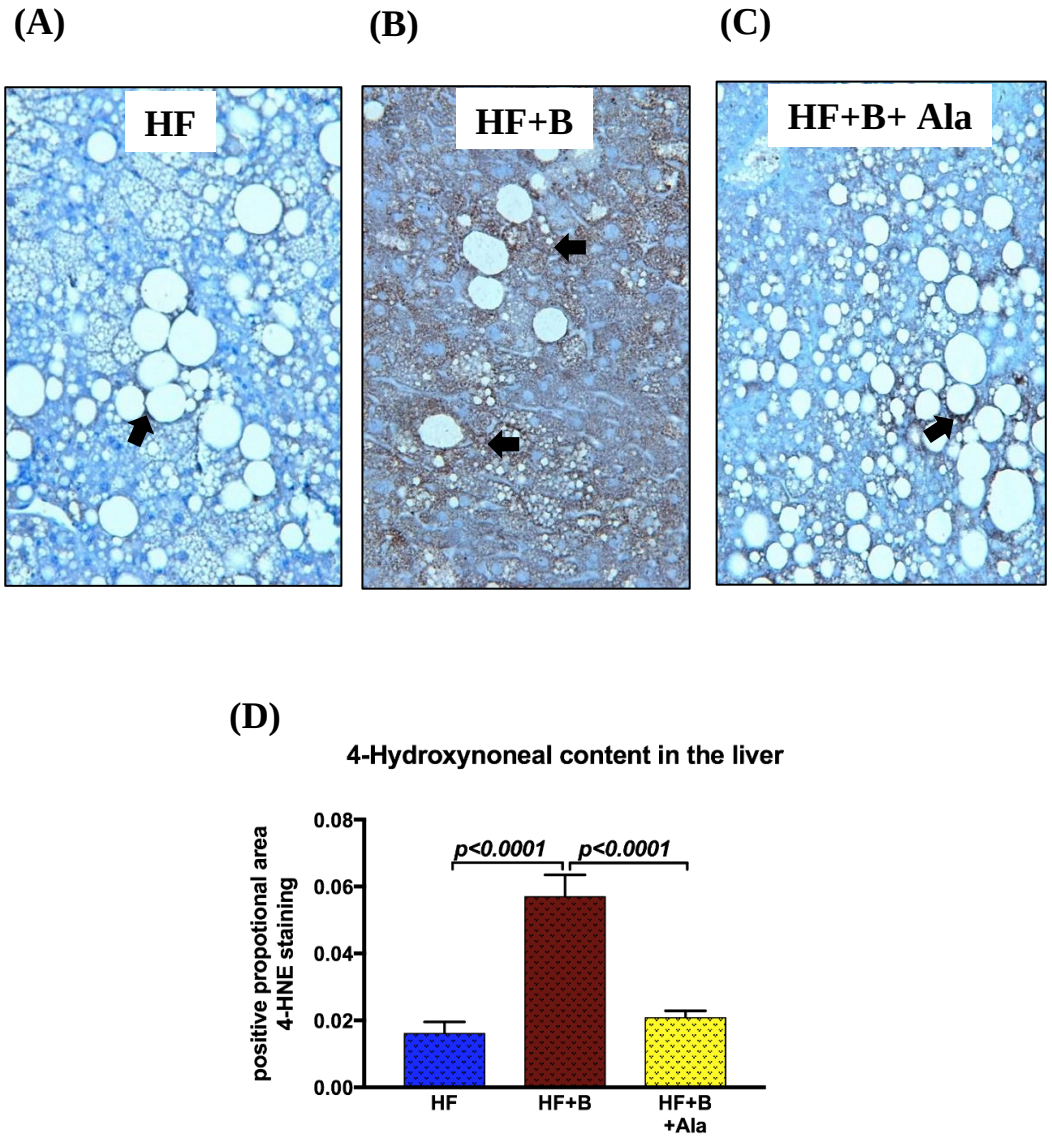

Figure 6.10 Alagebrium inhibited lipid peroxidation in the liver of high AGE fed mice

4-HNE adducts representing lipid peroxidation in liver sections from mice fed the HF diet for 40 weeks showed mild oxidative stress (A). High dietary AGEs (HF+B) significantly increased 4-HNE adducts compared to HF fed mice, represented by increased brown colour positive staining (B). However, high AGE fed mice also treated with Ala showed a profound reduction in lipid peroxidation/oxidative (C). Quantification of positively stained 4-HNE adducts in liver section showed that increased lipid peroxidation/oxidative

stress caused by high AGE diet was completely prevented by Ala treatment (D). Each bar represents the mean ± SEM profile of 10-15 mice per treatment group as calculated by one-way ANOVA with Tukey's comparison test. Arrows: 4-HNE adducts. Magnification x200. HF: high fat diet, B: baking, Ala: alagebrium.

6.3.9 Effects of alagebrium on RAGE gene expression in Kupffer cells

As shown in chapter 3, KUP5 cells exposed to high AGEs significantly ($p<0.0001$) increased gene expression of RAGE compared to untreated or RSA (rat serum albumin) treated cells after 6 hours. However, when these cells were treated with both AGEs and alagebrium, prophylactically or therapeutically, there was a significant ($p<0.05$) down-regulation of RAGE gene expression (Fig. 6.11), suggesting that alagebrium is effective in reducing effects of AGEs which are mediated via RAGE.

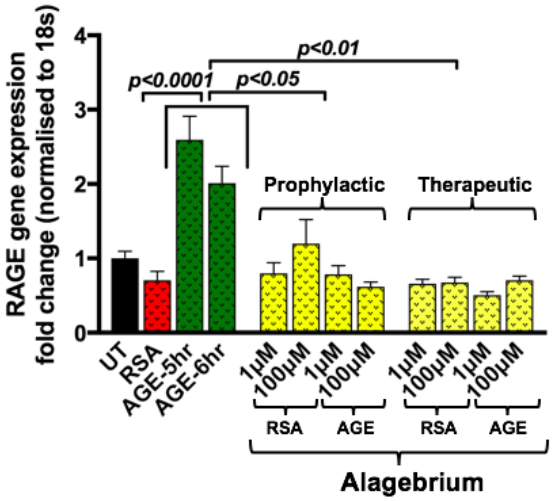

Figure 6.11 Alagebrium prevents RAGE up-regulation by AGEs in KUP5 cells
Gene expression of RAGE showed significant up-regulation in response to incubation with AGEs. Both prophylactic and therapeutic treatment with Ala in two different doses significantly reduced RAGE expression in AGEs-treated KUP5 cells. Gene expression at 5 hours (5hr) of incubation with AGEs is shown to indicate the up-regulated expression of RAGE when Ala was added to the cells (therapeutic approach). The data have been normalized to endogenous control gene, 18S and UT control was given an arbitrary value of 1. Each bar represents the mean ± SEM profile from 3 independent experiments as calculated by one-way ANOVA with Tukey's comparison test. Note: for clarity,

prophylactic and therapeutic groups are indicated by a single bracket for statistical comparison as there was no difference between the groups within each set. UT: untreated, RSA: rat serum albumin.

6.3.10 Effects of alagebrium on pro-inflammatory cytokine expression in Kupffer cells

In vivo experiments clearly showed that exposure to high AGEs dramatically increased gene expression of pro-inflammatory cytokines in the liver. Importantly, 10 weeks of Ala treatment significantly down-regulated the expression of these cytokines. In keeping with the findings of *in vivo* experiments, we measured gene expression of pro-inflammatory cytokines in KUP5 cells treated with Ala using the same protocol as that used to investigate RAGE gene expression above. We found that KUP5 cells exposed to AGEs showed significantly ($p<0.01$) up-regulated pro-inflammatory cytokine expression; TNF-α (Fig. 6.12A), IL-1β (Fig. 6.12B) and MCP-1 (Fig. 6.12C). However, when AGE-exposed cells were treated with Ala, both prophylactically and therapeutically, there were profound reductions ($p<0.05$) in the expression of these cytokines compared to AGE-exposed KUP5 cells without Ala treatment (Fig. 6.12). The finding that the complete prevention of KUP5 cell-expressed cytokines by Ala points to the possibility that in high AGE fed mice, Ala may have blocked pro-inflammatory cytokine secretion by Kupffer cells, preventing HSC activation and NAFLD progression to liver fibrosis.

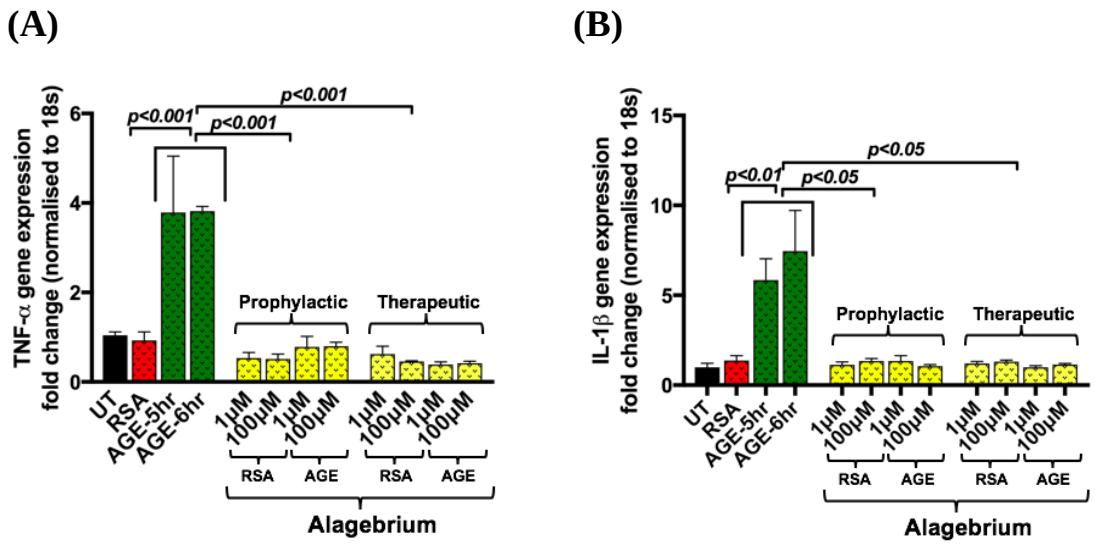

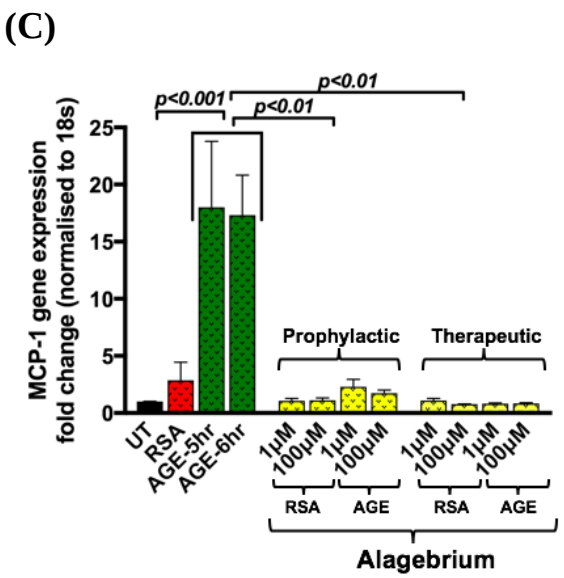

Figure 6.12 Alagebrium prevents up-regulation of pro-inflammatory cytokines by AGEs in KUP5 cells

Gene expression of pro-inflammatory cytokines showed significant up-regulation in response to incubation with AGEs. Both prophylactic and therapeutic treatment with Ala in two different doses significantly reduced TNF-α (A), IL-1β (B) and MCP-1 (C) expression in AGEs-treated KUP5 cells. Gene expression at 5 hours (5hr) of incubation with AGEs is shown to indicate the up-regulated expression of pro-inflammatory cytokines when Ala was added to the cells (therapeutic approach). The data have been normalized to endogenous control gene, 18S and UT control was given an arbitrary value of 1. Each bar represents the mean ± SEM profile from 3 independent experiments as calculated by one-way ANOVA with Tukey's comparison test. Note: for clarity, prophylactic and therapeutic groups are indicated by a single bracket for statistical comparison as there was no difference between the groups within each set. UT: untreated, RSA: rat serum albumin.

6.3.11 Effects of alagebrium on NOX enzyme subunit gene expression and ROS generation in KUP5 cells

We also measured gene expression of NOX enzyme subunits, NOX-4, a membrane bound catalytic subunit and $p47^{phox}$, a regulatory subunit. The expression of both subunit genes was significantly ($p<0.001$) up-regulated in response to AGEs after 6 hours of exposure compared to untreated or RSA treated cells. However, the expression of these genes was

significantly ($p<0.001$) down-regulated by Ala treatment and returned to those of untreated or RSA levels (Fig. 6.13A, B). Although NOX-4 expression after 5 hours showed a similar increase to that of 6 hour incubation, $p47^{phox}$ was not up-regulated by AGEs at this time point. Thus, Ala apparently showed no therapeutic effect on $p47^{phox}$ expression in this experiment (Fig. 6.13B).

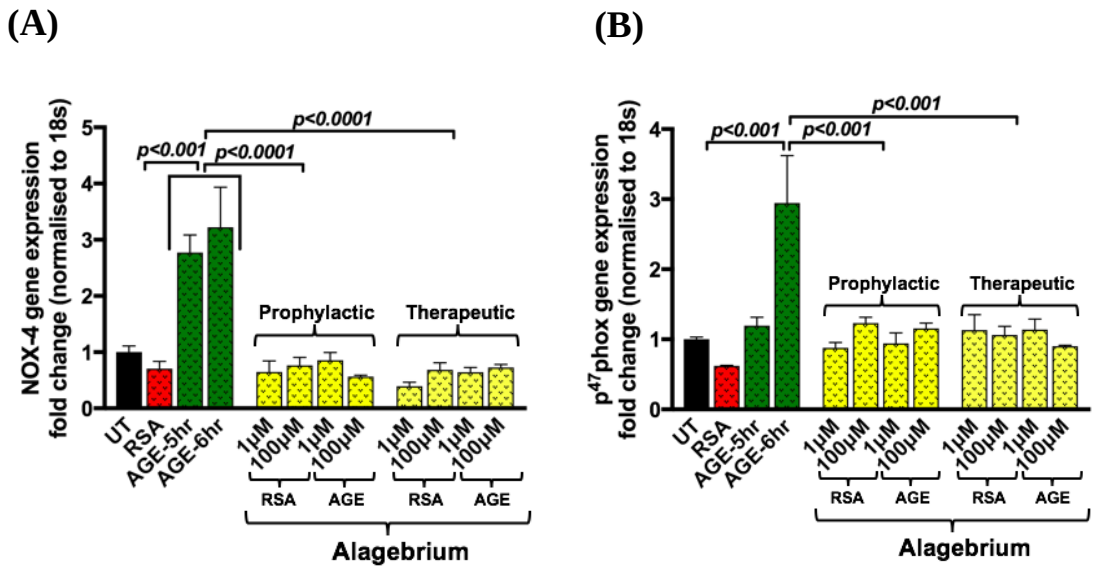

Figure 6.13 Alagebrium prevents up-regulation of NOX enzyme subunit expression by AGEs in KUP5 cells

Gene expression of NOX-4 was significantly up-regulated by AGE exposure compared to UT or RSA treated cells. However, both prophylactic and therapeutic treatment with Ala in two different doses significantly ($p<0.0001$) reduced NOX-4 gene expression compared to AGE exposure without Ala treatment in KUP5 cells. Gene expression at 5 hours (5hr) of incubation with AGEs is shown to indicate the up-regulated expression of NOX-4 when Ala was added to the cells (therapeutic approach) (A). Gene expression of $p47^{phox}$ was significantly up-regulated by AGEs after 6 hours but not 5 hours of exposure compared to UT or RSA treated cells. However, prophylactic and therapeutic treatments with Ala significantly reduced $p47^{phox}$ gene expression in KUP5 cells compared to cells exposed to AGEs for 6 hours, but not for 5 hours (B). The data have been normalized to endogenous control gene, 18S and UT control was given an arbitrary value of 1. Each bar represents the mean ± SEM profile from 3 independent experiments as calculated by one-way ANOVA with Tukey's comparison test. Note: for clarity, prophylactic and therapeutic groups are indicated by a single bracket for statistical comparison as there

was no difference between the groups within each set. UT: untreated, RSA: rat serum albumin.

Real time ROS generation by KUP5 cells measured using 2,4-DCFDA showed that AGEs significantly ($p<0.05$) increased fluorescence emission by KUP5 cells compared to untreated or RSA treated cells following 10 or 30 minutes of exposure (Fig. 6.14). However, when the cells were treated with Ala at the time of AGE addition, ROS generation was significantly ($p<0.05$) reduced compared to that of KUP5 cells exposed to AGEs without Ala treatment.

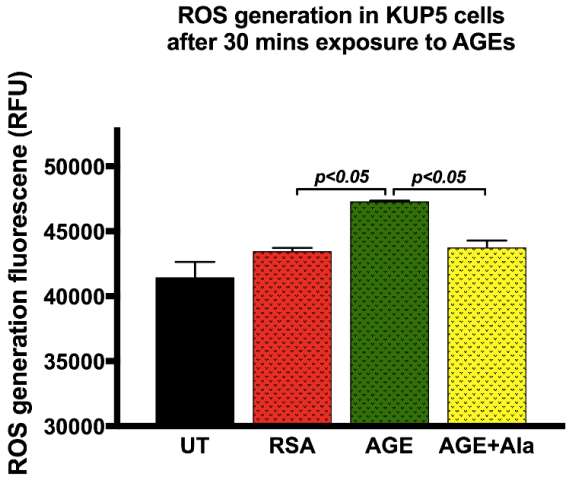

Figure 6.14 Alagebrium inhibits real time ROS generation by KUP5 cells
Exposure of KUP5 cells to AGEs for 30 minutes significantly ($p<0.05$) increased ROS generation compared to UT or RSA treated cells. However, in the presence of Ala, ROS generation was significantly abrogated. The data have been normalized to endogenous control gene, 18S and UT control was given an arbitrary value of 1. Each bar represents the mean $\pm$ SEM profile from 3 independent experiments as calculated by one-way ANOVA with Tukey's comparison test. UT: untreated, RSA: rat serum albumin, Ala: alagebrium.

6.3.12 Effects of alagebrium on the activation of HSCs

It was shown in chapter 3 that LX2 cells, immortalized human hepatic stellate cells, were not activated upon direct exposure to AGEs. In the present studies, we found the same phenomenon where direct exposure of LX2 cells to AGEs failed to activate LX2 cells, as reflected by an unaltered α-SMA gene expression (Fig. 6.15). However, as reported in chapter 3, LX2 cells were activated when conditioned media collected from AGEs treated KUP5 cells were added to LX2 cells compared to the addition of conditioned media from RSA treated or untreated (UT) KUP5 cells (Fig. 6.15). This was reflected by significant ($p<0.01$) increase in α-SMA gene expression by LX2 cells. Importantly, when LX2 cells treated with conditioned media collected from AGE-exposed KUP5 cells which had also been treated with Ala, we found that there was a significant ($p<0.01$) inhibition of α-SMA gene expression, suggesting an inhibition of LX2 activation (Fig. 6.15). In addition, we have used TGF-β1, a potent activator of HSCs, to activate LX2 cells as a positive control. However, when LX2 cells were treated with TGF-β1 and Ala, the drug failed to reduce α-SMA gene expression induced by TGF-β1 (data not shown). This confirmed that the mode of action of Ala in ameliorating HSC activation and fibrogenesis in high AGE fed mice is via inhibition of pro-inflammatory cytokine secretion by Kupffer cells (upstream of TGF-β1 pathway).

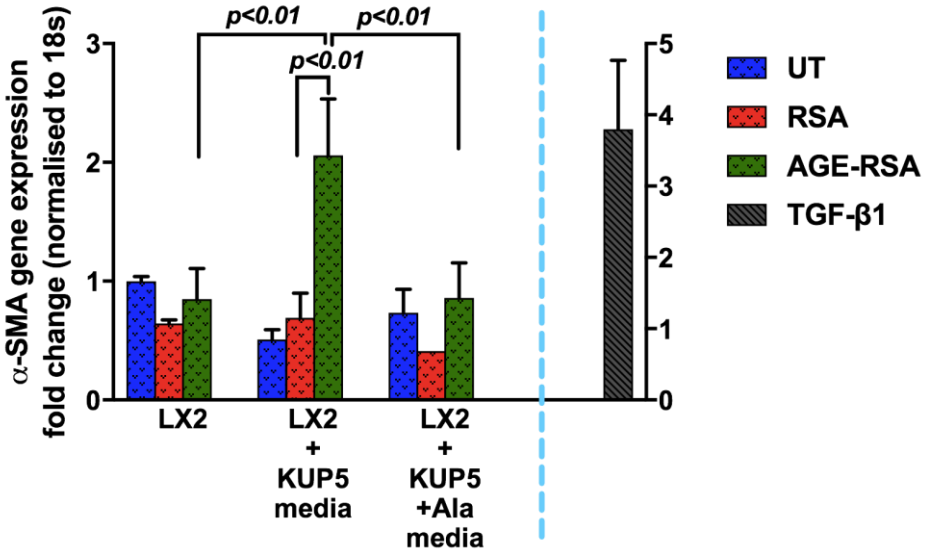

Figure 6.15 Alagebrium prevents the activation of hepatic stellate cells (LX2 cells) via inhibition of Kupffer cells-derived pro-inflammatory cytokines

LX2 cells exposed to AGEs failed to undergo activation. However, when LX2 cells were exposed to conditioned media collected from KUP5 cells which had been treated with AGEs for 6 hours, the cells were activated as reflected by significantly increased α-SMA gene expression compared to LX2 cells treated with AGEs or conditioned media collected from KUP5 cells treated with RSA. Importantly, the activation of LX2 cells was significantly reduced when LX2 cells were treated with conditioned media collected from KUP5 cells which had also been treated with Ala. The data have been normalized to endogenous control gene, 18S and UT control was given an arbitrary value of 1. Each bar represents the mean ± SEM profile from 3 independent experiments as calculated by one-way ANOVA with Tukey's comparison test. UT: untreated, RSA: rat serum albumin, Ala: alagebrium.

6.4 Discussion

In this study, we demonstrate for the first time that the AGE-crosslink breaker alagebrium markedly reduces liver injury and NAFLD progression to liver fibrosis. Moreover, we demonstrate that alagebrium apparently increases AGE clearance from the liver. The anti-fibrotic effect of alagebrium was associated with a marked reduction in circulating CML levels, RAGE expression, pro-inflammatory and pro-fibrotic cytokine release, inhibition of oxidative pathways and HSC activation. We provide further evidence that alagebrium, which has not been studied in NAFLD progression, improves the condition by primarily acting on hepatic Kupffer cells where it inhibits a number of pathways that ultimately results in reduced myofibroblastic HSC activation and fibrogenesis.

Alagebrium has been shown to be effective in many disorders associated with inflammation,[465] as well as reducing macrophage infiltration and potent pro-fibrotic cytokine TGF-β1 production.[466] In keeping with these studies, the current study showed that alagebrium markedly reduced liver injury in mice fed the high AGE diet compared to those exposed to high dietary AGEs without alagebrium treatment. Supporting the findings described in chapter 3, the present findings also showed that high dietary AGEs exacerbate liver RAGE expression and oxidative stress in Kupffer cells, the likely source of ROS generation. Further support for oxidative stress comes from the present findings

that increased lipid peroxidation in the liver of high AGE fed mice was likely attributable to increased expression of NOX subunits and ROS generation by KUP5 cells which were prevented by alagebrium treatment. In line with this, others have shown that alagebrium effectively prevented the membrane translocation of cytosolic regulatory NOX subunit $p47^{phox}$ and membrane bound catalytic NOX subunit NOX-4 gene expression in mesangial cells.[467] This would be in keeping with the suggestion that in the liver, AGEs activate RAGE with subsequent increases in oxidative stress,[383] which in turn increases AGE formation and contributes to a vicious cycle of AGE formation, generation of oxidative stress and further RAGE activation as depicted in Figure 4.17 of chapter 4.

What is intriguing is however that alagebrium markedly reduced circulating CML/AGEs and this was associated with reduced liver RAGE expression. Evidence that Kupffer cells are probably a major cell type that contribute to increased liver RAGE expression comes from KUP5 cell experiments where both prophylactic and therapeutic application of alagebrium prevented high AGE-induced RAGE expression. Thus, this phenomenon of reduced circulating AGEs and liver RAGE expression could be explained by the finding that alagebrium improves AGE clearance by a mechanism that is yet to be identified. This, however, leaves the liver exposed to reduced circulating AGEs that act on RAGE activation.

Supporting the findings described in chapters 3 and 4, the present findings also showed that high dietary AGEs caused increased expression of pro-inflammatory and pro-fibrotic cytokines. However, supporting a therapeutic role of alagebrium, we found that the drug markedly reduced the expression of pro-inflammatory cytokines such as TNF-α, MCP-1 and IL-6 and pro-fibrotic cytokines such as TGF-β1 with very little or no inflammatory cell infiltration in the livers of high AGE fed mice. It is possible that resident liver macrophages Kupffer cells play a pivotal role in the induction of inflammation because the immortalized mouse Kupffer cell line, KUP5 cells, responded with increased expression of these cytokines upon exposure to high AGEs and that both prophylactic and therapeutic application of alagebrium prevented their expression.

Perpetuation of inflammation is a major cause that activates myofibroblastic hepatic stellate cells (HSCs).[468] In many liver diseases, pathogenic stimuli directly activate and transform quiescent HSCs to their activated state which secretes ECM proteins. In the present study, we examined how LX2 cells, an immortalized human HSC cell line,

respond when the cells are exposed to AGEs. Surprisingly, we found that AGEs failed to activate LX2 cells, suggesting that AGEs may not directly activate HSCs, at least under our experimental conditions. We therefore investigated whether Kupffer cells, which reside in the same vicinity as the HSCs in liver sinusoids, crosstalk with HSCs. In supporting our hypothesis, the conditioned media collected from KUP5 cells that had been exposed to AGEs, but not to RSA, activated LX2 cells. This suggested that Kupffer cell products in the conditioned media collected from KUP5 cells stimulated HSC activation. What is more intriguing is that HSC activation could be prevented by addition of the conditioned media collected from KUP5 cells that have been exposed to AGEs but also treated with alagebrium, suggesting that the drug prevented the secretion of HSC stimulating products by Kupffer cells. These HSC stimulating products may well be pro-inflammatory cytokines[79] and ROS.[37] Thus, we propose that this is the likely mechanism by which Kupffer cells propagate inflammation which in turn activates HSCs which secrete pro-fibrotic TGF-β1 and ECM proteins. The present findings suggest that alagebrium acts directly on Kupffer cells to inhibit the release of pro-inflammatory cytokines and ROS which in turn is associated with a reduced activation of HSCs, leading to the improvement of NAFLD progression to liver fibrosis.

It should be noted however that methylglyoxal (MG), an intermediate product of glycation pathway, has been shown to induce mitochondrial oxidative stress, ATP production and mitochondrial dysfunction in vascular smooth muscle and cardiac cells, and mitochondrial dysfunction and cell death in the liver.[469-471] Alagebrium, on the other hand, has been reported to restore ATP content in cells, increase calcium flux and manganese superoxide dismutase activity, and reduce mitochondrial superoxide production which were associated with exposure to AGEs.[472] Although we have not measured mitochondrial function in the present study, it is possible that alagebrium may have also played a role in reducing mitochondrial ROS generation, contributing to anti-fibrotic effects of the drug.

Alagebrium was first introduced as an AGE-crosslink breaker. Most studies that explore the therapeutic efficacy of alagebrium have been focused on cardiovascular diseases. The drug has also been tested in clinical trials to investigate its effects on diabetic nephropathy. Although the mode of action of the drug is still unclear, many studies showed that it acts as an antioxidant,[452] inhibits glucose autooxidation[452] and chelate

metal ions that facilitate the advanced glycation reaction.[473] Despite the mode of action of alagebrium is yet to be defined, the drug has been shown be to be effective in reducing AGE accumulation in the kidneys.[474] In the present study, both *in vitro* and *in vivo* findings suggest that alagebrium may have directly affected AGE binding to RAGE because the drug prevented RAGE up-regulation. It is also possible that whilst RAGE is involved in inflammatory pathways,[475] other AGE receptors such as AGER-1 and AGER-3 may be involved in AGE clearance.[460] In fact, AGER-1 has been classified as an AGE scavenger receptor, a receptor involved in the removal of AGEs.[476] This may provide another explanation as to how alagebrium works to prevent AGE-associated detrimental effects in the liver. Thus, it is yet to be defined whether alagebrium prevents AGE/RAGE signalling or because it is described as an AGE-crosslink breaker it may facilitate AGE clearance by endocytosis,[477] either by binding to AGEs or promotes AGE binding to a scavenger receptor such as AGER-1.[476]

The latter explanation is more likely as alagebrium treated mice after 4 weeks of high AGE diet showed a similar fluorescence intensity in the liver and the kidneys to that of standard chow fed healthy mice. This suggests that alagebrium may have promoted increased endocytosis/clearance of labelled-AGEs, their metabolism in sinusoidal endothelial cells and Kupffer cells[353] and destined the processed AGE metabolites for excretion via the kidneys. Thus, the increased fluorescence intensity in the kidneys may well be due to the metabolized products of AGEs rather than full length labelled-AGEs which are approximately 65 kDa in size. However, a recent study reported that larger proteins such as 66 kDa BSA can still be filtered through the glomeruli.[478] Further investigations are necessary to confirm this.

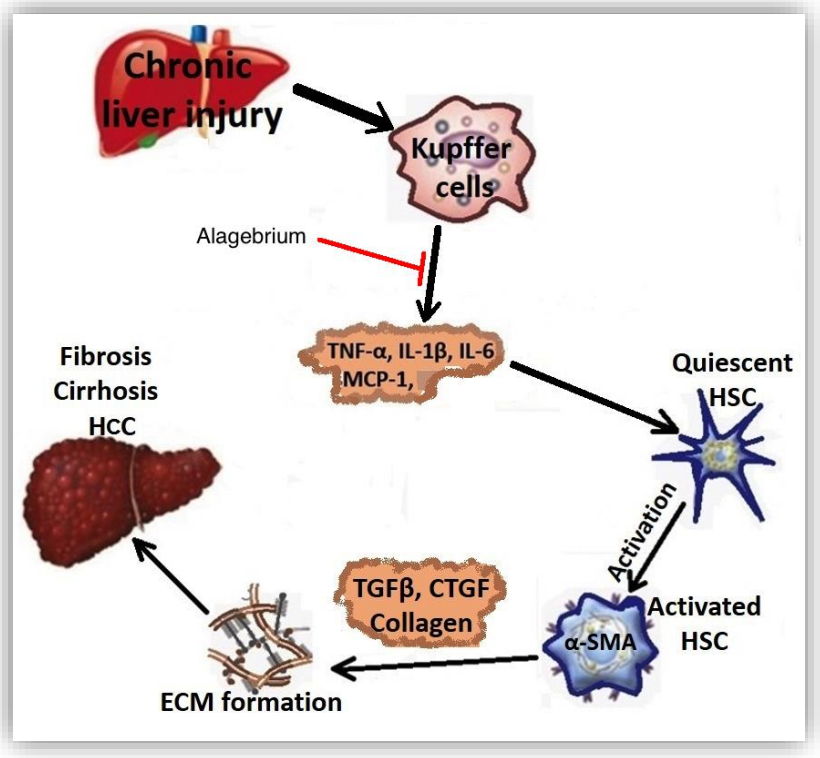

Figure 6.16 Alagebrium inhibition of crosstalk between Kupffer cells and HSCs that drives perpetuation of inflammation and fibrogenesis

Alagebrium directly inhibits pro-inflammatory cytokine release by Kupffer cells and thereby, indirectly inhibits activation of HSCs.

Most AGE trafficking studies has been carried out using AGEs tagged with radioactive labels.[479] These isotopes are not stable and subject to rapid release from labelled-AGEs upon lysosomal proteolysis.[353] Therefore, in our study we have chosen LI-COR IR dye-labels as it is stable.[480,481] In the short term study of 4 weeks, upon gavage of labelled-AGEs, we measured AGE accumulation in organs such as heart, lungs, brain, muscles, spleen, the kidneys and the liver at different time points. We found that the fluorescence intensity, which was highest in the liver amongst organs at all time points, showed the highest intensity after 20 minutes of labelled-AGE administration. This corroborated with previous findings that intravenously administrated AGEs were rapidly and almost exclusively taken up by the liver.[477] This agrees with a recent study using radio-labelled AGEs where more than 90% of radio-activity was recovered from the liver, irrespective of time following the administration of labelled-AGEs. Similar to our study, the kidneys also showed a high fluorescence; however, there was also some fluorescence in the spleen.[353] Moreover, similar to fluorescence intensity in our study, they reported that the

radio activity decayed with time. It is important to note that as mentioned above, in the present study, the highest fluorescence was detected in the livers of healthy mice fed the standard chow, suggesting that the healthy liver which expresses low levels of RAGE is capable of clearing AGEs rapidly compared to HF or high AGEs fed mice with relatively increased RAGE expression. Moreover, as mentioned above, alagebrium treatment apparently normalised AGE clearance in high AGE fed mice to that of standard chow fed healthy mice. On the other hand, alagebrium treatment in HF fed mice did not improve fluorescence intensity or possibly the clearance of AGEs, suggesting that alagebrium may be effective when specific pathways are activated by AGEs.

In summary, we demonstrate that alagebrium, originally described as an AGE-crosslink breaker, is a promising drug that prevents high dietary AGE-induced NAFLD progression to liver fibrosis. It has a plethora of beneficial effects associated with an ability to inhibit the activation of liver resident macrophages, Kupffer cells, and thereby reduces oxidative stress, inflammation, HSC activation and fibrogenesis. Thus, alagebrium, which has not been studied in AGE-induced NAFLD progression, displays potent anti-oxidative, anti-inflammatory and anti-fibrotic properties in the liver. Moreover, although it is yet to be confirmed whether alagebrium prevents AGE/RAGE signalling, it apparently promotes AGE uptake by the liver so that ingested AGEs can potentially be processed by the liver to excrete via the kidneys, limiting the availability of circulating AGEs to bind and activate RAGE. Therefore, we propose that alagebrium may have clinical utility in NAFLD patients where dietary modifications of high AGE diets are not feasible.

CHAPTER 7

General Discussion and conclusions

7.1 Introduction

Non-alcoholic fatty liver disease (NAFLD) is the most common liver disease in the world affecting up to 40% of Australian adult population. It is the leading cause for liver transplantations in the USA and expected to be the leading cause in the next 10 years in Australia. There is no proven medical treatment for NAFLD except for liver transplantation in patients with advanced liver disease. The management involves lifestyle modifications and dietary restrictions, which seem difficult to achieve practically. On the other hand, a decade of clinical trials involving a diversity of pharmaceutical agents targeting the pathological concepts of NAFLD did not reveal a single intervention that has convincingly improved all important outcomes for NAFLD/NASH patients. Hence, there remains a major need for cost-effective but efficacious therapies, particularly when NAFLD is isolated without other co-morbidities.[482]

NAFLD is a condition where excess amount of fat accumulation occurs in the liver, which is considered as the first hit of the two-hit hypothesis. NAFLD can progress to non-alcoholic steatohepatitis (NASH), a severe form of the disease or even cirrhosis or hepatocellular carcinoma. This process of NAFLD progression has been postulated to result from a so called ‘second-hit’. There are several factors that have been documented to act as the second hit. Among these factors, advanced glycation end products (AGEs) have been considered a potential contributor to progression of NAFLD to its severe forms.[212]

AGEs are formed when the reducing sugars non-enzymatically react with proteins through a series of reactions.[360] The first steps are reversible whereas the final step is irreversible and that makes AGEs more stable and less vulnerable to degradation. The rate of the glycation reaction is affected by several factors including sugar concentration, protein turn-over rate and the extent of oxidative stress and the nature of the media the reaction takes place in. Glycation is a natural phenomenon that occurs during aging. However, in conditions such as diabetes, the rate can be accelerated due to high blood glucose concentration (hyperglycaemia).[8] These AGEs formed in the body are known as endogenous AGEs. The glycation reaction can also occur during food processing, especially when foods are processed at high temperature in the absence of water, giving foods the characteristic golden-brown colour of AGEs.[483] Thus, foods with high fat, sugars and protein contents and those cooked at high temperatures have the highest AGE content.[483] High levels of AGEs are found in many commonly consumed foods such as toasted breads, biscuits, potato chips, toasted breakfast cereals and meats that are grilled, fried or roasted. Although intestinal absorption of AGEs is poor, high AGE diets increase circulating AGE levels whilst these levels fall in response to low AGE diets.[220,234] Animal models of diabetes have demonstrated that reducing the intake of dietary AGEs results in prevention of diabetic nephropathy.[254]

Irrespective of the source, AGEs can exert direct effects by crosslink formation with proteins in the body. A classic example of these crosslinks is the bond between AGEs and arterial walls in atherosclerosis.[484] AGEs can also exert indirect effects through activation of their receptors.[485] There are several receptors that have been identified as being the mediators of AGE effect and the receptor for advanced glycation end products or RAGE is the best characterized of all.[368] RAGE is a 35 kDa multi-ligand receptor that has multiple signalling cascades, leading to tissue inflammation, oxidative stress and fibrosis.[368]

The AGE-RAGE interaction has been implicated in the pathogenesis of a range of diseases. Given that the rate of AGE formation is accelerated in diabetes, most of the effects of AGE-RAGE axis have been studied in diabetic complications such as cardiovascular diseases,[7,363,376] erectile dysfunction[273] and diabetic nephropathy.[466] Other chronic diseases in which they have been implicated include Alzheimer's disease and amyloidosis,[486] rheumatoid arthritis[487] and liver diseases.[212] As a result, there is an

increasing interest in the therapies that could be used to target these compounds or their receptors and their downstream signalling pathways.

The experiments in this thesis were therefore designed to explore the role of AGE-RAGE axis in NAFLD progression to liver fibrosis with mechanistic insights derive from cell culture studies utilizing two of the most important liver cell types involved in inflammation and fibrogenesis, Kupffer cells and hepatic stellate cells, respectively. Moreover, as a therapeutic measure, we have also performed studies to investigate the effects of dietary modification and pharmacological interventions on NAFLD progression to liver fibrosis.

7.2 Role of endogenous AGEs on NAFLD progression

We hypothesized that endogenous AGEs formed in conditions such as diabetes may accelerate NAFLD progression. Therefore, it was important to determine the contribution of endogenous AGEs in NAFLD. Thus, we performed studies in mice fed a high fat (HF) diet for 40 weeks with fat intake approximated to that found in the Western diet. This time was chosen since mice fed this diet for 33 weeks showed no increase in inflammatory cytokine expression.[212] Interestingly, this model did not exhibit peripheral insulin resistance, however, it replicated all the other defining features of human NAFLD/NASH including obesity, steatohepatitis and fibrosis. Since we previously reported that intraperitoneal (i.p.) injections of *in vitro* prepared AGEs to rats with cholestatic liver injury augmented liver fibrosis,[210] we first employed exogenously administered AGEs to mimic the effect of endogenously formed AGEs on NAFLD progression (chapter 3).

Commencing at 30 weeks, we administered AGEs daily for 10 weeks at 3 doses via i.p. route. Mice treated with i.p. AGEs for 10 weeks were sacrificed at 40 weeks. We found that intraperitoneally injected AGEs elevated plasma ALT levels compared to HF fed mice, suggesting that AGEs cause liver injury. However, none of the doses of i.p. AGEs affected the expression of RAGE or LPS-binding genes compared to HF fed mice. Moreover, gene expression of pro-inflammatory cytokines and pro-fibrotic cytokines was not significantly elevated with AGE injections compared to HF fed mice. These findings were in keeping with the findings that i.p. AGEs did not exacerbate NAFLD progression to liver fibrosis compared to that of HF fed mice. Although intraperitoneally administered AGEs may not represent a full spectrum of changes that take place in diabetic subjects or

animals, the objective was to examine the effects due to AGEs alone before we endeavour to examine how diabetes, which likely elevates circulating AGEs, contributes to NAFLD progression.

NAFLD patients are commonly insulin resistant and may present with diabetes, and on the other hand, most diabetic patients develop NAFLD.[488,489] The objective of AGE administration was to mimic the endogenous AGEs that can be formed during diabetes. However, in the real-world scenario, it would be ideal to use diabetic animals. Therefore, we performed experiments in mice with diabetes to investigate the contribution of diabetes on NAFLD progression to liver fibrosis (chapter 4).

In comparison with intraperitoneally administered AGEs, diabetic mice showed an increased expression of RAGE, pro-inflammatory and pro-fibrotic cytokines in the liver. Moreover, diabetes significantly increased hepatic 4-hydroxynonenal content, reflecting that diabetes is associated with ROS generation and oxidative stress compared to HF fed mice. In addition, diabetic mice that were fed the high AGE diet showed the highest lipid peroxidation which will be discussed below. Previous studies with animals and humans show that oxidative stress is critical in NAFLD progression as steatosis makes hepatic tissue more susceptible to oxidative stress and subsequent inflammation and fibrosis.[490] Whilst it is difficult to make a solid inference that AGEs formed during diabetes drive NAFLD progression, we found that liver RAGE expression and plasma CML level, which represents circulating AGEs, were significantly elevated in diabetic mice compared to HF fed mice, suggesting that AGEs formed during diabetes may activate the AGE-RAGE axis to drive NAFLD progression. Indeed, diabetic mice fed the high AGE diet showed the highest plasma CML/AGE level compared to both diabetic or high AGE fed mice and because high dietary AGEs make liver fibrosis worse (see below), we can speculate that high CML/AGEs in diabetic mice likely contributed to NAFLD progression. Thus, the pathological changes in diabetic mice led to significantly increased liver fibrosis, which were most severe in mice that had been fed a diet high in AGEs, as described in the succeeding sections.

7.3 Role of dietary (exogenous) AGEs on NAFLD progression

Since high levels of AGEs are found in many commonly consumed foods,[443] we performed studies in mice fed a high AGE diet (by baking the high fat diet at 160^{o} C for 1 hour) to investigate the effects of dietary AGEs on NAFLD progression and compared with those of endogenously derived AGEs. In marked contrast to intraperitoneally administrated AGEs, we found that dietary AGEs caused profound effects on oxidative stress, pro-inflammatory and pro-fibrotic cytokine expression, LPS responsive genes and worsening liver fibrosis, suggesting that the dietary route is more harmful in NAFLD than endogenously produced AGEs.

As suggested by the findings in chapters 3, 4 and 5, mice fed a diet high in AGEs showed the highest liver injury. Moreover, in agreement with previous findings,[357,491] dietary AGEs markedly increased oxidative stress as reflected by an increased content of hepatic 4-hydroxynonenal, a marker of lipid peroxidation compared to HF fed control mice. Moreover, diabetic mice that were fed the high dietary AGEs showed the highest lipid peroxidation. We have also provided evidence that high dietary AGEs induce oxidative stress, likely via the activation of RAGE in liver resident macrophages Kupffer cells with subsequent ROS generation,[383] which, in turn, increases AGE formation and contributes to a vicious cycle of AGE formation, generation of oxidative stress and further RAGE activation. Thus, the present findings highlight the importance of AGEs, in particular, AGEs derived from dietary sources, in perpetuating oxidative stress. This suggests that AGE-RAGE axis is a potential pathway that could be implicated in the so called 'second-hit' that drives NAFLD progression to liver fibrosis. Previous studies with animals and humans show that oxidative stress is critical in NAFLD progression and steatosis makes hepatic tissue more susceptible to oxidative stress and subsequent inflammation and fibrosis.[490] Similar to diabetic mice, plasma CML levels were increased in response to high AGE diet. Interestingly, we found that there was a significant additive effect on plasma CML levels in high AGE fed mice when they were made diabetic, confirming that circulating CML formed during diabetes contributes to the same pool of AGEs added to the circulation by high AGE diet. This is important because irrespective of the source of AGEs, increased circulating CML/AGEs levels were positively and strongly associated with liver RAGE expression, a biological phenomenon strongly implicated in perpetuating oxidative stress and inflammation, leading to NAFLD progression.[485]

We show further evidence that diets high in AGEs have a remarkable effect on NAFLD progression to liver fibrosis, likely associated with detrimental effects of AGE/RAGE axis in the gut/microbiota as increased expression of endotoxin responsive genes in the liver of high AGEs fed diabetic mice was completely prevented by RAGE deletion. Although we did not measure circulating endotoxin levels or tight junction integrity in the present study, the present findings suggest that in agreement with previous reports,[354] dietary AGEs may contribute to leaky gut and dysbiosis which in turn increase the translocation of bacteria and bacterial products with subsequent activation of LPS responsive genes.[492,493] The possibility that RAGE deletion may have prevented downstream signalling of RAGE that may be necessary for induction of LPS responsive genes in Kupffer cells is supported by the KUP5 cell work which showed a complete inhibition of pro-inflammatory cytokine expression by RAGE blockade.

We have previously shown ROS production by primary Kupffer cells exposed to AGEs.[212] In this thesis, for the first time we studied the effects of AGEs on a immortalised murine Kupffer cell line (KUP5 cells).[349] As expected, we showed that RAGE expression was significantly increased in response to AGEs. In agreement with previous reports[494] and our *in vivo* experiments, pro-inflammatory cytokine expression was markedly elevated by AGEs. In addition, various subunits of NOX enzyme were markedly up-regulated in response to AGEs, leading to increased ROS generation.[212] Specificity of the effects of AGEs was verified by running a positive control of LPS stimulation, as has been used in previous studies.[432]

In our *in vivo* experiments, the mechanism by which HSCs were activated to ECM secreting myofibroblastic phenotype in diabetic mice or in mice fed the high AGE diet was not clear. It was therefore not possible to ascertain whether HSC activation is a direct consequence of AGE/RAGE activation on these cells or whether it is a consequence of preceding events such as oxidative stress or inflammation. It has been reported that HSCs can be activated by exposing to AGEs.[369] Therefore, *in vitro* studies were performed to explore the direct effects, if any, of AGEs on HSCs. An immortalized line of human HSCs (LX2 cells) were exposed directly to AGEs. Our findings however failed to support previous reports.[369] We then explored the possibility of crosstalk that Kupffer cells and HSCs may be involved. Thus, we found that by exposing LX2 cells to the conditioned media collected from KUP5 cells treated with AGEs, the cells were transformed to

myofibroblastic phenotype that expressed high levels of pro-fibrotic cytokine TGF-β1 and a major ECM component collagen 1. This conflicting outcome between our study and others[369] is probably due to the differences in experimental conditions and/or the difference in the cell type employed. Nevertheless, our findings are more consistent with the notion that Kupffer cells are the first defence line in the liver and are the main cell type that highly express RAGE, a molecule closely linked to inflammation and immune responses.[353] Because both Kupffer cells and HSCs reside in close proximity, HSCs can respond directly to signals emanating from Kupffer cells.[495] Thus, it appears that, AGEs act indirectly on HSCs to drive fibrogenesis. These findings collectively suggest that the gut/liver AGE-RAGE axis as well as AGE/RAGE signalling in the liver play an important role in the pathogenesis dietary AGE-induced NAFLD progression to liver fibrosis.

The experiments with $RAGE^{-/-}$ mice in the current study showed that following the induction of diabetes, $RAGE^{-/-}$ mice gained body weight rapidly than wild type (WT) mice despite the same food and water intake. Moreover, in the present study, $RAGE^{-/-}$ mice showed lower blood glucose levels compared to WT mice following the induction of diabetes and unlike in $RAGE^{-/-}$ mice, blood glucose levels continued to rise in WT mice throughout the experiment period. These findings may suggest that in the absence of RAGE, diabetic mice have improved insulin resistance[496] and/or insulin secretion. Although it is yet to be defined whether RAGE regulates insulin secretion in diabetes, especially when a majority of insulin producing pancreatic beta cell populations were compromised by streptozotocin injections, published studies provide support for our findings that RAGE negatively regulates peripheral insulin sensitivity.[496-498] In addition, Leuner *et al* reported that RAGE deletion promotes body weight gain in response to HF diet.[498] On the other hand, Song *et al* reported that RAGE promotes obesity and body weight gain,[496] and therefore, more studies are needed to clarify these discrepancies, especially in diabetic mice with compromised beta cell populations.

7.4 Therapeutic strategies of targeting the AGE/RAGE axis in the prevention of NAFLD progression

7.4.1 Dietary interventions

Since there is no proven medical treatment for NAFLD, the management involves lifestyle modifications and dietary restrictions, which seems difficult to achieve in most patients.[482] In comparison with the Western diet, where dry heat is applied creating a large amount of AGEs, the Mediterranean diet, where food preparation involves vinegar-marination prior to processing, has a low amount of AGEs.[212] The Mediterranean diet has been shown to have many health benefits which may include beneficial effect on gut microbiota.[427,446,499] It has been widely studied for many diseases and shown that AGE content in food can be reduced by marination with vinegar, even using the same cooking methods.[443] Therefore, to investigate the effect on NAFLD progression, we marinated the HF diet with vinegar prior to baking at 160^{o} C and found that AGE content was reduced by 20-50%. We then discovered that mice fed this diet had markedly improved liver injury.

The findings that there was reduction of RAGE expression to that of HF fed mice by vinegar marination suggests that AGEs trigger liver RAGE up-regulation by either acting on liver AGE-RAGE axis or via gut/microbiota/liver axis. Moreover, inhibition of liver pro-inflammatory cytokine expression by vinegar marinating the baked diet with subsequent inhibition on pro-fibrotic cytokine and collagen expression by HSCs supports the hypothesis that RAGE down-regulation is key to preventing the activation of Kupffer cells and HSCs. In addition, a major down-regulation of LPS-binding receptor expression in the liver the by vinegar marinated baked diet suggests that microbiota integrity and gut homeostasis were restored as LPS derived from gut microbiota is a strong stimulus for increased expression of LPS-binding receptors in the liver.[493] These beneficial effects of vinegar marinated diet led to a profound reduction in NAFLD progression to liver fibrosis in mice.

Supporting our findings, it has been shown that animal models of diabetes have demonstrated that reducing the intake of dietary AGEs results in prevention of diabetic nephropathy.[254] It has also been shown that the addition of natural cereal bran (rye or spring triticale) in meat patties effectively inhibited AGE formation during cooking.[500] A recent study in healthy overweight individuals demonstrated that low AGE diets improve

insulin sensitivity, thus reducing the risk of type 2 diabetes.[501] Similarly, a low AGE diet for 6 weeks in diabetic subjects resulted in decreased serum AGE levels which was associated with decreased inflammatory markers such as C reactive protein.[229] Thus, making diets low in AGEs by cooking food for less time and at lower temperatures or alternatively, vinegar marination should provide many health benefits for patients with NAFLD. Indeed, a dietary AGE database now exists which can be used for dietary manipulation. Collectively, this provides evidence that a simple dietary modification of food with vinegar or changes to cooking methods may provide unprecedented benefits for patients with NAFLD.

7.4.2 Pharmacological interventions

7.4.2.1 Inhibitors of AGE formation

The studies in chapter 5 investigated the efficacy of inhibition of AGE formation on NAFLD progression. We used two drugs, aminoguanidine and pyridoxamine to inhibit endogenous AGE formation. These drugs have been extensively used in clinical trials, mainly for diabetic complications such as nephropathy and cardiovascular diseases.[319,430,502] Despite their original classification as inhibitors of AGE formation, they have also been suggested to work via other pathways.[503]

In the present studies, we were not able to identify any beneficial effects of these drugs on NAFLD progression in diabetic or high AGE fed mice. Other than an inhibitory effect of aminoguanidine on liver TNF-α expression, the two drugs were in fact detrimental and accelerated liver fibrosis in HF fed mice. An inhibitory effect of pyridoxamine on TNF-α expression in adipose tissue and diabetic nephropathy[411,433] is consistent with the current findings in HF fed diabetic mice that the drugs may have inhibited endogenous AGE formation. Moreover, the deleterious effects of the drugs on liver fibrosis in HF fed mice was not apparent in diabetes or high AGE diet fed animals possibly because the harmful effects of the drugs were counterbalanced by inhibition of AGE formation. Thus, the findings of this study do not support published studies which reported both aminoguanidine and pyridoxamine inhibit AGE formation and improves AGE related disease.[435,436,504,505] On the other hand, however there are several studies which reported negative outcomes of aminoguanidine treatment. This includes a report showing no

beneficial effects of aminoguanidine in liver injury caused by diabetes.[438] development of pancreatic and renal-neoplastic tumours,[439] elevation of liver enzyme levels and development of autoantibodies or unfavourable risk to benefit ratios in clinical trials.[439,441] Similar to aminoguanidine, eight weeks of pyridoxamine treatment failed to produce positive results in patients with overt nephropathy.[442]

In most studies, the dosage of aminoguanidine was similar to that used in the present study.[506] Similar to aminoguanidine, pyridoxamine was also administered via drinking water at a dose which is similar to those of published studies.[507] It should be noted however that although aminoguanidine has been suggested to reduce AGE formation by trapping carbonyl moieties, excessive reactive carbonyl traps have been suggested to be toxic because of depletion of vitamin B6.[429] Thus, it is not known whether drug doses employed in the present study reached toxic levels under our experimental conditions. This therefore warrants further investigation employing smaller doses of the drugs.[429]

7.4.2.2 AGE-crosslink breaker

The second pharmacological approach we used to target AGE/RAGE axis in NAFLD progression was the use of AGE-crosslink breaker alagebrium as discussed in chapter 6. This drug has been extensively used in numerous pre-clinical studies of chronic diseases including artherosclerosis,[508] erectile dysfunction,[462] cardiovascular diseases,[509] renal injury[510] and hypertension.[511] Moreover, alagebrium has also been used in phase II clinical trials targeting cardiovascular diseases.[512,513]

In comparison with the inhibitors of AGE formation which failed to produce a positive outcome on liver fibrosis, we found that alagebrium markedly reduced liver injury, leading to a complete inhibition of NAFLD progression to liver fibrosis in high AGE fed mice. Moreover, alagebrium was found to be very effective in inhibiting many pathways involved in liver injury, highlighting the importance of this drug which apparently works by mechanisms other than its designated mode of action as a crosslink breaker.

The most intriguing action of alagebrium was that it completely reversed circulating AGE levels to those seen in HF fed animals. This effect appears to be of prime importance because there was a positive and strong correlation of circulating AGEs with liver RAGE expression. The present evidence suggests that at the cellular level, Kupffer cells are a

major cell type that contributes to increased liver RAGE expression in response to high AGEs which was completely prevented by alagebrium. This phenomenon of reduced circulating AGEs and liver RAGE expression could be explained by the finding that alagebrium improves AGE clearance, resulting in a reduced exposure of RAGE to AGEs. These findings are supported by previous studies which demonstrated reduced AGE-induced RAGE expression in the heart,[514] and less glomerular inflammation[515] with alagebrium treatment. Our AGE trafficking studies provide evidence that alagebrium improves AGE clearance by a mechanism that is likely associated with induction of receptors that facilitate AGE uptake by the liver with subsequent processing and secretion into the circulation for excretion via the kidneys.[477] To support this, we found that whilst the intensity of fluorescence labelled-AGEs was reduced in the liver of mice fed the HF or high AGE diet, mice that were fed the high AGE diet and treated with alagebrium showed an increased intensity of fluorescence in both the liver and kidneys which was similar to that of standard chow fed mice.

Moreover, alagebrium reduced liver oxidative stress and ROS production in Kupffer cells, indicating that the drug may have a direct effect on AGE/RAGE signalling in these cells. In most pathological conditions, ROS is upstream of inflammatory events because ROS activate redox sensitive transcription factors such as NF-Kβ, which then activate transcription of inflammatory molecules upon translocating into the nucleus.[516] In line with this, we found that alagebrium markedly reduced the expression of pro-inflammatory cytokines such as TNF-α, MCP1 and IL-6 in mice fed the high AGE diet. Mechanistically, it appears that these cytokines may be primarily secreted by Kupffer cells as increased cytokine expression by Kupffer cells exposed to AGEs was completed prevented by treatment with alagebrium. It is well known that Kupffer cells are the first line of defensive mechanism[517] and that inflammatory cytokines released by these cells correlate with early stage of steatohepatitis.[518]

The primary end point of this study was NAFLD progression to liver fibrosis. Thus, we conclusively showed that alagebrium markedly improved liver fibrosis in high AGE fed mice. To provide mechanistic insights into how alagebrium prevented liver fibrosis, we designed experiments to investigate cross-talking between inflammatory cells and ECM secreting cells. The primary cell type which is responsible for ECM deposition in the liver is HSCs. We showed above that Kupffer cells expressed an increased level of pro-

inflammatory cytokines in response to AGEs. We then found that application of AGEs to HSCs/LX2 cells directly failed to activate the cells. However, when LX2 cells were exposed to the conditioned media collected from Kupffer cells that had been exposed to AGEs, the cells were markedly activated and transformed into a myofibroblastic phenotype that secretes ECM, suggesting that products secreted by Kupffer cells likely the trigger for this activation. Importantly, in another series of experiments, when LX2 cells were exposed to the conditioned media collected from Kupffer cells that had been exposed to AGEs but also treated with alagebrium, the activation of LX2 cells was completely prevented. This provides a mechanism by which alagebrium likely prevented NAFLD progression to liver fibrosis in mice fed the high AGE diet. Thus, we provide new evidence that alagebrium, which has not been studied in NAFLD progression, improves the condition by acting on hepatic Kupffer cells where it inhibits a number of pathways that ultimately results in reduced myofibroblastic HSC activation and fibrogenesis.

7.5 Conclusions

In this thesis, we provide evidence that AGEs, formed during food preparation at high temperature and possibly during diabetes, act as a second hit that drives NAFLD progression to liver fibrosis. AGEs have direct effects on liver AGE-RAGE activation. However, we further discovered that dietary AGEs are more deleterious than endogenous AGEs, likely due to a possible effect of diet-derived AGEs on gut homeostasis and microbiota integrity, disruption of which leads to activation of gut/liver AGE/RAGE pathway, tight junction disruption and leaky gut. We also conclude that AGEs act directly on Kupffer cells which results in the activation of RAGE, release of ROS and pro-inflammatory cytokines, which in turn activate HSCs to ECM secreting myofibroblastic phenotype and contribute to NAFLD progression to liver fibrosis.

We also provide evidence that therapeutic strategies that target AGE/RAGE axis could be useful in ameliorating NAFLD progression to liver fibrosis. We also conclude that a simple dietary modification of food with vinegar marination or changes to cooking methods to reduce AGE content may provide many benefits to patients with NAFLD. We further conclude that pharmacological intervention with alagebrium is greatly effective in ameliorating many pathological pathways induced by AGEs. Other than possible direct

actions of AGEs on liver AGE-RAGE signalling, it appears that alagebrium also effectively improves NAFLD progression by promoting AGE clearance from the circulation.

7.6 Future directions

This thesis provides strong evidence that AGE/RAGE axis contributes to NAFLD progression to liver fibrosis. The findings presented in this thesis warrant further investigations to uncover the mechanism of action of alagebrium in the liver and gut and suggest that the drug is certainly worth investigating for its therapeutic potential in NAFLD patients. We also recommend further studies to explore the effect of AGEs on microbiota integrity and gut homeostasis with special emphasis on leaky gut. The findings also justify further studies examining the effects of specific RAGE blockers in NAFLD in the context of high AGE exposure including both dietary and endogenous sources.

We also believe there is sufficient evidence to justify a clinical trial comparing the effects on liver function and inflammatory markers of high and low AGE diets in both diabetic and non-diabetic patients with NAFLD.

BIBLIOGRAPHY

1 Global Health Estimates 2016: Deaths by Cause, A., Sex, by Country and by Region, 2000-2016. Geneva, World Health Organization; 2018. . (2018).

2 Asrani, S. K., Devarbhavi, H., Eaton, J. & Kamath, P. S. Burden of liver diseases in the world. *Journal of Hepatology* **70**, 151-171, doi:10.1016/j.jhep.2018.09.014 (2019).

3 Loomba, R. & Sanyal, A. J. The global NAFLD epidemic. *Nature Reviews Gastroenterology &Amp; Hepatology* **10**, 686, doi:10.1038/nrgastro.2013.171 (2013).

4 Bellentani, S. The epidemiology of non-alcoholic fatty liver disease. *Liver International* **37** 81–84, doi:DOI: 10.1111/liv.13299 (2017).

5 Day, C. P. & James, O. F. W. Steatohepatitis: A tale of two "hits"? *Gastroenterology* **114**, 842-845, doi:10.1016/S0016-5085(98)70599-2 (1998).

6 Uribarri, J. *et al.* Dietary advanced glycation end products and their role in health and disease. *Advances in nutrition (Bethesda, Md.)* **6**, 461-473, doi:10.3945/an.115.008433 (2015).

7 Singh, V. P., Bali, A., Singh, N. & Jaggi, A. S. Advanced glycation end products and diabetic complications. *The Korean journal of physiology & pharmacology : official journal of the Korean Physiological Society and the Korean Society of Pharmacology* **18**, 1-14, doi:10.4196/kjpp.2014.18.1.1 (2014).

8 Singh, R., Barden, A., Mori, T. & Beilin, L. J. D. Advanced glycation end-products: a review. **44**, 129-146, doi:10.1007/s001250051591 (2001).

9 Goldin, A., Beckman Joshua, A., Schmidt Ann, M. & Creager Mark, A. Advanced Glycation End Products. *Circulation* **114**, 597-605, doi:10.1161/CIRCULATIONAHA.106.621854 (2006).

10 Bierhaus, A. *et al.* Understanding RAGE, the receptor for advanced glycation end products. **83**, 876-886, doi:10.1007/s00109-005-0688-7 (2005).

11 Senatus, L. M. & Schmidt, A. M. The AGE-RAGE Axis: Implications for Age-Associated Arterial Diseases. *Frontiers in genetics* **8**, 187-187, doi:10.3389/fgene.2017.00187 (2017).

12 Villegas-Rodríguez, M. E. *et al.* The AGE-RAGE Axis and Its Relationship to Markers of Cardiovascular Disease in Newly Diagnosed Diabetic Patients. *PLOS ONE* **11**, e0159175, doi:10.1371/journal.pone.0159175 (2016).

13 Jandeleit-Dahm, K., Watson, A. & Soro-Paavonen, A. THE AGE/RAGE AXIS IN DIABETES-ACCELERATED ATHEROSCLEROSIS. **35**, 329-334, doi:doi:10.1111/j.1440-1681.2007.04875.x (2008).

14 Wang, H. *et al.* Visualizing liver anatomy, physiology and pharmacology using multiphoton microscopy. *J. Biophotonics* 1–15, doi: DOI 10.1002/jbio.201600083 (2016).

15 Malarkey, D. E., Johnson, K., Ryan, L., Boorman, G. & Maronpot, R. R. New Insights into Functional Aspects of Liver Morphology. *Toxicologic Pathology* **33**, 27-34, doi:10.1080/01926230590881826 (2005).
16 Hollander, C. F., van Bezooijen, C. F. A. & Solleveld, H. A. 244-250 (Springer Berlin Heidelberg).
17 Hosseini, M. *et al. BLUNT TRAUMA LIVER-CONSERVATIVE OR SURGICAL MANAGEMENT?* , (2018).
18 Saxena, R., Theise, N. D. & Craeford, J. M. Microanatomy of the Human Liver—Exploring the Hidden Interfaces. *Hepatology* **30**, 1339-1346 (1999).
19 Ricken, T. *et al. Modeling function–perfusion behavior in liver lobules including tissue, blood, glucose, lactate and glycogen by use of a coupled two-scale PDE–ODE approach.* (2014).
20 Kuntz, E. & Kuntz, H.-D. *Hepatology, Textbook and Atlas*. 3 edn, (Springers, 2008).
21 Kmieć, Z. in *Advanced Anatomy Embryol Cell Biol. 2001;161:III-XIII, 1-151* Vol. 161 1-151 (Springer, 2001).
22 Macchiarelli, G. & Motta, P. M. The three-dimensional microstructure of the liver. A review by scanning electron microscopy. *Scanning electron microscopy*, 1019 (1986).
23 Lalor, P. F., Lai, W. K., Curbishley, S. M., Shetty, S. & Adams, D. H. Human hepatic sinusoidal endothelial cells can be distinguished by expression of phenotypic markers related to their specialised functions in vivo. *World Journal of Gastroenterology : WJG* **12**, 5429-5439, doi:10.3748/wjg.v12.i34.5429 (2006).
24 Roberts, R. A. *et al.* Role of the Kupffer Cell in Mediating Hepatic Toxicity and Carcinogenesis. *Toxicological Sciences* **96**, 2-15, doi:10.1093/toxsci/kfl173 (2007).
25 Blouin, A., Bolender, R. P. & Weibel, E. R. Distribution of organelles and membranes between hepatocytes and nonhepatocytes in the rat liver parenchyma. *The Journal of Cell Biology* **72**, 441-455 (1977).
26 Friedman, S. L. Hepatic Stellate Cells: Protean, Multifunctional, and Enigmatic Cells of the Liver. **88**, 125–172, doi:doi:10.1152/physrev.00013.2007 (2008).
27 Ramadori, G. *et al.* Expression of the gene of the α-smooth muscle-actin isoform in rat liver and in rat fat-storing (ITO) cells. *Virchows Archiv B* **59**, 349, doi:10.1007/bf02899424 (1990).
28 Geerts, A. History, Heterogeneity, Developmental Biology, and Functions of Quiescent Hepatic Stellate Cells. *Semin Liver Dis* **21**, 311-336, doi:10.1055/s-2001-17550 (2001).
29 Rockey, D. C., Boyles, J. K., Gabbiani, G. & Friedman, S. L. Rat hepatic lipocytes express smooth muscle actin upon activation in vivo and in culture. *Journal of submicroscopic cytology and pathology* **24**, 193-203 (1992).
30 Rockey, D. C. Hepatic Blood Flow Regulation by Stellate Cells in Normal and Injured Liver. *Semin Liver Dis* **21**, 337-350, doi:10.1055/s-2001-17551 (2001).
31 Geerts, A. *et al.* Purification of rat hepatic stellate cells by side scatter–activated cell sorting. *Hepatology* **27**, 590-598, doi:10.1002/hep.510270238 (1998).
32 Bogert, T. P. & LaRusso, N. F. Cholangiocyte biology. *Current Opinion in Gastroenterology* **23**, 299–305 (2007).
33 Alvaro, D. *et al.* Proliferating Cholangiocytes: A Neuroendocrine Compartment in the Diseased Liver. *Gastroenterology* **132**, 415-431, doi:10.1053/j.gastro.2006.07.023 (2007).

34 Almeda-Valdes, P., Olivos, N. E. A., Barranco-Fragoso, B., Uribe, M. & Méndez-Sánchez, N. The Role of Dendritic Cells in Fibrosis Progression in Nonalcoholic Fatty Liver Disease. *BioMedical Research International* **2015**, 7, doi:doi.org/10.1155/2015/768071 (2015).

35 Connolly, M. K. *et al.* In liver fibrosis, dendritic cells govern hepatic inflammation in mice via TNF-α. *The Journal of Clinical Investigation* **119**, 3213–3225 doi:doi:10.1172/JCI37581 (2009).

36 Lau, A. H. & Thomson, A. W. Dendritic cells and immune regulation in the liver. *Gut* **52**, 307–314 (2003).

37 Bataller, R. & Brenner, D. A. Liver fibrosis. *The Journal of clinical investigation* **115**, 209-218, doi:10.1172/JCI24282 (2005).

38 Friedman, S. L. & Arthur, M. J. P. Vol. 8 (2002).

39 Hernandez-Gea, V. & Friedman, S. L. Pathogenesis of Liver Fibrosis. *Annual Review of Pathology: Mechanisms of Disease* **6**, 425–456 (2011).

40 Wells, R. G. Cellular Sources of Extracellular Matrix in Hepatic Fibrosis. *Clinics in liver disease* **12**, 759-viii, doi:10.1016/j.cld.2008.07.008 (2008).

41 Karsdal, M. A. *et al.* Novel insights into the function and dynamics of extracellular matrix in liver fibrosis. *American Journal of Physiology - Gastrointestinal and Liver Physiology* **308**, G807-G830, doi:10.1152/ajpgi.00447.2014 (2015).

42 Knittel, T. *et al.* Rat liver myofibroblasts and hepatic stellate cells: Different cell populations of the fibroblast lineage with fibrogenic potential. *Gastroenterology* **117**, 1205-1221, doi:10.1016/S0016-5085(99)70407-5 (1999).

43 Azevedo, C. M. *et al.* Bone marrow-derived cells migrate to the liver and contribute to the generation of different cell types in chronic Schistosoma mansoni infection. *Experimental Parasitology* **159**, 29-36, doi:https://doi.org/10.1016/j.exppara.2015.08.005 (2015).

44 Duval, F., Moreno-Cuevas, J. E., González-Garza, M. T., Rodríguez-Montalvo, C. & Cruz-Vega, D. E. Protective mechanisms of medicinal plants targeting hepatic stellate cell activation and extracellular matrix deposition in liver fibrosis. *Chinese Medicine* **9**, 27, doi:10.1186/s13020-014-0027-4 (2014).

45 Benyon, R. C. & Arthur, M. J. P. Extracellular Matrix Degradation and the Role of Hepatic Stellate Cells. *Semin Liver Dis* **21**, 373-384, doi:10.1055/s-2001-17552 (2001).

46 Rockey, D. C. & Bissell, D. M. Noninvasive measures of liver fibrosis. *Hepatology* **43**, S113-S120, doi:10.1002/hep.21046 (2006).

47 Jiang, H. *et al.* Alcohol Consumption and Liver Disease in Australia: ATime Series Analysis of the Period 1935–2006. *Alcohol and Alcoholism* **49**, 363–368, doi:doi: 10.1093/alcalc/agt143 (2014).

48 Ishak, K. G., Zimmerman, H. J. & Ray, M. B. Alcoholic Liver Disease: Pathologic, Pathogenetic and Clinical Aspects. *Alcoholism: Clinical and Experimental Research* **15**, 45-66 (1991).

49 O'Shea, R. S. Alcoholic Liver Disease. *Hepatology*, 307-328, doi:DOI10.1002/hep.23258 (2010).

50 Norström, T. & Skog, O.-J. Alcohol and mortality: methodological and analytical issues in aggregate analyses. *Addiction* **96**, S5-S17 (2001).

51 Girela, E., Villanueva, E., Hernandez-Cueto, C. & Luna, J. D. Comparison of the cage questionnaire versus some biochemical markers in the diagnosis of alcoholism. *Alcohol and Alcoholism* **29**, 337-343, doi:10.1093/oxfordjournals.alcalc.a045541 (1994).

52 Zuckerman, A. J. in *Medical Microbiology* (ed S. Baron) (University of Texas Medical Branch, 1996).

53 O'Sullivan, B. G. *et al.* Estimates of chronic hepatitis B virus infection in Australia, 2000. *Australian and New Zealand Journal of Public Health* **28**, 212-216, doi:10.1111/j.1467-842X.2004.tb00697.x (2004).

54 Modi, A. A. & Liang, T. J. Hepatitis C: a clinical review. *Oral Diseases* **14**, 10-14, doi:10.1111/j.1601-0825.2007.01419.x (2008).

55 Thompson, A. J. V. Australian recommendations for the management of hepatitis C virus infection: a consensus statement. *The Medical Journal of Australia* **204**, 268-272 (2016).

56 Leggett, B. A., Halliday, J. W., Brown, N. N., Bryant, S. & Powell, L. W. Prevalence of haemochromatosis amongst asymptomatic Australians. *British Journal of Haematology* **74**, 525-530, doi:10.1111/j.1365-2141.1990.tb06345.x (1990).

57 Feder, J. N. *et al.* A novel MHC class I–like gene is mutated in patients with hereditary haemochromatosis. *Nature Genetics* **13**, 399, doi:10.1038/ng0896-399 (1996).

58 Richardson, A., Prideaux, A. & Kiely, P. Haemochromatosis: unexplained metacarpophalangeal or ankle arthropathy should prompt diagnostic tests: findings from two UK observational cohort studies. *Scandinavian Journal of Rheumatology* **46**, 69-74, doi:10.3109/03009742.2016.1155645 (2017).

59 Brissot, P., Cavey, T., Ropert, M., Guggenbuhl, P. & Loréal, O. Genetic hemochromatosis: Pathophysiology, diagnostic and therapeutic management. *La Presse Médicale* **46**, e288-e295, doi:https://doi.org/10.1016/j.lpm.2017.05.037 (2017).

60 Boonstra, K., Beuers, U. & Ponsioen, C. Y. Epidemiology of primary sclerosing cholangitis and primary biliary cirrhosis: A systematic review. *Journal of Hepatology* **56**, 1181–1188 (2012).

61 Liu, K. *et al.* Epidemiology and outcomes of primary sclerosing cholangitis with and without inflammatory bowel disease in an Australian cohort. *Liver International* **37** 442–448 (2017).

62 Alizadeh, A. H. M. Cholangitis: Diagnosis, Treatment and Prognosis. *Journal of Clinical and Translational Hepatology* **5**, 404–413, doi:doi: 10.14218/JCTH.2017.00028 (2017).

63 Yimam, K. K. & Bowlus, C. L. Diagnosis and classification of primary sclerosing cholangitis. *Autoimmunity Reviews* **13**, 445-450, doi:https://doi.org/10.1016/j.autrev.2014.01.040 (2014).

64 Sood, S., Gow, P. J., Christie, J. M. & Angus, P. W. Epidemiology of Primary Biliary Cirrhosis in Victoria, Australia: High Prevalence in Migrant Populations. *Gastroenterology* **127**, 470–475, doi:doi:10.1053/j.gastro.2004.04.064 (2004).

65 Lleo, A., Marzorati, S., Anaya, J.-M. & Gershwin, M. E. Primary biliary cholangitis: a comprehensive overview. *Hepatology International* **11**, 485–499, doi:doi.org/10.1007/s12072-017-9830-1 (2017).

66 Almpanis, Z., Demonakou, M. & Tiniakos, D. Evaluation of liver fibrosis: "Something old, something new…". *Annals of Gastroenterology* **29**, 445-453 (2016).

67 Standish, R. A., Cholongitas, E., Dhillon, A., Burroughs, A. K. & Dhillon, A. P. AN APPRAISAL OF THE HISTOPATHOLOGICAL ASSESSMENT OF LIVER FIBROSIS. *Gut* **55**, 569–578, doi:doi: 10.1136/gut.2005.084475 (2006).

68 Friedman, S. L. Liver fibrosis – from bench to bedside. *Journal of Hepatology* **38** S38–S53, doi:doi:10.1016/S0168-8278(02)00429-4 (2003).

69 Pinzani, M. Liver fibrosis. *Springer seminars in immunopathology* **21**, 475 (1999).

70 Skoien, R. *et al.* Heterogeneity of fibrosis patterns in non-alcoholic fatty liver disease supports the presence of multiple fibrogenic pathways. *Liver International* **33**, 624–632, doi:DOI:10.1111/liv.12100 (2013).

71 Chengxi, L., Rentao, L. & Wei, Z. *Progress in non-invasive detection of liver fibrosis*. Vol. 15 (2018).

72 Burt, A. D., Griffiths, M. R., Schuppan, D., Voss, B. & Macsween, R. N. M. Ultrastructural localization of extracellular matrix proteins in liver biopsies using ultracryomicrotorny and' irnmuno-gold labelling. *Histopathology* **16**, 53-58 (1990).

73 Seyer, J. M., Hutcheson, E. T. & Kang, A. H. Collagen Polymorphism in Normal and Cirrhotic Human Liver. *The Journal of Clinical Investigation* **59**, 241-248 (1977).

74 Gressner, A. M. & Haarmann, R. HYALURONIC ACID SYNTHESIS AND SECRETION BY RAT LIVER FAT STORING CELLS (PERISINUSOIDAL LIPOCYTES) IN CULTURE. *BIOCHEMICAL AND BIOPHYSICAL RESEARCH COMMUNICATIONS* **151**, 222-229 (1988).

75 Schuppan, D. Structure of the extracellular matrix in normal and fibrotic liver: collagens and glycoproteins. *Seminars in liver disease* **10**, 1 (1990).

76 Benyon, R. C. & Iredale, J. P. Is liver fibrosis reversible? *Gut* **46**, 443–446 (2000).

77 Wynn, T. A. Common and unique mechanisms regulate fibrosis in various fibroproliferative diseases. *The Journal of Clinical Investigation* **117**, 524-529, doi:doi:10.1172/JCI31487 (2007).

78 Di Sario, A. *et al.* Selective Naɥ/Hɥ Exchange Inhibition by Cariporide Reduces Liver Fibrosis in the Rat. *HEPATOLOGY* **37**, 256-266, doi:doi:10.1053/jhep.2003.50028 (2003).

79 Lee, U. E. & Friedman, S. L. Mechanisms of hepatic fibrogenesis. *Best practice & research. Clinical gastroenterology* **25**, 195-206, doi:10.1016/j.bpg.2011.02.005 (2011).

80 Melton, A. C. & Yee, J., Hal.F. . Hepatic Stellate Cell Protrusions Couple PlateletDerived Growth Factor-BB to Chemotaxis. *Hepatology* **45**, 1446-1453, doi:DOI10.1002/hep.21606 (2007).

81 Rachfal, A. W. & Brigstock, D. R. Connective tissue growth factor (CTGF/CCN2) in hepatic fibrosis. *Hepatology research* **26**, 1-9 (2003).

82 Melton, A. C., Datta, A. & Yee, J., Hal.F. [Ca2+]i-independent contractile force generation by rat hepatic stellate cells in response to endothelin-1. *American journal of physiology* **290**, G7 (2006).

83 Herath, C. B., Grace, J. A. & Angus, P. W. Therapeutic potential of targeting the renin angiotensin system in portal hypertension. *World Journal of Gastrointestinal Pathophysiology* **4**, 1-11, doi:10.4291/wjgp.v4.i1.1 (2013).

84 Fiorucci, S. *et al.* PAR1 Antagonism Protects Against Experimental Liver Fibrosis. Role of Proteinase Receptors in Stellate Cell Activation. *Hepatology* **39**, 365–375 (2004).

85 Hammel, P. *et al.* REGRESSION OF LIVER FIBROSIS AFTER BILIARY DRAINAGE IN PATIENTS WITH CHRONIC PANCREATITIS AND STENOSIS OF THE COMMON BILE DUCT. *The New England Journal of Medicine* **23**, 344:418 (2001).

86 Shiratori, Y. *et al.* Histologic Improvement of Fibrosis in Patients with Hepatitis C Who Have Sustained Response to Interferon Therapy. *Annals of Internal Medicine* **132**, :517-552 (2000).
87 Kweon, Y.-O. *et al.* Decreasing fibrogenesis: an immunohistochemical study of paired liver biopsies following lamivudine therapy for chronic hepatitis B. *Journal of Hepatology* **35**, 749–755 (2001).
88 Wakim Fleming, J. & Mullen, K. D. Long-term Management of Alcoholic Liver Disease. *Clinics in liver disease* **9**, 135-149 (2005).
89 Dufour, J.-F., DeLellis, R. & Kaplan, M. M. Reversibility of Hepatic Fibrosis in Autoimmune Hepatitis. *Annals of Internal Medicine* **127:**, 981-989 (1997).
90 Dixon, J. B., Bhathal, P. S., Hughes, N. R. & O'Brien, P. E. Nonalcoholic Fatty Liver Disease: Improvement in Liver Histological Analysis With Weight Loss. *Hepatology* **39**, 1647–1654 (2004).
91 Radaeva, S. *et al.* Natural Killer Cells Ameliorate Liver Fibrosis by Killing Activated Stellate Cells in NKG2D-Dependent and Tumor Necrosis Factor–Related Apoptosis-Inducing Ligand–Dependent Manners. *Gastroenterology* **130**, 435–452 (2006).
92 Bloom, S., Kemp, W. & Lubel, J. Portal hypertension: pathophysiology, diagnosis and management. *Internal Medicine Journal* **45** 16-26, doi:doi:10.1111/imj.12590 (2015).
93 Heidelbugh, J. J. & Sherbondy, M. Cirrhosis and Chronic Liver Failure: Part II. Complications and Treatment. *American Family Physician* **74**, 667-676 (2006).
94 Grace, J. A. *et al.* Activation of the Mas Receptor by Angiotensin-(1–7) in the Renin–Angiotensin System Mediates Mesenteric Vasodilatation in Cirrhosis. *Gastroenterology* **145**, 874-884.e875, doi:10.1053/j.gastro.2013.06.036 (2013).
95 Nusrat, S., Khan, M. S., Fazili, J. & Madhoun, M. F. Cirrhosis and its complications: Evidence based treatment. *World Journal of Gastroenterology* **20**, 5442-5460 (2014).
96 El-Kader, S. M. A. & Ashmawy, E. M. S. E.-D. Non-alcoholic fatty liver disease: The diagnosis and management. *World Journal of Gastroenterology* **7** 846-858 (2015).
97 Yeh, M. M. & Brunt, E. M. Pathology of Nonalcoholic Fatty Liver Disease. *American Journal of Clinical Pathology* **128**, 837-847, doi:DOI: 10.1309/RTPM1PY6YGBL2G2R (2007).
98 Ludwig, J., Viggiano, T. R., McGill, D. B. & Oh, B. J. Nonalcoholic steatohepatitis: Mayo Clinic experiences with a hitherto unnamed disease. *Mayo Clinic Proceedings* **55**, 434-438 (1980).
99 Farrell, G. C. & Larter, C. Z. Nonalcoholic Fatty Liver Disease: From Steatosis to Cirrhosis. *Hepatology* **43**, S99-S112, doi:DOI10.1002/hep.20973 (2006).
100 Brunt, E. M., Kleiner, D. E., Wilson, L. A., Belt, P. & Neuschwander-Tetri, B. A. The NAS and The Histopathologic Diagnosis in NAFLD: Distinct Clinicopathologic Meanings. *Hepatology* **53**, 810–820, doi:doi:10.1002/hep.24127 (2011).
101 Ratziu, V. *et al.* Sampling Variability of Liver Biopsy in Nonalcoholic Fatty Liver Disease. *Gastroenterology* **128**, 1898–1906, doi:doi:10.1053/j.gastro.2005.03.084 (2005).
102 Sanyal, A. J. *et al.* Endpoints and clinical trial design for nonalcoholic steatohepatitis. *Hepatology* **54**, 344–353, doi:doi:10.1002/hep.24376 (2011).

103 Brown, G. T. & Kleiner, D. E. Histopathology of non-alcoholic fatty liver disease and non-alcoholic steatohepatitis. *Metabolism* **65**, 1080–1086, doi:doi:10.1016/j.metabol.2015.11.008 (2016).

104 Chalasani, N. *et al.* Relationship of steatosis grade and zonal location to histological features of steatohepatitis in adult patients with nonalcoholic fatty liver disease. *Journal of Hepatology* **48**, 829–834 (2008).

105 Kleiner, D. E. *et al.* Design and Validation of a Histological Scoring System for Nonalcoholic Fatty Liver Disease. *Hepatology* **41**, 1313-1324, doi:DOI10.1002/hep.20701 (2005).

106 Takahashi, Y. & Fukusato, T. Histopathology of non-alcoholic fatty liver disease/non-alcoholic steatohepatitis. *World Journal of Gastroenterology* **20**, 15539-15548 (2014).

107 Kleiner, D. E. & Makhlouf, H. R. Histology of NAFLD and NASH in Adults and Children. **20**, 293–312, doi:doi:10.1016/j.cld.2015.10.011 (2016).

108 Patton, H. *et al.* Clinical correlates of histopathology in pediatric nonalcoholic steatohepatitis (NASH). *Gastroenterology* **135**, 1961–1971, doi:doi:10.1053/j.gastro.2008.08.050 (2008).

109 Day, C. P. & James, O. F. W. Steatohepatitis: A Tale of Two ‘‘Hits’’? *Gastroenterology* **114**, 842-845 (1998).

110 Schwimmer, J. B. *et al.* Heritability of Nonalcoholic Fatty Liver Disease. *Gastroenterology* **136**, 1585–1592, doi:doi:10.1053/j.gastro.2009.01.050 (2009).

111 Sookoian, S. & Pirola, C. J. Genetic predisposition in nonalcoholic fatty liver disease. *Clinical and Molecular Hepatology* **23**, 1-12, doi:doi.org/10.3350/cmh.2016.0109 (2017).

112 Romeo, S. *et al.* Genetic variation in PNPLA3 confers susceptibility to nonalcoholic fatty liver disease. *Nature genetics* **40**, 1461-1465, doi:10.1038/ng.257 (2008).

113 Dongiovanni, P. *et al.* Transmembrane 6 superfamily member 2 gene variant disentangles nonalcoholic steatohepatitis from cardiovascular disease. **61**, 506-514, doi:10.1002/hep.27490 (2015).

114 Caligiuri, A., Gentilini, A. & Marra, F. Molecular Pathogenesis of NASH. *International Journal of Molecular Sciences* **17**, 1575 (2016).

115 Pirazzi, C. *et al.* Patatin-like phospholipase domain-containing 3 (PNPLA3) I148M (rs738409) affects hepatic VLDL secretion in humans and in vitro. *Journal of hepatology* **57**, 1276-1282 (2012).

116 Beer, N. L. *et al.* The P446L variant in GCKR associated with fasting plasma glucose and triglyceride levels exerts its effect through increased glucokinase activity in liver. *Human molecular genetics* **18**, 4081-4088 (2009).

117 Dongiovanni, P. *et al.* Genetic variants regulating insulin receptor signalling are associated with the severity of liver damage in patients with non-alcoholic fatty liver disease. *Gut* **59**, 267-273 (2010).

118 Macaluso, F. S., Maida, M. & Petta, S. Genetic background in nonalcoholic fatty liver disease: A comprehensive review. *World journal of gastroenterology* **21**, 11088-11111, doi:10.3748/wjg.v21.i39.11088 (2015).

119 Buzzetti, E., Pinzani, M. & Tsochatzis, E. A. The multiple-hit pathogenesis of non-alcoholic fatty liver disease (NAFLD). *Metabolism* **65**, 1038 – 1048 (2016).

120 Hochberg, Z. *et al.* Child health, developmental plasticity, and epigenetic programming. *Endocrine Reviews* **32**, 159–224 (2011).

121 Sun, C., Fan, J.-G. & Qiao, L. Potential Epigenetic Mechanism in Non-Alcoholic Fatty Liver Disease. *International Journal of Molecular Sciences* **16**, 5161 (2015).

122 Gallego-Durán, R. & Romero-Gómez, M. Epigenetic mechanisms in non-alcoholic fatty liver disease: An emerging field. *World Journal of Hepatology* **7**, 2497-2502 (2015).
123 Hardy, T. & Mann, D. A. Epigenetics in liver disease: from biology to therapeutics. *Gut* **65**, 1895–1905 (2016).
124 Pogribny, I. P. *et al.* Hepatic epigenetic phenotype predetermines individual susceptibility to hepatic steatosis in mice fed a lipogenic methyldeficient diet. *Journal of Hepatology* **51**, 176–186, doi:doi:10.1016/j.jhep.2009.03.021 (2009).
125 Pirola, C. J. *et al.* Epigenetic modification of liver mitochondrial DNA is associated with histological severity of nonalcoholic fatty liver disease. *Gut* **62**, 1356-1363, doi:10.1136/gutjnl-2012-302962 (2013).
126 Murphy, S. K. *et al.* Relationship Between Methylome and Transcriptome in Patients With Nonalcoholic Fatty Liver Disease. *Gastroenterology* **145**, 1076-1087, doi:10.1053/j.gastro.2013.07.047 (2013).
127 Yang, S.-M., Kim, B. J., Toro, L. N. & Skoultchi, A. I. H1 linker histone promotes epigenetic silencing by regulating both DNA methylation and histone H3 methylation. *PNAS* **110**, 1708–1713, doi:doi/10.1073/pnas.1213266110 (2013).
128 He, Y. *et al.* The potential of microRNAs in liver fibrosis. *Cellular Signalling* **24**, 2268–2272, doi:doi.org/10.1016/j.cellsig.2012.07.023 (2012).
129 Li, Y.-Y. Genetic and epigenetic variants influencing the development of nonalcoholic fatty liver disease. *World Journal of Gastroenterology* **18**, 6546-6551 (2012).
130 Malaguarnera, M., Di Rosa, M., Nicoletti, F. & Malaguarnera, L. Molecular mechanisms involved in NAFLD progression. *Journal of Molecular Medicine*, doi:DOI 10.1007/s00109-009-0464-1.
131 Sanyal, A. J. *et al.* Nonalcoholic steatohepatitis: Association of insulin resistance and mitochondrial abnormalities. *Gastroenterology* **120**, 1183-1192, doi:10.1053/gast.2001.23256 (2001).
132 Begriche, K., Massart, J., Robin, M.-A., Bonnet, F. & Fromenty, B. Mitochondrial adaptations and dysfunctions in nonalcoholic fatty liver disease. *Hepatology* **58**, 1497-1507, doi:10.1002/hep.26226 (2013).
133 Oliveira, C. P. M. S. *et al.* Oxidative stress in the pathogenesis of nonalcoholic fatty liver disease, in rats fed with a choline-deficient diet. *Journal of Cellulr and Molecular Medicine* **6**, 399-406 (2002).
134 Petrosillo, G. *et al.* Mitochondrial dysfunction in rat with nonalcoholic fatty liver: Involvement of complex I, reactive oxygen species and cardiolipin. *Biochimica et Biophysica Acta (BBA) - Bioenergetics* **1767**, 1260-1267, doi:https://doi.org/10.1016/j.bbabio.2007.07.011 (2007).
135 Pérez-Carreras, M. *et al.* Defective hepatic mitochondrial respiratory chain in patients with nonalcoholic steatohepatitis. *Hepatology* **38**, 999-1007, doi:10.1002/hep.1840380426 (2003).
136 Mak, K. Y. *et al.* ACE2 Therapy Using Adeno-associated Viral Vector Inhibits Liver Fibrosis in Mice. *Molecular Therapy* **23**, 1434-1443, doi:10.1038/mt.2015.92 (2015).
137 Paradies, G., Paradies, V., Ruggiero, F. M. & Petrosillo, G. Oxidative stress, cardiolipin and mitochondrial dysfunction in nonalcoholic fatty liver disease. *World Journal of Gastroenterology* **20**, 14205-14218 (2014).

138 Chavin, K. D. *et al.* Obesity Induces Expression of Uncoupling Protein-2 in Hepatocytes and Promotes Liver ATP Depletion. *The Journal of Biological Chemistry* **274**, 5692–5700 (1999).
139 Schulze-Osthoff, K. *et al.* Cytotoxic Activity of Tumor Necrosis Factor Is Mediated by Early Damage of Mitochondrial Functions. *The Journal of Biological Chemistry* **267**, 5317-5323 (1992).
140 Zhang, Y. *et al.* Positional cloning of the mouse obese gene and its humanhomologue. *Nature* **372**, 425-432 (1994).
141 Tilg, H. & Hotamisligil, G. S. Nonalcoholic Fatty Liver Disease: Cytokine-Adipokine Interplay and Regulation of Insulin Resistance. *Gastroenterology* **131**, 934-945, doi:10.1053/j.gastro.2006.05.054 (2006).
142 Polyzos, S. A., Kountouras, J. & Mantzoros, C. S. Adipokines in nonalcoholic fatty liver disease. *Metabolism - Clinical and Experimental* **65**, 1062-1079, doi:10.1016/j.metabol.2015.11.006 (2016).
143 Adolph, T. E., Grander, C., Grabherr, F. & Tilg, H. Adipokines and Non-Alcoholic Fatty Liver Disease: Multiple Interactions. *International Journal of Molecular Sciences* **18**, 1649-1664, doi:doi:10.3390/ijms18081649 (2017).
144 Scherer, P. E., Williams, S., Fogliano, M., Baldini, G. & Lodish, H. F. A Novel Serum Protein Similar to C1q, Produced Exclusively in Adipocytes. *Journal of Biological Chemistry* **270**, 26746-26749, doi:10.1074/jbc.270.45.26746 (1995).
145 Tsochatzis, E. A., Papatheodoridis, G. V. & Archimandritis, A. J. Adipokines in Nonalcoholic Steatohepatitis: From Pathogenesis to Implications in Diagnosis and Therapy. *Mediators of Inflammation* **2009**, doi:10.1155/2009/831670 (2009).
146 Steppan, C. M. *et al.* The hormone resistin links obesity to diabetes. *Nature* **409**, 307, doi:10.1038/35053000 (2001).
147 Wittamer, V. *et al.* The C-terminal Nonapeptide of Mature Chemerin Activates the Chemerin Receptor with Low Nanomolar Potency. *Journal of Biological Chemistry* **279**, 9956-9962, doi:10.1074/jbc.M313016200 (2004).
148 Leung, C., Rivera, L., Furness, J. B. & Angus, P. W. The role of the gut microbiota in NAFLD. *Nature Reviews Gastroenterology &Amp; Hepatology* **13**, 412, doi:10.1038/nrgastro.2016.85 (2016).
149 Aron-Wisnewsky, J., Gaborit, B., Dutour, A. & Clement, K. Gut microbiota and non-alcoholic fatty liver disease: new insights. *Clinical Microbiology and Infection* **19**, 338-348, doi:10.1111/1469-0691.12140 (2013).
150 Delaere, F. *et al.* The role of sodium-coupled glucose co-transporter 3 in the satiety effect of portal glucose sensing. *Molecular Metabolism* **2**, 47-53, doi:https://doi.org/10.1016/j.molmet.2012.11.003 (2013).
151 Wong, V. W.-S. *et al.* Molecular Characterization of the Fecal Microbiota in Patients with Nonalcoholic Steatohepatitis – A Longitudinal Study. *PLoS ONE* **8**, doi:doi:10.1371/journal.pone.0062885 (2013).
152 Miele, L. *et al.* Increased intestinal permeability and tight junction alterations in nonalcoholic fatty liver disease. *Hepatology* **49**, 1877-1887, doi:10.1002/hep.22848 (2009).
153 Volynets, V. *et al.* Nutrition, Intestinal Permeability, and Blood Ethanol Levels Are Altered in Patients with Nonalcoholic Fatty Liver Disease (NAFLD). *Digestive Diseases and Sciences* **57**, 1932-1941, doi:10.1007/s10620-012-2112-9 (2012).
154 Gäbele, E. *et al.* DSS induced colitis increases portal LPS levels and enhances hepatic inflammation and fibrogenesis in experimental NASH. *Journal of Hepatology* **55**, 1391-1399, doi:10.1016/j.jhep.2011.02.035 (2011).

155 Cope, K., Risby, T. & Diehl, A. M. Increased gastrointestinal ethanol production in obese mice: Implications for fatty liver disease pathogenesis. *Gastroenterology* **119**, 1340-1347, doi:10.1053/gast.2000.19267 (2000).
156 Nair, S., Cope, K., Terence, R. H. & Diehl, A. M. Obesity and female gender increase breath ethanol concentration: potential implications for the pathogenesis of nonalcoholic steatohepatitis. *American Journal Of Gastroenterology* **96**, 1200, doi:10.1111/j.1572-0241.2001.03702.x (2001).
157 Li, S. *et al.* Change of intestinal mucosa barrier function in the progress of non-alcoholic steatohepatitis in rats. *World Journal of Gastroenterology* **14**, 3254-3258 (2008).
158 Mao, J.-W. *et al.* Intestinal mucosal barrier dysfunction participates in the progress of nonalcoholic fatty liver disease. *International Journal of Clinical and Experimental Pathology* **8**, 3648-3658 (2015).
159 Zeisel, S. H. & da Costa, K.-A. Choline: An Essential Nutrient for Public Health. *Nutrition reviews* **67**, 615-623, doi:10.1111/j.1753-4887.2009.00246.x (2009).
160 Wang, Z. *et al.* Gut flora metabolism of phosphatidylcholine promotes cardiovascular disease. *Nature* **472**, 57, doi:10.1038/nature09922

https://www.nature.com/articles/nature09922#supplementary-information (2011).
161 Spencer, M. D. *et al.* Association Between Composition of the Human Gastrointestinal Microbiome and Development of Fatty Liver With Choline Deficiency. *Gastroenterology* **140**, 976-986, doi:10.1053/j.gastro.2010.11.049 (2011).
162 Yokota, A. *et al.* Is bile acid a determinant of the gut microbiota on a high-fat diet? *Gut Microbes* **3**, 455-459, doi:10.4161/gmic.21216 (2012).
163 Carr, R. M. & Reid, A. E. FXR agonists as therapeutic agents for non-alcoholic fatty liver disease. *Current Atherosclerosis Reports* **17**, doi:doi.org/10.1007/s11883-015-0500-2 (2015).
164 Trauner, M., Claudel, T., Fickert, P., Moustafa, T. & Wagner, M. Bile Acids as Regulators of Hepatic Lipid and Glucose Metabolism. *Digestive Diseases* **28**, 220-224 (2010).
165 Mudaliar, S. *et al.* Efficacy and Safety of the Farnesoid X Receptor Agonist Obeticholic Acid in Patients With Type 2 Diabetes and Nonalcoholic Fatty Liver Disease. *Gastroenterology* **145**, 574-582.e571, doi:10.1053/j.gastro.2013.05.042 (2013).
166 Neuschwander-Tetri, B. A. *et al.* Farnesoid X nuclear receptor ligand obeticholic acid for non-cirrhotic, non-alcoholic steatohepatitis (FLINT): a multicentre, randomised, placebo-controlled trial. *The Lancet* **385**, 956-965, doi:10.1016/S0140-6736(14)61933-4 (2015).
167 McCrory, M. A., Shaw, A. C. & Lee, J. A. Energy and Nutrient Timing for Weight Control: Does Timing of Ingestion Matter? *Endocrinology and Metabolism Clinics of North America* **45**, 689-718, doi:https://doi.org/10.1016/j.ecl.2016.04.017 (2016).
168 Tappy, L. Q&A: 'Toxic' effects of sugar: should we be afraid of fructose? *BMC Biology* **10**, 42, doi:10.1186/1741-7007-10-42 (2012).
169 Musso, G. *et al.* Dietary habits and their relations to insulin resistance and postprandial lipemia in nonalcoholic steatohepatitis. *Hepatology* **37**, 909-916, doi:10.1053/jhep.2003.50132 (2003).
170 Marriott, B. P., Olsho, L., Hadden, L. & Connor, P. Intake of Added Sugars and Selected Nutrients in the United States, National Health and Nutrition Examination

Survey (NHANES) 2003—2006. *Critical Reviews in Food Science and Nutrition* **50**, 228-258, doi:10.1080/10408391003626223 (2010).
171 Aragno, M. & Mastrocola, R. Dietary Sugars and Endogenous Formation of Advanced Glycation Endproducts: Emerging Mechanisms of Disease. *Nutrients* **9**, 385 (2017).
172 Yao, M. *et al.* Relative influence of diet and physical activity on cardiovascular risk factors in urban Chinese adults. *International Journal Of Obesity* **27**, 920, doi:10.1038/sj.ijo.0802308 (2003).
173 Stanhope, K. L. *et al.* Consuming fructose-sweetened, not glucose-sweetened, beverages increases visceral adiposity and lipids and decreases insulin sensitivity in overweight/obese humans. *The Journal of Clinical Investigation* **119**, 1322-1334, doi:10.1172/JCI37385 (2009).
174 Nomura, K. & Yamanouchi, T. The role of fructose-enriched diets in mechanisms of nonalcoholic fatty liver disease. *The Journal of Nutritional Biochemistry* **23**, 203-208, doi:https://doi.org/10.1016/j.jnutbio.2011.09.006 (2012).
175 Goran, M. I., Walker, R. & Allayee, H. Genetic-related and carbohydrate-related factors affecting liver fat accumulation. *Current Opinion in Clinical Nutrition & Metabolic Care* **15**, 392-396, doi:10.1097/MCO.0b013e3283544477 (2012).
176 Barrera, F. & George, J. The Role of Diet and Nutritional Intervention for the Management of Patients with NAFLD. *Clinics in Liver Disease* **18**, 91-112, doi:https://doi.org/10.1016/j.cld.2013.09.009 (2014).
177 Fan, J.-G. & Cao, H.-X. Role of diet and nutritional management in non-alcoholic fatty liver disease. *Journal of Gastroenterology and Hepatology* **28** 81–87, doi:doi:10.1111/jgh.12244 (2013).
178 Savard, C. *et al.* Synergistic interaction of dietary cholesterol and dietary fat in inducing experimental steatohepatitis. *Hepatology* **57**, 81-92, doi:10.1002/hep.25789 (2013).
179 van Rooyen, D. M. *et al.* Hepatic Free Cholesterol Accumulates in Obese, Diabetic Mice and Causes Nonalcoholic Steatohepatitis. *Gastroenterology* **141**, 1393–1403 (2011).
180 Dongiovanni, P. & Valenti, L. A Nutrigenomic Approach to Non-Alcoholic Fatty Liver Disease. *International Journal of Molecular Sciences* **18**, 1534 (2017).
181 Carvalhana, S., Machado, M. V. & Cortez-Pinto, H. Improving dietary patterns in patients with nonalcoholic fatty liver disease. *Current Opinion in Clinical Nutrition & Metabolic Care* **15**, 468-473, doi:10.1097/MCO.0b013e3283566614 (2012).
182 Kargulewicz, A., Stankowiak-Kulpa, H. & Grzymisławski, M. Dietary recommendations for patients with nonalcoholic fatty liver disease. *Przegląd Gastroenterologiczny* **9**, 18-23, doi:10.5114/pg.2014.40845 (2014).
183 Wit, N. d. *et al.* Saturated fat stimulates obesity and hepatic steatosis and affects gut microbiota composition by an enhanced overflow of dietary fat to the distal intestine. *American Journal of Physiology-Gastrointestinal and Liver Physiology* **303**, G589-G599, doi:10.1152/ajpgi.00488.2011 (2012).
184 Corbin, K. D. & Zeisel, S. H. Choline metabolism provides novel insights into nonalcoholic fatty liver disease and its progression. *Current Opinion in Gastroenterology* **28**, 159–165, doi:DOI:10.1097/MOG.0b013e32834e7b4b (2012).
185 Valenti, L. *et al.* HFE Genotype, Parenchymal Iron Accumulation, and Liver Fibrosis in Patients With Nonalcoholic Fatty Liver Disease. *Gastroenterology* **138**, 905-912, doi:10.1053/j.gastro.2009.11.013 (2010).

186 Targher, G. *et al.* Associations between serum 25-hydroxyvitamin D₃ concentrations and liver histology in patients with non-alcoholic fatty liver disease. *Nutrition, Metabolism and Cardiovascular Diseases* **17**, 517-524, doi:10.1016/j.numecd.2006.04.002 (2007).
187 Bouwens, L., Baekeland, M., de Zanger, R. & Wisse, E. Quantitation, tissue distribution and proliferation kinetics of kupffer cells in normal rat liver. *Hepatology* **6**, 718-722, doi:10.1002/hep.1840060430 (1986).
188 Thomson, A. W. & Knolle, P. A. Antigen-presenting cell function in the tolerogenic liver environment. *Nature Reviews Immunology* **10**, 753, doi:10.1038/nri2858 (2010).
189 Maher, J. J., Leon, P. & Ryan, J. C. Beyond insulin resistance: Innate immunity in nonalcoholic steatohepatitis. *Hepatology* **48**, 670-678, doi:10.1002/hep.22399 (2008).
190 Baffy, G. Kupffer cells in non-alcoholic fatty liver disease: The emerging view. *Journal of Hepatology* **51**, 212-223, doi:10.1016/j.jhep.2009.03.008 (2009).
191 Lanthier, N. Targeting Kupffer cells in non-alcoholic fatty liver disease/non-alcoholic steatohepatitis: Why and how? *World Journal of Hepatology* **7**, 2184-2188, doi:10.4254/wjh.v7.i19.2184 (2015).
192 Dixon, L. J., Barnes, M., Tang, H., Pritchard, M. T. & Nagy, L. E. in *Comprehensive Physiology* (John Wiley & Sons, Inc., 2013).
193 Harte, A. L. *et al.* Elevated endotoxin levels in non-alcoholic fatty liver disease. *Journal of Inflammation* **7**, 15, doi:10.1186/1476-9255-7-15 (2010).
194 Wenfeng, Z. *et al.* Kupffer cells: increasingly significant role in nonalcoholic fatty liver disease. *Annals of Hepatology* **13**, 489-495 (2014).
195 Rivera, C. A. *et al.* Toll-like receptor-4 signaling and Kupffer cells play pivotal roles in the pathogenesis of non-alcoholic steatohepatitis. *Journal of hepatology* **47**, 571-579, doi:10.1016/j.jhep.2007.04.019 (2007).
196 Malhi, H. & Gores, G. J. Molecular Mechanisms of Lipotoxicity in Nonalcoholic Fatty Liver Disease. *Semin Liver Dis* **28**, 360-369, doi:10.1055/s-0028-1091980 (2008).
197 Marí, M. *et al.* Mitochondrial free cholesterol loading sensitizes to TNF- and Fas-mediated steatohepatitis. *Cell Metabolism* **4**, 185-198, doi:10.1016/j.cmet.2006.07.006 (2006).
198 Lambeth, J. D. NOX enzymes and the biology of reactive oxygen. *Nature Reviews Immunology* **4**, 181, doi:10.1038/nri1312 (2004).
199 Brunt, E. M. & Tiniakos, D. G. Histopathology of nonalcoholic fatty liver disease. *World Journal of Gastroenterology : WJG* **16**, 5286-5296, doi:10.3748/wjg.v16.i42.5286 (2010).
200 Neyrinck, A. M. *et al.* Critical role of Kupffer cells in the management of diet-induced diabetes and obesity. *Biochemical and Biophysical Research Communications* **385**, 351-356, doi:https://doi.org/10.1016/j.bbrc.2009.05.070 (2009).
201 Fülöp, P. *et al.* Lack of UCP2 reduces fas-mediated liver injury in ob/ob mice and reveals importance of cell-specific UCP2 expression. *Hepatology* **44**, 592-601, doi:10.1002/hep.21310 (2006).
202 Liu, S. *et al.* Role of Toll-Like Receptors in Changes in Gene Expression and NF-□B Activation in Mouse Hepatocytes Stimulated with Lipopolysaccharide. *Infection and Immunity* **70**, 3433–3442 (2002).

203 Meli, R., Mattace Raso, G. & Calignano, A. Role of Innate Immune Response in Non-Alcoholic Fatty Liver Disease: Metabolic Complications and Therapeutic Tools. *Frontiers in Immunology* **5**, 177, doi:10.3389/fimmu.2014.00177 (2014).
204 Lukacs-Kornek, V. & Schuppan, D. Dendritic cells in liver injury and fibrosis: Shortcomings and promises. *Journal of Hepatology* **59**, 1124-1126, doi:10.1016/j.jhep.2013.05.033 (2013).
205 Miyao, M. *et al.* Pivotal role of liver sinusoidal endothelial cells in NAFLD/NASH progression. *Laboratory Investigation* **95**, 1130, doi:10.1038/labinvest.2015.95

https://www.nature.com/articles/labinvest201595#supplementary-information (2015).
206 Ishikawa, T., Yokoyama, H., Matsuura, T. & Fujiwara, Y. Fc gamma RIIb expression levels in human liver sinusoidal endothelial cells during progression of non-alcoholic fatty liver disease. *PLOS ONE* **14**, e0211543, doi:10.1371/journal.pone.0211543 (2019).
207 Harris, E. N. & Gopalakrishnan, S. Profile of the liver sinusoidal endothelial cell in non-alcohol fatty liver. **27**, 565.564-565.564, doi:10.1096/fasebj.27.1_supplement.565.4 (2013).
208 Carpino, G., Renzi, A., Onori, P. & Gaudio, E. Role of Hepatic Progenitor Cells in Nonalcoholic Fatty Liver Disease Development: Cellular Cross-Talks and Molecular Networks. *International Journal of Molecular Sciences* **14**, 20112 (2013).
209 Roskams, T. *et al.* Oxidative stress and oval cell accumulation in mice and humans with alcoholic and nonalcoholic fatty liver disease. *The American journal of pathology* **163**, 1301-1311, doi:10.1016/S0002-9440(10)63489-X (2003).
210 Goodwin, M. *et al.* Advanced glycation end products augment experimental hepatic fibrosis. *Journal of Gastroenterolgy and Hepatology* **28**, 369–376, doi:doi:10.1111/jgh.12042 (2013).
211 Leung, C. *et al.* Dietary glycotoxins exacerbate progression of experimental fatty liver disease. *Journal of Hepatology* **60** 832–838 (2014).
212 Leung, C. *et al.* Dietary advanced glycation end-products aggravate non-alcoholic fatty liver disease. *World Journal of Gastroenterology* **22**, 8026-8040 (2016).
213 Singh, R., Barden, A., Mori, T. & Beilin, L. Advanced glycation end-products: a review. *Diabetologia* **44**, 129±146 (2001).
214 Busch, M., Franke, S., Ru¨ster, C. & Wolf, G. Advanced glycation end-products and the kidney. *European Journal of Clinical Investigation* **40**, 742-755, doi:DOI: 10.1111/j.1365-2362.2010.02317.x (2010).
215 Skovsted, I., Christensen, M., Breinholt, J. & Mortensen, S. *Characterisation of a novel AGE-compound derived from lysine and 3-deoxyglucosone*. Vol. 44 (1998).
216 Kokkinidou, S. & Peterson, D. G. Control of Maillard-type off-flavor development in ultrahigh-temperature- processed bovine milk by phenolic chemistry. *Journal of Agricultural and Food Chemistry* **62**, 8023-8033 (2014).
217 Tian, C. *et al.* REACTIVE CARBONYL SPECIES AND THEIR ROLES IN SARCOPLASMIC RETICULUM Ca2+ CYCLING DEFECT IN THE DIABETIC HEART. *Heart Failure Reviews* **19**, 101–112, doi:doi:10.1007/s10741-013-9384-9 (2014).
218 Mano, J. i. Reactive carbonyl species: Their production from lipid peroxides, action in environmental stress, and the detoxification mechanism. *Plant Physiology and Biochemistry* **59** 90-97, doi:doi:10.1016/j.plaphy.2012.03.010 (2012).
219 Gkogkolou, P. & Böhm, M. Advanced glycation end products Key players in skin aging? *Dermato-Endocrinology* **4**, 259–270 (2012).

220 Vlassara, H. & Palace, M. R. Diabetes and advanced glycation endproducts. *Journal of Internal Medicine* **251**, 87±101 (2002).
221 Jenkins, D. J. A. *et al.* Glycemic index of foods: a physiological basis for carbohydrate exchange. *American Journal of Clinical Nutrition* **34**, 362-366 (1981).
222 Abid, A. *et al.* Soft drink consumption is associated with fatty liver disease independent of metabolic syndrome. *Journal of Hepatology* **51**, 918–924 (2009).
223 Nseir, W., Nassar, F. & Assy, N. Soft drinks consumption and nonalcoholic fatty liver disease. *World Journal of Gastroenterology : WJG* **16**, 2579-2588, doi:10.3748/wjg.v16.i21.2579 (2010).
224 Crescenzo, R. *et al.* Increased hepatic de novo lipogenesis and mitochondrial efficiency in a model of obesity induced by diets rich in fructose. *European Journal of Nutrition* **52**, 537–545 (2013).
225 Whitcomb, E. A., Chiu, C.-J. & Taylor, A. Dietary glycemia as a determinant of health and longevity. *Molecular Aspects of Medicine* **46**, 14-20, doi:https://doi.org/10.1016/j.mam.2015.08.005 (2015).
226 Uchiki, T. *et al.* Glycation-altered proteolysis as a pathobiologic mechanism that links dietary glycemic index, aging, and age-related disease (in nondiabetics). *Aging Cell* **11**, 1-13, doi:10.1111/j.1474-9726.2011.00752.x (2012).
227 Kostolanska, J., Jakus, V. & Barák, L. HbA1c and Serum Levels of Advanced Glycation and Oxidation Protein Products in Poorly and Well Controlled Children and Adolescents with Type 1 Diabetes Mellitus. *Journal of pediatric endocrinology & metabolism* **22**, 433 (2009).
228 Guilbaud, A., Niquet-Leridon, C., Boulanger, E. & Tessier, F. J. How Can Diet Affect the Accumulation of Advanced Glycation End-Products in the Human Body? *Foods* **5**, 84, doi:10.3390/foods5040084 (2016).
229 Vlassara, H. *et al.* Inflammatory mediators are induced by dietary glycotoxins, a major risk factor for diabetic angiopathy. *PNAS* **99**, 15596–15601 (2002).
230 Baynes, J. W. Role of Oxidative Stress in Development of Complications in Diabetes. *Diabetes* **40**, 405-412, doi:10.2337/diab.40.4.405 (1991).
231 Anderson, M. M., Requena, J. R., Crowley, J. R., Thorpe, S. R. & Heinecke, J. W. The myeloperoxidase system of human phagocytes generates Nε-(carboxymethyl)lysine on proteins: a mechanism for producing advanced glycation end products at sites of inflammation. *Journal of Clinical Investigation* **104**, 103–113 (1999).
232 Uribarri, J. *et al.* Circulating Glycotoxins and Dietary Advanced Glycation Endproducts: Two Links to Inflammatory Response, Oxidative Stress, and Aging. *J Gerontol A Biol Sci Med Sci.* **62**, 427–433 (2007).
233 Leslie, R. D. G. *et al.* Level of an Advanced Glycated End Product Is Genetically Determined A Study of Normal Twins. *Diabetes* **52**, 2441-2444 (2003).
234 Koschinsky, T. *et al.* Orally absorbed reactive glycation products (glycotoxins): An environmental risk factor in diabetic nephropathy. *Proceedings of the National Academy of Sciences of the United States of America* **94**, 6474–6479 (1997).
235 Ames, J. M. Control of the Maillard reaction in food systems. *Trends in Food Science & Technology* **1**, 150-154, doi:https://doi.org/10.1016/0924-2244(90)90113-D (1990).
236 van Boekel, M. A. J. S. Kinetic aspects of the Maillard reaction: a critical review. *Food / Nahrung* **45**, 150-159, doi:10.1002/1521-3803(20010601)45:3<150::AID-FOOD150>3.0.CO;2-9 (2001).

237 Goldberg, T. *et al.* Advanced Glycoxidation End Products in Commonly Consumed Foods. *Journal of The American Dietitic Association* **104**, 1287-1291, doi:doi: 10.1016/j.jada.2004.05.214 (2004).
238 Uribarri, J. *et al.* Advanced Glycation End Products in Foods and a Practical Guide to Their Reduction in the Diet. **110**, 911-916, doi:doi:10.1016/j.jada.2010.03.018 (2010).
239 Kellow, N. J. & Coughlan, M. T. Effect of diet-derived advanced glycation end products on inflammation. *Nutrition Reviews* **73**, 737–759, doi:doi: 10.1093/nutrit/nuv030 (2015).
240 Cerami, C. *et al.* Tobacco smoke is a source of toxic reactive glycation products. *Proceedings of the National Academy of Sciences of the United States of America* **94**, 13915-13920 (1997).
241 Nicholl, I. D. & Bucala, R. Advanced glycation endproducts and cigarette smoking. *Cell Mol Biol (Noisy-le-grand)* **44**, 1025-1033 (1998).
242 Araki, N. *et al.* Macrophage Scavenger Receptor Mediates the Endocytic Uptake and Degradation of Advanced Glycation End Products of the Maillard Reaction. *European Journal of Biochemistry* **230**, 408-415, doi:10.1111/j.1432-1033.1995.0408h.x (1995).
243 Miyata, T. *et al.* Renal catabolism of advanced glycation end products: The fate of pentosidine. *Kidney International* **53**, 416-422 (1998).
244 Smedsrød, B., Melkko, J., Araki, N., Sano, H. & Horiuchi, S. Advanced glycation end products are eliminated by scavenger-receptor-mediated endocytosis in hepatic sinusoidal Kupffer and endothelial cells. *Biochemical Journal* **322**, 567-573 (1997).
245 Sebekova´, K. n., Kupcˇova´, V., Schinzel, R. & Heidland, A. Markedly elevated levels of plasma advanced glycation end products in patients with liver cirrhosis – amelioration by liver transplantation. *Journal of Hepatology* **36**, 66-71 (2002).
246 Goldin, A., Beckman, J. A., Schmidt, A. M. & Creager, M. A. Advanced Glycation End Products Sparking the Development of Diabetic Vascular Injury. *Circulation* **114**, 597-605 (2006).
247 Tan, A. L. Y., Forbes, J. M. & Cooper, M. E. AGE, RAGE, and ROS in Diabetic Nephropathy. *Seminars in Nephrology* **27**, 130-143 (2007).
248 Aso, Y., Inukai, T., Tayama, K. & Takemura, Y. Serum concentrations of advanced glycation endproducts are associated with the development of atherosclerosis as well as diabetic microangiopathy in patients with type 2 diabetes. *Acta Diabetologica* **37**, 87-92 (2000).
249 Bierhaus, A., Hofmann, M. A., Ziegler, R. & Nawroth, P. P. AGEs and their interaction with AGE-receptors in vascular disease and diabetes mellitus. I. The AGE concept. *Cardiovascular Research* **37**, 586–600 (1998).
250 Sims, T. J., Rasmussen, L. M., Oxlund, H. & Bailey, A. J. The role of glycation cross-links in diabetic vascular stiffening. *Diabetologia* **39**, 946-951 (1996).
251 Monnier, V. M., Glomb, M., Elgawish, A. & Sell, D. R. The Mechanism of Collagen Cross-Linking in Diabetes: A Puzzle Nearing Resolution. *Diabetes* **45**, S67-S72, doi:10.2337/diab.45.3.S67 (1996).
252 Gautieri, A. *et al.* Advanced glycation end-products: Mechanics of aged collagen from molecule to tissue. *Matrix Biology* **59**, 95–108, doi:doi.org/10.1016/j.matbio.2016.09.001 (2017).
253 Bucala, R., Tracey, K. J. & Cerami, A. Advanced glycosylation products quench nitric oxide and mediate defective endothelium-dependent vasodilatation in

experimental diabetes. *The Journal of Clinical Investigation* **87**, 432-438, doi:10.1172/JCI115014 (1991).

254 Zheng, F. *et al.* Prevention of diabetic nephropathy in mice by a diet low in glycoxidation products. *Diabetes/Metabolism Research and Reviews* **18**, 224-237, doi:10.1002/dmrr.283 (2002).

255 Vlassara, H. *et al.* Advanced glycation end products induce glomerular sclerosis and albuminuria in normal rats. *Proceedings of the National Academy of Sciences of the United States of America* **91**, 11704-11708 (1994).

256 Uribarri, J. *et al.* Restriction of Dietary Glycotoxins Reduces Excessive Advanced Glycation End Products in Renal Failure Patients. *Journal of American Society of Nephrology* **14**, 728–731 (2003).

257 Busch, M. *et al.* Vitamin B6 metabolism in chronic kidney disease--relation to transsulfuration, advanced glycation and cardiovascular disease. *Nephron. Clinical Practice* **114**, c38-c46, doi:10.1159/000245068 (2010).

258 Makita , Z. *et al.* Advanced Glycosylation End Products in Patients with Diabetic Nephropathy. *New England Journal of Medicine* **325**, 836-842, doi:10.1056/nejm199109193251202 (1991).

259 Beisswenger, P. J. *et al.* Formation of Immunochemical Advanced Glycosylation End Products Precedes and Correlates With Early Manifestations of Renal and Retinal Disease in Diabetes. *Diabetes* **44**, 824-829, doi:10.2337/diab.44.7.824 (1995).

260 Berg, T. J. *et al.* Advanced glycation end products in serum predict changes in the kidney morphology of patients with insulin-dependent diabetes mellitus. *Metabolism* **46**, 661-665, doi:https://doi.org/10.1016/S0026-0495(97)90010-X (1997).

261 Koska, J. *et al.* Advanced Glycation End Products, Oxidation Products, and Incident Cardiovascular Events in Patients With Type 2 Diabetes. *Diabetes Care* **41**, 570-576, doi:10.2337/dc17-1740 (2018).

262 Stirban, A., Gawlowski, T. & Roden, M. Vascular effects of advanced glycation endproducts: Clinical effects and molecular mechanisms. *Molecular Metabolism* **3** 94–108 (2014).

263 Soro-Paavonen, A. *et al.* Advanced glycation end-products induce vascular dysfunction via resistance to nitric oxide and suppression of endothelial nitric oxide synthase. *Journal of Hypertension* **28**, 780–788, doi:DOI:10.1097/HJH.0b013e328335043e (2010).

264 Leurs, P. & Lindholm, B. The AGEeRAGE Pathway and Its Relation to Cardiovascular Disease in Patients with Chronic Kidney Disease. *Archives of Medical Research* **44** 601-610 (2013).

265 Chang, J.-B., Chu, N.-F., Syu, J.-T., Hsieh, A.-T. & Hung, Y.-R. Advanced glycation end products (AGEs) in relation to atherosclerotic lipid profiles in middleaged and elderly diabetic patients. *Lipids in Health and Disease* **10**, 228 (2011).

266 Cai, W. *et al.* Oral Glycotoxins Determine the Effects of Calorie Restriction on Oxidant Stress, Age-Related Diseases, and Lifespan. *The American Journal ofPathology* **173**, doi:DOI: 10.2353/ajpath.2008.080152 (2008).

267 McCance, D. R. *et al.* Maillard reaction products and their relation to complications in insulin-dependent diabetes mellitus. *The Journal of Clinical Investigation* **91**, 2470-2478, doi:10.1172/JCI116482 (1993).

268 Peppa, M. *et al.* Adverse Effects of Dietary Glycotoxins on Wound Healing in Genetically Diabetic Mice. *Diabetes* **52**, 2805-2813 (2003).
269 Thornalley, P. J. Glycation in Diabetic Neuropathy: Characteristics, Consequences, Causes, and Therapeutic Options. *INTERNATIONAL REVIEW OF NEUROBIOLOGY*, 38 (2002).
270 Smith, M. A. *et al.* Advanced Maillard reaction end products are associated with Alzheimer disease pathology. *Proceedings of the National Academy of Sciences of the United States of America* **91**, 5710-5714 (1994).
271 Seftel, A. D. Erectile dysfunction--the paradigm changes but the challenges remain. *The Journal of urology* **158**, 1768 (1997).
272 Cartledge, J. J., Eardley, I. & Morrison, J. F. B. Nitric oxide-mediated corpus cavernosal smooth muscle relaxation is impaired in ageing and diabetes. *BJU International* **87**, 402-407, doi:10.1046/j.1464-410x.2001.00067.x (2001).
273 Usta, M. F. *et al.* The Breakdown of Preformed Advanced Glycation End Products Reverses Erectile Dysfunction in Streptozotocin‐Induced Diabetic Rats: Preventive Versus Curative Treatment. *The Journal of Sexual Medicine* **3**, 242-252, doi:10.1111/j.1743-6109.2006.00217.x (2006).
274 Tatone, C. & Amicarelli, F. The aging ovary—the poor granulosa cells. *Fertility and Sterility* **99**, 12-17, doi:10.1016/j.fertnstert.2012.11.029 (2013).
275 Merhi, Z. Advanced glycation end products and their relevance in female reproduction. *Human Reproduction* **29**, 135–145, doi:doi:10.1093/humrep/det383 (2014).
276 Chen, P., Zhao, J. & Gregersen, H. Up-Regulated Expression of Advanced Glycation End-Products and Their Receptor in the Small Intestine and Colon of Diabetic Rats. *Digestive Diseases and Sciences* **57**, 48–57 (2012).
277 Liu, X. *et al.* Toxicological evaluation of advanced glycation end product Nε(carboxymethyl)lysine: Acute and subacute oral toxicity studies. *Regulatory Toxicology and Pharmacology* **77** 65-74 (2016).
278 Hyogo, H. & Yamagishi, S.-i. Advanced Glycation End Products (AGEs) and their Involvement in Liver Disease. *Current Pharmaceutical Design* **14**, 969-972 (2008).
279 Yagmur, E. *et al.* Elevation of Nε-(carboxymethyl)lysine-modified advanced glycation end products in chronic liver disease is an indicator of liver cirrhosis. *Clinical Biochemistry* **39**, 39-45 (2006).
280 Hyogo, H. *et al.* Elevated levels of serum advanced glycation end products in patients with non-alcoholic steatohepatitis. *Hepatology* **22**, 1112-1119 (2007).
281 Sayej, W. N. *et al.* Advanced Glycation End Products Induce Obesity and Hepatosteatosis in CD-1 Wild-Type Mice. *BioMedical Research International* **2016**, 12, doi:doi.org/10.1155/2016/7867852 (2016).
282 Li, M. *et al.* Effects of Long-Term Exposure to Free Nε(Carboxymethyl)lysine on Rats Fed a High-Fat Diet. *Journal of Agriculture and Food Chemistry* **63**, 10995−11001, doi:DOI: 10.1021/acs.jafc.5b05750 (2015).
283 Li, M. *et al.* Increased Accumulation of Protein-Bound Nε-(Carboxymethyl)lysine in Tissues of Healthy Rats after Chronic Oral Nε-(Carboxymethyl)lysine. *Journal of Agricultural and Food Chemistry* **63**, 1658-1663, doi:10.1021/jf505063t (2015).
284 Svistounov, D. *et al.* Hepatic disposal ofadvanced glycation end products during maturation and aging. *Experimental Gerontology* **48**, 549-556 (2013).
285 Fehrenbach, H., Weiskirchen, R., Kasper, M. & Gressner, A. M. Up-regulated Expression of the Receptor for Advanced Glycation End Products in Cultured Rat

Hepatic Stellate Cells During Transdifferentiation to Myofibroblasts. *Hepatology* **34**, 943-952 (2001).

286 Guimarães, E. L. M., Empsen, C., Geerts, A. & Grunsven, L. A. v. Advanced glycation end products induce production of

reactive oxygen species via the activation of NADPH oxidase in murine hepatic stellate cells. *Journal of Hepatology* **52**, 389-397 (2010).

287 Iwamoto, K. *et al.* Advanced glycation end products enhance the proliferation and activation of hepatic stellate cells. *Journal of Gastroenterology* **43**, 298-304, doi:DOI 10.1007/s00535-007-2152-7 (2008).

288 He, Y., Zhu, J., Huang, Y., Gao, H. & Zhao, Y. Advanced glycation end product (AGE)-induced hepatic stellate cell activation via autophagy contributes to hepatitis C-related fibrosis. *Acta Diabetol* **52**, 959969, doi:DOI 10.1007/s00592-015-0763-7 (2015).

289 Stitt, A. W., He, C. & Vlassara, H. Characterization of the Advanced Glycation End-Product Receptor Complex in Human Vascular Endothelial Cells. *Biochemical and Biophysical Research Communications* **256**, 549-556, doi:https://doi.org/10.1006/bbrc.1999.0291 (1999).

290 Bierhaus, A. *et al.* Understanding RAGE, the receptor for advanced glycation end products. *Journal of Molecular Medicine* **83**, 876–886, doi:DOI 10.1007/s00109-005-0688-7 (2005).

291 Zhuang, A. & Forbes, J. M. Diabetic kidney disease: a role for advanced glycation end-product receptor 1 (AGE-R1)? *Glycoconjugate Journal* **33**, 645-652, doi:10.1007/s10719-016-9693-z (2016).

292 Lu, C. *et al.* Advanced glycation endproduct (AGE) receptor 1 is a negative regulator of the inflammatory response to AGE in mesangial cells. *Proceedings of the National Academy of Sciences of the United States of America* **101**, 11767-11772, doi:10.1073/pnas.0401588101 (2004).

293 Forough, R. *et al.* Elevated 80K-H protein in breast cancer: A role for FGF-1 stimulation of 80K-H. *The International Journal of Biological Markers* **18**, 89 (2003).

294 Strieter, R. M. & Keane, M. P. Innate immunity dictates cytokine polarization relevant to the development of pulmonary fibrosis. *Journal of Clinical Investigation* **114**, 165-168, doi:10.1172/JCI200422398 (2004).

295 Henderson, N. C. *et al.* Galectin-3 regulates myofibroblast activation and hepatic fibrosis. *Proceedings of the National Academy of Sciences of the United States of America* **103**, 5060-5065, doi:10.1073/pnas.0511167103 (2006).

296 Li, L.-c., Li, J. & Gao, J. Functions of Galectin-3 and Its Role in Fibrotic Diseases. *Journal of Pharmacology and Experimental Therapeutics* **351**, 336-343, doi:10.1124/jpet.114.218370 (2014).

297 Li, P. *et al.* Hematopoietic-Derived Galectin-3 Causes Cellular and Systemic Insulin Resistance. *Cell* **167**, 973-984.e912, doi:https://doi.org/10.1016/j.cell.2016.10.025 (2016).

298 Brett, J. *et al.* Survey of the Distribution of a Newly Characterized Receptor for Advanced Glycation End Products in Tissues. *The American Journal of Pathology* **143**, 1699-1712 (1993).

299 Hofmann, M. A. *et al.* RAGE Mediates a Novel Proinflammatory Axis. *Cell* **97**, 889-901, doi:10.1016/S0092-8674(00)80801-6 (1999).

300 Buckley, S. T. & Ehrhardt, C. The Receptor for Advanced Glycation End Products (RAGE) and the Lung. *Journal of Biomedicine and Biotechnology* **Volume 2010** 11 (2010).
301 Yonekura, H. *et al.* Novel splice variants of the receptor for advanced glycation end-products expressed in human vascular endothelial cells and pericytes, and their putative roles in diabetes-induced vascular injury. *Biochemical Journal* **370**, 1097-1109, doi:10.1042/bj20021371 (2003).
302 Oliveira, M. I. A. *et al.* RAGE receptor and its soluble isoforms in diabetes mellitus complications. *Jornal Brasileiro de Patologia e Medicina Laboratorial* **49**, 97-108 (2013).
303 Lee, E. J. & Park, J. H. Receptor for Advanced Glycation Endproducts (RAGE), Its Ligands, and Soluble RAGE: Potential Biomarkers for Diagnosis and Therapeutic Targets for Human Renal Diseases. *Genomics & Informatics* **11**, 224-229, doi:10.5808/GI.2013.11.4.224 (2013).
304 Younessi, P. & Yoonessi, A. Advanced Glycation End-Products and Their Receptor-Mediated Roles: Inflammation and Oxidative Stress. *Iran Journal of Medical Science* **36**, 154-166 (2011).
305 Huang, J.-S. *et al.* Role of receptor for advanced glycation end-product (RAGE) and the JAK/STAT-signaling pathway in AGE-induced collagen production in NRK-49F cells. *Journal of Cellular Biochemistry* **81**, 102–113, doi:DOI: 10.1002/1097-4644(20010401)81:1<102::AID-JCB1027>3.0.CO;2-Y (2001).
306 Bierhaus, A. *et al.* Diabetes-Associated Sustained Activation of the Transcription Factor Nuclear Factor-κB. *Diabetes* **50**, 2792-2808, doi:10.2337/diabetes.50.12.2792 (2001).
307 Schwenger, V. *et al.* Damage to the Peritoneal Membrane by Glucose Degradation Products Is Mediated by the Receptor for Advanced Glycation End-Products. *Journal of the American Society of Nephrology* **17**, 199 (2006).
308 Wendt, T. M. *et al.* RAGE Drives the Development of Glomerulosclerosis and Implicates Podocyte Activation in the Pathogenesis of Diabetic Nephropathy. *The American Journal of Pathology* **162**, 1123-1137 (2003).
309 Gu, L. *et al.* Role of receptor for advanced glycation end-products and signalling events in advanced glycation end-product-induced monocyte chemoattractant protein-1 expression in differentiated mouse podocytes. *Nephrology Dialysis Transplantation* **21**, 299-313, doi:10.1093/ndt/gfi210 (2006).
310 Schmidt, A. M., Yan, S. D., Yan, S. F. & Stern, D. M. The multiligand receptor RAGE as a progression factor amplifying immune and inflammatory responses. *Journal of Clinical Investigation* **108**, 949-955 (2001).
311 Shen, C. *et al.* RAGE-Specific Inhibitor FPS-ZM1 Attenuates AGEs-Induced Neuroinflammation and Oxidative Stress in Rat Primary Microglia. *Neurochemical Research* **42**, 2902-2911, doi:10.1007/s11064-017-2321-x (2017).
312 Yu, Y. *et al.* Advanced glycation end products receptor RAGE controls myocardial dysfunction and oxidative stress in high-fat fed mice by sustaining mitochondrial dynamics and autophagy-lysosome pathway. *Free Radical Biology and Medicine* **112**, 397-410, doi:https://doi.org/10.1016/j.freeradbiomed.2017.08.012 (2017).
313 Moser, B., Herold, K. C. & Schmidt, A. M. Receptor for Advanced Glycation End Products and Its Ligands: Initiators or Amplifiers of Joint Inflammation—a Bit of Both? *Arthritis & Rheumatism* **54**, 14-18 (2006).
314 Monnier, V. M. *et al.* Skin Collagen Glycation, Glycoxidation, and Crosslinking Are Lower in Subjects With Long-Term Intensive Versus Conventional Therapy of

Type 1 Diabetes: Relevance of Glycated Collagen Products Versus HbA(1c) as Markers of Diabetic Complications. *Diabetes* **48**, 870-880 (1999).

315 Rahbar, S. *et al.* Evidence that pioglitazone, metformin and pentoxifylline are inhibitors of glycation. *Clinica Chimica Acta* **301**, 65-77, doi:https://doi.org/10.1016/S0009-8981(00)00327-2 (2000).

316 Beisswenger, P. J., Howell, S. K., Touchette, A. D., Lal, S. & Szwergold, B. S. Metformin reduces systemic methylglyoxal levels in type 2 diabetes. *Diabetes* **48**, 198-202, doi:10.2337/diabetes.48.1.198 (1999).

317 Lin, R.-Y. *et al.* Lowering of dietary advanced glycation endproducts (AGE) reduces neointimal formation after arterial injury in genetically hypercholesterolemic mice. *Atherosclerosis* **163** 303/ 311 (2002).

318 Engelen, L., Stehouwer, C. D. A. & Schalkwijk, C. G. Current therapeutic interventions in the glycation pathway: evidence from clinical studies. *Diabetes, Obesity and Metabolism* **15**, 677–689 (2013).

319 Borg, D. J. & Forbes, J. M. Targeting advanced glycation with pharmaceutical agents: where are we now? *Glycoconjugate Journal* **33**, 653-670, doi:10.1007/s10719-016-9691-1 (2016).

320 Bhatwadekar, A. *et al.* A new advanced glycation inhibitor, LR-90, prevents experimental diabetic retinopathy in rats. *British Journal of Ophthalmology* **92**, 545-547, doi:10.1136/bjo.2007.127910 (2008).

321 Liao, W. *et al.* Intracellular Antioxidant Detoxifying Effects of Diosmetin on 2,2-Azobis(2-amidinopropane) Dihydrochloride (AAPH)-Induced Oxidative Stress through Inhibition of Reactive Oxygen Species Generation. *Journal of Agricultural and Food Chemistry* **62**, 8648-8654, doi:10.1021/jf502359x (2014).

322 Figarola, J. L., Shanmugam, N., Natarajan, R. & Rahbar, S. Anti-Inflammatory Effects of the Advanced Glycation End Product Inhibitor LR-90 in Human Monocytes. *Diabetes* **56**, 647–655 (2007).

323 Beisswenger, P. J. & Ruggiero-Lopez, D. Metformin inhibition of glycation processes. *Diabetes & amp; Metabolism* **29**, 6103, doi:Doi : DM-09-2003-29-4-1262-3636-101019-ART12 (2003).

324 Brown, B. E., Mahroof, F. M., Cook, N. L., van Reyk, D. M. & Davies, M. J. Hydrazine compounds inhibit glycation of low-density lipoproteins and prevent the in vitro formation of model foam cells from glycolaldehyde-modified low-density lipoproteins. *Diabetologia* **49**, 775-783, doi:10.1007/s00125-006-0137-3 (2006).

325 Rahbar, S. & Figarola, J. L. Novel inhibitors of advanced glycation endproducts. *Archives of Biochemistry and Biophysics* **419**, 63-79, doi:https://doi.org/10.1016/j.abb.2003.08.009 (2003).

326 Miyata, T., van Ypersele de Strihou, C., Kurokawa, K. & Baynes, J. W. Alterations in nonenzymatic biochemistry in uremia: Origin and significance of “carbonyl stress” in long-term uremic complications. *Kidney International* **55**, 389-399, doi:10.1046/j.1523-1755.1999.00302.x (1999).

327 Miyata, T., Kurokawa K & C., V. Y. D. S. Advanced Glycation and Lipoxidation End Products: Role of Reactive Carbonyl Compounds Generated during Carbohydrate and Lipid Metabolism. *Journal of the American Society of Nephrology* **11**, 1744 (2000).

328 Cooper, M. E. *et al.* The cross-link breaker, N-phenacylthiazolium bromide prevents vascular advanced glycation end-product accumulation. *Diabetologia* **43**, 660-664, doi:10.1007/s001250051355 (2000).

329 Nenna, A. *et al.* Pharmacologic approaches against Advanced Glycation End Products (AGEs) in diabetic cardiovascular disease. *Research in Cardiovascular Medicine* **4**, 5-5, doi:10.5812/cardiovascmed.4(2)2015.26949 (2015).
330 Koyama, H., Yamamoto, H. & Nishizawa, Y. RAGE and Soluble RAGE: Potential Therapeutic Targets for Cardiovascular Diseases. *Molecular Medicine* **13**, 625-635, doi:doi: 10.2119/2007-00087.Koyama (2007).
331 Monteiro, F. A., Cardoso, I., Sousa, M. M. & Saraiva, M. J. In vitro inhibition of transthyretin aggregate-induced cytotoxicity by full and peptide derived forms of the soluble receptor for advanced glycation end products (RAGE). *FEBS Letters* **580**, 3451-3456, doi:10.1016/j.febslet.2006.05.020 (2006).
332 Bucciarelli, L. G. *et al.* RAGE Blockade Stabilizes Established Atherosclerosis in Diabetic Apolipoprotein E–Null Mice. *Circulation* **106**, 2827-2835 (2002).
333 Sakaguchi, T. *et al.* Central role of RAGE-dependent neointimal expansion in arterial restenosis. *The Journal of Clinical Investigation* **111**, 959-972, doi:10.1172/JCI17115 (2003).
334 Taguchi, A. *et al.* Blockade of RAGE/amphoterin suppresses tumor growth and metastases. *Nature* **405**, 354-360 (2000).
335 Goova, M. T. *et al.* Blockade of Receptor for Advanced Glycation End-Products Restores Effective Wound Healing in Diabetic Mice. *The American Journal of Pathology* **159**, 513-525, doi:10.1016/S0002-9440(10)61723-3 (2001).
336 Wang, Q. *et al.* Blocking AGE-RAGE Signaling Improved Functional Disorders of Macrophages in Diabetic Wound. *Journal of Diabetes Research* **2017**, 1428537, doi:10.1155/2017/1428537 (2017).
337 Arancio, O. *et al.* RAGE potentiates Aβ-induced perturbation of neuronal function in transgenic mice. *The EMBO Journal* **23**, 4096-4105, doi:10.1038/sj.emboj.7600415 (2004).
338 Barile, G. R. *et al.* The RAGE Axis in Early Diabetic Retinopathy. *Investigative Ophthalmology & Visual Science* **46**, 2916-2924, doi:10.1167/iovs.04-1409 (2005).
339 Izushi, Y. *et al.* Soluble form of the receptor for advanced glycation end-products attenuates inflammatory pathogenesis in a rat model of lipopolysaccharide-induced lung injury. *Journal of Pharmacological Sciences* **130**, 226-234, doi:https://doi.org/10.1016/j.jphs.2016.02.005 (2016).
340 Shoji, T. *et al.* Receptor for Advanced Glycation End Products Is Involved in Impaired Angiogenic Response in Diabetes. *Diabetes* **55**, 2245–2255 (2006).
341 Forbes, J. M. *et al.* Modulation of Soluble Receptor for Advanced Glycation End Products by Angiotensin-Converting Enzyme-1 Inhibition in Diabetic Nephropathy. *Journal of the American Society of Nephrology* **16**, 2363 (2005).
342 Marx, N. *et al.* Thiazolidinediones Reduce Endothelial Expression of Receptors for Advanced Glycation End Products. *Diabetes* **53**, 2662-2668, doi:10.2337/diabetes.53.10.2662 (2004).
343 Cuccurullo, C. *et al.* Suppression of Rage as a Basis of Simvastatin-Dependent Plaque Stabilization in Type 2 Diabetes. *Arteriosclerosis, Thrombosis and Vascular Biology* **26-**, doi:DOI: 10.1161/01.ATV.0000249630.02085.12 (2006).
344 Browning, J. D. *et al.* Prevalence of hepatic steatosis in an urban population in the United States: impact of ethnicity. *Hepatology* **40**, 1387-1395 (2004).
345 Loomba, R. & Sanyal, A. J. The global NAFLD epidemic. *Nat Rev Gastroenterol Hepatol* **10**, 686-690 (2013).

346 Liliensiek, B. *et al.* Receptor for advanced glycation end products (RAGE) regulates sepsis but not the adaptive immune response. *Journal of Clinical Investigation* **113**, 1641-1650, doi:10.1172/JCI200418704 (2004).
347 Kim, Y. O., Stoll, M., Hebich, B., Wang, X. & Schuppan, D. Tu1815 Mice Fed a High-Fat High-Fructose Diet and Treated With Low Dose Streptozotocin Develop Insulin Resistance, NASH and Liver Fibrosis. *Gastroenterology* **142**, S-1024, doi:10.1016/S0016-5085(12)63961-4 (2012).
348 Lo, L. *et al.* Diabetes is a progression factor for hepatic fibrosis in a high fat fed mouse obesity model of non-alcoholic steatohepatitis. *Journal of Hepatology* **55**, 435-444, doi:10.1016/j.jhep.2010.10.039 (2011).
349 Kitani, H. *et al.* Establishment of c-myc-immortalized Kupffer cell line from a C57BL/6 mouse strain. *Results in immunology* **4**, 68-74, doi:10.1016/j.rinim.2014.08.001 (2014).
350 Van Rooyen, D. M. *et al.* Hepatic Free Cholesterol Accumulates in Obese, Diabetic Mice and Causes Nonalcoholic Steatohepatitis. *Gastroenterology* **141**, 1393-1403.e1395, doi:https://doi.org/10.1053/j.gastro.2011.06.040 (2011).
351 De Minicis, S., Bataller, R. & Brenner, D. A. NADPH Oxidase in the Liver: Defensive, Offensive, or Fibrogenic? *Gastroenterology* **131**, 272-275, doi:10.1053/j.gastro.2006.05.048 (2006).
352 Dooley, S., ten Dijke, P. J. C. & Research, T. TGF-β in progression of liver disease. **347**, 245-256, doi:10.1007/s00441-011-1246-y (2012).
353 Svistounov, D. *et al.* Hepatic disposal of advanced glycation end products during maturation and aging. *Experimental gerontology* **48**, 549-556, doi:10.1016/j.exger.2013.03.005 (2013).
354 Rapin, J. R. & Wiernsperger, N. Possible links between intestinal permeability and food processing: A potential therapeutic niche for glutamine. *Clinics (Sao Paulo, Brazil)* **65**, 635-643, doi:10.1590/S1807-59322010000600012 (2010).
355 Davis, K. E., Prasad, C., Vijayagopal, P., Juma, S. & Imrhan, V. Advanced Glycation End Products, Inflammation, and Chronic Metabolic Diseases: Links in a Chain? *Critical Reviews in Food Science and Nutrition* **56**, 989-998, doi:10.1080/10408398.2012.744738 (2016).
356 Byun, K. *et al.* Advanced glycation end-products produced systemically and by macrophages: A common contributor to inflammation and degenerative diseases. *Pharmacology & Therapeutics* **177**, 44-55, doi:https://doi.org/10.1016/j.pharmthera.2017.02.030 (2017).
357 Nowotny, K., Jung, T., Höhn, A., Weber, D. & Grune, T. Advanced glycation end products and oxidative stress in type 2 diabetes mellitus. *Biomolecules* **5**, 194-222, doi:10.3390/biom5010194 (2015).
358 Yoo, J. Y. *et al.* 16S rRNA gene-based metagenomic analysis reveals differences in bacteria-derived extracellular vesicles in the urine of pregnant and non-pregnant women. *Experimental &Amp; Molecular Medicine* **48**, e208, doi:10.1038/emm.2015.110

https://www.nature.com/articles/emm2015110#supplementary-information (2016).
359 Marrone, G., Shah, V. H. & Gracia-Sancho, J. Sinusoidal communication in liver fibrosis and regeneration. *Journal of hepatology* **65**, 608-617, doi:10.1016/j.jhep.2016.04.018 (2016).
360 Singh, R., Barden, A., Mori, T. & Beilin, L. Advanced glycation end-products: a review. *Diabetologia* **44**, 129-146, doi:10.1007/s001250051591 (2001).

361 Stinghen, A. E. M., Massy, Z. A., Vlassara, H., Striker, G. E. & Boullier, A. Uremic Toxicity of Advanced Glycation End Products in CKD. *Journal of the American Society of Nephrology* **27**, 354-370, doi:10.1681/asn.2014101047 (2016).
362 Bohlender, J. M., Franke, S., Stein, G. & Wolf, G. Advanced glycation end products and the kidney. *American Journal of Physiology-Renal Physiology* **289**, F645-F659, doi:10.1152/ajprenal.00398.2004 (2005).
363 Rhee, S. Y. & Kim, Y. S. The Role of Advanced Glycation End Products in Diabetic Vascular Complications. *Diabetes & metabolism journal* **42**, 188-195, doi:10.4093/dmj.2017.0105 (2018).
364 Zakaria, M. N., El-Bassossy, H. M. & Barakat, W. Targeting AGEs Signaling Ameliorates Central Nervous System Diabetic Complications in Rats. *Advances in pharmacological sciences* **2015**, 346259-346259, doi:10.1155/2015/346259 (2015).
365 Tolman, K. G., Fonseca, V., Dalpiaz, A. & Tan, M. H. Spectrum of Liver Disease in Type 2 Diabetes and Management of Patients With Diabetes and Liver Disease. *Diabetes Care* **30**, 734-743, doi:10.2337/dc06-1539 (2007).
366 Forouhi, N. G., Misra, A., Mohan, V., Taylor, R. & Yancy, W. Dietary and nutritional approaches for prevention and management of type 2 diabetes. *BMJ* **361**, k2234, doi:10.1136/bmj.k2234 (2018).
367 Ley, S. H., Hamdy, O., Mohan, V. & Hu, F. B. Prevention and management of type 2 diabetes: dietary components and nutritional strategies. *Lancet (London, England)* **383**, 1999-2007, doi:10.1016/S0140-6736(14)60613-9 (2014).
368 Bierhaus, A. *et al.* Understanding RAGE, the receptor for advanced glycation end products. *Journal of Molecular Medicine* **83**, 876-886, doi:10.1007/s00109-005-0688-7 (2005).
369 Iwamoto, K. *et al.* Advanced glycation end products enhance the proliferation and activation of hepatic stellate cells. *Journal of Gastroenterology* **43**, 298-304, doi:10.1007/s00535-007-2152-7 (2008).
370 Li, J., Liu, D., Sun, L., Lu, Y. & Zhang, Z. Advanced glycation end products and neurodegenerative diseases: Mechanisms and perspective. *Journal of the Neurological Sciences* **317**, 1-5, doi:10.1016/j.jns.2012.02.018 (2012).
371 Sasaki, N. *et al.* Advanced Glycation End Products in Alzheimer's Disease and Other Neurodegenerative Diseases. *The American Journal of Pathology* **153**, 1149-1155, doi:10.1016/S0002-9440(10)65659-3 (1998).
372 Hudson, B. I. & Lippman, M. E. Targeting RAGE Signaling in Inflammatory Disease. *Annual Review of Medicine* **69**, 349-364, doi:10.1146/annurev-med-041316-085215 (2018).
373 Yamagishi, S.-i. & Matsui, T. Role of receptor for advanced glycation end products (RAGE) in liver disease. *European journal of medical research* **20**, 15-15, doi:10.1186/s40001-015-0090-z (2015).
374 Brenner, T. *et al.* Reactive metabolites and AGE-RAGE-mediated inflammation in patients following liver transplantation. *Mediators of inflammation* **2013**, 501430-501430, doi:10.1155/2013/501430 (2013).
375 Cataldegirmen, G. *et al.* RAGE limits regeneration after massive liver injury by coordinated suppression of TNF-α and NF-κB. *The Journal of Experimental Medicine* **201**, 473-484, doi:10.1084/jem.20040934 (2005).
376 Zhao, J., Randive, R. & Stewart, J. A. Molecular mechanisms of AGE/RAGE-mediated fibrosis in the diabetic heart. *World journal of diabetes* **5**, 860-867, doi:10.4239/wjd.v5.i6.860 (2014).

377 Zeng, S. *et al.* Blockade of receptor for advanced glycation end product (RAGE) attenuates ischemia and reperfusion injury to the liver in mice. *Hepatology* **39**, 422-432, doi:doi:10.1002/hep.20045 (2004).
378 Poli, G., Biasi, F. & Leonarduzzi, G. 4-Hydroxynonenal–protein adducts: A reliable biomarker of lipid oxidation in liver diseases. *Molecular Aspects of Medicine* **29**, 67-71, doi:https://doi.org/10.1016/j.mam.2007.09.016 (2008).
379 Arumugam, T., Ramachandran, V., Gomez, S. B., Schmidt, A. M. & Logsdon, C. D. S100P-Derived RAGE Antagonistic Peptide Reduces Tumor Growth and Metastasis. **18**, 4356-4364, doi:10.1158/1078-0432.CCR-12-0221 %J Clinical Cancer Research (2012).
380 Deane, R. *et al.* A multimodal RAGE-specific inhibitor reduces amyloid β–mediated brain disorder in a mouse model of Alzheimer disease. *The Journal of Clinical Investigation* **122**, 1377-1392, doi:10.1172/JCI58642 (2012).
381 Polimeni, L. *et al.* Oxidative stress: New insights on the association of non-alcoholic fatty liver disease and atherosclerosis. *World journal of hepatology* **7**, 1325-1336, doi:10.4254/wjh.v7.i10.1325 (2015).
382 Zarkovic, N. 4-Hydroxynonenal as a bioactive marker of pathophysiological processes. *Molecular Aspects of Medicine* **24**, 281-291, doi:https://doi.org/10.1016/S0098-2997(03)00023-2 (2003).
383 Yan, S. F., Ramasamy, R. & Schmidt, A. M. Mechanisms of Disease: advanced glycation end-products and their receptor in inflammation and diabetes complications. *Nature Clinical Practice Endocrinology &Amp; Metabolism* **4**, 285, doi:10.1038/ncpendmet0786 (2008).
384 Huang, J.-S. *et al.* Role of receptor for advanced glycation end-product (RAGE) and the JAK/STAT-signaling pathway in AGE-induced collagen production in NRK-49F cells. *Journal of Cellular Biochemistry* **81**, 102-113, doi:doi:10.1002/1097-4644(20010401)81:1<102::AID-JCB1027>3.0.CO;2-Y (2001).
385 Julio, C. T.-V., Elvis, C. & Mónica, A. T.-R. Receptor for AGEs (RAGE) as Mediator of NF-kB Pathway Activation in Neuroinflammation and Oxidative Stress. *CNS & Neurological Disorders - Drug Targets* **13**, 1615-1626, doi:http://dx.doi.org/10.2174/1871527313666140806144831 (2014).
386 Song, F. *et al.* RAGE Regulates the Metabolic and Inflammatory Response to High-Fat Feeding in Mice. **63**, 1948-1965, doi:10.2337/db13-1636 %J Diabetes (2014).
387 Hiroyuki, U. & Sho-ichi, Y. Advanced Glycation End Products and Insulin Resistance. *Current Pharmaceutical Design* **14**, 987-989, doi:http://dx.doi.org/10.2174/138161208784139747 (2008).
388 Mohamed, J., Nazratun Nafizah, A. H., Zariyantey, A. H. & Budin, S. B. Mechanisms of Diabetes-Induced Liver Damage: The role of oxidative stress and inflammation. *Sultan Qaboos University medical journal* **16**, e132-e141, doi:10.18295/squmj.2016.16.02.002 (2016).
389 Loria, P., Lonardo, A. & Anania, F. Liver and diabetes. A vicious circle. *Hepatology research : the official journal of the Japan Society of Hepatology* **43**, 51-64, doi:10.1111/j.1872-034X.2012.01031.x (2013).
390 Brownlee, M., Vlassara, H., Kooney, A., Ulrich, P. & Cerami, A. Aminoguanidine prevents diabetes-induced arterial wall protein cross-linking. *Science* **232**, 1629-1632, doi:10.1126/science.3487117 (1986).

391 Youssef, S. *et al.* Effect of diabetes and aminoguanidine therapy on renal advanced glycation end-product binding. *Kidney International* **55**, 907-916, doi:https://doi.org/10.1046/j.1523-1755.1999.055003907.x (1999).
392 Kelly, D. J. *et al.* 2098 (WILLIAMS & WILKINS, United States, 2001).
393 Li, Q. *et al.* Effects of aminoguanidine and vitamin C on collagen type IV in diabetic nephropathy rats. *Endocrine*, 251 (2011).
394 Vadla, G. P. A. & Vellaichamy, E. Beneficial effects of aminoguanidine against streptozotocin-induced pathological changes in diabetic mice kidney. *Biomedicine & Preventive Nutrition* **3**, 221 (2013).
395 Wada, J. Advanced glycation end products-cytokine-nitric oxide sequence pathway in the development of diabetic nephropathy: aminoguanidine ameliorates the overexpression of tumour necrosis factor-alpha and inducible nitric oxide synthase in diabetic rat glomeruli. *DIABETOLOGIA* **42**, 878-886 (1999).
396 Stadler, K., Jenei, V., Somogyi, A. & Jakus, J. Beneficial effects of aminoguanidine on the cardiovascular system of diabetic rats. *Diabetes/Metabolism Research and Reviews* **21**, 189-196, doi:10.1002/dmrr.501 (2005).
397 Nenna, A. *et al.* Pharmacologic Approaches Against Advanced Glycation End Products (AGEs) in Diabetic Cardiovascular Disease. *Research in Cardiovascular Medicine* **4**, e26949, doi:10.5812/cardiovascmed.4(2)2015.26949 (2015).
398 Yong Ming, L. *et al.* Prevention of Cardiovascular and Renal Pathology of Aging by the Advanced Glycation Inhibitor Aminoguanidine. *Proceedings of the National Academy of Sciences of the United States of America*, 3902 (1996).
399 Mishra, A. & Newman, E. A. Aminoguanidine Reverses the Loss of Functional Hyperemia in a Rat Model of Diabetic Retinopathy. *Frontiers in Neuroenergetics* **3**, 10, doi:10.3389/fnene.2011.00010 (2011).
400 Luo, D., Fan, Y. & Xu, X. The effects of aminoguanidine on retinopathy in STZ-induced diabetic rats. *Bioorganic & Medicinal Chemistry Letters* **22**, 4386-4390, doi:https://doi.org/10.1016/j.bmcl.2012.04.130 (2012).
401 Roufail, E., Soulis, T., Boel, E., Cooper, M. E. & Rees, S. Depletion of nitric oxide synthase-containing neurons in the diabetic retina: reversal by aminoguanidine. *Diabetologia* **41**, 1419-1425, doi:10.1007/s001250051087 (1998).
402 Tian, M. *et al.* Aminoguanidine cream ameliorates skin tissue microenvironment in diabetic rats. *Archives of Medical Science : AMS* **12**, 179-187, doi:10.5114/aoms.2016.57595 (2016).
403 Carvalho, V. F. *et al.* Inhibition of advanced glycation end products by aminoguanidine restores mast cell numbers and reactivity in alloxan-diabetic rats. *European Journal of Pharmacology* **669**, 143-148, doi:https://doi.org/10.1016/j.ejphar.2011.08.004 (2011).
404 Usta, M. F. *et al.* The Protective Effect of Aminoguanidine on Erectile Function in Streptozotocin Diabetic Rats. *The Journal of Urology* **170**, 1437-1442, doi:10.1097/01.ju.0000077557.45582.f3 (2003).
405 Orman, D., Vardi, N., Ates, B., Taslidere, E. & Elbe, H. Aminoguanidine mitigates apoptosis, testicular seminiferous tubules damage, and oxidative stress in streptozotocin-induced diabetic rats. *Tissue and Cell* **47**, 284-290, doi:https://doi.org/10.1016/j.tice.2015.03.006 (2015).
406 Majd, A. A., Goodarzi, M. T., Hassanzadeh, T., Tavilani, H. & Karimi, J. Aminoguanidine partially prevents the reduction in liver pyruvate kinase activity in diabetic rats. *Advanced Biomedical Research* **3**, 260, doi:10.4103/2277-9175.148233 (2014).

407 Edeas, M., Attaf, D., Mailfert, A. S., Nasu, M. & Joubet, R. Maillard Reaction, mitochondria and oxidative stress: Potential role of antioxidants. *Pathologie Biologie* **58**, 220-225, doi:https://doi.org/10.1016/j.patbio.2009.09.011 (2010).
408 Metz, T. O., Alderson, N. L., Thorpe, S. R. & Baynes, J. W. Pyridoxamine, an inhibitor of advanced glycation and lipoxidation reactions: a novel therapy for treatment of diabetic complications. *Archives of Biochemistry and Biophysics* **419**, 41-49, doi:https://doi.org/10.1016/j.abb.2003.08.021 (2003).
409 Tanimoto, M. *et al.* Effect of pyridoxamine (K-163), an inhibitor of advanced glycation end products, on type 2 diabetic nephropathy in KK-A^y/Ta mice. *Metabolism - Clinical and Experimental* **56**, 160-167, doi:10.1016/j.metabol.2006.08.026 (2007).
410 Murakoshi, M. *et al.* Pleiotropic effect of pyridoxamine on diabetic complications via CD36 expression in KK-A^y/Ta mice. *Diabetes Research and Clinical Practice* **83**, 183-189, doi:10.1016/j.diabres.2008.11.008 (2009).
411 Elseweidy, M. M., Elswefy, S. E., Younis, N. N. & Zaghloul, M. S. Pyridoxamine, an inhibitor of protein glycation, in relation to microalbuminuria and proinflammatory cytokines in experimental diabetic nephropathy. *Experimental Biology and Medicine* **238**, 881-888, doi:10.1177/1535370213494644 (2013).
412 Abouzed, T. K. *et al.* Preventive Effect of Salicylate and Pyridoxamine on Diabetic Nephropathy. *Journal of Diabetes Research* **2016**, 1786789, doi:10.1155/2016/1786789 (2016).
413 Degenhardt, T. P. *et al.* Pyridoxamine inhibits early renal disease and dyslipidemia in the streptozotocin-diabetic rat. *Kidney International* **61**, 939-950, doi:10.1046/j.1523-1755.2002.00207.x.
414 Ren, X. *et al.* Protective function of pyridoxamine on retinal photoreceptor cells via activation of the p-Erk1/2/Nrf2/Trx/ASK1 signalling pathway in diabetic mice. *Molecular Medicine Reports*, 420, doi:10.3892/mmr.2016.5270 (2016).
415 Padival, S. & Nagaraj, R. H. Pyridoxamine Inhibits Maillard Reactions in Diabetic Rat Lenses. *Ophthalmic Research* **38**, 294-302 (2006).
416 Hiroyuki, U.-K., Sho-ichi, Y., Masayoshi, T., Hideaki, B. & Yasushi, S. Pyridoxamine, an Inhibitor of Advanced Glycation End Product (AGE) Formation Ameliorates Insulin Resistance in Obese, Type 2 Diabetic Mice. *Protein & Peptide Letters* **17**, 1177-1181, doi:http://dx.doi.org/10.2174/092986610791760423 (2010).
417 Pereira-Simon, S. *et al.* Inhibition of Advanced Glycation End Products (AGEs) Accumulation by Pyridoxamine Modulates Glomerular and Mesangial Cell Estrogen Receptor α Expression in Aged Female Mice. *PLoS ONE* **11**, 1-14, doi:10.1371/journal.pone.0159666 (2016).
418 Chang, K.-C. *et al.* Prevention of arterial stiffening by pyridoxamine in diabetes is associated with inhibition of the pathogenic glycation on aortic collagen. *BRITISH JOURNAL OF PHARMACOLOGY* **157**, 1419-1426 (2009).
419 Santos Silva, D. *et al.* Pyridoxamine Reverts Methylglyoxal-induced Impairment of Survival Pathways During Heart Ischemia. *CARDIOVASCULAR THERAPEUTICS* **31**, E79-E85 (2013).
420 Syngle, A., Vohra, K., Garg, N., Kaur, L. & Chand, P. Advanced glycation end-products inhibition improves endothelial dysfunction in rheumatoid arthritis. *International Journal of Rheumatic Diseases* **15**, 45-55, doi:10.1111/j.1756-185X.2011.01679.x (2012).

421 e Nico, E. T. M. *et al.* The action of aminoguanidine on the liver of trained diabetic rats. *Journal of Diabetes & Metabolic Disorders* **12**, 9 (2013).
422 Schuppe-Koistinen, I., Frisk, A.-L. & Janzon, L. Molecular profiling of hepatotoxicity induced by a aminoguanidine carboxylate in the rat: gene expression profiling. *Toxicology* **179**, 197-219, doi:https://doi.org/10.1016/S0300-483X(02)00355-4 (2002).
423 Roman, B., Carta, L., Martínez-González, M. A. & Serra-Majem, L. Effectiveness of the Mediterranean diet in the elderly. *Clinical interventions in aging* **3**, 97-109 (2008).
424 Romagnolo, D. F. & Selmin, O. I. Mediterranean Diet and Prevention of Chronic Diseases. *Nutrition today* **52**, 208-222, doi:10.1097/NT.0000000000000228 (2017).
425 Castro-Quezada, I., Román-Viñas, B. & Serra-Majem, L. The Mediterranean diet and nutritional adequacy: a review. *Nutrients* **6**, 231-248, doi:10.3390/nu6010231 (2014).
426 Billingsley, H. E. & Carbone, S. The antioxidant potential of the Mediterranean diet in patients at high cardiovascular risk: an in-depth review of the PREDIMED. *Nutrition & Diabetes* **8**, 13, doi:10.1038/s41387-018-0025-1 (2018).
427 George, E. S. *et al.* A Mediterranean Diet Model in Australia: Strategies for Translating the Traditional Mediterranean Diet into a Multicultural Setting. *Nutrients* **10**, 465, doi:10.3390/nu10040465 (2018).
428 Borg, D. J. & Forbes, J. M. J. G. J. Targeting advanced glycation with pharmaceutical agents: where are we now? **33**, 653-670, doi:10.1007/s10719-016-9691-1 (2016).
429 Nagai, R., Murray, D. B., Metz, T. O. & Baynes, J. W. Chelation: a fundamental mechanism of action of AGE inhibitors, AGE breakers, and other inhibitors of diabetes complications. *Diabetes* **61**, 549-559, doi:10.2337/db11-1120 (2012).
430 Nenna, A. *et al.* Pharmacologic Approaches Against Advanced Glycation End Products (AGEs) in Diabetic Cardiovascular Disease. *Research in cardiovascular medicine* **4**, e26949-e26949, doi:10.5812/cardiovascmed.4(2)2015.26949 (2015).
431 Cardoso, S. *et al.* Effects of methylglyoxal and pyridoxamine in rat brain mitochondria bioenergetics and oxidative status. *Journal of Bioenergetics and Biomembranes* **46**, 347-355, doi:10.1007/s10863-014-9551-2 (2014).
432 Su, G. L. *et al.* Activation of human and mouse Kupffer cells by lipopolysaccharide is mediated by CD14. *American Journal of Physiology-Gastrointestinal and Liver Physiology* **283**, G640-G645, doi:10.1152/ajpgi.00253.2001 (2002).
433 Maessen, D. E. *et al.* Delayed Intervention With Pyridoxamine Improves Metabolic Function and Prevents Adipose Tissue Inflammation and Insulin Resistance in High-Fat Diet–Induced Obese Mice. *Diabetes* **65**, 956-966, doi:10.2337/db15-1390 (2016).
434 Hammes, H. P., Martin, S., Federlin, K., Geisen, K. & Brownlee, M. Aminoguanidine treatment inhibits the development of experimental diabetic retinopathy. **88**, 11555-11558, doi:10.1073/pnas.88.24.11555 %J Proceedings of the National Academy of Sciences (1991).
435 Soulis, T., Cooper, M. E., Vranes, D., Bucala, R. & Jerums, G. Effects of aminoguanidine in preventing experimental diabetic nephropathy are related to the duration of treatment. *Kidney International* **50**, 627-634, doi:https://doi.org/10.1038/ki.1996.358 (1996).

436 KELLY, D. J. *et al.* Aminoguanidine Ameliorates Overexpression of Prosclerotic Growth Factors and Collagen Deposition in Experimental Diabetic Nephropathy. **12**, 2098-2107 (2001).
437 Lewis, E. J. *et al.* Pyridorin in type 2 diabetic nephropathy. *Journal of the American Society of Nephrology : JASN* **23**, 131-136, doi:10.1681/ASN.2011030272 (2012).
438 e Nico, E. T. M. *et al.* The action of aminoguanidine on the liver of trained diabetic rats. **12**, 40, doi:10.1186/2251-6581-12-40 (2013).
439 Boel, E., Selmer, J., Flodgaard, H. J. & Jensen, T. Diabetic late complications: Will aldose reductase inhibitors or inhibitors of advanced glycosylation endproduct formation hold promise? *Journal of Diabetes and its Complications* **9**, 104-129, doi:https://doi.org/10.1016/1056-8727(94)00025-J (1995).
440 Bolton, W. K. *et al.* Randomized Trial of an Inhibitor of Formation of Advanced Glycation End Products in Diabetic Nephropathy. *American Journal of Nephrology* **24**, 32-40, doi:10.1159/000075627 (2004).
441 Freedman, B. I. *et al.* Design and Baseline Characteristics for the Aminoguanidine Clinical Trial in Overt Type 2 Diabetic Nephropathy (ACTION II). *Controlled Clinical Trials* **20**, 493-510, doi:https://doi.org/10.1016/S0197-2456(99)00024-0 (1999).
442 Nascimento, M. M. *et al.* Effect of High-Dose Thiamine and Pyridoxine on Advanced Glycation End Products and Other Oxidative Stress Markers in Hemodialysis Patients: A Randomized Placebo-Controlled Study. *Journal of Renal Nutrition* **16**, 119-124, doi:10.1053/j.jrn.2006.01.002 (2006).
443 Goldberg, T. *et al.* Advanced glycoxidation end products in commonly consumed foods. *Journal of the American Dietetic Association* **104**, 1287-1291, doi:10.1016/j.jada.2004.05.214 (2004).
444 Luers, L., Rysiewski, K., Dumpitak, C. & Birkmann, E. Kinetics of Advanced Glycation End Products Formation on Bovine Serum Albumin with Various Reducing Sugars and Dicarbonyl Compounds in Equimolar Ratios. **15**, 201-205, doi:10.1089/rej.2011.1284 (2012).
445 Piya, M., Harte, A. & McTernan, P. Metabolic endotoxaemia: is it more than just a gut feeling? . *Current Opinion in Lipidology* **24**, 78-85, doi:10.1097/MOL.0b013e32835b4431 (2013).
446 Garcia-Mantrana, I., Selma-Royo, M., Alcantara, C. & Collado, M. C. Shifts on Gut Microbiota Associated to Mediterranean Diet Adherence and Specific Dietary Intakes on General Adult Population. *Frontiers in microbiology* **9**, 890-890, doi:10.3389/fmicb.2018.00890 (2018).
447 Baratta, F. *et al.* Adherence to Mediterranean Diet and Non-Alcoholic Fatty Liver Disease: Effect on Insulin Resistance. *American Journal of Gastroenterology* **112**, 1832-1839, doi:10.1038/ajg.2017.371 (2017).
448 Ryan, M. C. *et al.* The Mediterranean diet improves hepatic steatosis and insulin sensitivity in individuals with non-alcoholic fatty liver disease. *Journal of Hepatology* **59**, 138-143, doi:10.1016/j.jhep.2013.02.012 (2013).
449 Fraser, A., Abel, R., Lawlor, D. A., Fraser, D. & Elhayany, A. A modified Mediterranean diet is associated with the greatest reduction in alanine aminotransferase levels in obese type 2 diabetes patients: results of a quasi-randomised controlled trial. *Diabetologia* **51**, 1616-1622, doi:10.1007/s00125-008-1049-1 (2008).

450 Tzima, N. *et al.* Adherence to the Mediterranean diet moderates the association of aminotransferases with the prevalence of the metabolic syndrome; the ATTICA study. *Nutrition & metabolism* **6**, 30-30, doi:10.1186/1743-7075-6-30 (2009).
451 Seth, H., Prajitha, T., Tito, V. & C., A. E. Cleavage of in vitro and in vivo formed lens protein cross-links by a novel cross-link breaker. *Molecular and Cellular Biochemistry* **243**, 73-80, doi:https://doi.org/10.1023/A:1021660105893 (2003).
452 Mentink, C. J. A. L., Hendriks, M., Levels, A. A. G. & Wolffenbuttel, B. H. R. Glucose-mediated cross-linking of collagen in rat tendon and skin. *Clinica Chimica Acta* **321**, 69-76, doi:https://doi.org/10.1016/S0009-8981(02)00097-9 (2002).
453 Yamagishi, S.-i. *et al.* Inhibitors of Advanced Glycation End Products (AGEs): Potential Utility for the Treatment of Cardiovascular Disease. *Cardiovascular Drug Reviews* **26**, 50-58, doi:10.1111/j.1527-3466.2007.00038.x (2008).
454 Candido, R. *et al.* A Breaker of Advanced Glycation End Products Attenuates Diabetes-Induced Myocardial Structural Changes. *Circulation Research* **92**, 785-792, doi:10.1161/01.res.0000065620.39919.20 (2003).
455 Kass, D. A. *et al.* Improved Arterial Compliance by a Novel Advanced Glycation End-Product Crosslink Breaker. *Circulation* **104**, 1464-1470, doi:10.1161/hc3801.097806 (2001).
456 Carrick-Ranson, G. *et al.* The effect of 1 year of Alagebrium and moderate-intensity exercise training on left ventricular function during exercise in seniors: a randomized controlled trial. *Journal of Applied Physiology* **121**, 528-536 (2016).
457 Fischer, T. AGE-RELATED MACULAR DEGENERATION IS A VASCULAR DISEASE, PART OF VASCULOPATHY: HOLISTIC APPROACH OF THE AMD'S PATHOPHYSIOLOGY, PREVENTION AND PREVENTIVE TREATMENT. *Journal of Pharmaceutical & Scientific Innovation* **1**, 15 (2012).
458 Fujimoto, N. *et al.* Pericardial/Myocardial Disease/Pulmonary Hypertension: CARDIOVASCULAR EFFECTS OF ONE YEAR OF ALAGEBRIUM AND ENDURANCE EXERCISE TRAINING IN HEALTHY OLDER INDIVIDUALS. *Journal of the American College of Cardiology* **61**, E1257, doi:10.1016/S0735-1097(13)61257-7 (2013).
459 Laurent, S. & Boutouyrie, P. Arterial Stiffness and Stroke in Hypertension: Therapeutic Implications for Stroke Prevention. *CNS Drugs* **19**, 1-11 (2005).
460 Coughlan, M. T., Forbes, J. M. & Cooper, M. E. Role of the AGE crosslink breaker, alagebrium, as a renoprotective agent in diabetes. *Kidney International* **72**, S54-S60, doi:https://doi.org/10.1038/sj.ki.5002387 (2007).
461 Nawaz, M. I. *et al.* Novel drugs and their targets in the potential treatment of diabetic retinopathy. *Medical science monitor : international medical journal of experimental and clinical research* **19**, 300-308, doi:10.12659/MSM.883895 (2013).
462 Wang, L. *et al.* AGE-Breaker ALT-711 Plus Insulin Could Restore Erectile Function in Streptozocin-Induced Type 1 Diabetic Rats. *The Journal of Sexual Medicine* **11**, 1452-1462, doi:https://doi.org/10.1111/jsm.12533 (2014).
463 DA, K. *et al.* Improved arterial compliance by a novel advanced glycation end-product crosslink breaker. *Circulation* **104**, 464-470 (2001).
464 A., M. C. *et al.* Nonalcoholic fatty liver disease: A spectrum of clinical and pathological severity. *Gastroenterology* **116**, 1413-1419, doi:10.1016/S0016-5085(99)70506-8 (1999).

465 Yamagishi, S.-i. Potential Clinical Utility of Advanced Glycation End Product Cross-Link Breakers in Age- and Diabetes-Associated Disorders. *Rejuvenation Research* **15**, 564-572, doi:10.1089/rej.2012.1335 (2012).

466 Sourris, K. C., Forbes, J. M. & Cooper, M. E. Therapeutic Interruption of Advanced Glycation in Diabetic Nephropathy. *Annals of the New York Academy of Sciences* **1126**, 101-106, doi:doi:10.1196/annals.1433.048 (2008).

467 Park, J. *et al.* Renoprotective antioxidant effect of alagebrium in experimental diabetes. *Nephrology Dialysis Transplantation* **26**, 3474-3484, doi:10.1093/ndt/gfr152 (2011).

468 Friedman, S. L. Molecular Regulation of Hepatic Fibrosis, an Integrated Cellular Response to Tissue Injury. **275**, 2247-2250, doi:10.1074/jbc.275.4.2247 (2000).

469 Wang, H., Liu, J. & Wu, L. Methylglyoxal-induced mitochondrial dysfunction in vascular smooth muscle cells. *Biochemical Pharmacology* **77**, 1709-1716, doi:https://doi.org/10.1016/j.bcp.2009.02.024 (2009).

470 Ward, M. S., Fotheringham, A. K., Cooper, M. E. & Forbes, J. M. Targeting advanced glycation endproducts and mitochondrial dysfunction in cardiovascular disease. *Current Opinion in Pharmacology* **13**, 654-661, doi:https://doi.org/10.1016/j.coph.2013.06.009 (2013).

471 Seo, K., Ki, S. H. & Shin, S. M. Methylglyoxal induces mitochondrial dysfunction and cell death in liver. *Toxicological research* **30**, 193-198, doi:10.5487/TR.2014.30.3.193 (2014).

472 Coughlan, M. T. *et al.* Advanced glycation end products are direct modulators of β-cell function. *Diabetes* **60**, 2523-2532, doi:10.2337/db10-1033 (2011).

473 Thomas, M. C., Baynes, J. W., Thorpe, S. R. & Cooper, M. E. The Role of AGEs and AGE Inhibitors in Diabetic Cardiovascular Disease. *Current Drug Targets* **6**, doi:https://doi.org/10.2174/1389450054021873 (2005).

474 FORBES, J. M. *et al.* The breakdown of preexisting advanced glycation end products is associated with reduced renal fibrosis in experimental diabetes. *The FASEB Journal* **17**, 1762-1764, doi:10.1096/fj.02-1102fje (2003).

475 Chuah, Y. K., Basir, R., Talib, H., Tie, T. H. & Nordin, N. Receptor for Advanced Glycation End Products and Its Involvement in Inflammatory Diseases. *International Journal of Inflammation* **2013**, doi:https://doi.org/10.1155/2013/403460 (2013).

476 Lu, C. *et al.* Advanced glycation endproduct (AGE) receptor 1 is a negative regulator of the inflammatory response to AGE in mesangial cells. **101**, 11767-11772, doi:10.1073/pnas.0401588101 %J Proceedings of the National Academy of Sciences of the United States of America (2004).

477 Smedsrød, B., Melkko, J., Araki, N., Sano, H. & Horiuchi, S. Advanced glycation end products are eliminated by scavenger-receptor-mediated endocytosis in hepatic sinusoidal Kupffer and endothelial cells. *The Biochemical journal* **322 (Pt 2)**, 567-573 (1997).

478 Lawrence, M. G. *et al.* Permeation of macromolecules into the renal glomerular basement membrane and capture by the tubules. **114**, 2958-2963, doi:10.1073/pnas.1616457114 %J Proceedings of the National Academy of Sciences (2017).

479 Hultscha, C. *et al.* Biodistribution and catabolism of 18F-labeled N-q-fructoselysine as a model of Amadori products. *Nuclear Medicine and Biology* **33**, 865–873 (2006).

480 Korb, M. L. *et al.* Use of monoclonal antibody-IRDye800CW bioconjugates in the resection of breast cancer. *The Journal of surgical research* **188**, 119-128, doi:10.1016/j.jss.2013.11.1089 (2014).
481 Kovar, J. L., Curtis, E., Othman, S. F., Simpson, M. A. & Michael Olive, D. Characterization of IRDye 800CW chlorotoxin as a targeting agent for brain tumors. *Analytical Biochemistry* **440**, 212-219, doi:https://doi.org/10.1016/j.ab.2013.05.013 (2013).
482 Chalasani, N. *et al.* The diagnosis and management of nonalcoholic fatty liver disease: Practice guidance from the American Association for the Study of Liver Diseases. **67**, 328-357, doi:10.1002/hep.29367 (2018).
483 Uribarri, J. *et al.* Advanced glycation end products in foods and a practical guide to their reduction in the diet. *Journal of the American Dietetic Association* **110**, 911-916.e912, doi:10.1016/j.jada.2010.03.018 (2010).
484 Basta, G., De Caterina, R. & Schmidt, A. M. Advanced glycation end products and vascular inflammation: implications for accelerated atherosclerosis in diabetes. *Cardiovascular Research* **63**, 582-592, doi:10.1016/j.cardiores.2004.05.001 (2004).
485 Yan, S. D. *et al.* Enhanced cellular oxidant stress by the interaction of advanced glycation end products with their receptors/binding proteins. **269**, 9889-9897 (1994).
486 Vitek, M. P. *et al.* Advanced glycation end products contribute to amyloidosis in Alzheimer disease. *Proceedings of the National Academy of Sciences* **91**, 4766-4770, doi:10.1073/pnas.91.11.4766 (1994).
487 de Groot, L. *et al.* Advanced glycation endproducts are increased in rheumatoid arthritis patients with controlled disease. *Arthritis research & therapy* **13**, R205-R205, doi:10.1186/ar3538 (2011).
488 Tilg, H., Moschen, A. R. & Roden, M. NAFLD and diabetes mellitus. *Nature Reviews Gastroenterology &Amp; Hepatology* **14**, 32, doi:10.1038/nrgastro.2016.147 (2016).
489 Hazlehurst, J. M., Woods, C., Marjot, T., Cobbold, J. F. & Tomlinson, J. W. Non-alcoholic fatty liver disease and diabetes. *Metabolism: clinical and experimental* **65**, 1096-1108, doi:10.1016/j.metabol.2016.01.001 (2016).
490 Santos, J. C. d. F., Valentim, I. B., de Araújo, O. R. P., Ataide, T. d. R. & Goulart, M. O. F. Development of nonalcoholic hepatopathy: contributions of oxidative stress and advanced glycation end products. *International journal of molecular sciences* **14**, 19846-19866, doi:10.3390/ijms141019846 (2013).
491 Guimarães, E. L. M., Empsen, C., Geerts, A. & van Grunsven, L. A. Advanced glycation end products induce production of reactive oxygen species via the activation of NADPH oxidase in murine hepatic stellate cells. *Journal of Hepatology* **52**, 389-397, doi:https://doi.org/10.1016/j.jhep.2009.12.007 (2010).
492 Qu, W. *et al.* Dietary advanced glycation end products modify gut microbial composition and partially increase colon permeability in rats. **61**, 1700118, doi:10.1002/mnfr.201700118 (2017).
493 Seki, E. & Schnabl, B. Role of innate immunity and the microbiota in liver fibrosis: crosstalk between the liver and gut. *The Journal of physiology* **590**, 447-458, doi:10.1113/jphysiol.2011.219691 (2012).
494 Kellow, N. J. & Coughlan, M. T. Effect of diet-derived advanced glycation end products on inflammation. *Nutrition Reviews* **73**, 737-759, doi:10.1093/nutrit/nuv030 (2015).

495 Kolios, G., Valatas, V. & Kouroumalis, E. Role of Kupffer cells in the pathogenesis of liver disease. *World journal of gastroenterology* **12**, 7413-7420, doi:10.3748/wjg.v12.i46.7413 (2006).

496 Song, F. *et al.* RAGE Regulates the Metabolic and Inflammatory Response to High-Fat Feeding in Mice. *Diabetes* **63**, 1948-1965, doi:10.2337/db13-1636 (2014).

497 Sullivan, C. M. *et al.* RAGE polymorphisms and the heritability of insulin resistance: the Leeds Family Study. *Diabetes and Vascular Disease Research* **2**, 42-44, doi:10.3132/dvdr.2005.005 (2005).

498 Leuner, B. *et al.* RAGE influences obesity in mice. **45**, 102-108, doi:10.1007/s00391-011-0279-x (2012).

499 Gotsis, E. *et al.* Health Benefits of the Mediterranean Diet:An Update of Research Over the Last 5 Years. *Angiology* **66**, 304-318, doi:10.1177/0003319714532169 (2015).

500 Chen, G., Madl, R. L. & Smith, J. S. Inhibition of advanced glycation endproducts in cooked beef patties by cereal bran addition. *Food Control* **73**, 847-853, doi:https://doi.org/10.1016/j.foodcont.2016.09.037 (2017).

501 Soldatos, G. *et al.* Diet low in advanced glycation end products increases insulin sensitivity in healthy overweight individuals: a double-blind, randomized, crossover trial. *The American Journal of Clinical Nutrition* **103**, 1426-1433, doi:10.3945/ajcn.115.125427 (2016).

502 Bowman, M. A. *et al.* Pharmacokinetics of aminoguanidine administration and effects on the diabetes frequency in nonobese diabetic mice. *Journal of Pharmacology and Experimental Therapeutics* **279**, 790-794 (1996).

503 Onorato, J. M., Jenkins, A. J., Thorpe, S. R. & Baynes, J. W. Pyridoxamine, an Inhibitor of Advanced Glycation Reactions, Also Inhibits Advanced Lipoxidation Reactions: MECHANISM OF ACTION OF PYRIDOXAMINE. **275**, 21177-21184, doi:10.1074/jbc.M003263200 (2000).

504 Degenhardt, T. P. *et al.* Pyridoxamine inhibits early renal disease and dyslipidemia in the streptozotocin-diabetic rat. *Kidney International* **61**, 939-950, doi:https://doi.org/10.1046/j.1523-1755.2002.00207.x (2002).

505 Stitt, A. *et al. The AGE Inhibitor Pyridoxamine Inhibits Development of Retinopathy in Experimental Diabetes*. Vol. 51 (2002).

506 Wilkinson-Berka, J. L. *et al.* ALT-946 and Aminoguanidine, Inhibitors of Advanced Glycation, Improve Severe Nephropathy in the Diabetic Transgenic (mREN-2)27 Rat. **51**, 3283-3289 (2002).

507 Ericson, K. L., Coburn, S. P., Gallant, M. A., Reinwald, S. & Burr, D. B. Metabolic studies of pyridoxamine (Vitamin B6) metabolism in rats. **25**, 608.603-608.603, doi:10.1096/fasebj.25.1_supplement.608.3 (2011).

508 Watson, A. M. D. *et al.* Delayed intervention with AGE inhibitors attenuates the progression of diabetes-accelerated atherosclerosis in diabetic apolipoprotein E knockout mice. **54**, 681-689, doi:10.1007/s00125-010-2000-9 (2011).

509 Frohlich, E. D., Varagic, J. & Susic, D. Cardiovascular and renal effects of a collagen cross-link breaker (ALT 711) in adult and aged spontaneously hypertensive rats*. *American Journal of Hypertension* **17**, 328-333, doi:10.1016/j.amjhyper.2003.12.015 %J American Journal of Hypertension (2004).

510 Lassila, M. *et al.* Accelerated Nephropathy in Diabetic Apolipoprotein E-Knockout Mouse: Role of Advanced Glycation End Products. **15**, 2125-2138, doi:10.1097/01.ASN.0000133025.23732.46 %J Journal of the American Society of Nephrology (2004).

511 Zhang, B. *et al.* Alagebrium (ALT-711) improves the anti-hypertensive efficacy of nifedipine in diabetic-hypertensive rats. *Hypertension Research* **37**, 901, doi:10.1038/hr.2014.98 (2014).
512 Bakris, G. L. *et al.* Advanced glycation end-product cross-link breakers: A novel approach to cardiovascular pathologies related to the aging process. *American Journal of Hypertension* **17**, 23S-30S, doi:10.1016/j.amjhyper.2004.08.022 %J American Journal of Hypertension (2004).
513 Little, W. C. *et al.* The Effect of Alagebrium Chloride (ALT-711), a Novel Glucose Cross-Link Breaker, in the Treatment of Elderly Patients With Diastolic Heart Failure. *Journal of Cardiac Failure* **11**, 191-195, doi:https://doi.org/10.1016/j.cardfail.2004.09.010 (2005).
514 Seo, H.-S., Lee, N.-H., Cho, Y.-H., Choi Hyung, O. & Suh, J. Abstract 12878: The Effect of Advanced Glycation End Products (AGE) Breaker, Alagebrium on the Cardiac Structural and Functional Change in Type I Diabetic Rat Model. *Circulation* **132**, A12878-A12878, doi:10.1161/circ.132.suppl_3.12878 (2015).
515 Watson, A. M. D. *et al.* Alagebrium reduces glomerular fibrogenesis and inflammation beyond preventing RAGE activation in diabetic apolipoprotein E knockout mice. *Diabetes* **61**, 2105-2113, doi:10.2337/db11-1546 (2012).
516 Tak, P. P. & Firestein, G. S. NF-kappaB: a key role in inflammatory diseases. *The Journal of clinical investigation* **107**, 7-11, doi:10.1172/JCI11830 (2001).
517 Dixon, L. J., Barnes, M., Tang, H., Pritchard, M. T. & Nagy, L. E. Kupffer cells in the liver. *Comprehensive Physiology* **3**, 785-797, doi:10.1002/cphy.c120026 (2013).
518 Leroux, A. *et al.* Toxic lipids stored by Kupffer cells correlates with their pro-inflammatory phenotype at an early stage of steatohepatitis. *Journal of Hepatology* **57**, 141-149, doi:https://doi.org/10.1016/j.jhep.2012.02.028 (2012).